

NASA/CP—1998-208414



17th International Microgravity  
Measurements Group Meeting

---

June 1998

## The NASA STI Program Office . . . in Profile

Since its founding, NASA has been dedicated to the advancement of aeronautics and space science. The NASA Scientific and Technical Information (STI) Program Office plays a key part in helping NASA maintain this important role.

The NASA STI Program Office is operated by Langley Research Center, the Lead Center for NASA's scientific and technical information. The NASA STI Program Office provides access to the NASA STI Database, the largest collection of aeronautical and space science STI in the world. The Program Office is also NASA's institutional mechanism for disseminating the results of its research and development activities. These results are published by NASA in the NASA STI Report Series, which includes the following report types:

- **TECHNICAL PUBLICATION.** Reports of completed research or a major significant phase of research that present the results of NASA programs and include extensive data or theoretical analysis. Includes compilations of significant scientific and technical data and information deemed to be of continuing reference value. NASA's counterpart of peer-reviewed formal professional papers but has less stringent limitations on manuscript length and extent of graphic presentations.
- **TECHNICAL MEMORANDUM.** Scientific and technical findings that are preliminary or of specialized interest, e.g., quick release reports, working papers, and bibliographies that contain minimal annotation. Does not contain extensive analysis.
- **CONTRACTOR REPORT.** Scientific and technical findings by NASA-sponsored contractors and grantees.

- **CONFERENCE PUBLICATION.** Collected papers from scientific and technical conferences, symposia, seminars, or other meetings sponsored or cosponsored by NASA.
- **SPECIAL PUBLICATION.** Scientific, technical, or historical information from NASA programs, projects, and missions, often concerned with subjects having substantial public interest.
- **TECHNICAL TRANSLATION.** English-language translations of foreign scientific and technical material pertinent to NASA's mission.

Specialized services that complement the STI Program Office's diverse offerings include creating custom thesauri, building customized data bases, organizing and publishing research results . . . even providing videos.

For more information about the NASA STI Program Office, see the following:

- Access the NASA STI Program Home Page at <http://www.sti.nasa.gov>
- E-mail your question via the Internet to [help@sti.nasa.gov](mailto:help@sti.nasa.gov)
- Fax your question to the NASA Access Help Desk at (301) 621-0134
- Telephone the NASA Access Help Desk at (301) 621-0390
- Write to:  
NASA Access Help Desk  
NASA Center for AeroSpace Information  
7121 Standard Drive  
Hanover, MD 21076

NASA/CP—1998-208414



# 17th International Microgravity Measurements Group Meeting

Proceedings of a conference held at  
Ohio Aerospace Institute  
Brook Park, Ohio  
and sponsored by PI Microgravity Services Project;  
Microgravity Measurements & Analysis Program;  
Microgravity Science Division; NASA Lewis Research  
Center; and the NASA Microgravity Research Program  
March 24–26, 1998

National Aeronautics and  
Space Administration

Lewis Research Center

---

June 1998

Available from

NASA Center for Aerospace Information  
7121 Standard Drive  
Hanover, MD 21076  
Price Code: A13

National Technical Information Service  
5287 Port Royal Road  
Springfield, VA 22100  
Price Code: A13



17th International  
Microgravity Measurements Group  
Meeting

Final Report

March 24 - 26, 1998

*Hosted by:*

Ohio Aerospace Institute  
Brook Park, Ohio

*Sponsored by:*

PI Microgravity Services Project  
Microgravity Measurement & Analysis Program  
Microgravity Science Division  
NASA Lewis Research Center

and the  
NASA Microgravity Research Program

# Table of Contents

---

|   |      |
|---|------|
| Table of Contents .....                     | i    |
| List of Sessions, Papers, and Authors ..... | iii  |
| Agenda .....                                | vii  |
| Attendees .....                             | xiii |
| Meeting Summary .....                       | 1    |
| Papers .....                                | 4    |



## Session, Papers, and Authors

Presentation Title

Presenter

Paper #

Welcoming remarks & logistics

*R. DeLombard (NASA Lewis Research Center)*

Welcoming remarks

*J. Salzman (NASA Lewis Research Center)*

Introductory remarks

*R. Henderson (NASA Marshall Space Flight Center)*

### Session A

#### SUMMARY OF SHUTTLE MICROGRAVITY ENVIRONMENT

Chair: M. Rogers

Review of Shuttle microgravity acceleration data (vibratory and transient)

*K. Hrovat (Tal-Cut Corp.) and Richard DeLombard (NASA Lewis Research Center)*

1

A review of microgravity levels on ten OARE shuttle missions

*K. McPherson (NASA Lewis Research Center)*

2

Review of MMA measurements on four shuttle missions

*A. Schütte (Daimler Benz Aerospace AG), et. al.*

3

Firsthand perspective on the microgravity environment

*D. Thomas (NASA Johnson Space Center)*

4

Fifteen years of European experience in microgravity characterization-from  
Spacelab to the International Space Station

*H. Hamacher (Deutsches Zentrum fuer Luft- und Raumfahrt), et. al.*

5

### Session B

#### SUMMARY OF MIR MICROGRAVITY ENVIRONMENT

Chair: J. Acevedo

Acceleration disturbances in the Mir microgravity environment

*M. E. Moskowitz (Tal-Cut Corp.)*

6

Acceleration measurements with MIM on Mir and Shuttle mission STS-85

*B. Tryggvason (Canadian Space Agency), et. al.*

7

Gravitational sensitivity analysis of microgravity environment on Mir space  
station

*V. Polezhaev (Russian Academy of Sciences)*

8

## Session, Papers, and Authors

Presentation Title  
Presenter

---

Paper #

### Session C ISS MICROGRAVITY ENVIRONMENT Chair: A. Karchmer

|  |    |
|--|----|
| Introduction of International Microgravity Strategic Planning Group<br><i>R. Rhome (NASA Headquarters)</i>                     | 9  |
| Quasi-steady state microgravity performance assessment<br><i>M. Laible (Boeing Company)</i>                                    | 10 |
| Review of DAC-6 microgravity environment<br><i>S. Thampi (Boeing Company)</i>  | 11 |
| ARIS final design and flight test results<br><i>G. Bushnell (Boeing Company)</i>   | 12 |
| ISS microgravity requirements and environment discussion<br><i>Discussion Leader: A. Karchmer (NASA Lewis Research Center)</i> |    |

### Session D SUMMARY OF FREE FLYER MICROGRAVITY ENVIRONMENT Chair: K. McPherson

|  |    |
|--|----|
| Terrier-Black Brant sounding rocket microacceleration environment<br><i>T. Kacpura (Aerospace Design &amp; Fabrication) and<br/>J. C. Acevedo (NASA Lewis Research Center)</i>   | 13 |
| Review of 3-DMA measurements on six shuttle missions and nine suborbital flights<br><i>J. Bijvoet and P. D. Nerren (University of Alabama in Huntsville)</i>   | 14 |
| First microgravity measurement results of FOTON-11 by QSAM<br><i>H. Hamacher and H. E. Richter (Deutsches Zentrum fuer Luft- und Raumfahrt)</i>  | 15 |
| Some Results of Measuring Microgravity in the Process of "FOTON no. 11"<br>Microgravitational Space Platform Flight<br><i>V. F. Agarkov and V. D. Kozlov (Central Specialized Design Bureau, Samara, Russia)</i>   | 16 |
| Results of Synchro Experiment on Simultaneous Measurement and Estimation using Digital Model of Microgravity in places of Accelerometer Installation during "FOTON no. 11" Flight for Digital Model Accuracy Assessment<br><i>V. F. Agarkov and V. D. Kozlov (Central Specialized Design Bureau, Samara, Russia)</i> | 17 |

## Session, Papers, and Authors

Presentation Title  
*Presenter*

Paper #

---

### Session E SCIENCE AFFECTED BY MICROGRAVITY ENVIRONMENT Chair: M. Rogers

|   |    |
|---|----|
| Fluids and Materials Science Studies Utilizing the Microgravity-vibration Isolation Mount (MIM)<br><i>R. Herring (Canadian Space Agency), et. al.</i>   | 18 |
| Fundamental physics microgravity sensitivity<br><i>U. Israelsson (Jet Propulsion Laboratory), et. al.</i>   | 19 |
| Materials science experiment microgravity sensitivity<br>• <i>Programmatic issues - D. Gillies (NASA Marshall Space Flight Center)</i><br>• <i>Case studies - I. Alexander (National Center for Microgravity Research on Fluids and Combustion/Case Western Reserve University)</i> | 20 |
| A short collation of g-jitter effects on combustion experiments in microgravity<br><i>H. Ross (NASA Lewis Research Center)</i>  | 21 |
| NASA's microgravity fluid physics program - tolerability to residual accelerations<br><i>R. Skarda (NASA Lewis Research Center)</i>   | 22 |
| Microgravity sensitivity of typical fluid physics experiment<br><i>R. Monti (U. of Naples, Italy), et. al.</i>  | 23 |
| Containerless processing in reduced gravity using the TEMPUS facility during MSL-1 and MSL-1R<br><i>J. Rogers (NASA Marshall Space Flight Center)</i>   | 24 |
| Planning experiments for a microgravity environment<br><i>M. Rogers (National Center for Microgravity Research on Fluids and Combustion)</i>  | 25 |

## Session, Papers, and Authors

Presentation Title

Presenter

Paper #

---

### Session F

#### MICROGRAVITY MEASUREMENT OPERATIONS DURING ISS ERA

Chair: T. Sutliff

|  |    |
|--|----|
| g-LIMIT: A vibration isolation system for the microgravity science glovebox<br><i>M. Whorton (NASA Marshall Space Flight Center)</i>                               | 26 |
| Acceleration measurements in JEM<br><i>T. Ikeda and K. Murakami (National Space Development Agency of Japan)</i>   | 27 |
| Status of ESA taskforce on microgravity levels on the International Space Station<br><i>P. Clancy (European Space Agency)</i>                                      | 28 |
| Procedures and microgravity measurements for commercial materials development in space<br><i>J. Bijvoet and P. D. Nerren (University of Alabama in Huntsville)</i> | 29 |
| KSC ISS payload processing and facilities<br><i>K. Zari (Kennedy Space Center)</i>   | 30 |
| The International Space Station Microgravity Acceleration Measurement System<br><i>J. Fox (Canopus Systems, Inc.)</i>  | 31 |
| SAMS-II Requirements & Operations<br><i>L. Wald (NASA Lewis Research Center)</i>   | 32 |
| PI Microgravity Services role for International Space Station operations<br><i>R. DeLombard (NASA Lewis Research Center)</i>                                       | 33 |
| PIMS data storage, access, and neural network processing<br><i>K. McPherson (NASA Lewis Research Center) and M. E. Moskowitz (Tal-Cut Corp.)</i>                   | 34 |

# Agenda

---

## Agenda

| Title  | Presenter                                  | Paper #                  |
|--|--|--------------------------|
| <b>Tuesday, March 24, 1998</b>   |  |                          |
| 8:00 A 8:15 A Welcoming remarks & logistics  | R. DeLombard (LeRC)                        |                          |
| 8:15 A 8:30 A Introductory remarks   | R. Henderson (MSFC)                        |                          |
| <b>Session A</b>   |  |                          |
| <b>SUMMARY OF SHUTTLE MICROGRAVITY ENVIRONMENT</b>   |  | <i>Chair: M. Rogers</i>  |
| 8:30 A 9:00 A Review of Shuttle microgravity acceleration data (vibratory and transient)                                   | K. Hrovat (Tal-Cut)                        | 1                        |
| 9:00 A 9:30 A A review of microgravity levels on ten OARE shuttle missions   | K. McPherson (LeRC)                        | 2                        |
| 9:30 A 10:00 A Review of MMA measurements on four shuttle missions   | A. Schütte (DASA)                          | 3                        |
| 10:00 A 10:15 A <b>BREAK</b>   |  |                          |
| 10:15 A 11:00 A Firsthand perspective on the microgravity environment  | D. Thomas (JSC)                            | 4                        |
| 11:00 A 11:30 A Fifteen years of European experience in microgravity characterization - from Spacelab to the Space Station | H. Hamacher (DLR)                          | 5                        |
| 11:30 A 1:00 P <b>LUNCH</b>  |  |                          |
| <b>Session B</b>   |  |                          |
| <b>SUMMARY OF MIR MICROGRAVITY ENVIRONMENT</b>   |  | <i>Chair: J. Acevedo</i> |
| 1:00 P 1:10 P Welcoming remarks  | J. Salzman (LeRC)                          |                          |
| 1:10 P 1:40 P Acceleration disturbances in the Mir microgravity environment  | J. Acevedo (LeRC)                          | 6                        |
| 1:40 P 2:10 P First microgravity measurement results of FOTON-11 by QSAM   | H. Hamacher (DLR)                          | 16                       |
| 2:10 P 2:25 P <b>BREAK</b>   |  |                          |
| 2:25 P 3:05 P Acceleration measurements with MIM on Mir and Shuttle mission STS-85   | B. Tryggvason (CSA)                        | 7                        |
| 3:05 P 3:40 P Gravitational sensitivity analysis of microgravity environment on Mir space station                          | V. Polezhaev (Russian Academy of Sciences) | 8                        |
| 3:40 P 4:10 P KSC ISS payload processing and facilities  | K. Zari (KSC)                              | 31                       |

# Agenda

Title

Presenter

Paper #

*Wednesday, March 25, 1998 (Morning)*

## Session C

ISS MICROGRAVITY ENVIRONMENT

*Chair: A. Karchmer*

**NOTE:** The MGMG was joined by the International Microgravity Strategic Planning Group during the morning session.

|         |         |   |                                       |    |
|---------|---------|---|---------------------------------------|----|
| 8:00 A  | 8:15 A  | Introduction of International Microgravity Strategic Planning Group | R. Rhome (NASA HQ)                    | 9  |
| 8:15 A  | 8:55 A  | Quasi-steady state microgravity performance assessment              | M. Laible (Boeing)                    | 10 |
| 8:55 A  | 9:30 A  | Review of DAC-6 microgravity environment                            | S. Thampi (Boeing)                    | 11 |
| 9:30 A  | 9:45 A  | <b>BREAK</b>  |                                       |    |
| 9:45 A  | 10:45 A | ARIS final design and flight test results                           | G. Bushnell (Boeing)                  | 12 |
| 10:45 A | 11:30 A | ISS microgravity requirements and environment discussion            | Discussion Leader: A. Karchmer (LeRC) |    |
| 11:30 A | 1:00 P  | <b>LUNCH</b>  |                                       |    |

# Agenda

| Title | Presenter | Paper # |
|-------|-----------|---------|
|-------|-----------|---------|

---

*Wednesday, March 25, 1998 (Afternoon)*

|                  |
|------------------|
| <b>Session D</b> |
|------------------|

|   |                            |
|---|----------------------------|
| <b>SUMMARY OF FREE FLYER MICROGRAVITY ENVIRONMENT</b> | <i>Chair: K. McPherson</i> |
|---|----------------------------|

|        |        |  |                  |    |
|--------|--------|--|------------------|----|
| 1:05 P | 1:30 P | Terrier-Black Brant sounding rocket microacceleration environment                | T. Kacpura (ADF) | 13 |
| 1:35 P | 2:00 P | Review of 3-DMA measurements on six shuttle missions and nine suborbital flights | J. Bijvoet (UAH) | 14 |
| 2:00 P | 2:15 P | <b>BREAK</b>   |                  |    |

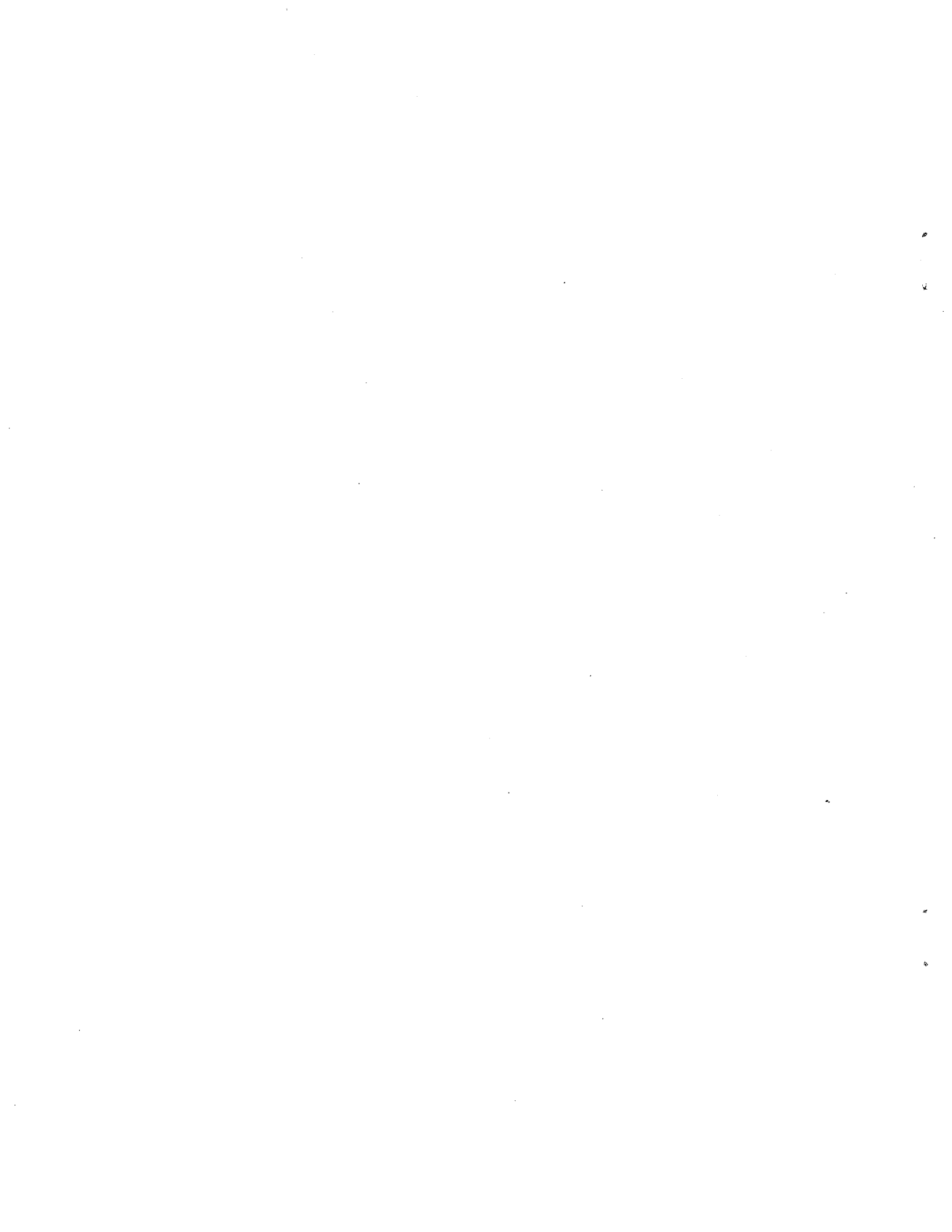
|                  |
|------------------|
| <b>Session E</b> |
|------------------|

|   |                         |
|---|-------------------------|
| <b>SCIENCE AFFECTED BY MICROGRAVITY ENVIRONMENT</b> | <i>Chair: M. Rogers</i> |
|---|-------------------------|

|        |        |  |  |    |
|--------|--------|--|--|----|
| 2:15 P | 2:50 P | Fluids and materials science studies utilizing the Microgravity-vibration Isolation Mount (MIM)  | R. Herring (CSA),<br>W. Duval (LeRC)     | 18 |
| 2:50 P | 3:25 P | Fundamental physics microgravity sensitivity   | U. Israelsson (JPL)                      | 19 |
| 3:25 P | 3:50 P | Materials science experiment microgravity sensitivity <ul style="list-style-type: none"> <li>• Programmatic issues</li> <li>• Case studies</li> </ul>  | D. Gillies (MSFC)<br>I. Alexander (NCMR) | 20 |
| 3:50 P | 4:25 P | A short collation of g-jitter effects on combustion experiments in microgravity  | H. Ross (LeRC)                           | 21 |
| 4:25 P | 4:50 P | Some results of measuring microgravity in the process of "FOTON no. 11" microgravitational space platform flight   | V. F. Agarkov<br>(CSDB/Russia)           | 16 |
| 4:50 P | 5:15 P | Results of synchro experiment on simultaneous measurement and estimation using digital model of microgravity in places of scelerometer installation during "FOTON no. 11" flight for digital model accuracy assessment | V. F. Agarkov<br>(CSDB/Russia)           | 17 |

## Agenda

| Title   | Presenter  | Paper #                           |
|---|--|-----------------------------------|
| <b>Thursday, March 26, 1998</b>                           |  |                                   |
| <b>Session E (continued)</b>                              |  |                                   |
| <b>SCIENCE AFFECTED BY MICROGRAVITY ENVIRONMENT</b>       |  | <i>Chair: I. Alexander</i>        |
| 8:07 A  | 8:37 A NASA's microgravity fluid physics program - tolerability to residual accelerations            | R. Skarda (LeRC) 22               |
| 8:37 A  | 9:25 A Microgravity sensitivity of typical fluid physics experiment                                  | R. Monti (U. of Naples) 23        |
| 9:25 A  | 9:50 A Containerless processing in reduced gravity using the TEMPUS facility during MSL-1 and MSL-1R | J. Rogers (MSFC) 24               |
| 9:50 A  | 10:08 A <b>BREAK</b>   |                                   |
| 10:08 A   | 10:27 A Planning experiments for a microgravity environment  | M. Rogers (NCMR) 25               |
| <b>Session F</b>  |  |                                   |
| <b>MICROGRAVITY MEASUREMENT OPERATIONS DURING ISS ERA</b> |  | <i>Chair: T. Sutliff</i>          |
| 10:27 A   | 11:00 A g-LIMIT: A vibration isolation system for the microgravity science glovebox                  | M. Whorton (MSFC) 26              |
| 11:00 A   | 12:00 P <b>LUNCH</b>   |                                   |
| 12:05 P   | 12:50 P Acceleration measurements in JEM   | T. Ikeda & K. Murakami (NASDA) 27 |
| 12:50 P   | 1:15 P Status of ESA taskforce on microgravity levels on the International Space Station             | P. Clancy (ESA) 28                |
| 1:15 P  | 1:30 P Procedures and microgravity measurements for commercial materials development in space        | J. Bijvoet (UAH) 29               |
| 1:30 P  | 2:15 P The International Space Station Microgravity Acceleration Measurement System                  | J. Fox (Canopus) 31               |
| 2:15 P  | 2:30 P <b>BREAK</b>  |                                   |
| 2:30 P  | 3:00 P SAMS-II Requirements & Operations   | L. Wald (LeRC) 32                 |
| 3:00 P  | 3:30 P PI Microgravity Services role for International Space Station operations                      | R. DeLombard (LeRC) 33            |
| 3:30 P  | 4:00 P PIMS data storage, access, and neural network processing                                      | K. McPherson (LeRC) 34            |
| <b>Meeting Summary</b>                                    |  |                                   |
| 4:00 P  | 4:20 P Summary discussion of MGMG #17  | R. DeLombard (LeRC)               |



## Attendee List

---

## Attendees

Julio C. Acevedo  
NASA Lewis Research Center  
MS 500-216  
21000 Brookpark Road  
Cleveland, OH 44135  
Telephone: 216-433-2471  
Fax: 216-433-8660  
Julio.C.Acevedo@lerc.nasa.gov

Valentin Agarkov  
Russia, Samara, 443009  
Pskovskaya Str. 18  
Telephone: 8462-271907  
Fax: 8462-272070

Iwan Alexander  
NCMR/CWRU  
Mechanical and Aerospace Engineering  
416 Glennan  
Case Western Reserve University  
Cleveland, OH 44106  
Telephone: (216)368 6045  
Fax: (216) 368 6445  
ida2@po.cwru.edu

David Allen  
Allen Aerospace Corp.  
P. O. Box 66042  
Cleveland, OH 44116  
Telephone: 440-333-2834  
Fax: 440-333-9290  
dallen@stratos.net

Christoph Bartscher  
Technical University Munich  
Institute A for Thermodynamics  
Boltzmannstr. 15  
85748 Garching, Germany  
Telephone: ++49 89 289 16232  
Fax: ++49 89 289 16218  
bartsch@thermo-a.mw.tu-muenchen.de

Jan A. Bijvoet  
Consortium for Materials Development in Space  
Research Institute Building, Rm M65  
The University of Alabama in Huntsville  
Huntsville AL. 35899  
Telephone: 256.890 6620  
Fax: 256.890 6791  
bijvoetj@email.uah.edu

Dan Bloom  
NYMA  
2001 Aerospace Parkway  
Brook Park, OH 44143  
Telephone: 216-977-1172  
Fax: 216-977-1269  
dbloom@lerc.nasa.gov

Glenn S. Bushnell  
Boeing Information, Space & Defense Systems  
P.O. Box 3999  
Seattle, WA 98124-2499  
Telephone: 253-773-7677  
Fax: 253-773-2250  
glenn.s.bushnell@boeing.com

Dr. Bradley M. Carpenter  
NASA Headquarters  
Code UG  
Washington DC 20546-0001  
Telephone: 202-358-0826  
Fax: 202-358-3091  
bcarpent@mail.hq.nasa.gov

Jean de Carufel  
Canadian Space Agency  
6767 Route de l'Aéroport  
St. Hubert, Quebec, Canada  
J3Y 8Y9  
Telephone: 514-926-4680  
Fax: 514 926-4707  
Jean.DeCarufel@space.gc.ca

Paul Clancy  
European Space Agency / ESTEC  
Keplerlaan 1  
2200 AG Noordwijk  
The Netherlands  
Telephone: 31-71-565-8735  
Fax: 31-71-565-3042  
pclancy@estec.esa.nl

Rafael Bureo Dacal  
European Space Agency  
Keplerlaan 1  
2200 AG Noordwijk  
The Netherlands  
Telephone: +31-71-565-4156  
Fax: +31-71-565-5427  
rbureo@estec.esa.nl

## Attendees

Steve DelBasso  
Boeing Defense & Space Group  
MS HS-24  
2100 Space Park Drive  
Nassau Bay, Tx 77058  
Telephone: 281-336-4768  
Fax: 281-336-5070  
Steve.Delbasso@SW.Boeing.com

Richard DeLombard  
NASA Lewis Research Center  
Mail Stop 500-216  
21000 Brookpark Road  
Cleveland, OH 44135  
Telephone: 216-433-5285  
Fax: 216-433-8660  
richard.delombard@lerc.nasa.gov

Patricia M. Doty  
NASA Marshall Space Flight Center  
Code MG21  
Marshall Space Flight Center, AL 35812  
Phone: 256-544-4136  
Fax: 256-544-5848  
Pat.Doty@msfc.nasa.gov

Walter H. B. Duval  
NASA Lewis Research Center  
Mail Stop 105-1  
21000 Brookpark Road  
Cleveland, OH 44135  
Telephone: 216-433-5023  
Fax: 216-433-5033  
Walter.M.Duval@lerc.nasa.gov

Dr. Don Edberg  
The Boeing Company  
5301 Bolsa Ave.  
H013-C316  
Huntington Beach, CA 92647  
Telephone: 714-896-5210  
Fax: 714-896-2305  
don.edberg@boeing.com

Dr. David G. Elliott  
Jet Propulsion Laboratory  
M/S 79-24  
4800 Oak Grove Dr.  
Pasadena, CA 91109  
Telephone: 818-354-3486  
Fax: 818-393-3707  
delliott@squid.jpl.nasa.gov

Jim Fountain  
Boeing  
499 Boeing Blvd.  
MS-JN-04  
P.O. Box 240002  
Huntsville, AL 35899  
Telephone: 256-461-3634  
Fax: 256-461-2772  
jim.fountain@boeing.com

James C. Fox  
Canopus Systems, Inc.  
2010 Hogback Rd., Ste. 3  
Ann Arbor, MI 48105  
Telephone: 734-971-4422  
Fax: 734-971-5243  
fox@canopus.com

Shinichi Furumoto  
Tsukuba Space Center  
Sengen 2-1-1  
Tsukuba City  
Ibaraki 305  
JAPAN  
Telephone: +81-298-52-2777  
Fax: +81-298-50-2233  
Furumoto.Shinichi@nasda.go.jp

Dave Gantose  
ADF Corp  
2001 Aerospace Pkwy  
Brook Park, OH 44142  
Telephone: 216-977-1376  
Fax: 216-977-1269  
gantose@lerc.nasa.gov

Philip Gregory  
Manager Microgravity Sciences Program  
Canadian Space Agency  
6767 route de l'Aéroport  
St-Hubert  
Quebec CANADA  
J3Y 8Y9  
Telephone: (514) 926 4770  
Fax: (514) 926 4766  
philip.gregory@space.gc.ca

## Attendees

Hans Hamacher  
DLR  
Institute for Space Simulation  
51170 Koeln  
GERMANY  
Telephone: +49-2203-6012330  
Fax: +49-2203-61768  
hans.hamacher@dlr.de

Rob Haslett  
NASA Lewis Research Center / Tal-Cut  
MS 500-216  
21000 Brookpark Rd.  
Cleveland, OH 44135  
Telephone: 440-716-3266  
Fax: 440-716-3267  
haslett@lerc.nasa.gov

John Heese  
ADF Inc.  
2001 Aerospace Parkway  
Brook Park, OH 44142  
Telephone: 216-977-1187  
Fax: 216-977-1269  
heese@lerc.nasa.gov

Fred Henderson  
Teledyne Brown Engineering  
2100 Space Park Drive HS-44  
Nassau Bay, TX 77058  
Telephone: (281) 336-4256  
Fax: (281) 336-5341  
fred.henderson@sw.boeing.com

Robin Henderson  
NASA Marshall Space Flight Center  
MG01 / Microgravity Research Program Office  
MSFC, AL 35812  
Telephone: 256-544-1738  
Fax: 256-544-5848  
robin.henderson@msfc.nasa.gov

Rodney Herring  
Program Scientist  
Microgravity Sciences Program  
Canadian Space Agency  
6767 route de l'Aéroport  
St-Hubert, Quebec  
Canada J3Y 8Y9  
Telephone: 514-926-4773  
Fax:  
Rodney.Herring@space.gc.ca

Myron Hill  
NASA Lewis Research Center  
MS 500-102  
21000 Brookpark Rd.  
Cleveland, OH 44135  
Telephone: 216-433-5279  
Fax: 216-433-8660  
Myron.E.Hill@lerc.nasa.gov

Kenneth Hrovat  
NASA Lewis Research Center / Tal-Cut  
Mail Stop 500-216  
21000 Brookpark Road  
Cleveland, OH 44135  
Telephone: (216) 433-3564  
Fax: (216) 433-8545  
Kenneth.Hrovat@lerc.nasa.gov

William O. Hughes  
NASA Lewis Research Center  
M/S 86-10  
21000 Brookpark Road  
Cleveland, OH 44135  
Telephone: (216) 433-2597  
Fax: (216) 433-6382  
William.O.Hughes@lerc.nasa.gov

Toshitami Ikeda  
NASDA  
Space Experiment Department  
Tsukuba Space Center,  
2-1-1, Sengen, Tsukuba-city  
Ibaraki, 305-8505, JAPAN  
Telephone: +81-298-52-2778  
Fax: +81-298-50-2233  
toikeda@RD.TKSC.NASDA.GO.JP

Ulf Israelsson  
Jet Propulsion Laboratory  
MS 79-5  
4800 Oak Grove Drive  
Pasadena, CA 91109  
Telephone: (818)-354-9255  
Fax: (818)393-6383  
ulf@squid.jpl.nasa.gov

Robert J. Jackson  
NASA Marshall Space Flight Center  
Code MG20  
Marshall Space Flight Center, AL 35812  
Telephone: 256-544-6582  
Fax: 256-544-5848  
Robert.J.Jackson@msfc.nasa.gov

## Attendees

Thomas Kacpura  
NYMA SETAR/ADF  
2001 Aerospace Parkway  
Brook Park, OH 44143  
Telephone: 216-977-1057  
Fax: 216-977-1269  
thomas.kacpura@lerc.nasa.gov

Dr. Allen Karchmer  
NASA Lewis Research Center  
21000 Brookpark Rd.  
MS 500-216  
Cleveland, OH 44135  
Telephone: 216-433-5180  
Fax: 216-433-8660  
allen.karchmer@lerc.nasa.gov

Rainer Kuhl  
DLR  
Koenigswinterer Str. 522  
D-53227 Bonn  
GERMANY  
Telephone: +49-228-447-387  
Fax: +49-228-447-700  
rainer.kuhl@dlr.de

Michael Laible  
Boeing Defense & Space Group  
MS HS-24  
2100 Space Park Drive  
Nassau Bay, Tx 77058  
Telephone: 281-336-4718  
Fax:  
Michael.Laible@SW.Boeing.com

Sandor L. Lehoczky  
NASA Marshall Space Flight Center  
ES71  
Huntsville, AL 35812  
Telephone: 256-544-7758  
Fax: 256-544-8762  
sandor.lehoczky@msfc.nasa.gov

Jack Lekan  
NASA Lewis Research Center  
Mail Stop 500-216  
21000 Brookpark Road  
Cleveland, Ohio 44135  
Telephone: (216) 433-3459  
Fax: (216) 433-8660  
Jack.Lekan@lerc.nasa.gov

Eugene Liberman  
NASA Lewis Research Center / Tal-Cut  
MS 500-216  
21000 Brookpark Road  
Cleveland, OH 44135  
Telephone: (216)-433-8518  
Fax: (216)-433-8660  
Gene.Liberman@lerc.nasa.gov

Nissim Lugasy  
NASA Lewis Research Center / Tal-Cut  
21000 Brookpark Rd.  
MS 500-216  
Cleveland, OH 44135  
Telephone: 216-433-2708  
Fax: 216-433-8660  
nissim.lugasy@lerc.nasa.gov

Mark E. McNelis  
NASA Lewis Research Center  
Mail Stop 86-10  
21000 Brookpark Road  
Cleveland, Ohio 44135  
Telephone: (216)433-8395  
Mark.E.McNelis@lerc.nasa.gov

John Merry  
NYMA  
2001 Aerospace Parkway  
Brook Park, OH 44143  
Telephone: 216-977-1135  
Fax: 216-977-1269  
Jesse.J.Merry@lerc.nasa.gov

David L. Miller  
NYMA  
2001 Aerospace Parkway  
Brook Park, OH 44143  
Telephone: 216-977-1275  
Fax: 216-977-1269  
David.L.Miller@lerc.nasa.gov

Rodolfo Monti  
Faculty of Engineering  
University of Naples  
Dept. of Space Science and Engineering  
Piazzale V. Tecchio, 80  
80125 Naples - ITALY  
Telephone: + 39 - 81 - 7682359  
Fax: + 39 - 81 - 5932044  
monti@unina.it

## Attendees

Dale Mortensen  
NYMA  
2001 Aerospace Parkway  
Brook Park, OH 44143  
Telephone: 216-977-1062  
Fax: 216-977-1269  
Dale.J.Mortensen@lerc.nasa.gov

Emily Nelson  
NASA Lewis Research Center  
Mail Stop 105-1  
21000 Brookpark Road  
Cleveland, OH 44135  
Telephone: 216-433-3268  
Fax: 216-433-5033  
Emily.S.Nelson@lerc.nasa.gov

Toshihiko Oida  
NASDA / Visiting Engineer @LeRC  
NASA Lewis Research Center  
Mail Stop 500-217  
21000 Brookpark Road  
Cleveland, Ohio 44135  
Telephone: 216.433.3084  
Fax: 216.433.3790  
toshihiko.oida@lerc.nasa.gov

Vadim I. Polezhaev  
The Institute for Problems in Mechanics  
Russian Academi of Scienses  
117526, Moscow  
Prospect Vernadskogo 101,  
Russia  
Telephone: (7-095) 434-32-83 (work)  
(7-095) 151-77-07 (home)  
Fax: (7-095) 938-20-48  
polezh@ipmnet.ru

Robert Rhome  
NASA Headquarters  
Code UG  
Washington DC 20546-0001  
Telephone: 202-358-1490  
Fax: 202-358-3091  
robert.rhomb@hq.nasa.gov

Dr. James E. Rice  
Canopus Systems, Inc.  
2010 Hogback Rd., Ste. 3  
Ann Arbor, MI 48105  
Telephone: 734-971-4422  
Fax: 734-971-5243  
rice@canopus.com

Judith L. Robey  
NASA Headquarters  
Code UG  
Washington DC 20546-0001  
Telephone: 202-358-0823  
Fax: 202-358-3091  
judith.robey@hq.nasa.gov

Jan Rogers  
NASA Marshall Space Flight Center  
Mail Code ES76  
Huntsville, AL 35812  
Telephone: 256-544-1081  
Fax: 256-544-2101  
jan.rogers@msfc.nasa.gov

Melissa J. B. Rogers  
National Center for Microgravity Research on  
Fluids and Combustion  
MS 110-3  
21000 Brookpark Road  
Cleveland, OH 44135  
Telephone: 216-433-2332  
Fax: 216-433-3973  
Melissa.Rogers@lerc.nasa.gov

Howard Ross  
NASA Lewis Research Center  
MS 500-115  
21000 Brookpark Road  
Cleveland, Ohio 44135  
Telephone: 216-433-2562  
Fax: 216-433-8660  
Howard.D.Ross@lerc.nasa.gov

Neil Rowe  
NYMA  
2001 Aerospace Parkway  
Brook Park, OH 44143  
Telephone: 216-977-1221  
Fax: 216-977-1269  
Neil.D.Rowe@lerc.nasa.gov

Jack Salzman  
NASA Lewis Research Center  
MS 500-205  
21000 Brookpark Road  
Cleveland, OH 44135  
Telephone: 216-433-2868  
Fax: 216-433-8660  
Jack.A.Salzman@lerc.nasa.gov

## Attendees

Subramanian Sankaran  
National Center for Microgravity Research on  
Fluids and Combustion  
MS-110-3  
21000 Brookpark Rd.  
Cleveland, OH 44135  
Telephone: 216-433-9335  
Fax: 216-433-3973  
Subramanian.Sankaran@lerc.nasa.gov

Craig Schafer  
NASA Johnson Space Center  
Code OZ4  
2101 NASA Road 1  
Houston, Tx 77058  
Telephone: 281-244-8939  
Fax: 281-244-8292  
craig.p.schafer1@jsc.nasa.gov

Andreas Schuette, RIO72  
Daimler-Benz Aerospace  
Space Infrastructure  
Postfach 28 61 56  
D-28361 Bremen  
Germany  
Telephone: +49 421 539 5354  
Fax: +49 421 539 5413  
Andreas.Schuette@ri.dasa.de

Nancy J. Shaw  
NASA Lewis Research Center  
MS 500-102  
21000 Brookpark Road  
Cleveland, OH 44135  
Telephone: 216-433-3285  
Fax: 216-433-8050  
Nancy.J.Shaw@lerc.nasa.gov

Dr. John V. Shebalin  
NASA Johnson Space Center  
ISS Payloads Office  
NASA/JSC Mail Code OZ4  
Houston, TX 77058-3696  
Telephone: 281 244-7118  
Fax: 281 244-8292  
john.v.shebalin1@jsc.nasa.gov

Alok Sinha  
Dept. Mech. Engg  
Penn State University  
University Park, PA 16802  
Telephone: 814-863-3079  
Fax: 814-863-4848  
axs22@psu.edu

Bruce Smith  
NYMA  
2001 Aerospace Parkway  
Brook Park, OH 44143  
Telephone: 216-977-1373  
Fax: 216-977-1269  
Alfred.B.Smith@lerc.nasa.gov

Thomas H. St. Onge  
NASA Lewis Research Center  
MS 500-217  
21000 Brookpark Road  
Cleveland, Ohio 44135  
Telephone: (216) 433-3557  
Fax: (216) 433-8660  
Thomas.H.StOnge@lerc.nasa.gov

William Y. Stewart  
Canadian Space Agency  
6767 Route de l'Aéroport  
St. Hubert, Quebec, Canada  
J3Y 8Y9  
Telephone: 514-926-4735  
Fax: 514 926-4707  
bill.stewart@space.gc.ca

Thomas Sutliff  
NASA Lewis Research Center  
MS 500-216  
21000 Brookpark Road  
Cleveland, Ohio 44135  
Telephone: (216) 433-3887  
Fax: (216) 433-8660  
Thomas.Sutliff@lerc.nasa.gov

Sreekumar K. Thampi  
Boeing Defense & Space Group  
MS HS-24  
2100 Space Park Drive  
Nassau Bay, Tx 77058  
Telephone: 281-336-5280  
Fax: 281-336-5070  
Sreekumar.Thampi@SW.Boeing.com

Dr. Donald A. Thomas  
NASA Johnson Space Center  
Code CB  
2101 NASA Road 1  
Houston, TX 77058  
Telephone: 281 244-8979  
donald.a.thomas1@jsc.nasa.gov

## Attendees

Duc Truong  
NASA Lewis Research Center  
MS 500-216  
21000 Brookpark Road  
Cleveland, Ohio 44135  
Telephone: (216) 433-8394  
Fax: (216) 433-8660  
Duc.k.truong@lerc.nasa.gov

Bjarni V Tryggvason  
Canadian Space Agency  
6767 Route de l'Aeroport  
St. Hubert, Quebec, Canada  
J3Y 8Y9  
Telephone: 514 926-4731  
Fax: 514 926-4707  
Bjarni.Tryggvason@space.gc.ca

Lawrence Vezina  
Mission Operations Engineer  
Canadian Space Agency  
6767 route de l'Aeroport  
St-Hubert, Quebec  
Canada J3Y 8Y9  
Telephone: 514-926-4768  
Lawrence.Vezina@space.gc.ca

William O. Wagar  
NASA Lewis Research Center  
MS 500-216  
21000 Brookpark Road  
Cleveland, Ohio 44135  
Telephone: (216) 433-3665  
Fax: (216) 433-8660  
william.o.wagar@lerc.nasa.gov

Lawrence W. Wald  
NASA Lewis Research Center  
MS 500-216  
21000 Brookpark Road  
Cleveland, Ohio 44135  
Telephone: (216) 433-5219  
Fax: (216) 433-8660  
lwald@lerc.nasa.gov

Dr. Mark S. Whorton  
NASA Marshall Space Flight Center  
ED12/Pointing Control Systems  
MSFC, AL 35812  
Telephone: (256) 544-1435  
Fax: (256) 544-5416  
mark.whorton@msfc.nasa.gov

Bruce W. Wilson  
The Boeing Company  
5301 Bolsa Avenue  
Mail Code H014-B412  
Huntington Beach, CA 92647-2099  
Telephone: 714-372-2363  
Fax: 714-896-1094  
bruce.w.wilson@boeing.com

Kevin Zari  
NASA Kennedy Space Center  
BC-D1  
KSC, FL 32899  
Telephone: 407-867-1104  
Fax: 407-867-7282  
kevin.zari-1@ksc.nasa.gov

Martin Zell  
Daimler-Benz Aerospace Dornier  
Av der Bundesstrasse 31  
88090 Immenstaad  
GERMANY  
Telephone: +49-7545-82963  
Fax: +49-7545-84429  
A008592@DBMAIL.DASA.DE

# MEETING SUMMARY

---

The Seventeenth International Microgravity Measurements Group (MGMG) meeting was held 24-26 March 1998 at the Ohio Aerospace Institute (OAI) in Brook Park, Ohio. This meeting focused on the transition of microgravity science research from the Shuttle, Mir, and free flyers to the International Space Station. The agenda shows that the presentations provided focused discussions toward that goal.

The MGMG series of meetings are conducted by the Principal Investigator Microgravity Services (PIMS) project of the Microgravity Science Division at the NASA Lewis Research Center (LeRC). The MGMG meetings provide a forum for the exchange of information and ideas about the microgravity environment and microgravity acceleration research in the Microgravity Research Program.

The meeting had participation from investigators in all areas of microgravity research, including science experiment principal investigators and project scientists, numerical modelers, instrumentation developers, and acceleration data analysts. The attendees included representatives from:

NASA centers: Headquarters, LeRC, Marshall Space Flight Center (MSFC), Johnson Space Center (JSC), Jet Propulsion Laboratory (JPL), and Kennedy Space Center (KSC)

Representatives from National Space Development Agency of Japan (NASDA), European Space Agency (ESA), Daimler Benz Aerospace AG (DASA), Deutsches Zentrum fuer Luft- und Raumfahrt (DLR), Centre National d'Etudes Spatiales (CNES), and Canadian Space Agency (CSA)

National Center for Microgravity Research on Fluids and Combustion

Universities in U.S., Italy, Germany, and Russia

Boeing Company (International Space Station (ISS) Prime Contractor)

Commercial companies in U.S. and Russia

Several agencies presented summaries of the measurement, analysis, and characterization of the microgravity environment of the Shuttle, Mir, and sounding rockets over the past fifteen years. This extensive effort has laid a foundation for pursuing a similar course during future microgravity science experiment operations on the ISS.

A special invited speaker was Dr. Donald Thomas, an astronaut from JSC who has flown on four Shuttle flights. He presented an excellent talk on crew effects on the microgravity environment and what can be done to minimize these effects. Many of the crew effects are not included in the predictions for the ISS microgravity environment, so education and awareness of the crew for their effect on the environment is an important factor. The PIMS group plans to pursue such a course with the astronaut office at JSC.

Bjarni Tryggvason, an astronaut from the Canadian Space Agency, also participated in the meeting with his perspective of the microgravity environment. Mr. Tryggvason conducted microgravity experiments while he served as a payload specialist on STS-85. Mr. Tryggvason has participated in the MGMG meetings for many years.

The MGMG coordinated with the International Microgravity Strategic Planning Group (IMSPG) meeting being held that same week at LeRC. The IMSPG members attended the Wednesday morning MGMG session as a joint meeting of the MGMG and the IMSPG. That session concentrated on the ISS microgravity environment. ISS program representatives presented the current predictions for the ISS microgravity environment along with the final design and flight testing results for the Active Rack Isolation System (ARIS). There was considerable discussion concerning the levels of acceleration (microgravity disturbances) to be expected on the ISS and how that compares with what has been experienced on the Shuttle and Mir. The MGMG has, for a long time, served as a mechanism for cooperation between the international space agencies participating in microgravity science research. The seventeenth MGMG served as a formal setting for the IMSPG to address the concerns of the microgravity environment on the ISS.

Future activities of microgravity environment characterization were discussed by several agencies who plan to operate on the ISS. The current state of plans to measure the environment in the U.S. Laboratory Module, the Japanese Experiment Module, and the

Columbus Orbital Facility were described. The PIMS project summarized the plans for the analysis and characterization of the environment.

All in all, this meeting was a success with only one speaker unable to attend. That presentation slot was filled with an optional paper on another topic. The accommodations afforded by the OAI were excellent with the comfortable auditorium, the service support, and ease of access for our international guests.

For additional information about the MGMG, please contact the PIMS project at NASA LeRC, send an e-mail inquiry to [MGMG@LERC.NASA.GOV](mailto:MGMG@LERC.NASA.GOV), or visit the MGMG WWW site at:

<http://www.lerc.nasa.gov/WWW/MMAP/PIMS/MGMG/mgmmain.html>

**MGMG #17**  
**PAPERS**

---

Compiled by: Richard DeLombard, NASA Lewis Research Center, Cleveland, Ohio

**Session A**

**SUMMARY OF SHUTTLE MICROGRAVITY  
ENVIRONMENT**

---

Chair: Melissa J. B. Rogers, National Center for Microgravity Research on Fluids and Combustion, Cleveland, Ohio

# **Review of Shuttle Microgravity Acceleration Data (Vibratory and Transient)**

---

Kenneth Hrovat, Tal-Cut Company, North Olmsted, Ohio

Richard DeLombard, NASA Lewis Research Center, Cleveland, Ohio

# **Review of Shuttle Microgravity Acceleration Data (Vibratory and Transient)**

Authors:

Kenneth Hrovat, Tal-Cut Company/NASA Lewis Research Center, Cleveland, Ohio

Richard DeLombard, NASA Lewis Research Center, Cleveland, Ohio

## **ABSTRACT**

Knowledge about the acceleration environment on the National Aeronautics and Space Administration's Space Shuttle plays an important role in conducting many microgravity science experiments. The Microgravity Measurement and Analysis Program at the Lewis Research Center measures and characterizes the acceleration environment of the Shuttle and other free-fall platforms. The Space Acceleration Measurement System has been the primary source of Shuttle vibratory and transient acceleration data. These data, along with those from other accelerometer systems, have been analyzed by the Principal Investigator Microgravity Services team in order to identify, qualify, and quantify the effects of various acceleration disturbances. This paper highlights and summarizes the results of these analyses.

## **INTRODUCTION**

The Microgravity Measurement and Analysis Program (MMAP) at the NASA Lewis Research Center measures and characterizes the acceleration environment of various free-fall platforms in support of microgravity science experiments. Accelerometer systems have been flown on the Shuttle, KC-135, Mir, and sounding rockets to measure the acceleration conditions during flight. Analyses are then conducted to gain an understanding of these accelerations as a function of both time and frequency in order to assist scientists with correlation (or lack of correlation) between the acceleration data and the results of their experiments.

## **ACCELERATION MEASUREMENTS**

Several different accelerometer systems have flown on the Shuttle, but the primary source of vibratory and transient acceleration data has been the Space Acceleration Measurement

System (SAMS). SAMS has supported twenty Shuttle missions since 1991. During this time, it has collected nearly 50 gigabytes of data in support of principal investigators (PIs) from various science disciplines including materials science, fluid physics, combustion science, biotechnology, and fundamental physics. SAMS has had the opportunity to measure the acceleration environment of various types of missions on a number of Shuttle carrier configurations as shown in these tables:

| SORTED BY CARRIER |         |
|-------------------|---------|
| CARRIER           | ACRONYM |
| Spacelab          | SLS-1   |
|                   | IML-1   |
|                   | USML-1  |
|                   | SL-J    |
|                   | IML-2   |
|                   | USML-2  |
|                   | LMS     |
|                   | MSL-1   |
|                   | USMP-1  |
|                   | USMP-2  |
|                   | USMP-3  |
|                   | USMP-4  |
| SPACEHAB          | SH-1    |
|                   | SH-2    |
|                   | SH-3    |
|                   | SH-5    |
|                   | SH-10   |
| Middeck           | STS-43  |
|                   | ATLAS-3 |

| SORTED BY DATE                 |        |         |  |
|--------------------------------|--------|---------|--|
| DATE                           | FLIGHT | ACRONYM | PAYLOAD  |
| June 5-14, 1991                | STS-40 | SLS-1   | 1st Spacelab Life Sciences                               |
| August 2-11, 1991              | STS-43 |         | TDRS deployment  |
| January 22-30, 1992            | STS-42 | IML-1   | 1st International Microgravity Laboratory                |
| June 25 - July 9, 1992         | STS-50 | USML-1  | 1st US Microgravity Laboratory                           |
| September 12-20, 1992          | STS-47 | SL-J    | Spacelab-J   |
| October 22 - November 1, 1992  | STS-52 | USMP-1  | 1st US Microgravity Payload                              |
| June 21 - July 1, 1993         | STS-57 | SH-1    | 1st SPACEHAB   |
| February 3-11, 1994            | STS-60 | SH-2    | 2nd SPACEHAB   |
| March 4-18, 1994               | STS-62 | USMP-2  | 2nd US Microgravity Payload                              |
| July 8-23, 1994                | STS-65 | IML-2   | 2nd International Microgravity Laboratory                |
| November 3-14, 1994            | STS-66 | ATLAS-3 | 3rd Atmospheric Laboratory for Applications and Sciences |
| February 3-11, 1995            | STS-63 | SH-3    | 3rd SPACEHAB, Mir Rendezvous                             |
| October 20 - November 5, 1995  | STS-73 | USML-2  | 2nd US Microgravity Laboratory                           |
| February 22 - March 9, 1996    | STS-75 | USMP-3  | 3rd US Microgravity Payload                              |
| June 20 - July 7, 1996         | STS-78 | LMS     | Life and Microgravity Spacelab                           |
| September 16-26, 1996          | STS-79 | SH-5    | 5th SPACEHAB, 4th Mir docking                            |
| April 4-8, 1997                | STS-83 | MSL-1   | 1st Microgravity Sciences Laboratory                     |
| July 1-17, 1997                | STS-94 | MSL-1   | 1st Microgravity Sciences Laboratory Reflight            |
| November 19 - December 5, 1997 | STS-87 | USMP-4  | 4th US Microgravity Payload                              |
| January 22-31, 1998            | STS-89 | SH-10   | 10th SPACEHAB, 8th Mir docking                           |

## DATA ANALYSIS

In the area of acceleration data analysis, the Principal Investigator Microgravity Services (PIMS) team at the NASA Lewis Research Center has continued the work initiated by the Acceleration Characterization and Analysis Project (ACAP). PIMS has analyzed data from a variety of sources, including SAMS, the Orbital Acceleration Research Experiment (OARE),

and the Microgravity Measurement Assembly (MMA). As a result, PIMS has characterized the microgravity environment of the Shuttle, which includes the effects of vehicle subsystems, crew activity, and experiment-related equipment.

The logistics of maintaining the Shuttle in a controlled free-fall and numerous other housekeeping issues dictate that vehicle-related activities and equipment are a necessity and their impact on the microgravity environment of the vehicle must be accounted for. One such class of vehicle systems is the Orbiter's attitude adjustment and maintenance subsystems. In order to compensate for orbital dynamics and accommodate various attitude requirements, the Shuttle employs one of three systems: the Orbital Maneuvering System (OMS), the Primary Reaction Control System (PRCS), or the Vernier Reaction Control System (VRCS). The OMS is used for major on-orbit velocity changes and therefore, rarely used. Its effects consist of an initial transient, which can be in excess of 50 mg and net accelerations on the order of 20 mg lasting as long as 40 seconds as seen in Figure 1. This disturbance is primarily aligned with the Orbiter structural X-axis owing to the fact that the OMS engines are directed out the Orbiter's tail. The PRCS and VRCS are used for attitude adjustment and maintenance. Thruster firings from these systems are considered transient disturbances typically lasting for a fraction a second, although, they can last longer. For the PRCS, peak accelerations are on the order of tens of mg. A series of PRCS firings are shown in the top plot of Figure 2, and a longer duration firing (greater than 10 seconds) is shown in the bottom plot of Figure 2. These PRCS thrusters are not used nearly as often as those of the VRCS. Peak accelerations for VRCS firings are on the order of tenths of mg, and usually last for less than a tenth of a second (see Figure 3). Another common Orbiter subsystem is the Ku-band antenna, which is located on the forward bulkhead (starboard side) of the Orbiter's cargo bay. Throughout a mission, the antenna is dithered nearly continuously at 17 Hz to prevent mechanical stiction as it slews to track communications satellites. This nearly incessant dithering produces a relatively intense oscillatory disturbance at 17 Hz, which is seen as the red horizontal streak in the spectrogram of Figure 4; harmonic components, particularly the 2<sup>nd</sup> and 3<sup>rd</sup> harmonics are usually also prominent. Calculations show that the root-mean-square (RMS) acceleration level in the 16.93 to 17.13 Hz band vary from tens of  $\mu\text{g}_{\text{RMS}}$  to a couple hundred  $\mu\text{g}_{\text{RMS}}$ , with a nominal level on the order of 100  $\mu\text{g}_{\text{RMS}}$ . Less prevalent, yet equally important for vehicle maintenance, are disturbances introduced by the Orbiter's hydraulic systems. These serve as the driving force for actuators on control surfaces, engine gimbals, valves, and so on. On orbit, hydraulic fluid is circulated periodically by motor-driven pumps for heat distribution. Pump motors operate at 10,000 rpm (166.7 Hz), but the only noticeable impact has been the turn-on transient (at about the 22-second mark of Figure 5) with an acceleration vector magnitude on the order of 1 mg.

One final vehicle subsystem considered here is the Active Thermal Control System. Radiator panels on the forward payload doors are part of this system and are deployed by motor-driven latches when needed for heat rejection during a mission. Transient peak accelerations on the order of 0.3 mg have been observed when these are deployed; one such occurrence is shown at about the 80-second mark of Figure 6. Successful Shuttle missions rely not only on a healthy vehicle, but on a healthy and well-prepared crew as well.

In general, the crew is mindful of their actions and potential impacts on the microgravity environment. However, on occasion (normally out of necessity) they impart disturbances to the acceleration environment. For health reasons, one such necessity is physical exercise. As seen in the frequency domain, crew exercise imparts fundamental twin peak disturbances, both of which are usually below 4 Hz. These traces are seen in the spectrogram of Figure 7; the pedaling signature is the orange-red horizontal trace in the 2 to 2.5 Hz range, and the shoulder-sway signature is the yellowish horizontal trace at approximately half of the pedaling frequency. Exercise also tends to excite structural modes below 10 Hz. Considerable intensity variations have been observed during crew exercise. This intensity variation is primarily a function of crewmember. A typical RMS acceleration increase from the twin peak fundamental disturbances is usually on the order of  $10^{-4}$  to  $10^{-3}$   $g_{RMS}$ . In addition to exercise, in-flight maintenance or corrective actions may be required of the crew. For example, during IML-2, experiment operations required a crewmember to essentially serve as a human centrifuge by swinging a bag of liquid around for mixing. Post-mission correlation of Spacelab module video and the acceleration data recorded during this activity showed this event quite clearly; 8 arm revolutions are seen in the X-axis (top) plot of Figure 8. While disturbances introduced by the crew may last for half an hour at a time, experiment-related disturbances can last for tens of hours at a time.

Were it not for space science experiments, the Microgravity Measurements Group would most likely not exist. These experiments typically require experiment apparatus to conduct or support the experiment. Consequently, experiment-related equipment disturbances, such as those caused by refrigerator/freezers (R/Fs), fans, pumps, centrifuges, and the like must be considered. Examples of experiment-related R/Fs are the Stirling Orbiter R/F (SOR/F), the Life Sciences Laboratory Equipment R/F (LSLE), and the Enhanced Orbiter R/F (EOR/F). The compressors of these R/Fs have been the source of strong oscillatory disturbances. For example, during the IML-2 mission, the LSLE compressor operated with a fundamental frequency around 22 Hz, and imparted a RMS acceleration of about 400  $\mu g_{RMS}$  while it was on. It was operational for nearly the duration of the mission with a duty cycle of 9 to 13 minutes on, and 16 to 25 minutes off. The spectrogram of Figure 9 shows the almost regularly spaced

signature of this disturbance. An extremely strong disturbance during the SPACEHAB-2 mission was the SOR/F. Its fundamental frequency was close to 60 Hz, and it imposed a RMS acceleration in 59.9-60 Hz range in excess of  $2 \text{ mg}_{\text{RMS}}$ . The power spectral density of Figure 10 shows this as the strongest disturbance registered despite the 50 Hz cutoff frequency of the sensor head. Another piece of experiment equipment that has been measured to impart a substantial oscillatory disturbance (4 to  $5 \text{ mg}_{\text{RMS}}$ ) was the TEMPUS water pump, which flew on the IML-2 mission. The rotational rate of this pump was 4800 rpm (80 Hz), and it operated for a duration ranging from 10 minutes to over 7 hours. The spectral signature of the water pump is seen as the horizontal red streak at about 80 Hz between about MET 001/02:38 and 001/03:22 of Figure 9. Somewhat less invasive than the TEMPUS water pump on IML-2, was the Combustion Module (CM-1) gas chromatograph vacuum pump flown on MSL-1. Its disturbance was comprised of two oscillatory components at about 46 and 55 Hz (see Figure 11). Its duration was about 4 minutes at a time, with a RMS acceleration level of approximately  $250 \mu\text{g}_{\text{RMS}}$  for the primary disturbance in the 44 to 49 Hz range (see Figure 12). A final experiment-related equipment disturbance to note was the JSC projects centrifuge flown on LMS. The centrifuge had a rotational rate of about 2400 rpm (40 Hz), with related disturbances at about 16 and 24 Hz (see spectrogram of Figure 13). Each centrifugation lasted about 15 minutes, and the RMS acceleration level in the 39 to 40.7 Hz range increased by nearly an order of magnitude from around  $40 \mu\text{g}_{\text{RMS}}$  when it was off to nearly  $500 \mu\text{g}_{\text{RMS}}$  when it was on. For further details regarding these and other microgravity disturbances, refer to the Microgravity Environment Description Handbook, which may be viewed on the World Wide Web from:

<http://www.lerc.nasa.gov/WWW/MMAP/PIMS/HTMLS/Micro-descpt.html>

## OVERALL MISSION CHARACTERISTICS

### **Principal component spectral analysis examination of mission environment**

On a mission-length basis, the mission microgravity environment is affected by several major factors. The specific payload equipment on-board, crew activities, Shuttle maneuvers, and Shuttle subsystems all contribute a significant amount of disturbance to the overall microgravity environment, as stated earlier. Many of these factors are controllable by mission design and crew awareness. For example, during the mission design process, experiments that are sensitive to frequencies related to crew exercise may be scheduled at times other than scheduled crew exercise periods. Another example is the assignment of Shuttle attitudes to meet the needs of the experiments to minimize the effects of thruster firings and attitude

changes. On the other hand, it is difficult to schedule experiment operations away from the disturbance of a R/F compressor which operates every ten minutes or so during the mission. As covered earlier, the disturbance levels of a refrigerator are significant throughout the mission.

By comparing the microgravity environments of the LMS and USML-1 missions as shown in the principal component spectral analysis (PCSA) plots of Figures 15 and 16, respectively, the absence of the LSLE R/F is apparent by the absence of the major disturbance around 22-23 Hz.

The attitudes assigned for microgravity missions have been, in general, in response to the payload's requirements. Typically for microgravity missions, a stable Earth-oriented attitude has usually been used. Refining the attitude to a gravity-gradient stabilized attitude, which has been trimmed to balance aerodynamic forces results in an attitude with relatively few thruster firings. On some microgravity missions, this has resulted in thrusters being intentionally fired to maintain their temperatures above a threshold value.

The STS-78 mission with the LMS payload had a single shift crew which meant that all seven crew members were on the same daily wake/sleep cycle. This mode of operation on the Orbiter produced two distinct microgravity environment characteristics. During the crew active time, equipment operation and crew motion contributed toward higher acceleration levels as compared with times for which the crew members were resting and sleeping. Crew active periods contributed to the higher magnitude disturbances seen in the LMS PCSA (Figure 15) between  $10^{-7}$  and  $10^{-6}$   $g^2/Hz$  from about 8 to 21 Hz. Similarly, crew rest periods (reduced equipment operation and lack of crew motion) contribute to the lower microgravity levels between  $10^{-9}$  and  $10^{-7}$   $g^2/Hz$  in the same frequency band.

The two large "humps" in the STS-78 PCSA plot at around 22 and 23 Hz were caused by the two LSLE R/Fs located in rack 9 of the Spacelab module. These R/Fs operate with a motorized compressor/evaporator and the rotational speed and operating duty cycle vary according to the load and power supply characteristics. This produces a vibration that varies in both magnitude and frequency, so the PCSA signature is not a tightly controlled frequency trace. For these two R/Fs, the vibrations produced by the motor/compressors was slightly different and they cycled on and off at regular but independent intervals during the course of the mission. Thus, there are times when the environment around 22 and 23 Hz is not dominated by the vibrations from one or both of these R/Fs. This results in histogram "hits" below the  $10^{-5}$   $g^2/Hz$  level in that frequency range, as opposed to the white area at 17 Hz from the nearly constant dither of the Ku-band antenna.

The STS-78 mission had equipment which, when operated, produced vibrations at tightly controlled frequencies at just under 16 Hz and around 24 Hz. The cause for this disturbance

was the JSC centrifuge, as stated earlier. When on, it produced vibrations at the SAMS sensor head location at a level of  $10^{-5}$  g<sup>2</sup>/Hz, as evidenced by the short red vertical lines near 16 and 24 Hz in Figure 15.

The primary payload on the STS-50 mission was the first U.S. Microgravity Laboratory (USML-1). This mission had a dual crew shift throughout the mission. The PCSA plot for this mission (Figure 16) exhibits a single level as opposed to the two levels seen on a single crew shift mission, such as STS-78 (Figure 15). This is indicative of the two crew shifts, thus keeping activity at similar levels throughout the mission. A LSLE R/F was not flown on this mission, and the data do not show the peaks at about 22 Hz, which are normally caused by this equipment.

One of the primary payloads on the STS-62 mission was the second U.S. Microgravity Payload (USMP-2). A PCSA plot for the USMP-2 payload microgravity time on the STS-62 mission is shown in Figure 17. This mission had a single crew shift and the PCSA plot exhibits the two basic magnitude levels between 10 Hz and 15 Hz associated with crew active and crew quiet time periods. This is similar to the characteristics described above for the STS-78 mission.

The faint "clusters" of points in the 1.25 Hz and 2.5 Hz region with magnitudes between  $10^{-7}$  and  $10^{-5}$  g<sup>2</sup>/Hz appear to be due to crew exercise on an ergometer. The two frequencies arise from the crew members' body motions and pedaling rates. This activity occurs on a daily basis for each crew member throughout the mission.

Two missions with Spacelab MPESSE carriers but with different crew activity schedules (USMP-2 with a single crew shift and USMP-3 with a dual crew shift) may be compared by examining Figures 17 and 18, respectively. It is interesting to note that the predominant levels for USMP-3 are comparable to the crew rest times of USMP-2. This seems to corroborate that the crew of USMP-3 were consciously attempting to work quietly during the microgravity experimentation period. When discussing the use of the acceleration data display for the STS-75 crew, Franklin Chang-Diaz, the Payload Commander, said

"The application was easy to use and useful for crew feedback. It influenced our activities greatly and made us much more aware of the potential crew-induced disturbances. It is a great on-orbit training tool for crews to develop an efficient low-g way of doing things. It also shows that we can do effective work without interfering with micro-g operations..." This appears to hold promise as a valuable microgravity level reduction technique.

### **One-third octave histogram examination of mission environment**

The ISS microgravity requirement specifies the levels in the vibratory regime by means of a root-mean-square level for one-third octave intervals in the frequency range from 0.01 Hz to

300 Hz. A procedure is being developed to process acceleration data to directly compare the measured environment against the ISS requirement levels. SAMS data from selected times in some microgravity missions have been processed in this one-third octave histogram procedure. The steps in this procedure create a time-based histogram of the root-mean-square levels in each one-third octave frequency interval. The time interval involved is approximately 2 minutes, which gives the closest integer power of 2 number of points to the 100 second interval specified in the ISS microgravity requirement.

The one-third octave histogram plot from a SAMS 25 Hz sensor head on the STS-78 mission is Figure 19. The ISS requirement levels are shown by the bold stepped lines from the lower left to upper right in the plot.

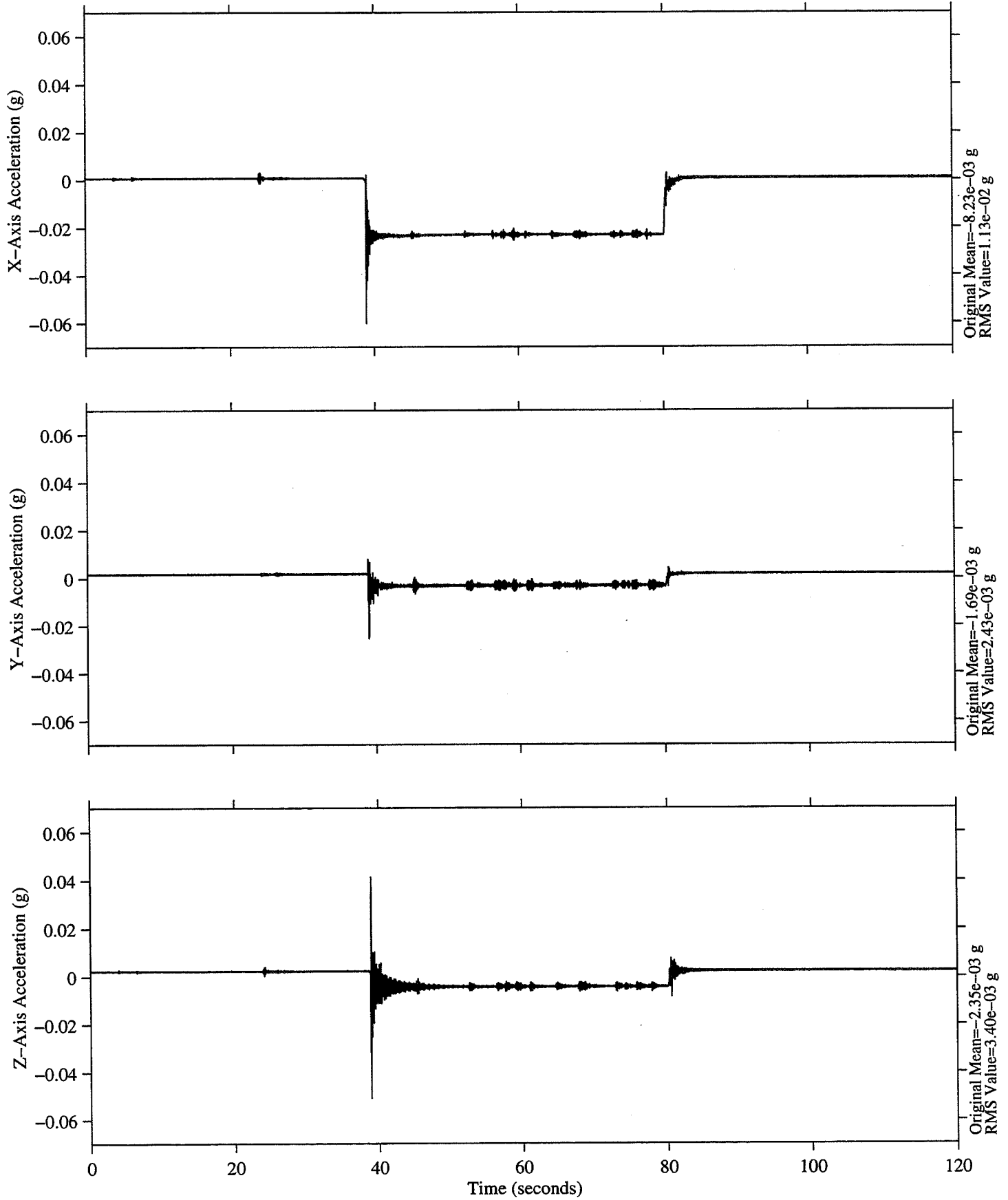
The Shuttle microgravity levels are generally above the ISS requirement level for frequencies below about 0.5 Hz. The Shuttle levels are generally below the ISS requirement level for frequencies above about 0.5 Hz. As seen previously with the PCSA plots, the levels for the crew active shift are higher than the crew sleep shift with the single shift crew on this mission.

For some disturbance sources on the Shuttle, the levels do exceed the levels of the ISS microgravity requirement. The R/F on the STS-78 mission caused the levels in the 20 Hz frequency range to exceed the ISS requirement level.

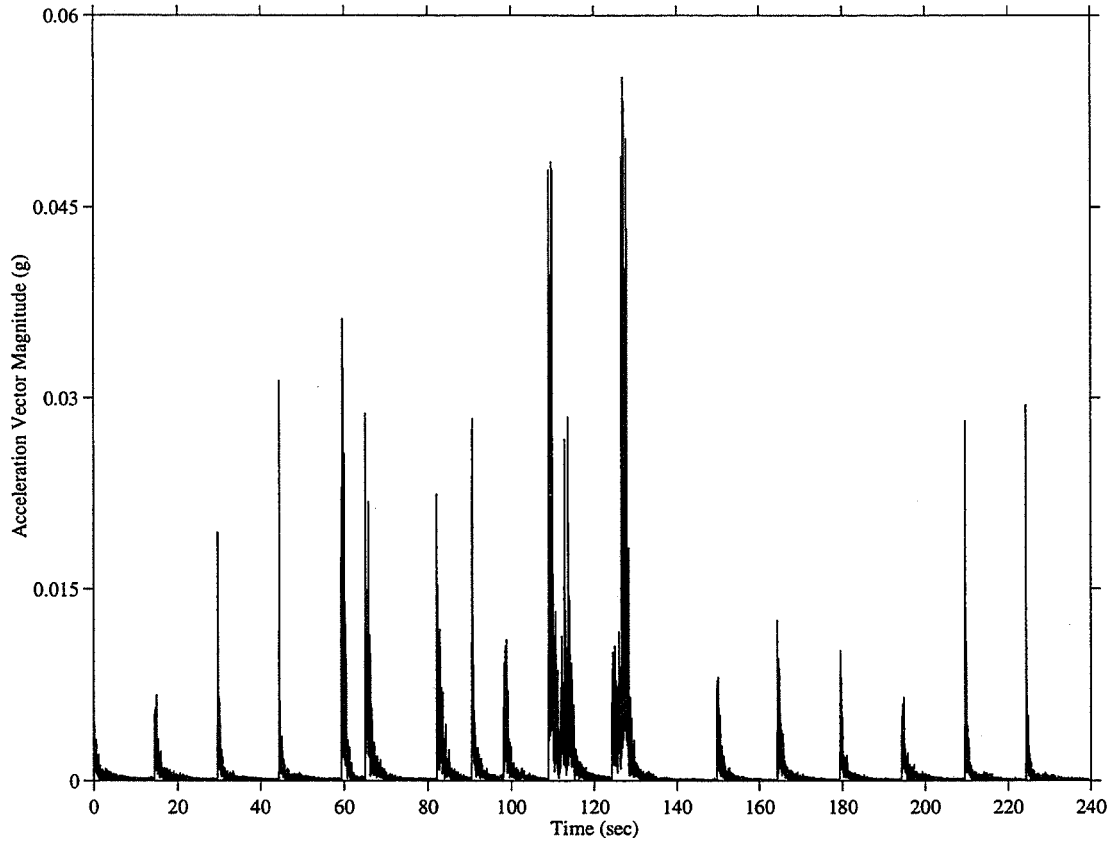
In the one-third octave histogram plot for the STS-65 mission (Figure 20), the TEMPUS water pump generated a high level at 80 Hz during much of the mission. This can be seen to exceed the ISS requirement for that one-third octave.

## SUMMARY

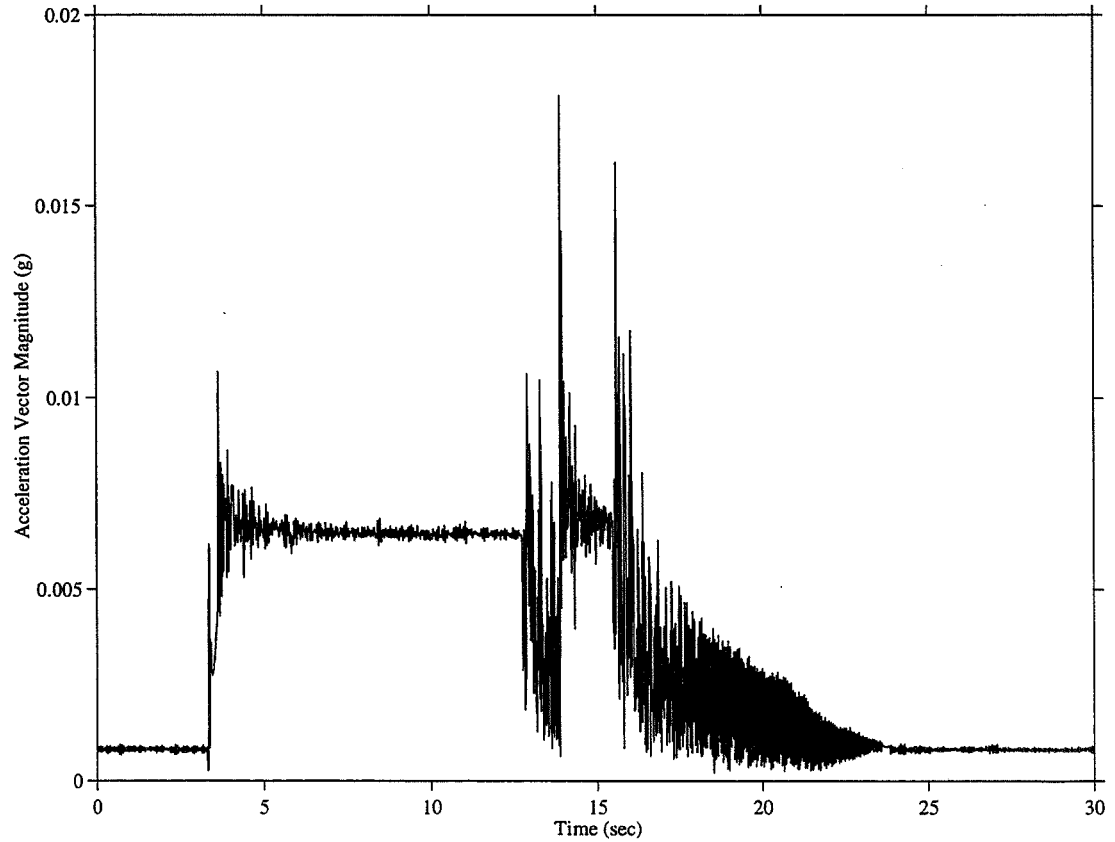
The Microgravity Measurement and Analysis Program, which is sponsored by the Microgravity Research Division has served to measure and characterize the acceleration environment of the Shuttle and other free-fall platforms. Analysis of the acceleration data shows that the vibratory environment of the Shuttle is primarily shaped by oscillatory disturbances originating from vehicle subsystems, crew activity, and experiment-related equipment. Transient disturbances, principally those arising from thruster firings, also play a key role in defining the acceleration environment.



2



MATLAB 4-Mar-97, 07:54 am

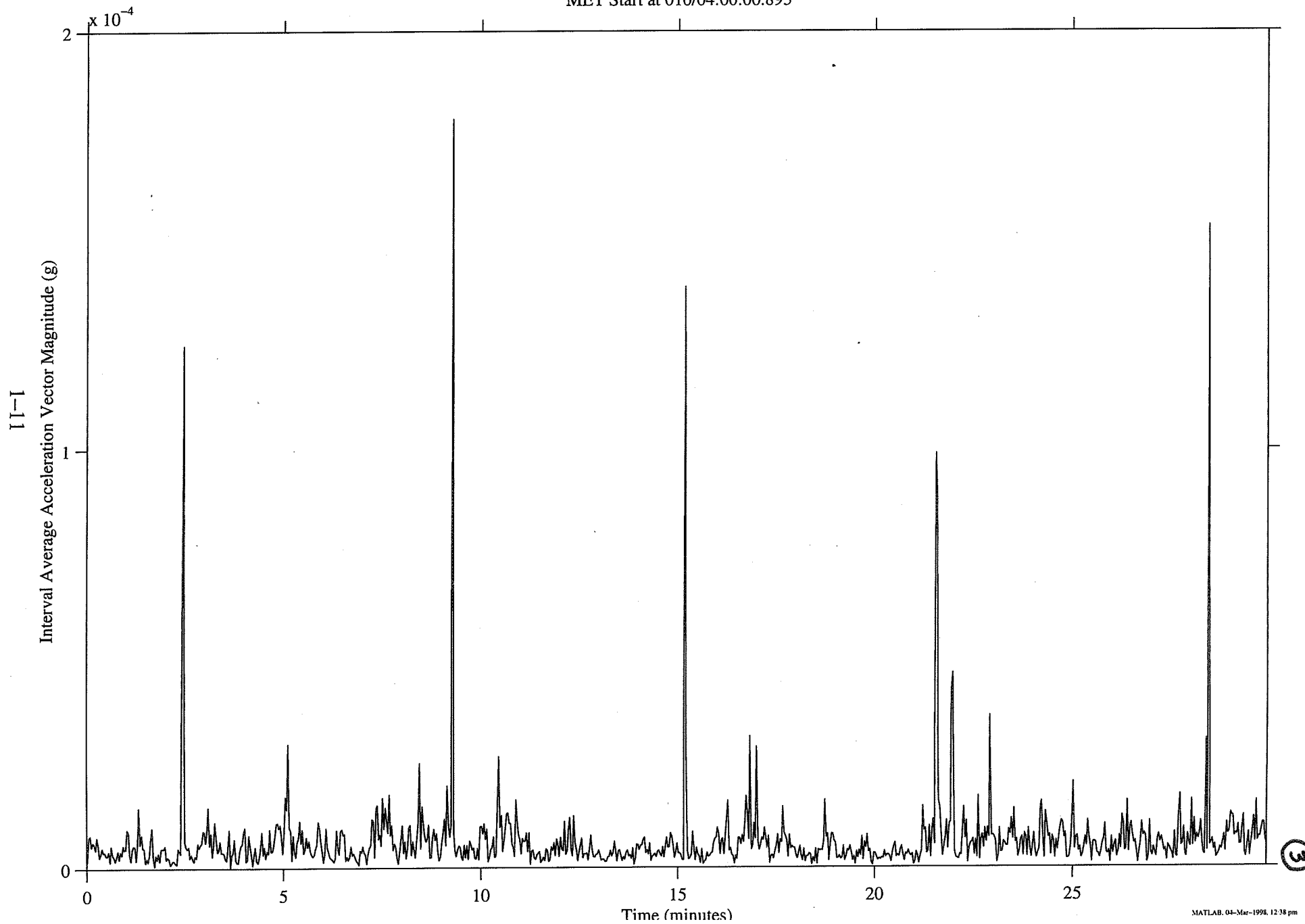


MATLAB 4-Mar-97, 07:54 am

Head B, 25.0 Hz  
fs=125.0 samples per second  
Interval=2.00 seconds

USMP-3F  
Structural Coordinates  
T=30.0 minutes

VRCS Firings (F5L and F5R)  
MET Start at 010/04:00:00.895

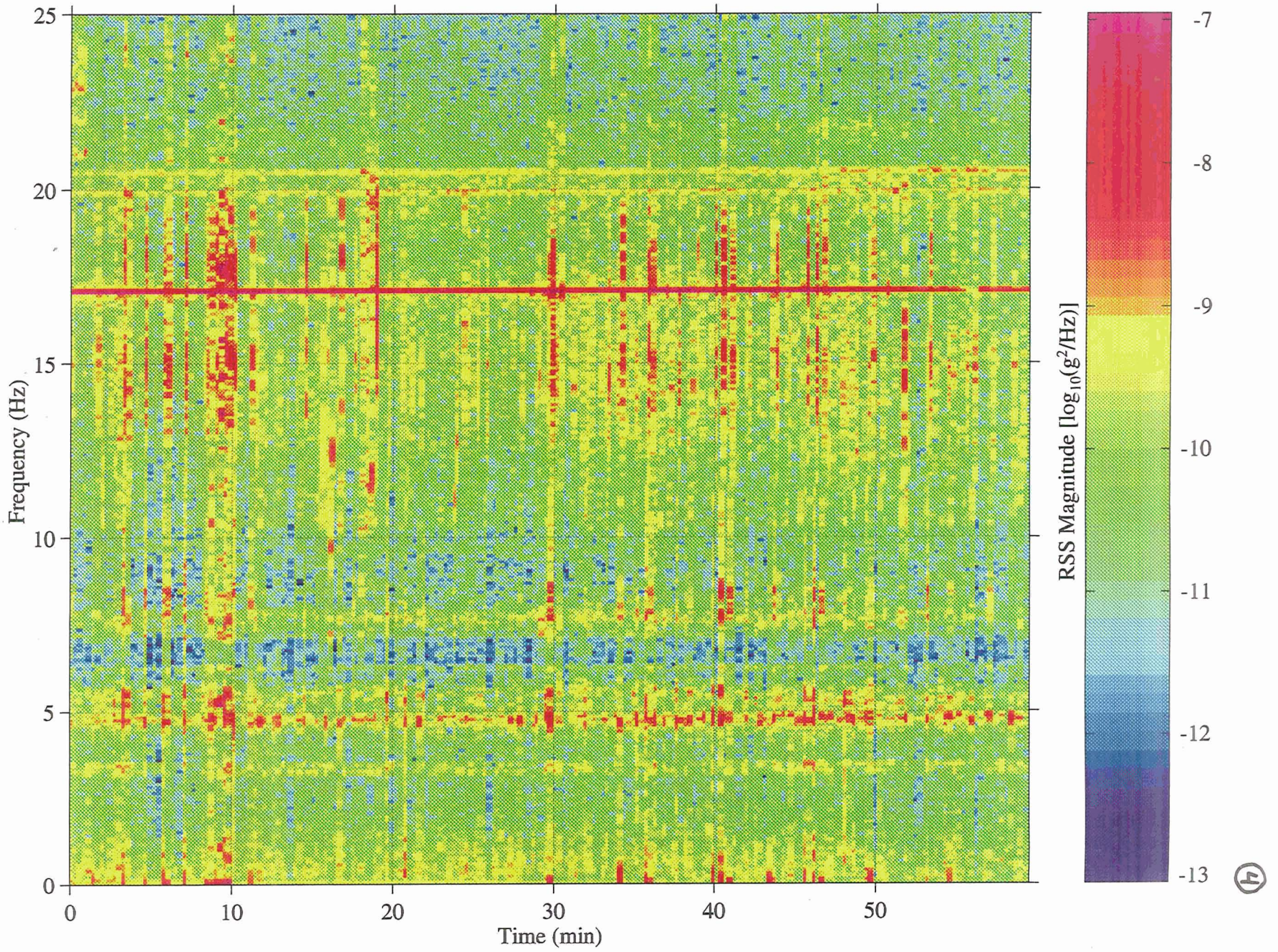


Head B, 25.0 Hz  
fs = 125.0 samples per second  
ΔF = 0.0610 Hz  
ΔT = 0.2731 min

MET Start at 011/21:00:00.321, Hanning k= 219  
MEDS: Ku-Band Antenna Dither (MPRESS Measurement)

USMP-2F  
Structural Coordinates

1-12



Head A, 10.0 Hz

fs= 50.0 samples per second

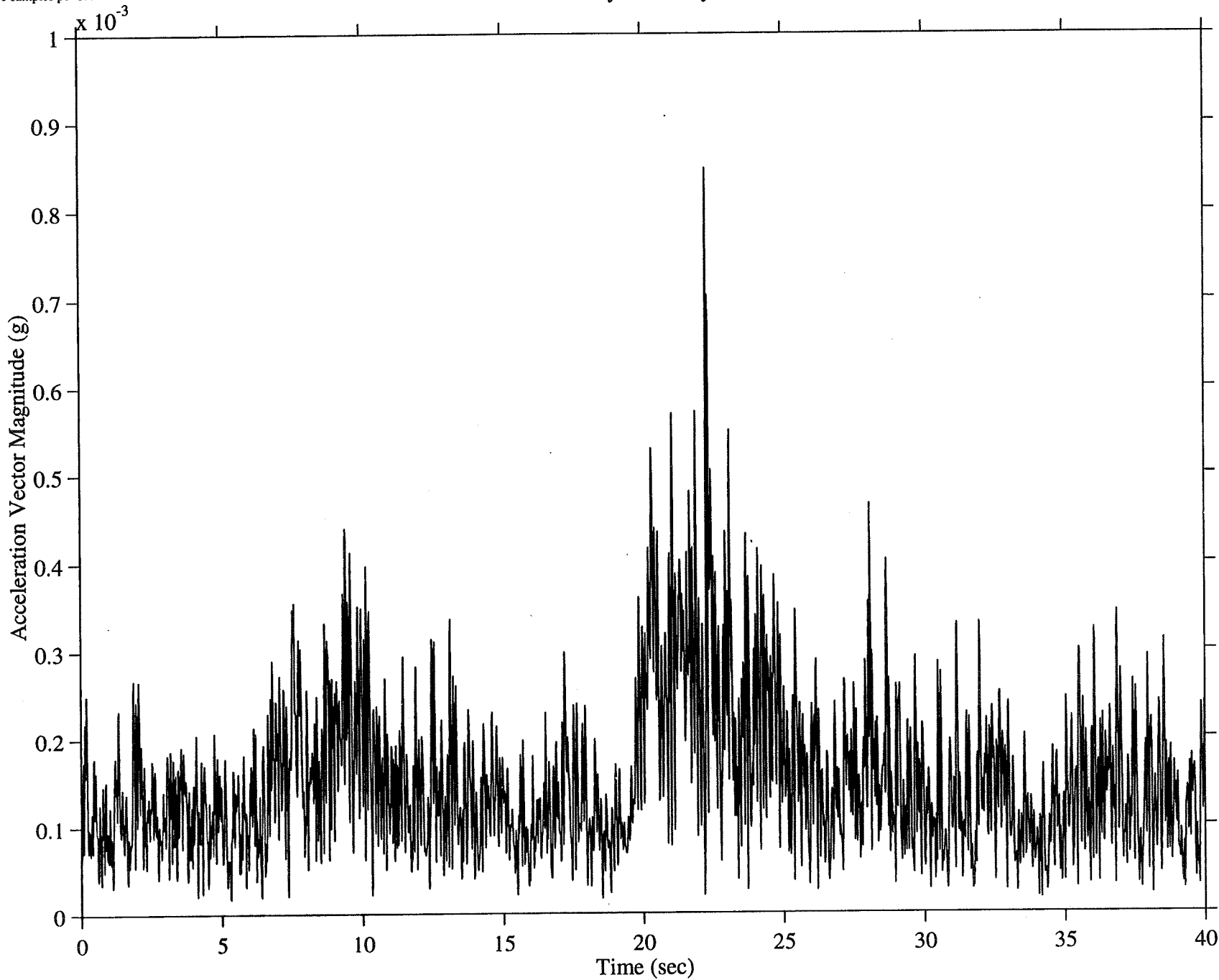
MET Start at 001/07:34:51.989

MEDS: Hydraulic System

IML-2

Structural Coordinates

I-13



5

Head A, 10.0 Hz

fs= 50.0 samples per second

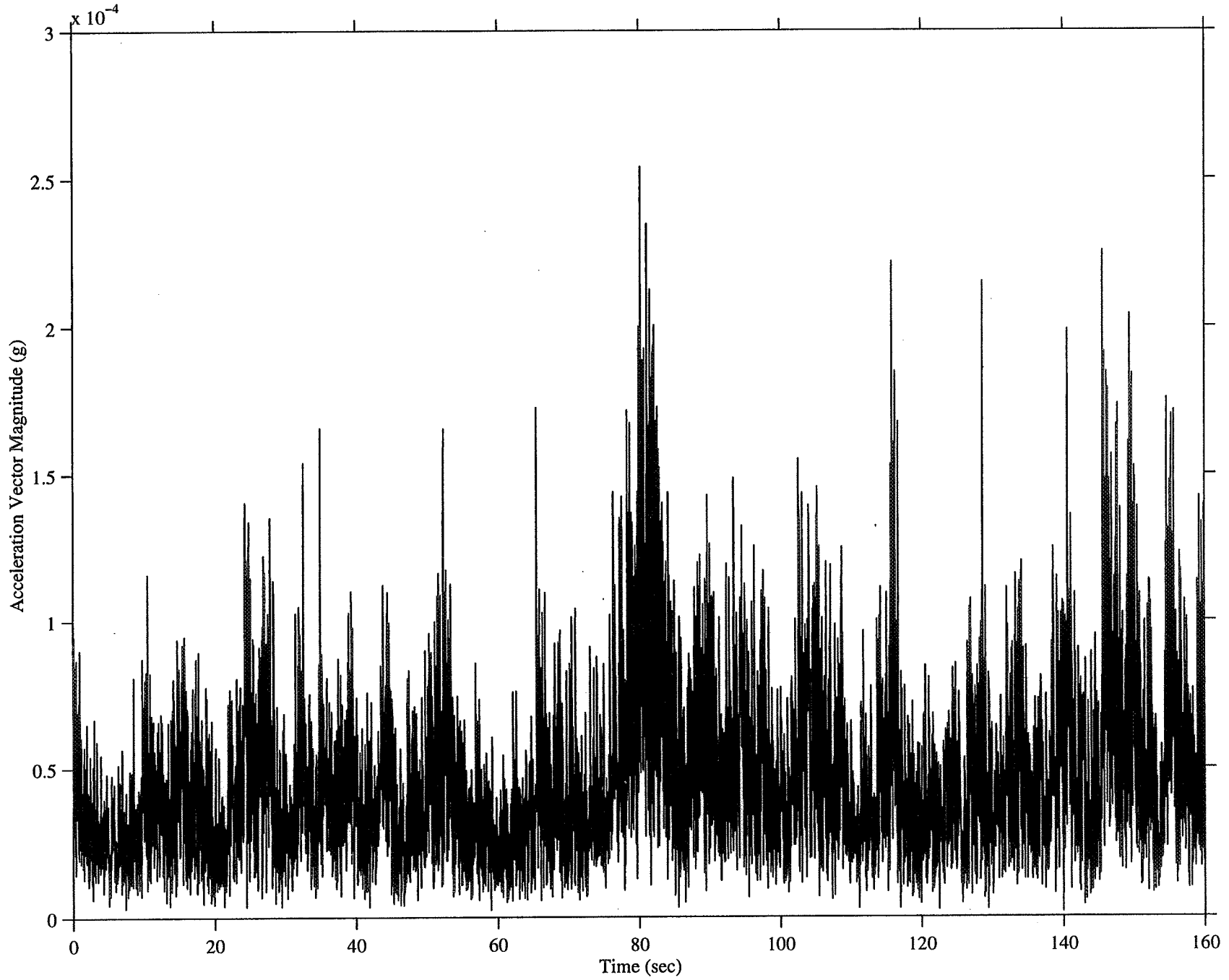
MET Start at 000/03:09:59.999

USMP-2F

Radiator Panel Deploy

Structural Coordinates

1-14

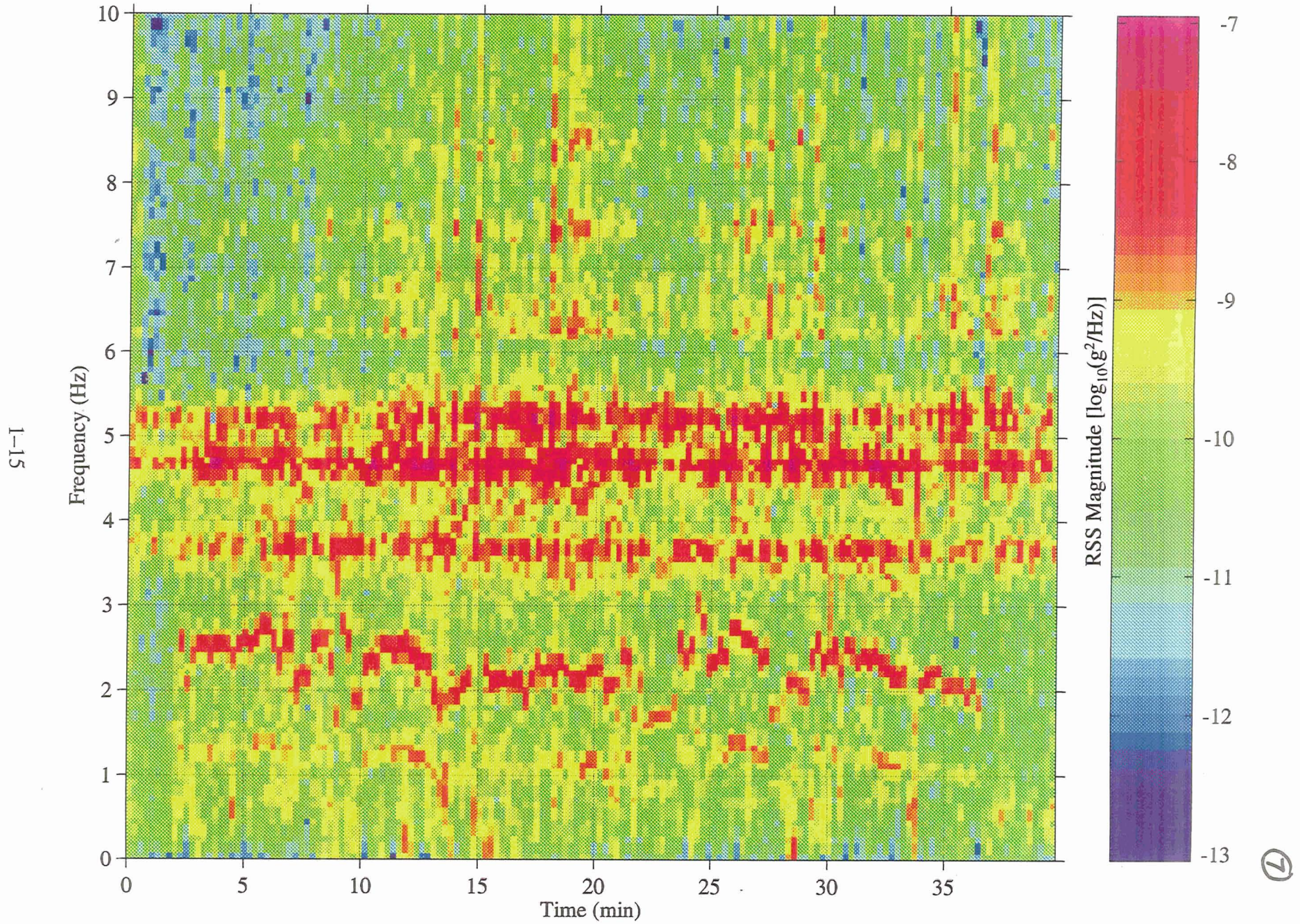


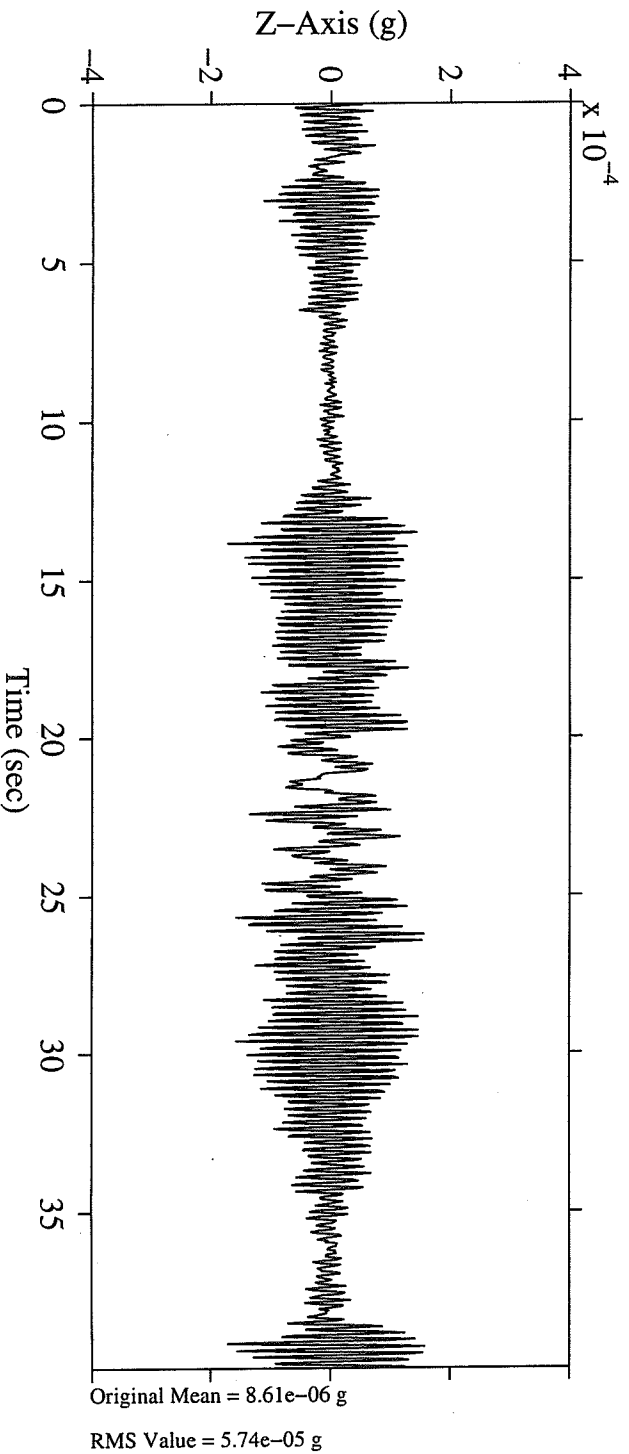
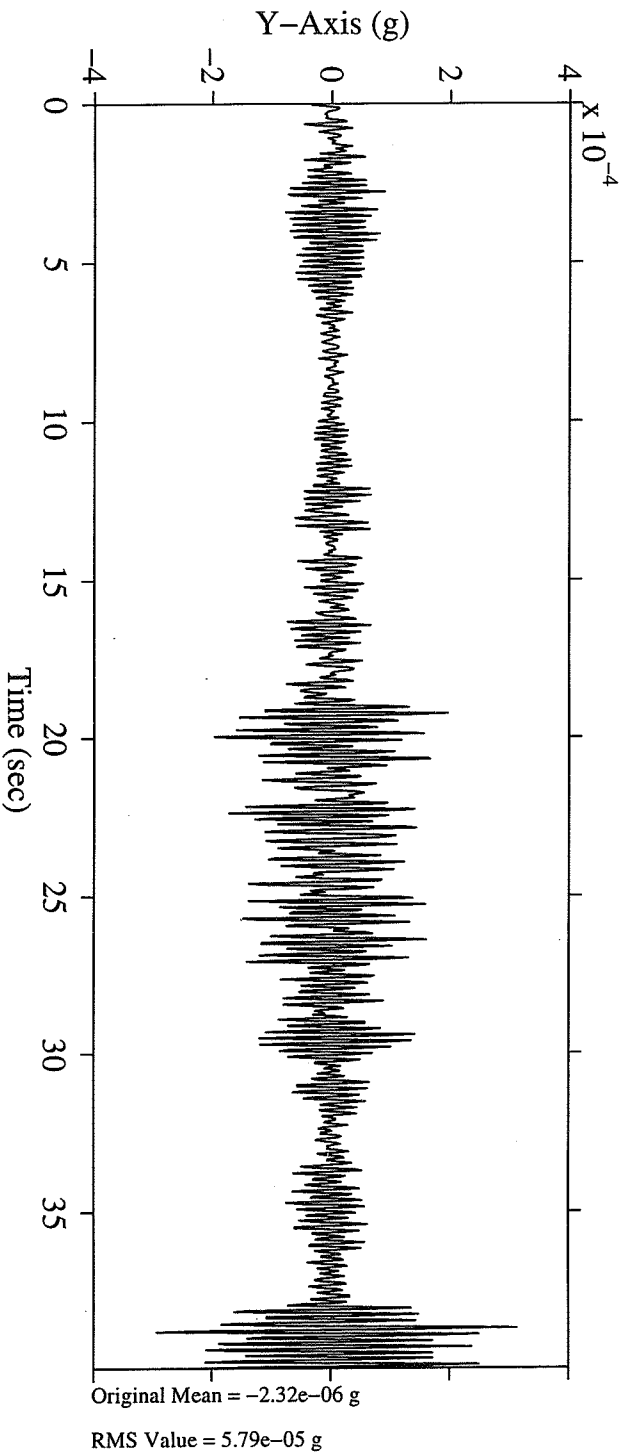
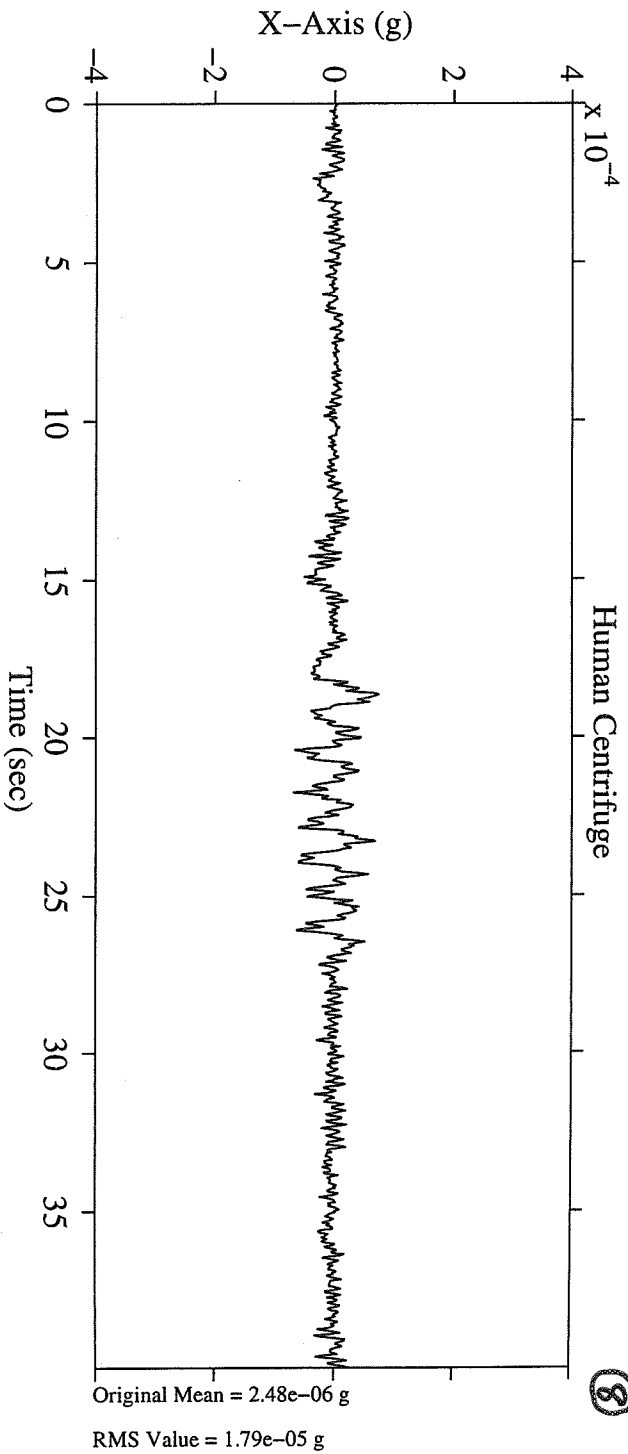
9

Head A, 10.0 Hz  
fs = 50.0 samples per second  
df = 0.0977 Hz  
dT = 0.1707 min

MET Start at 002/05:19:59.995, Hanning k= 234  
MEDS: Ergometer Exercise

IML-2  
Structural Coordinates

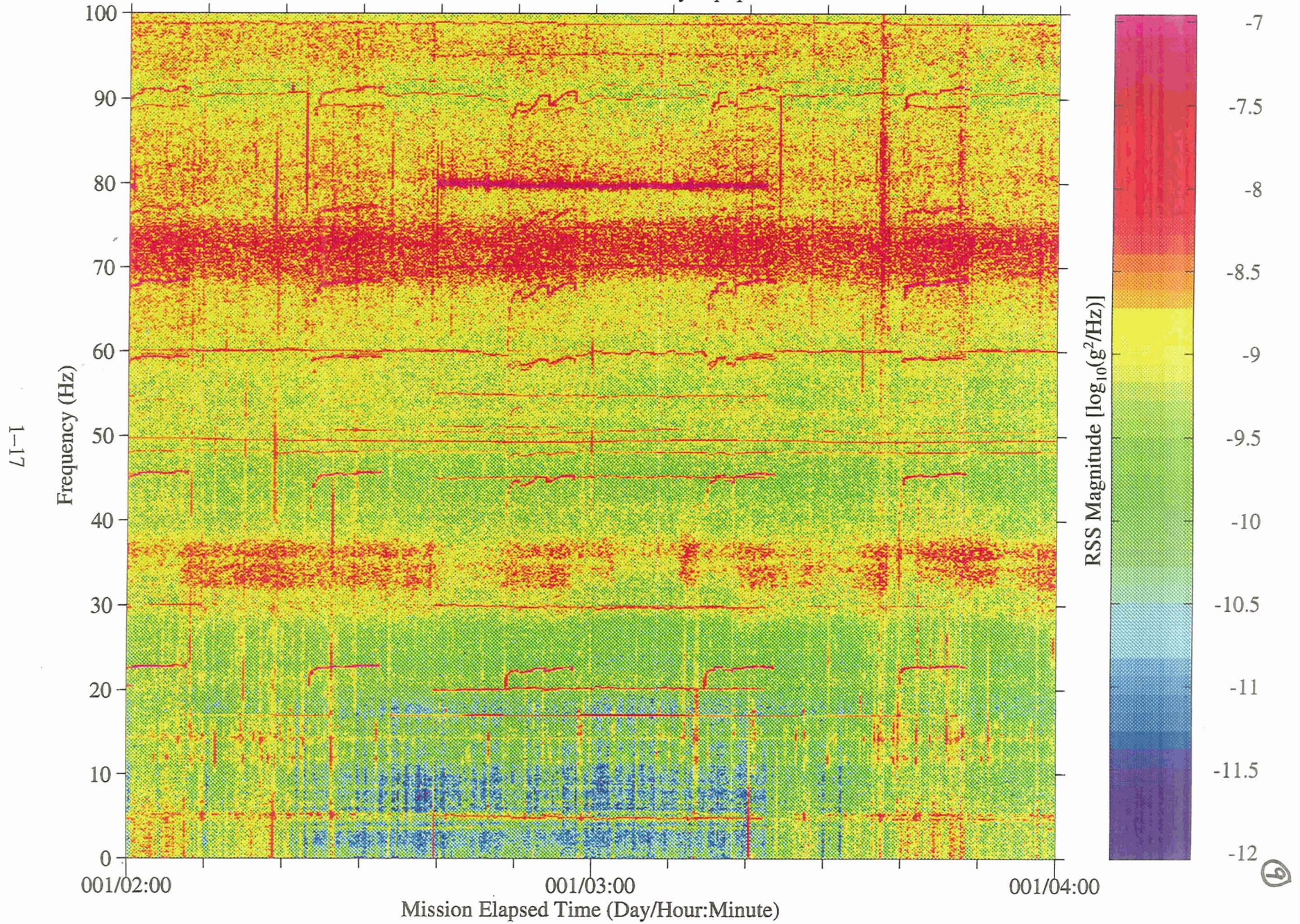




Head C, 100.0 Hz  
fs = 500.0 samples per second  
ΔF = 0.0610 Hz  
ΔT = 16.3840 sec

### MEDS: Life Science Laboratory Equipment

IML-2  
Structural Coordinates



Head B, 50.0 Hz

fs= 250.0 samples per second

dF= 0.06104 Hz

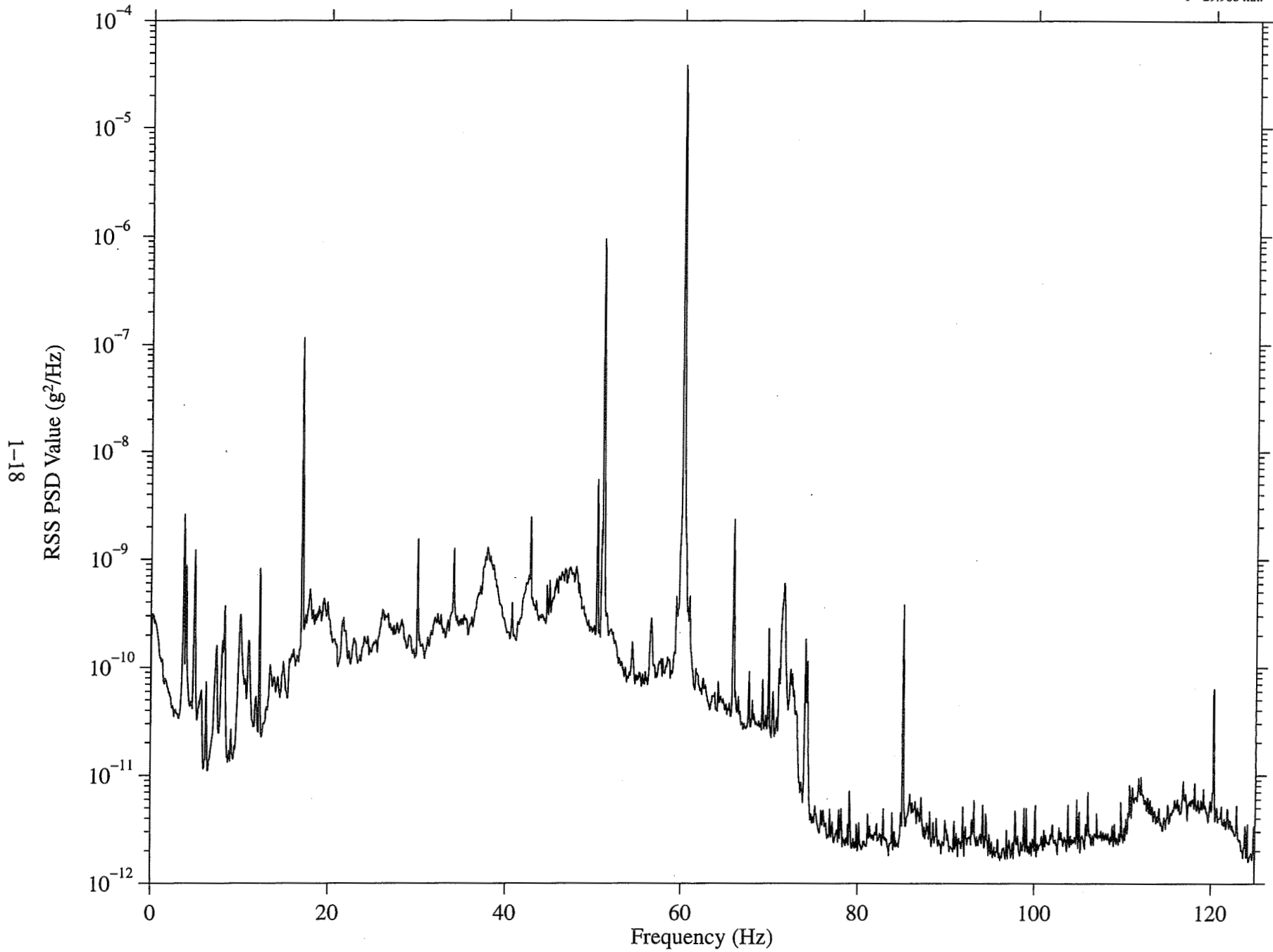
MET Start at 002/13:00:00.747, Hanning k=109

Stirling Orbiter Refrigerator/Freezer

SPACEHAB-2

Structural Coordinates

T= 29.988 min

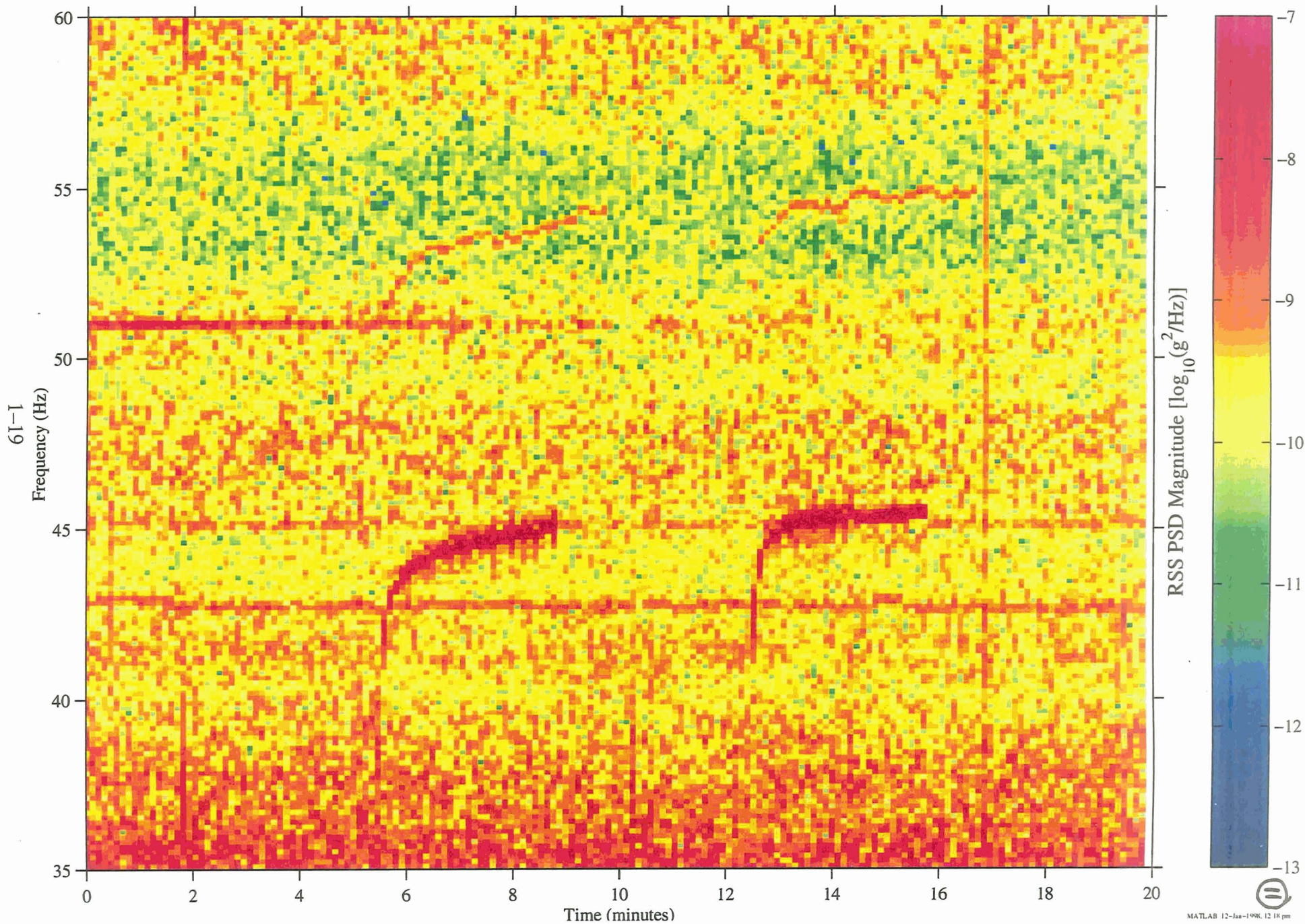


10

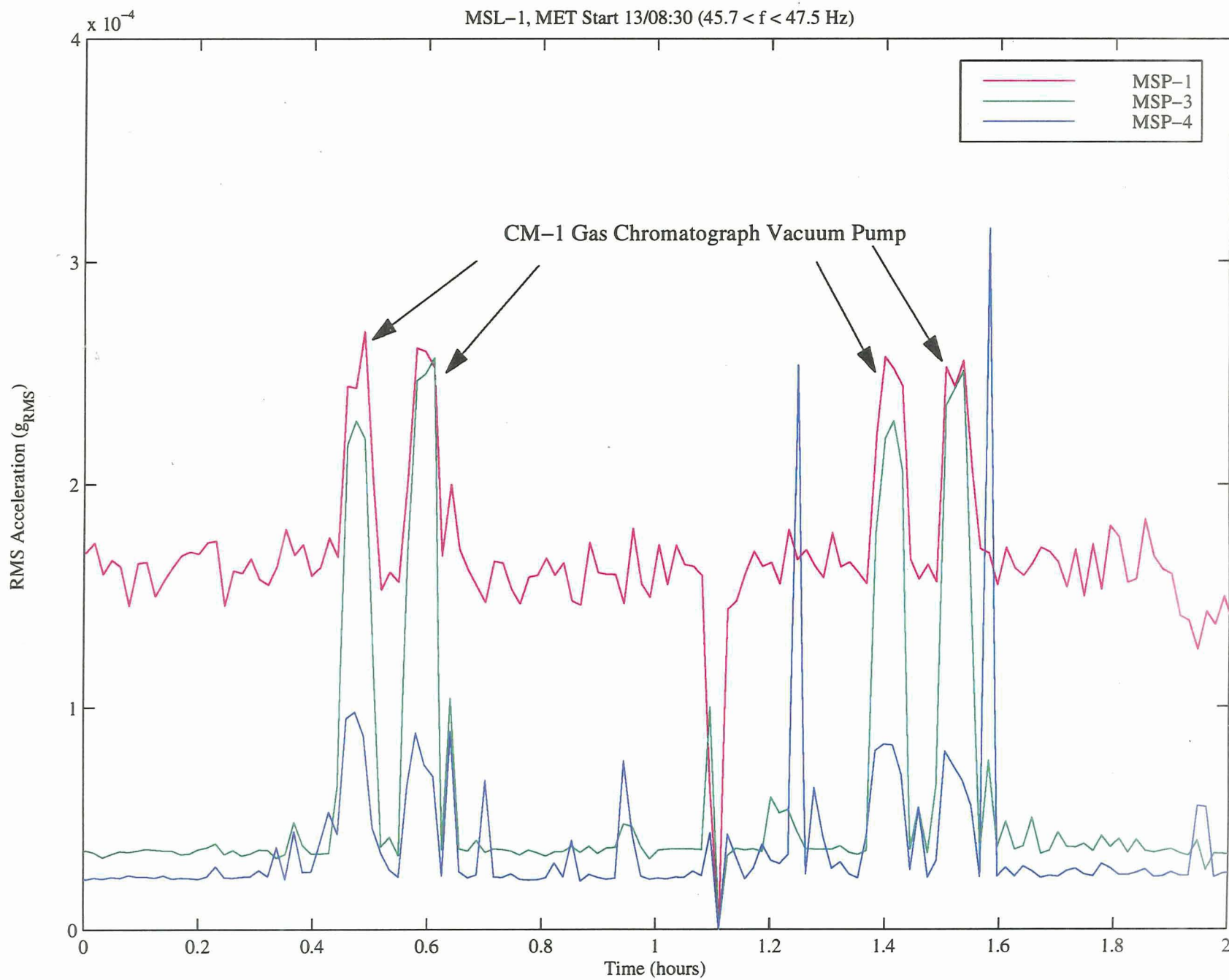
Head MSP3, 100 Hz  
fs=300.0 samples per second  
dF=0.1465 Hz  
dT=6.8267 seconds

STS-94  
MSP Coordinates  
20.0 minutes

### Gas Chromatograph Vacuum Pump MET Start at 006/20:36:00.000 (Hanning, k=175)

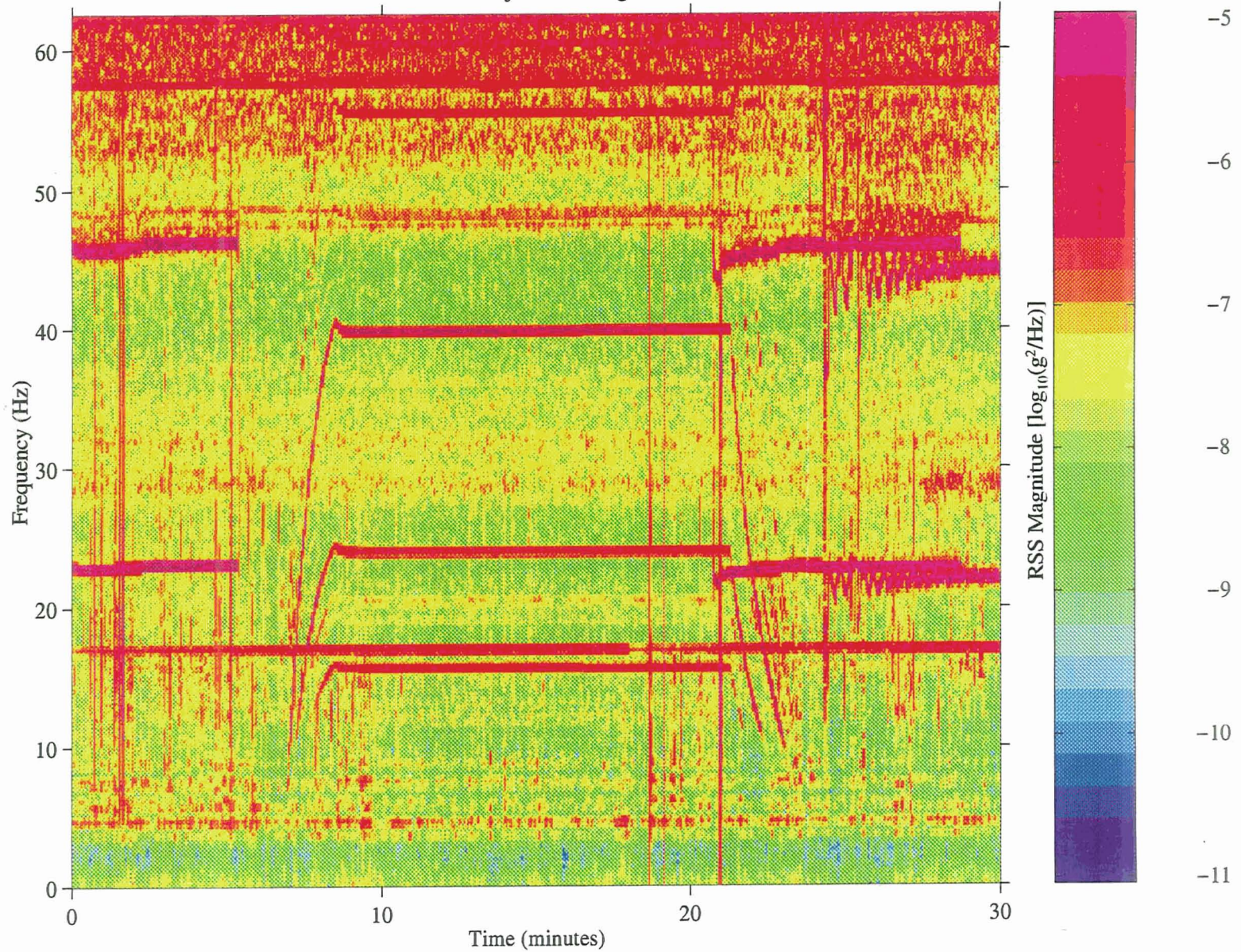


1-20



MET Start at 006/18:50:00

JSC Project Centrifuge



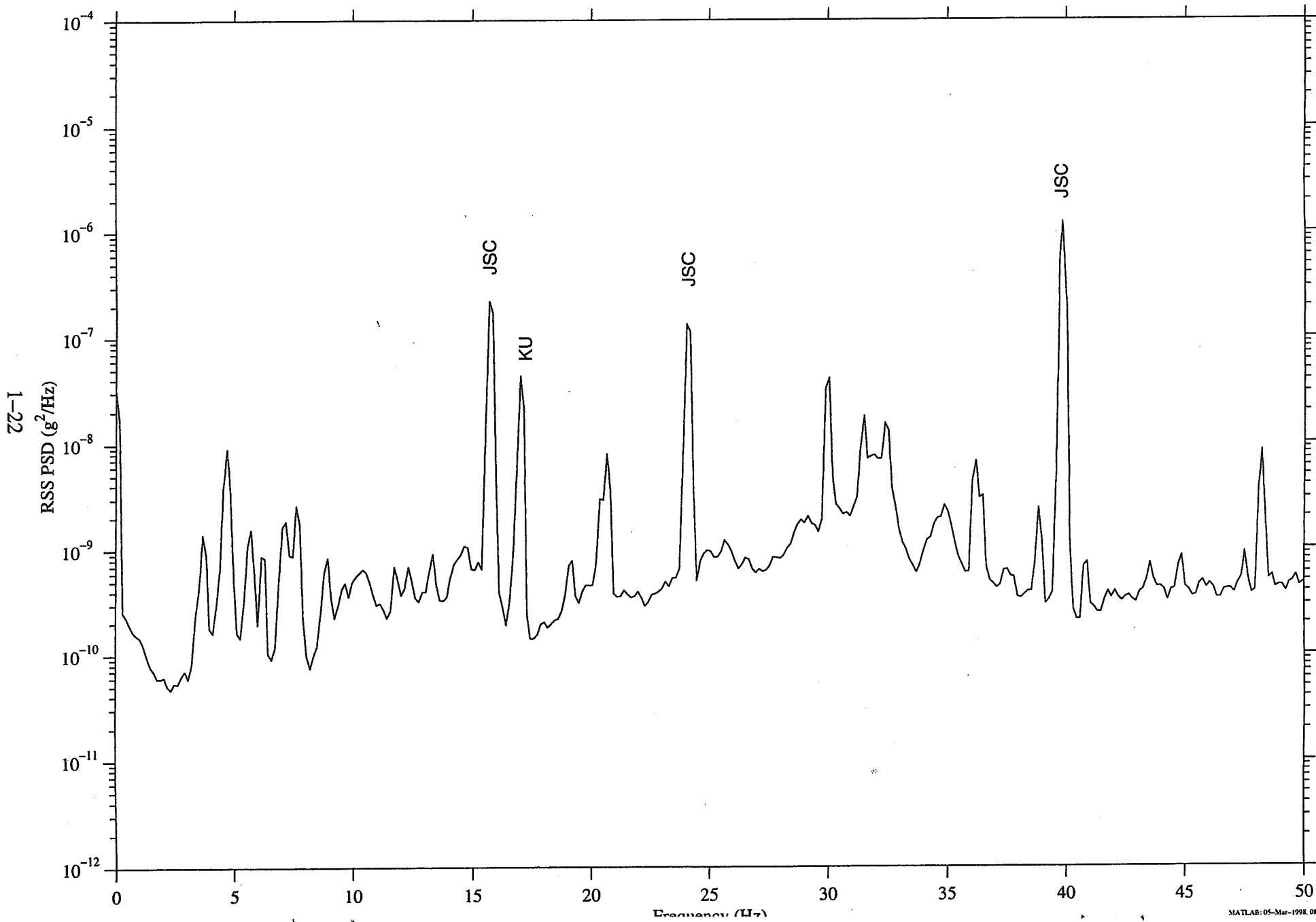
1-21

Figure 24. MMA MSP ACPF spectrogram showing JSC Projects Centrifuge accelerations. MET start at 006/18:50:00.

Head MSP4, 100 Hz  
fs=300 samples per second  
dF=0.1465 Hz

LMS  
MSP Coordinates  
T=10.0 minutes

JSC Projects Centrifuge  
MET Start at 006/19:00:00 (Hanning, k=88)



1-22



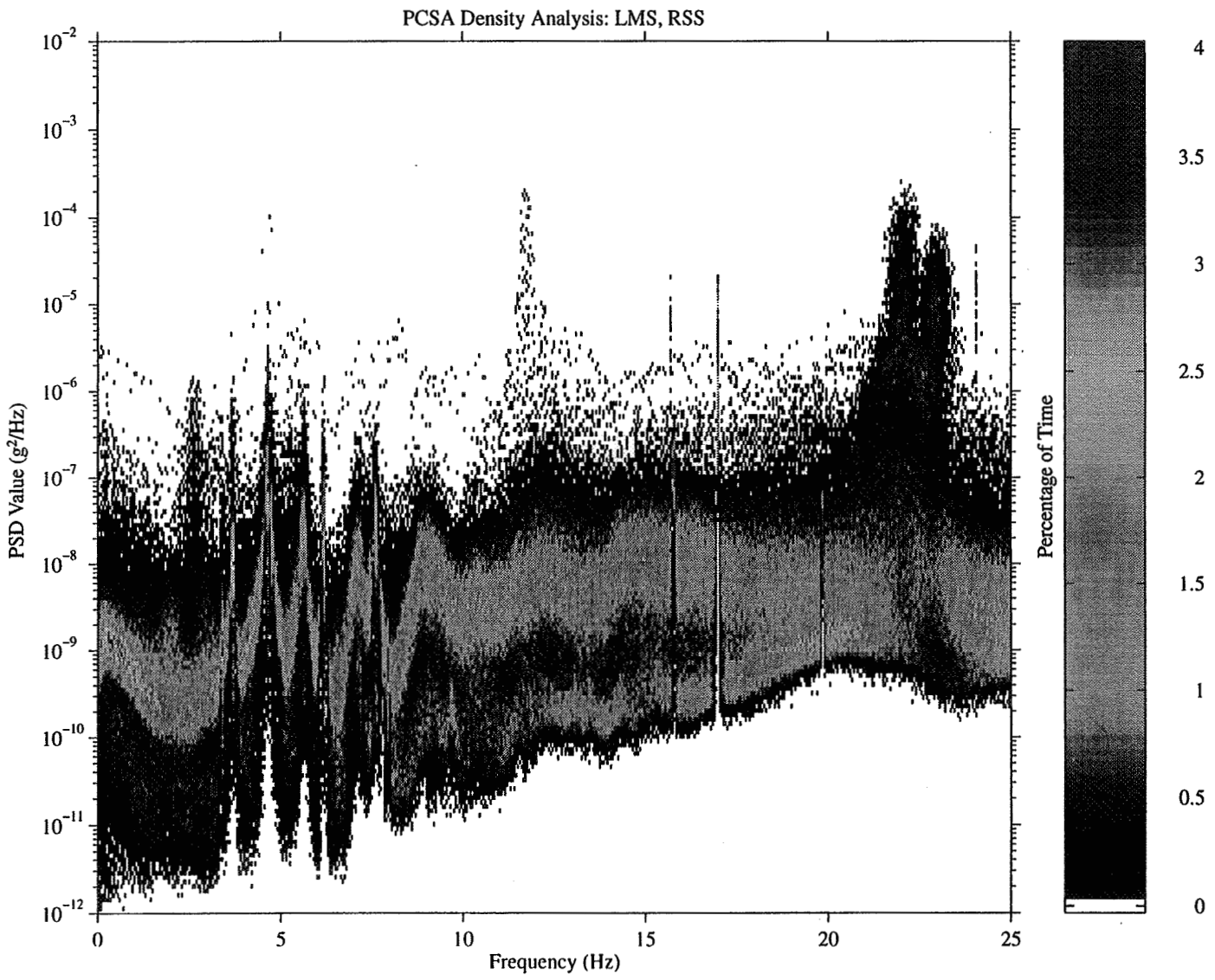


Figure 1: Principal Component Spectral Analysis plot for STS-78 / LMS

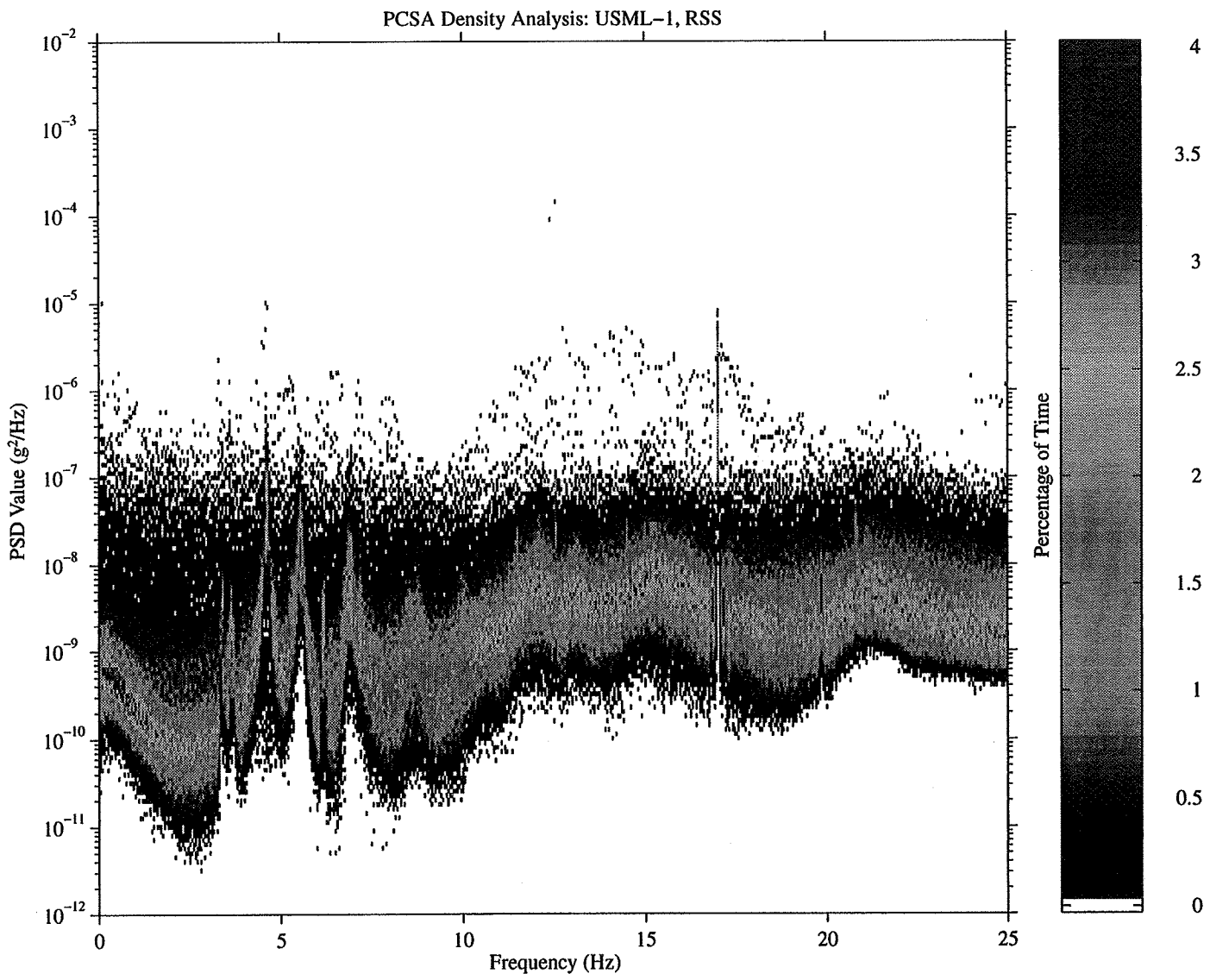


Figure 4: PCSA plot for STS-50 / USML-1

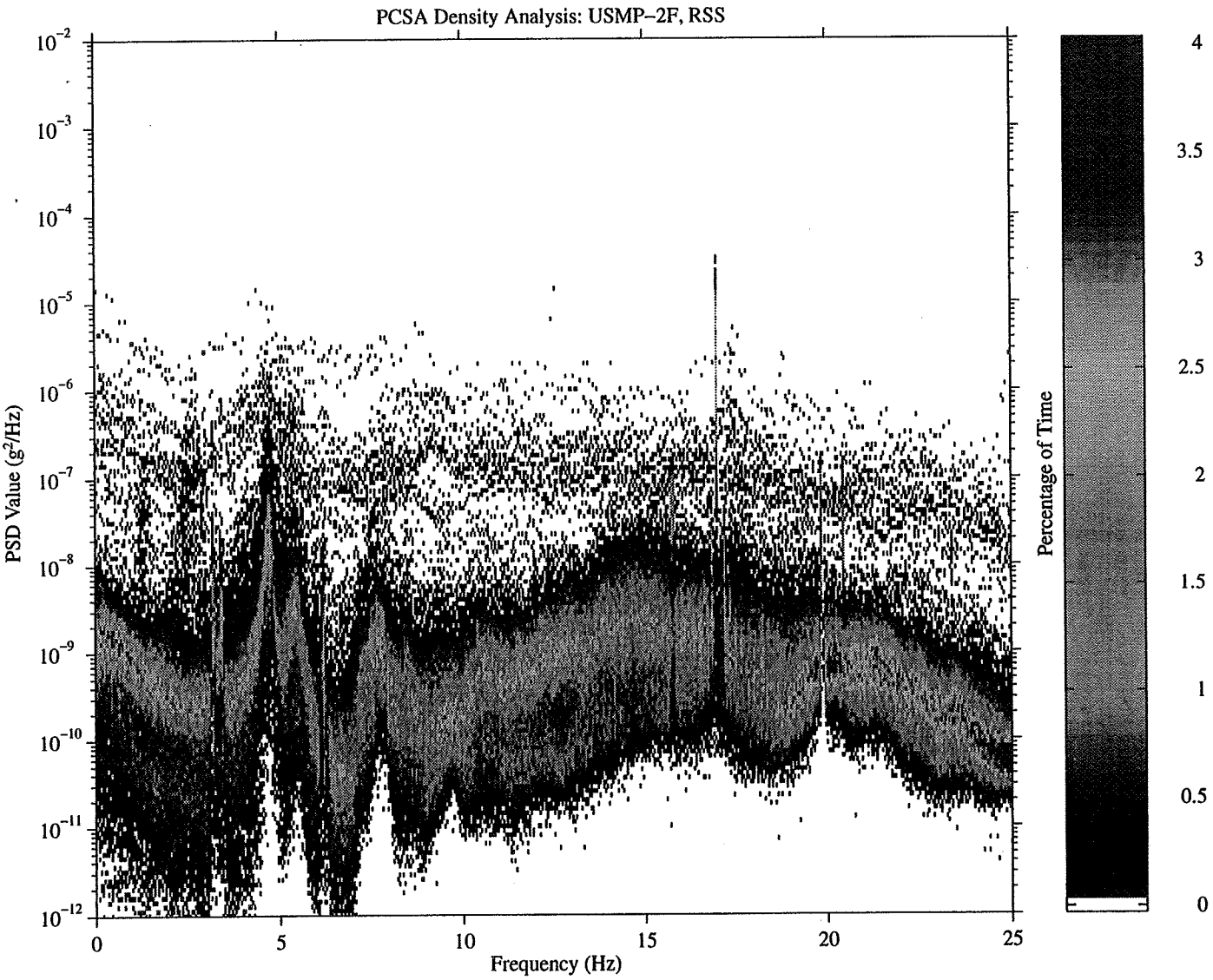


Figure 5: PCSA plot for USMP-2 microgravity portion of STS-62

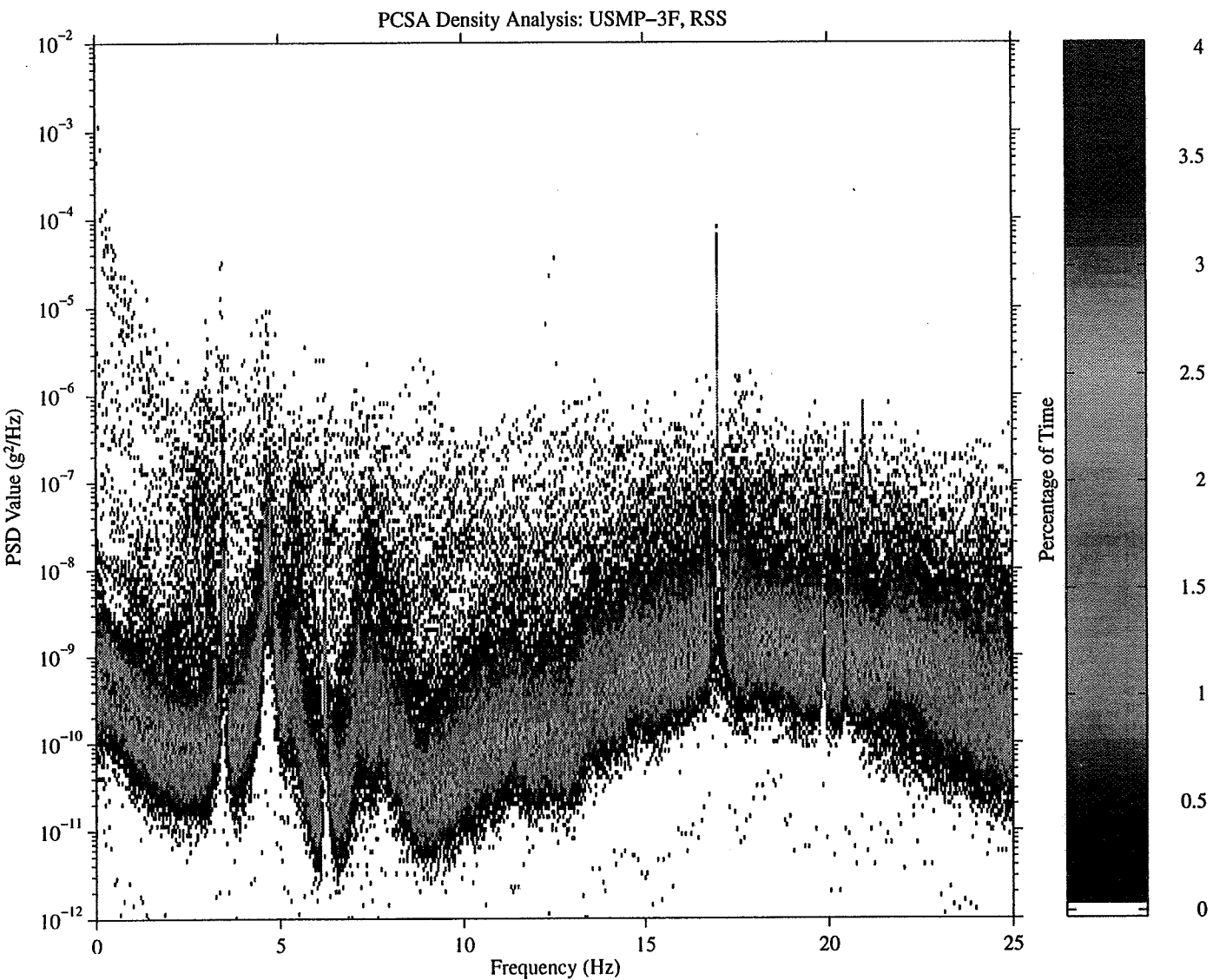


Figure 6: PCSA plot for USMP-3 microgravity portion of STS-75

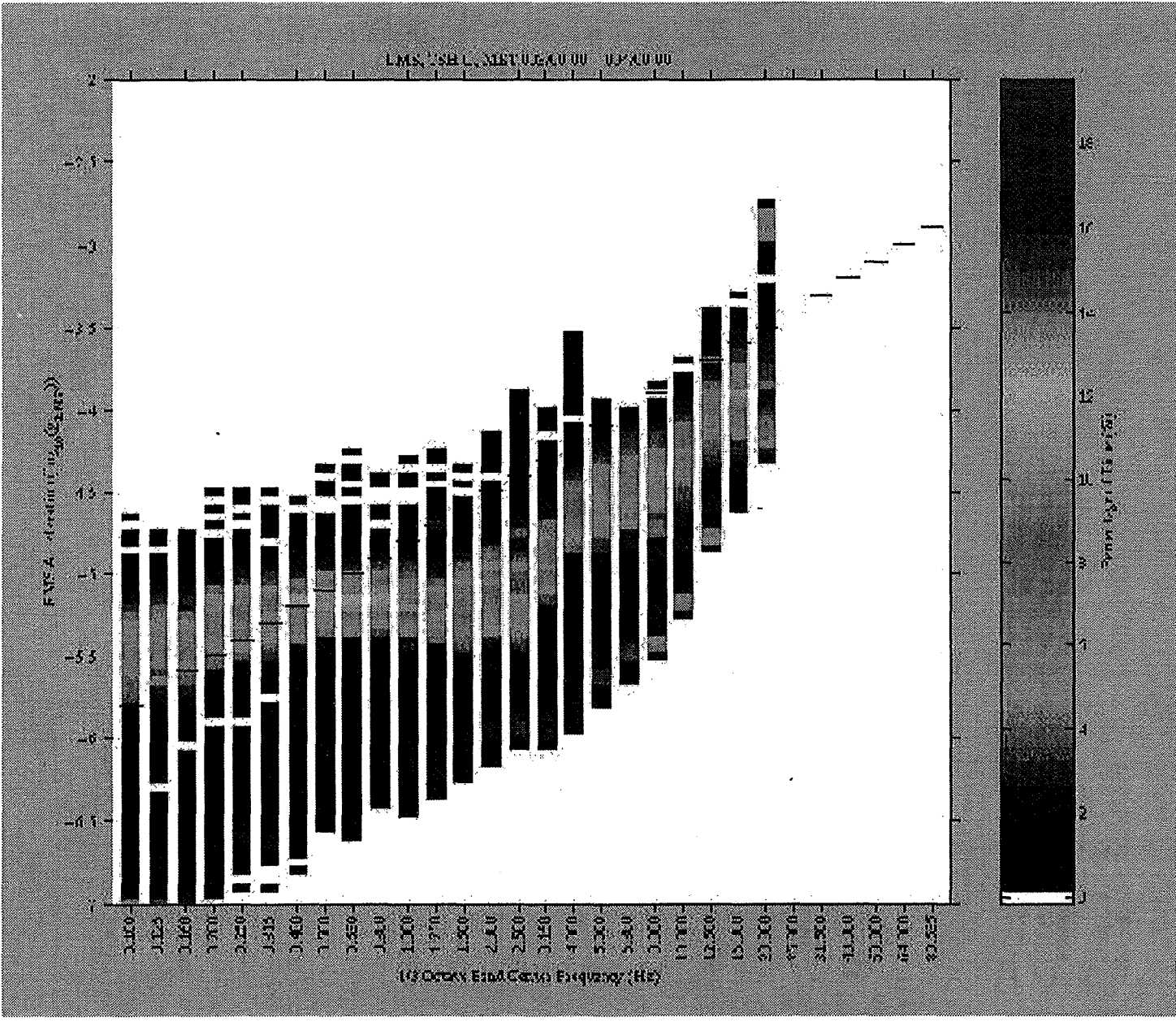
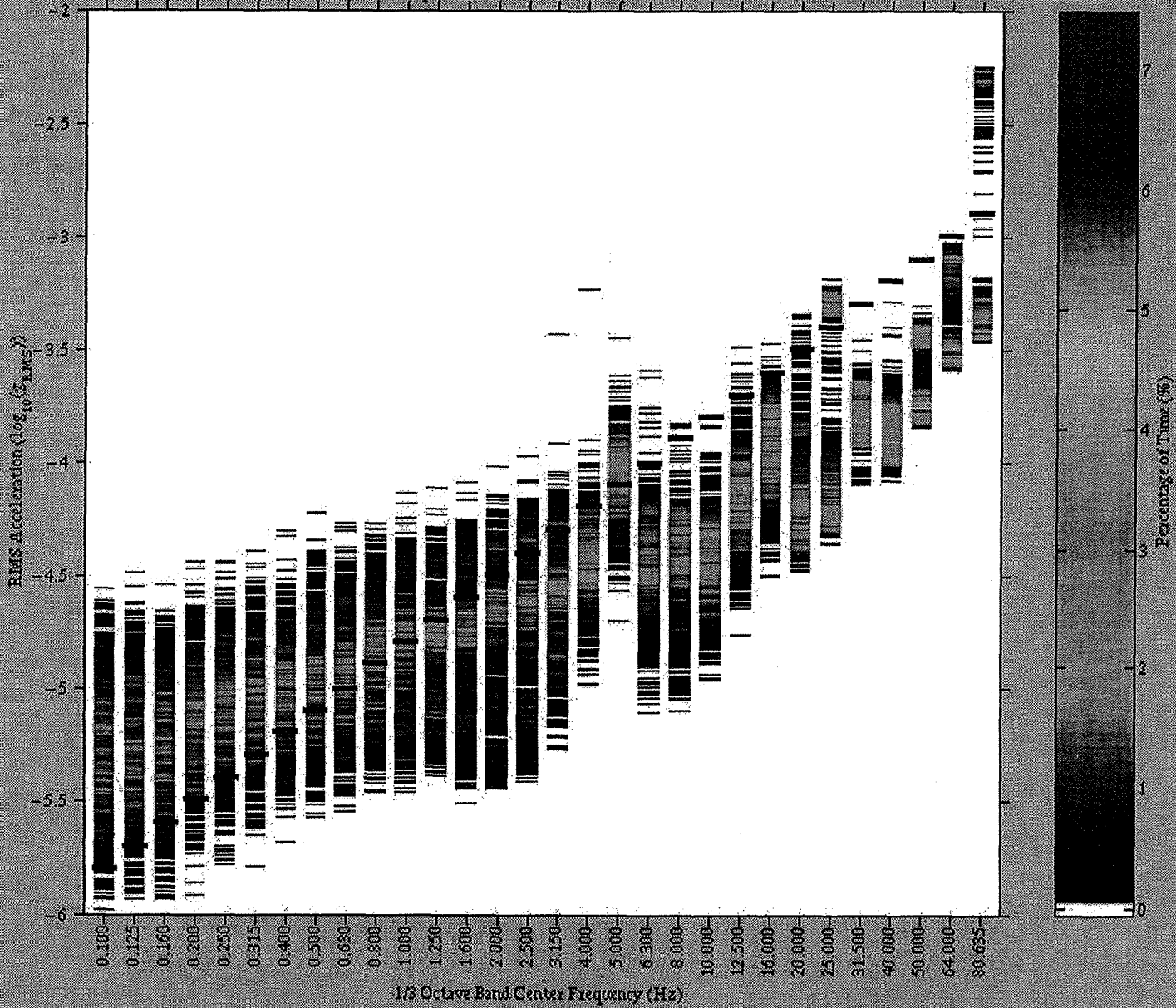


Figure 7: One-third octave histogram for day 3 of STS-78 / LMS

Sample IML-2 Versus ISS Requirement



Paper Number: 2

## **A Review of Microgravity Levels on Ten OARE Shuttle Missions**

---

Kevin M. McPherson, NASA Lewis Research Center, Cleveland, Ohio

# **A Review of Microgravity Levels on Ten OARE Shuttle Missions**

Author:

Kevin M. McPherson

NASA Lewis Research Center, Cleveland, OH 44135

## **ABSTRACT**

The Orbital Acceleration Research Experiment (OARE) is an accelerometer package with nano-g sensitivity and on-orbit bias calibration capabilities. The OARE consists of a three axis miniature electrostatic accelerometer (MESA), a full in-flight bias and scale factor calibration station, and an on-board microprocessor for experiment control and data storage. Originally designed to measure and record the aerodynamic acceleration environment of the NASA Space Shuttles during re-entry, the OARE has been used on ten shuttle missions to measure the quasi-steady acceleration environment ( $< 1$  Hz) of the Orbiter while in low-Earth orbit. The effects on the quasi-steady acceleration environment from Orbiter systems, Orbiter attitude, Orbiter altitude, and crew activity are well understood as a result of these ten shuttle missions. This knowledge of the quasi-steady acceleration realm has direct application to understanding the quasi-steady acceleration environment expected for the International Space Station (ISS). This paper will summarize the more salient aspects of this quasi-steady acceleration knowledge base.

## **INTRODUCTION**

NASA's Orbiters provide a reduced gravity environment during the Orbiter's continuous free-fall state in low-Earth orbit. The OARE is an accelerometer system managed by the NASA Lewis Research Center. The system contains a triaxial accelerometer that utilizes a single non-pendulous electrostatically suspended proof mass, an in-flight bias and scale factor calibration station, and an on board microprocessor for instrument control and data storage. The OARE is capable of better than 10 nano-g resolution. Errors in scale factor determination and bias estimation limit the on-orbit accuracy to approximately 50 nano-g's.<sup>1</sup>

Data in this report are presented in Orbiter body coordinates and in an Orbiter frame of reference. Excepting Figure 1, all data are presented at the OARE location. The Orbiter body coordinate system consists of the positive  $X_b$ -axis directed toward the Orbiter nose, the positive  $Y_b$ -axis directed out the starboard wing, and the positive  $Z_b$ -axis directed out the Orbiter belly.

An Orbiter frame of reference is one in which an observer is 'attached' to the Orbiter and observing a free-floating particle within the vehicle. Hence, a forward acceleration of the Orbiter would be reported as a negative  $X_b$ -axis acceleration because a free particle would appear to translate in the negative  $X_b$ -axis direction relative to the Orbiter's acceleration in the positive  $X_b$ -axis direction.

Plots of the OARE data are typically presented in either trimmean filter (TMF) acceleration versus time or in quasi-steady three dimensional histogram (QTH) format. Table 1 summarizes the presentation options for OARE data. The TMF is applied to the raw OARE data and is necessary to mitigate the effects of higher amplitude, higher frequency accelerations and to allow the quasi-steady acceleration information to be extracted. Operating on a sliding window of pre-defined length (typically 50 seconds), the TMF returns a trimmed average<sup>1</sup> for the window of data presented. The QTH plot is generated by counting the number of times the quasi-steady acceleration vector (typically TMF data) falls within a 2-dimensional bin. This summary of the acceleration vector magnitude and alignment is displayed using a 2-dimensional histogram for each combination of the three orthogonal axes:  $X_b Y_b$ ,  $X_b Z_b$ , and  $Y_b Z_b$ .<sup>2,3</sup>

Table 1: General OARE Processing Techniques

| Analysis Technique           | Usage  |
|------------------------------|--|
| TMF Acceleration versus Time | Reject transient, higher magnitude contributions                         |
| QTH Plot                     | Summarize acceleration vector magnitude and direction                    |
| Mapping of OARE Data         | Calculate the acceleration environment at other locations in the Orbiter |

Using Orbiter rotational rates and body angles, the distance between the OARE and the Orbiter Center of Gravity (CG), and the distance between the Orbiter CG and an alternate location, the OARE data can be presented or mapped to locations other than the OARE location. This calculation of the OARE accelerations at an alternate location is made possible by separating the three primary components of the quasi-steady acceleration vector: aerodynamic drag at the Orbiter CG, gravity gradient effects, and Euler effects. The aerodynamic drag component is affected by Orbiter attitude, Orbiter altitude, and diurnal effects on the atmosphere. Gravity gradient and Euler effects are influenced by Orbiter attitude. Figure 1 is a comparison of the OARE data at the OARE location and, alternately, the OARE data mapped to the Advanced Gradient Heating Facility (AGHF) in the Spacelab module during STS-78. The differences observed in the  $X_b$ -axis acceleration levels result from this facility being further

from the Orbiter CG in the  $X_b$ -axis direction than the OARE.

## ORBITER SYSTEM EFFECTS

The Orbiter has many systems that affect the acceleration environment during microgravity missions. While most of these systems manifest themselves as disturbances visible above the quasi-steady region ( $> 1$  Hz), two Orbiter systems in particular present their effects most apparently in the quasi-steady acceleration environment. The Orbiter food, water, and waste management subsystem provides dumping capabilities for potable and waste water.<sup>4</sup> Water dumps utilizing this subsystem are performed periodically throughout a mission using a nozzle located on the port side of the Orbiter. Figures 2 and 3 clearly illustrate the effects of water dumps on the quasi-steady acceleration environment. Figure 2 shows a supply water dump and its distinct level change of a relatively constant magnitude in the  $Y_b$ -axis and the  $Z_b$ -axis. A pair of distinct level changes is associated with the simultaneous supply and waste water (SIMO) dump shown in Figure 3. The second level change is attributed to the waste water dump cycling on and off throughout the supply water dump.

Another Orbiter system's effects clearly visible in the OARE data is cabin de-pressurization in preparation for an Extra Vehicular Activity (EVA). The cabin de-pressurization performed in association with an EVA performed during STS-87 (Figure 4) demonstrates these effects, an offset from the nominal accelerations most apparent on the  $Y_b$ - and  $Z_b$ -axes.

## CREW EFFECTS

The impact of the crew on the quasi-steady environment is a function of crew shift schedules, crew activity, and non-microgravity crew activities such as satellite deployments. As one might expect, the signature of the OARE data during a single-shift mission is distinctly different from a multi-shift mission. The quiet periods present throughout Figure 5 are associated with the sleep cycles of the STS-78 crew. Comparing the tight clustering of the data in Figure 6 (crew asleep) to the scattering of the data in Figure 7 (crew awake) further illustrates the impact of crew sleep cycles on the quasi-steady environment during the STS-78 mission.

The impact of crew activity on the environment is apparent in a comparison between the USMP-2 (STS-62) environment (Figure 8) and the LMS (STS-78) environment (Figure 5). As a direct result of the numerous life science experiments conducted in the Spacelab module during the LMS mission, the acceleration environment is noticeably noisier than the USMP-2 mission. In general, Spacelab missions exhibit a generally noisier microgravity environment than USMP missions because of the crew activity level in the Spacelab module and the

proximity of the crew to the OARE measurement location.

As expected, an activity such as a satellite deployment would have a noticeable negative impact on the overall microgravity environment. Figure 9 shows the specific effects on the quasi-steady acceleration environment during the deployment of the Tethered Satellite System (TSS) during USMP-3 (STS-75). Additional negative effects on the environment occur as the Orbiter is maneuvered into a satellite's deployment attitude.

## VEHICLE ATTITUDE EFFECTS

Orbiter attitude greatly influences the quasi-steady acceleration environment. Table 2 summarizes several of the missions the OARE has supported as a function of attitude and nominal g-level experienced in those attitudes. The information in this table was extracted from QTH plots generated for each of the missions listed in the table. As an example of this process, Figure 10 clearly shows the two primary attitudes flown during the LMS (STS-78) mission, indicated by the light gray regions in the center of the black region. The g-levels (Orbiter frame of reference) for these attitudes are extracted from the plot.

Table 2: Mission Summary Table

| Mission | STS Flight       | Primary Attitudes (LVLH Coords) | Orbiter Body Angles (Pitch, Yaw, Roll) | Nominal Micro-g Levels (X, Y, Z) |
|---------|------------------|---------------------------------|--|----------------------------------|
| USMP-2  | STS-62           | -ZLV,+YVV                       | 180,90,0                               | 0.3, 0.2, 0.7                    |
|         |                  | -XLV,-ZVV                       | 90,180,0                               | -0.6, 0.2,-0.4                   |
| IML-2   | STS-65           | -XLV,+YVV                       | 90,2,78                                | -0.9, 0.1, 0.0                   |
|         |                  | -ZLV,+YVV                       | 180,90,0                               | 0.4, 0.3, 0.8                    |
| USML-2  | STS-73           |                                 | 96,287,358                             | -0.8,-0.5,-0.2                   |
| USMP-3  | STS-75           | -XLV,+ZVV                       | 90,0,0                                 | -0.6,-0.1, 0.3                   |
| LMS     | STS-78           | -XLV,+ZVV                       | 97,0,0                                 | -0.5,-0.1, 0.3                   |
|         |                  | -ZLV, -XVV                      | 175,0,0                                | -0.1,-0.1, 0.5                   |
| MSL-1   | STS-83<br>STS-94 | -ZN/55ROLL                      | 180,0,55                               | 0.2, 0.4, 0.0                    |

In general, the axis in the direction (the aerodynamic drag axis) of flight experiences the greatest variation. This is shown in Figure 11 where a +ZSI attitude (+Z solar inertial, Orbiter belly oriented toward the Sun) was flown. In this attitude, the  $Y_b$ - and  $Z_b$ -axes alternate as the axis in the direction of flight. Consequently, their variation resulting from aerodynamic drag is

quite apparent. Figure 12 shows the effects of a +ZSI attitude in the QTH plot format.

The +ZSI attitude is useful in demonstrating another feature of OARE data processing, the Microgravity Analysis Work Station (MAWS). The MAWS model is used to predict the quasi-steady acceleration environment at any point in the Orbiter. Figure 13 shows the strong agreement between the MAWS model and the OARE data during the USML-2 (STS-73) mission.

## CONCLUSION

The OARE data obtained during ten shuttle missions have been instrumental in characterizing the quasi-steady acceleration environment of the Orbiter. This knowledge base will be used to predict and understand the quasi-steady environment of the International Space Station.

## References

1. Canopus Systems, Inc., OARE Technical Report #149, STS-78 (LMS-1) Final Report. CSI-9604, September, 1996.
2. Rogers, M.J.B., Hrovat, K., McPherson, K., Moskowitz, M., and Reckart, T.: *Accelerometer Data Analysis and Presentation Techniques*, NASA TM-113173, September 1997.
3. DeLombard, R., Hrovat, K., Moskowitz, M., and McPherson, K.: *Comparison Tools for Assessing the Microgravity Environment of Missions, Carriers, and Conditions*, NASA TM-107446, April 1997
4. Shuttle Operational Data Book, Volume 1, JSC-08934, Rev. E, Johnson Space Center, Houston, TX, January 1988.

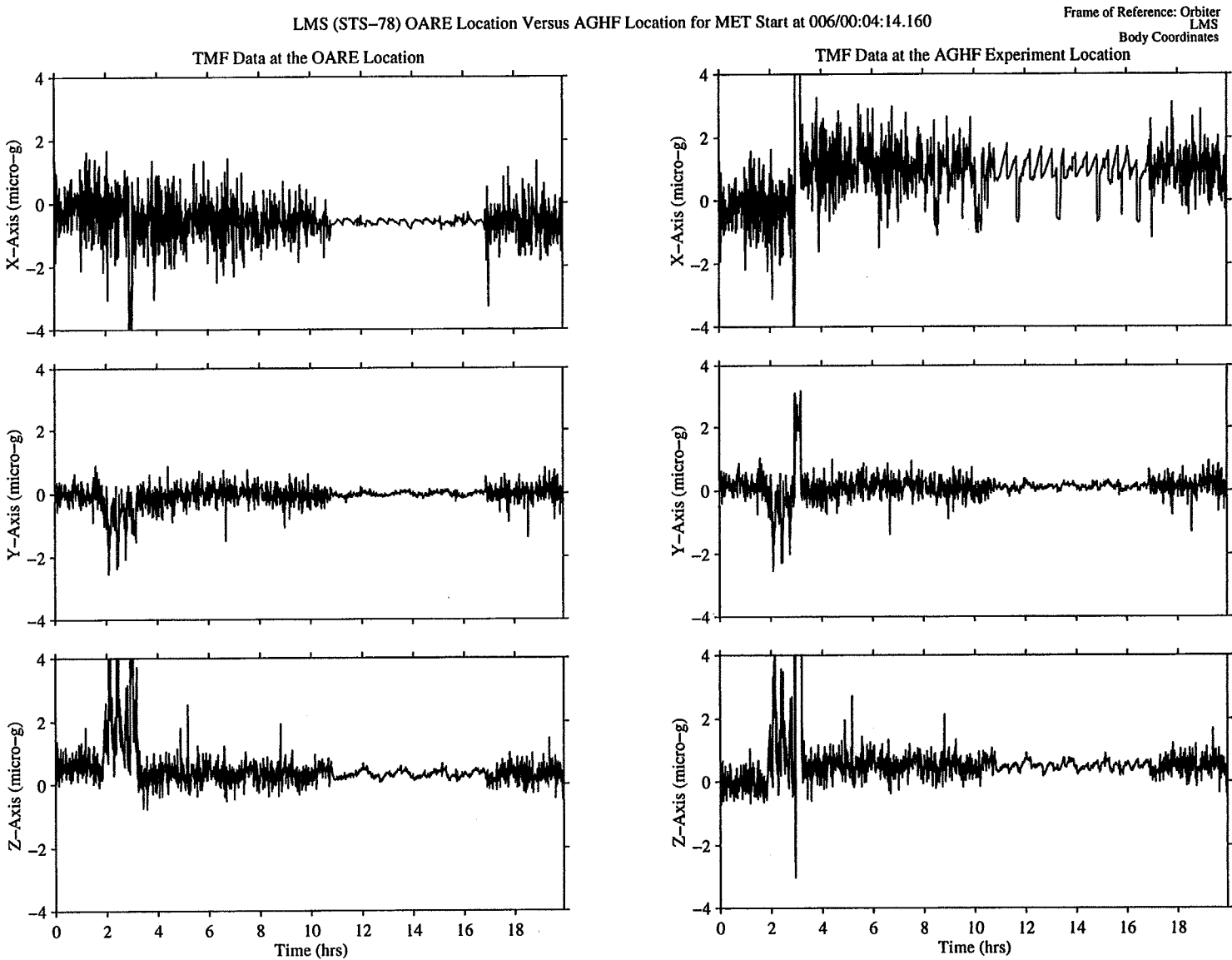


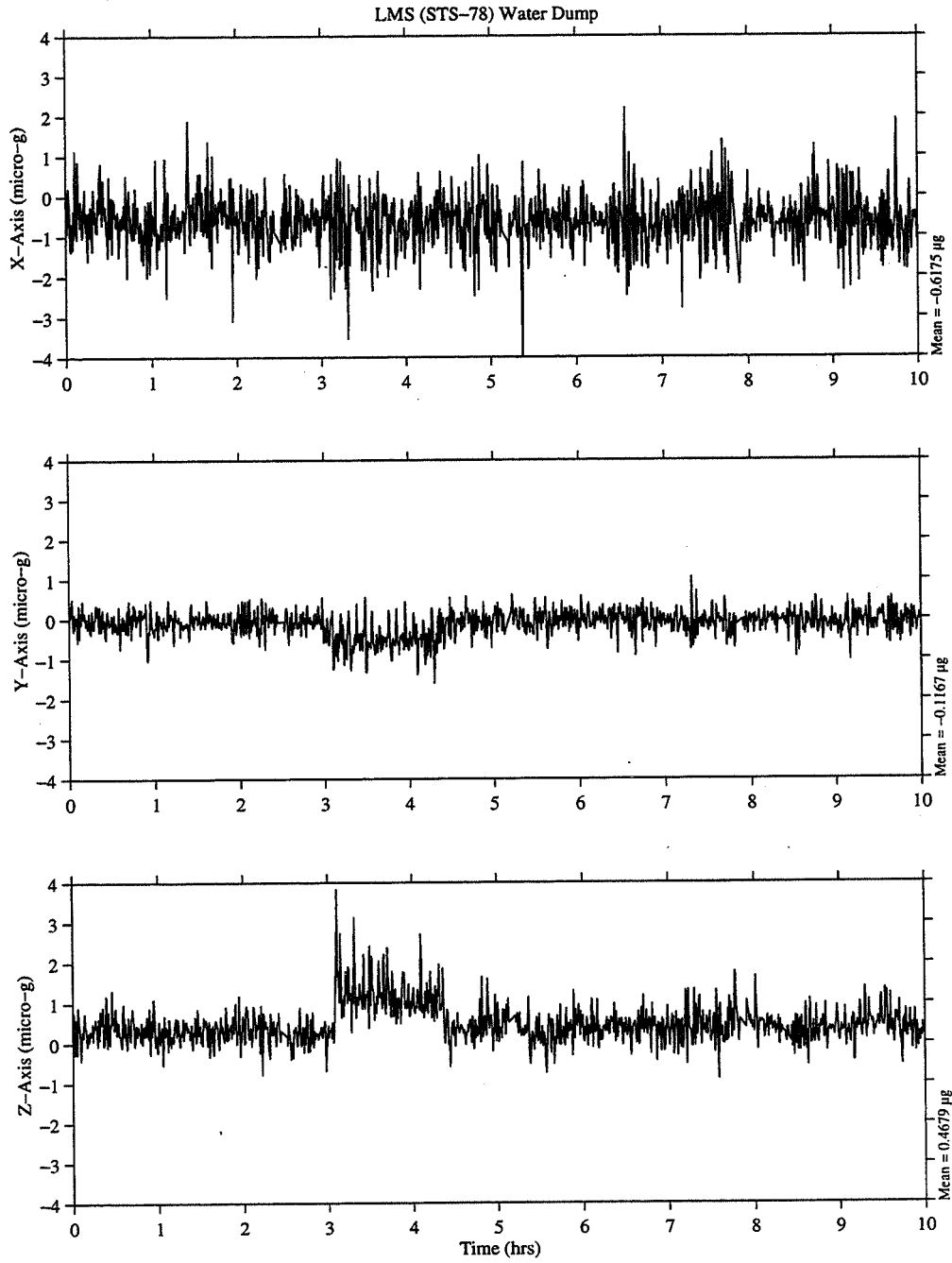
Figure 1: Comparison of OARE Data at OARE Location and AGHF Location from STS-78 (LMS)

# A Review of Microgravity Levels on Ten OARE Shuttle Missions

OARE Trimmed Mean Filtered  
OARE Location

MET Start at 007/22:00:11.160

Frame of Reference: Orbiter  
LMS  
Body Coordinates



MATLAB: 04-20-1994 09:11:00

**Figure 2: OARE TMF Data During Water Dump from STS-78 (LMS)**

*A Review of Microgravity Levels on Ten OARE Shuttle Missions*

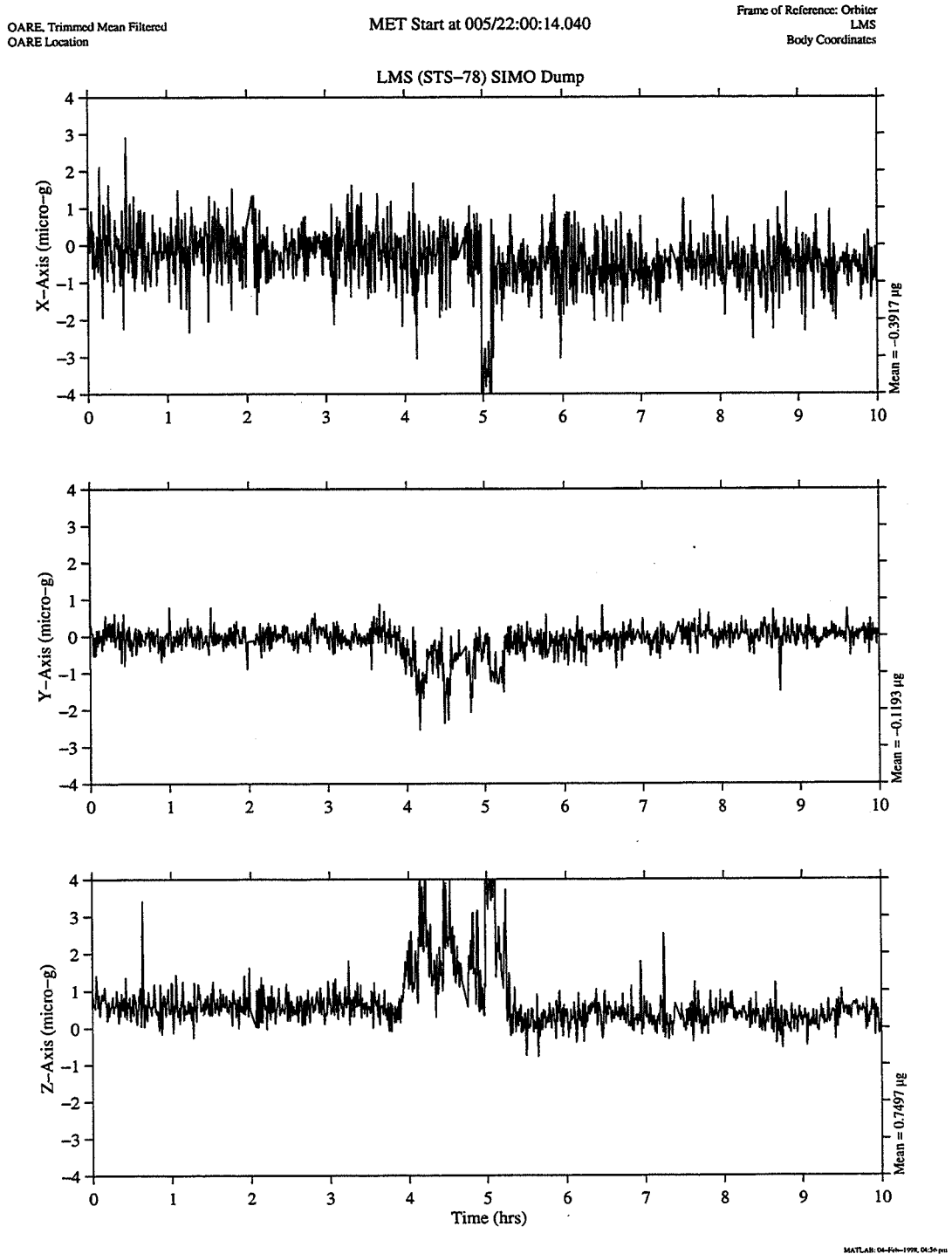


**Figure 3: OARE TMF Data During SIMO Dump from STS-78 (LMS)**

*A Review of Microgravity Levels on Ten OARE Shuttle Missions*

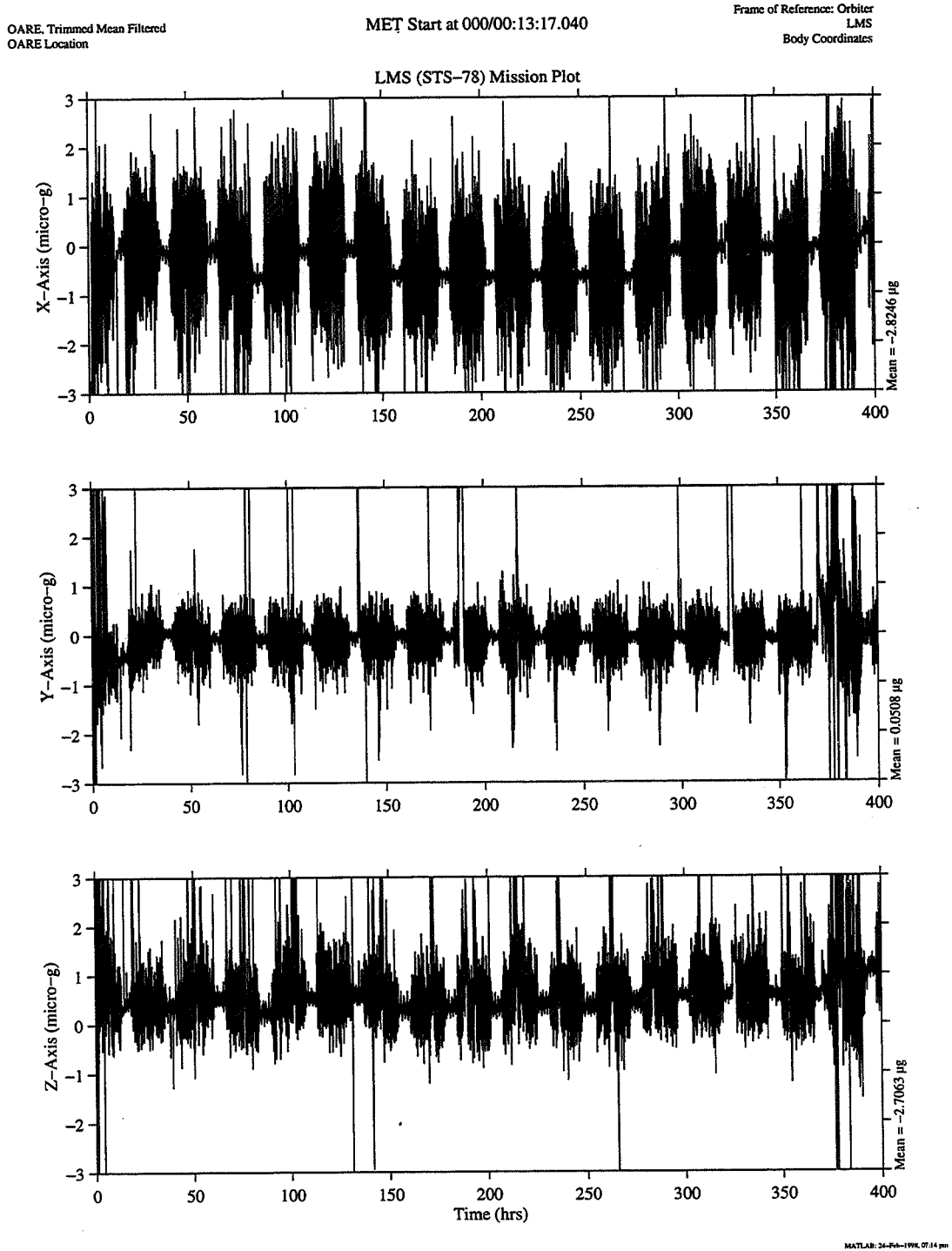


**Figure 5: OARE TMF Data for Entire Mission from STS-78 (LMS)**

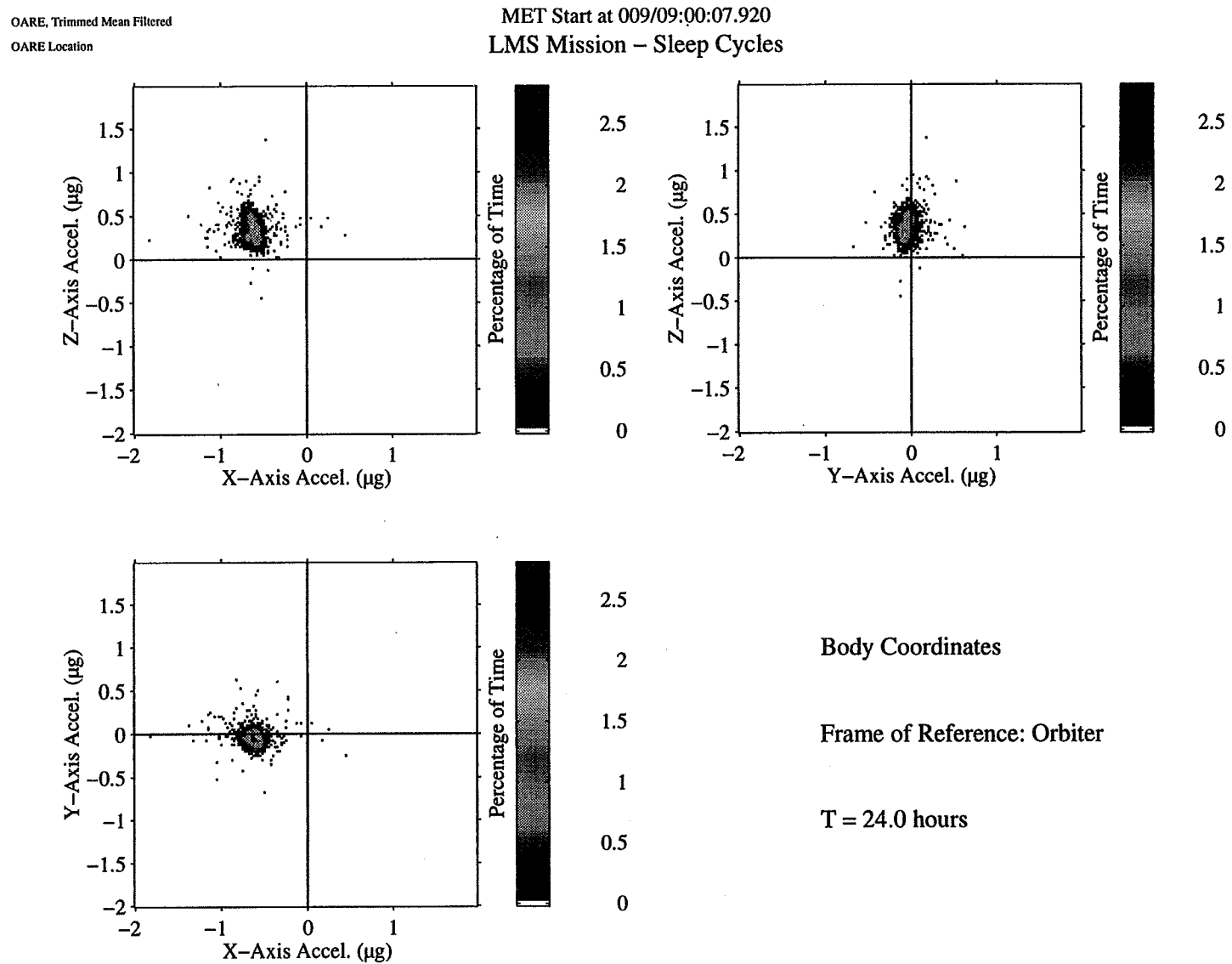
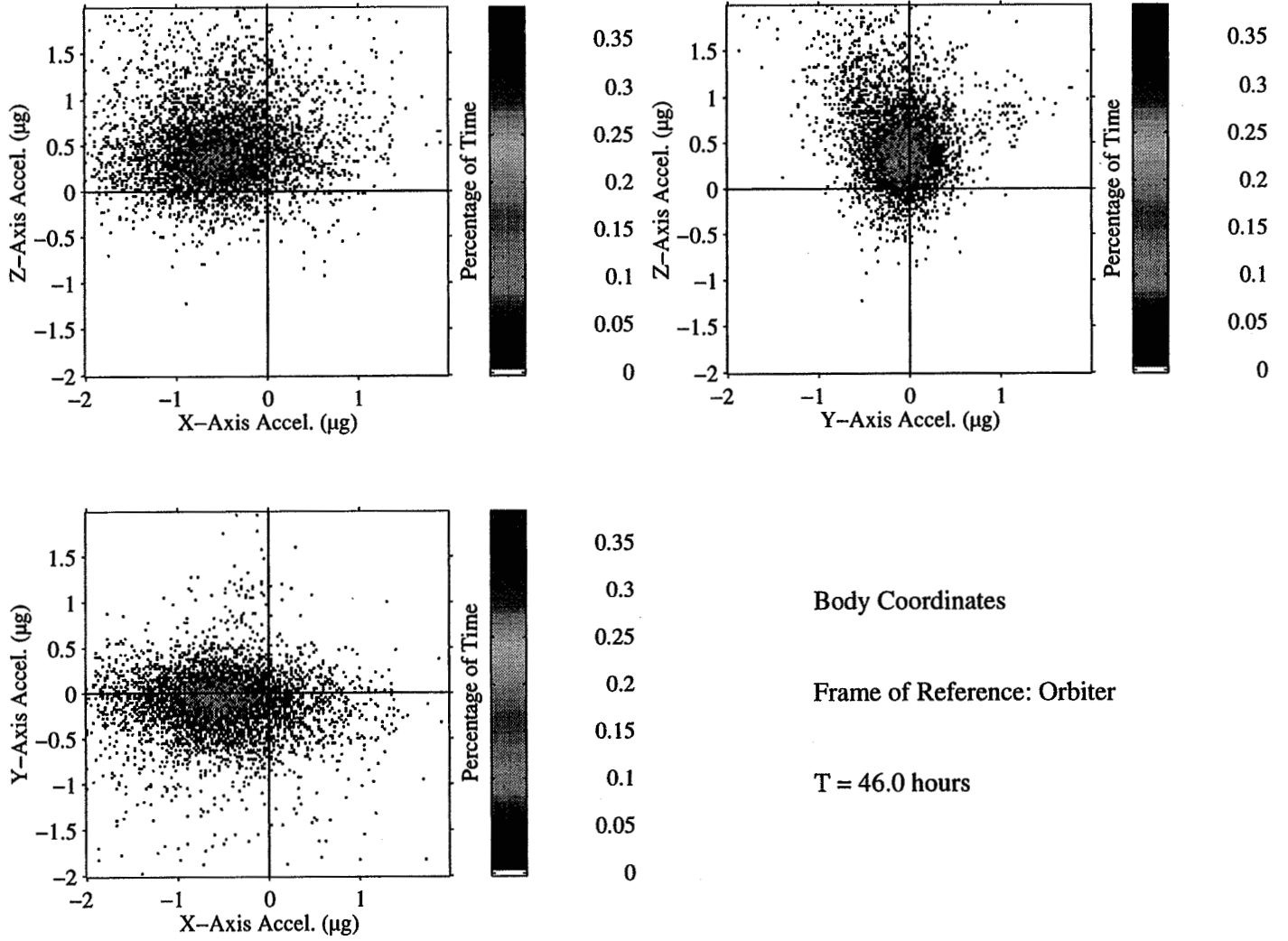


Figure 6: OARE TMF Data for Crew Sleep Period from STS-78 (LMS)

OARE, Trimmed Mean Filtered  
OARE Location

MET Start at 008/17:00:16.920  
LMS Mission – Crew Active Periods



*A Review of Microgravity Levels on Ten OARE Shuttle Missions*

Figure 7: OARE TMF Data for Crew Active Period from STS-78 (LMS)

*A Review of Microgravity Levels on Ten OARE Shuttle Missions*

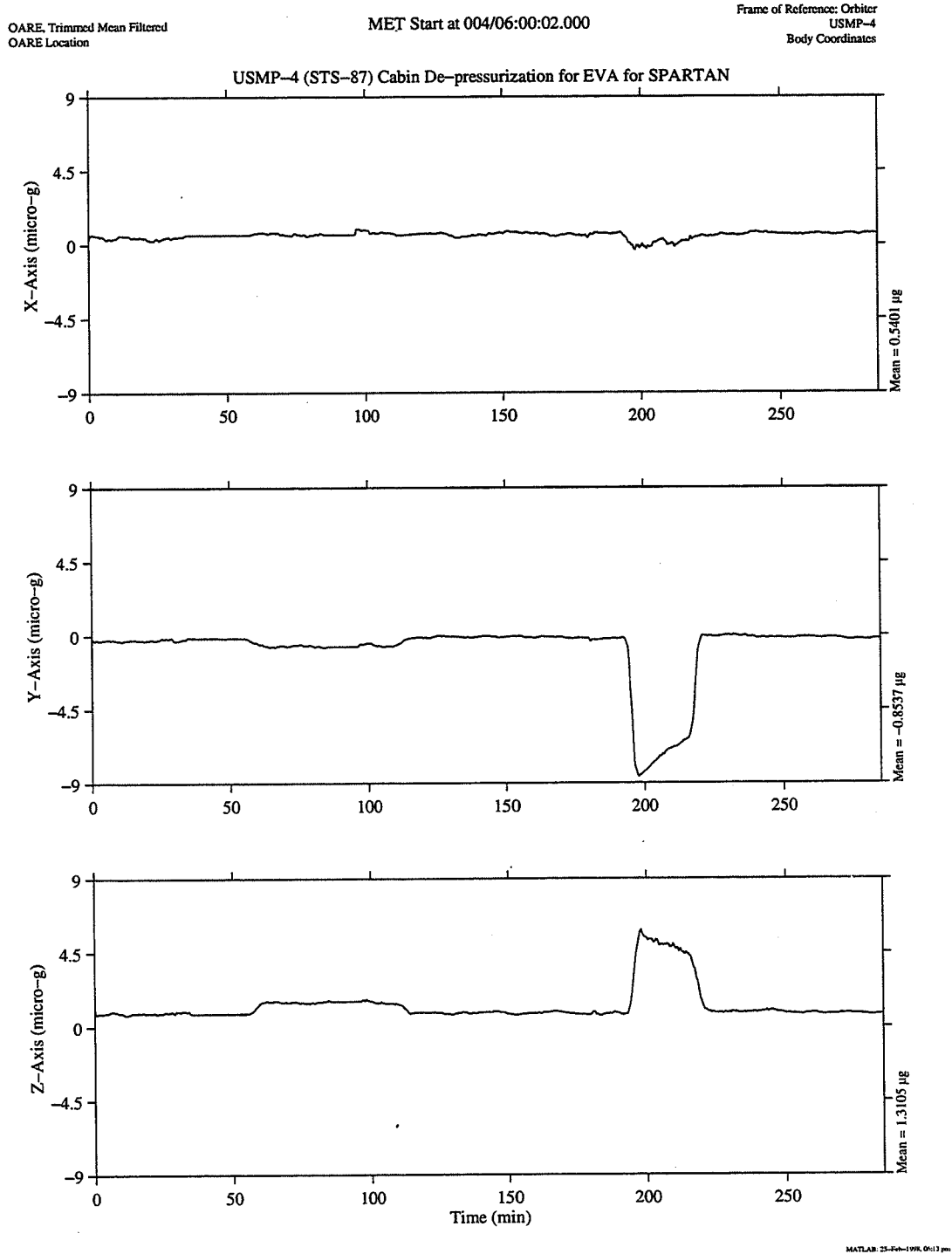


**Figure 4: OARE TMF Data During Cabin De-pressurization from STS-87 (USMP-4)**

*A Review of Microgravity Levels on Ten OARE Shuttle Missions*

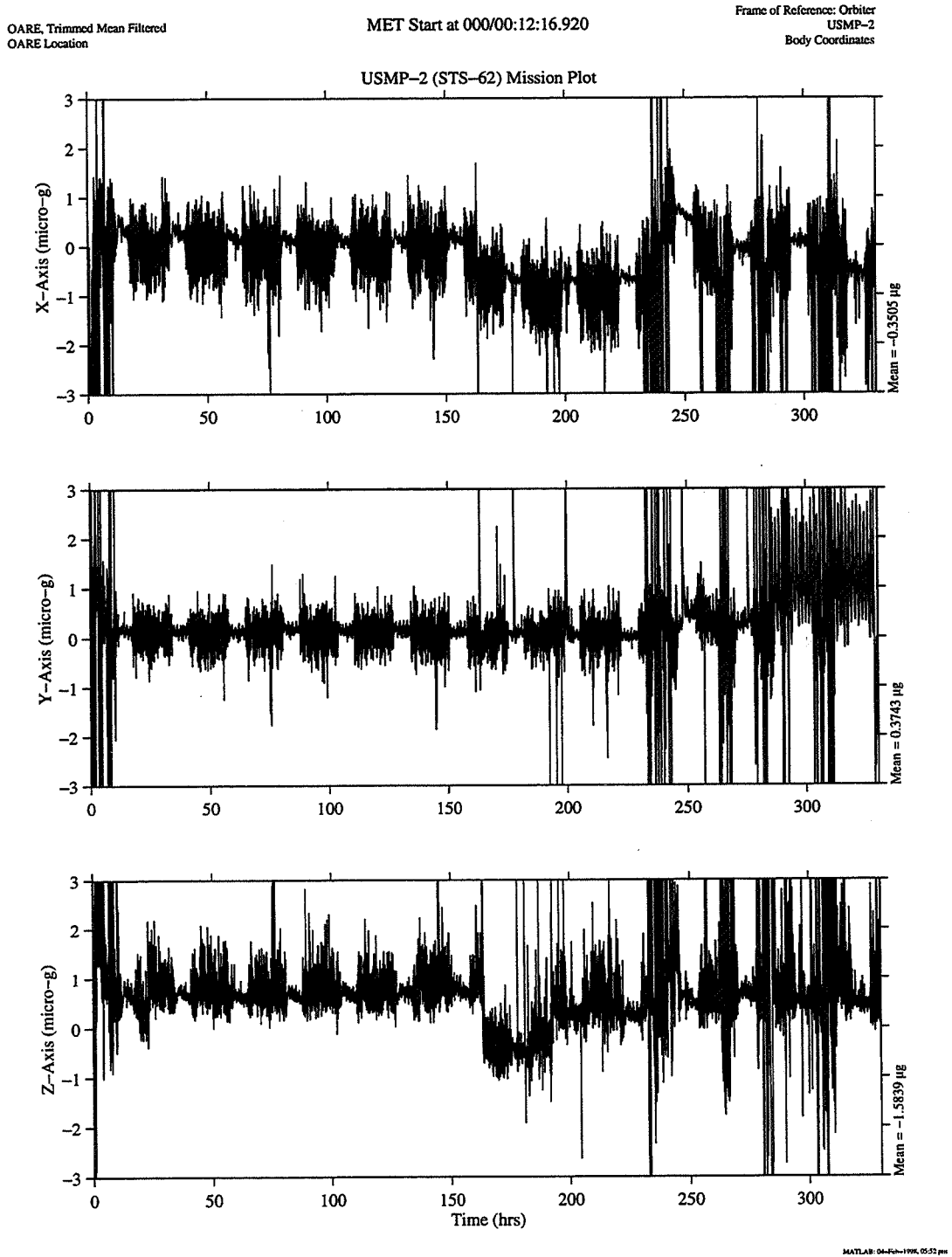


**Figure 8: OARE TMF Data for Entire Mission STS-62 (USMP-2)**

*A Review of Microgravity Levels on Ten OARE Shuttle Missions*

OARE, Trimmed Mean Filtered  
OARE Location

MET Start at 003/00:20:45.600

Frame of Reference: Orbiter  
USMP-3  
Body Coordinates

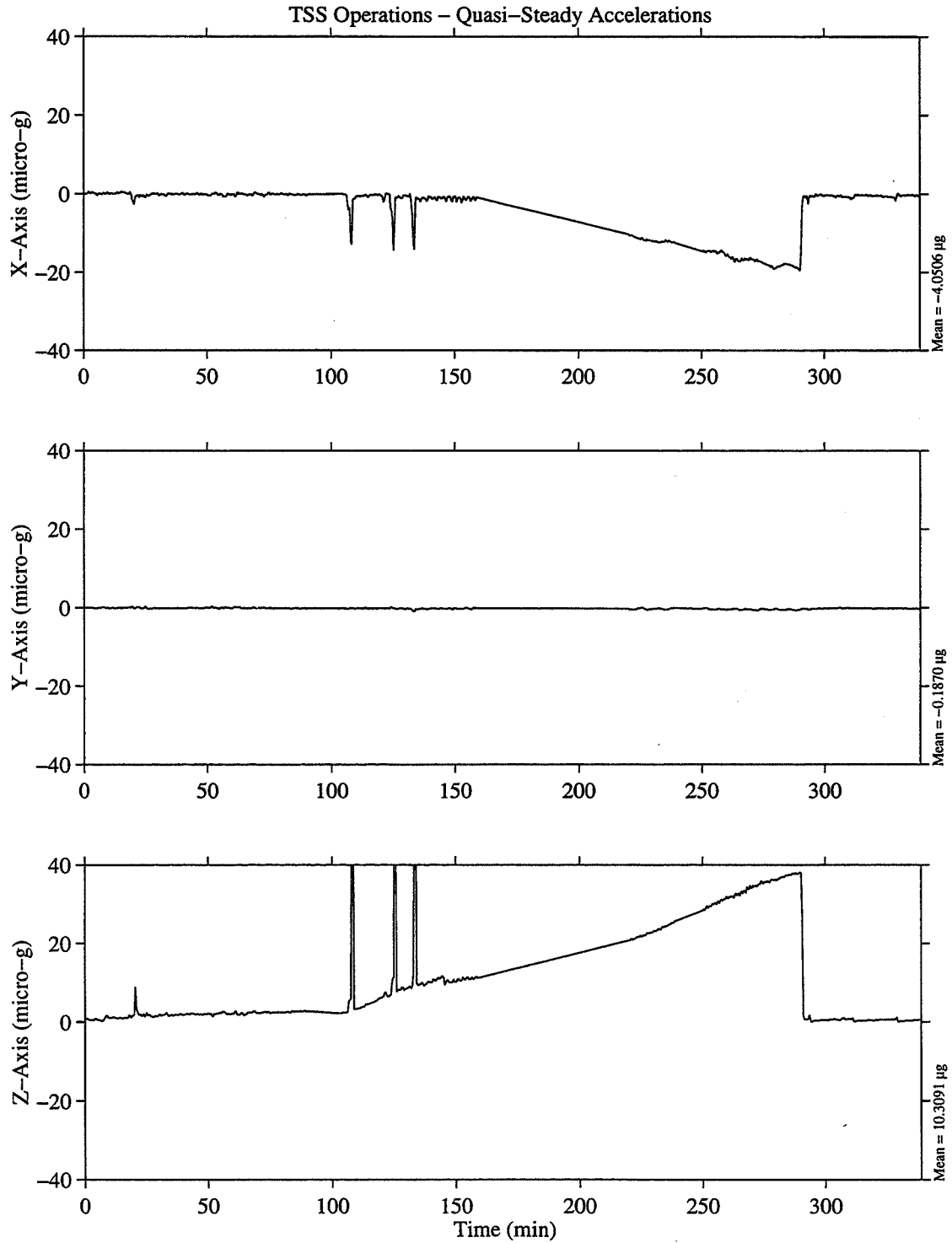
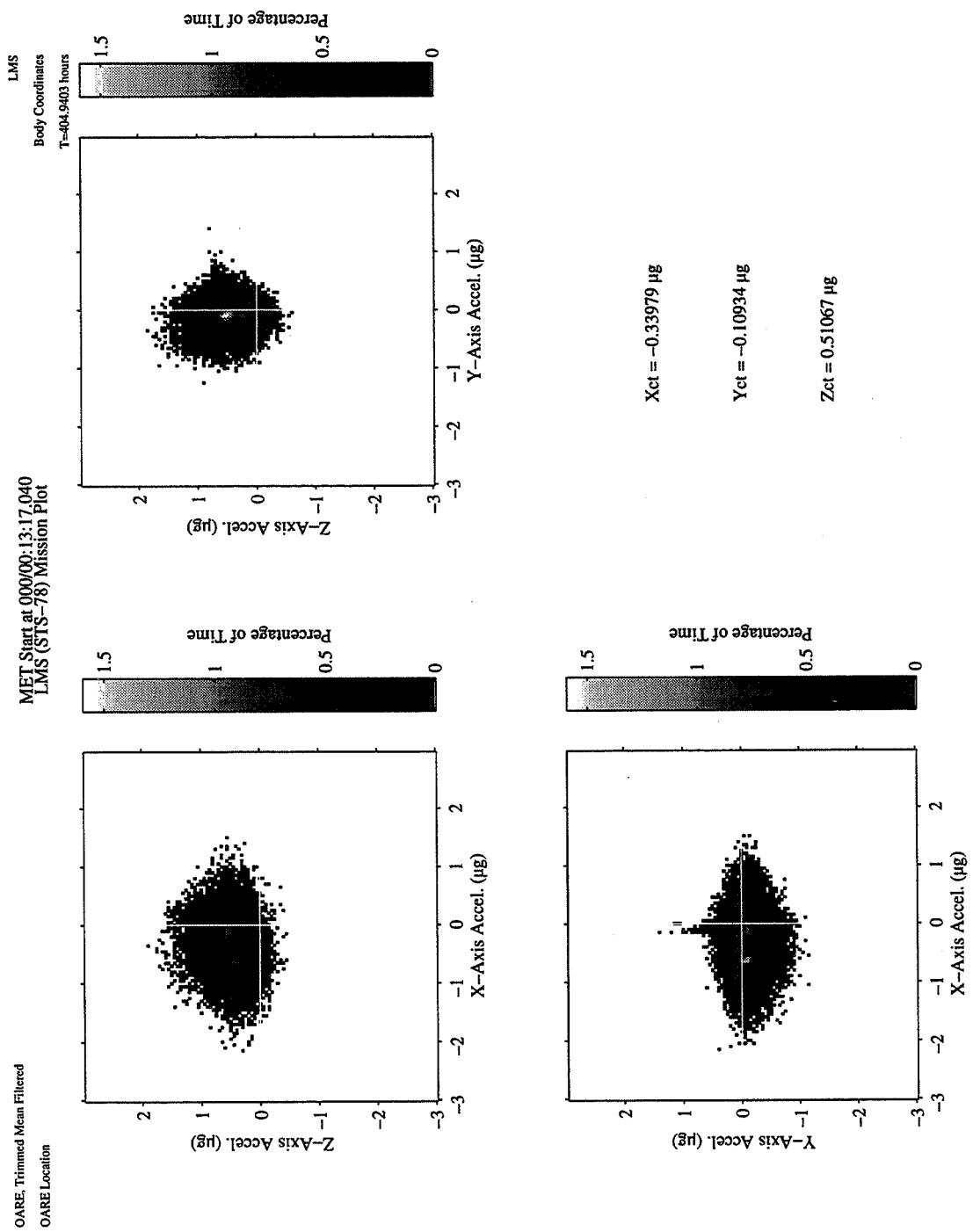


**Figure 9: OARE TMF Data During Deployment of Tether Satellite System from USMP-3 (STS-75)**



SMU-13-14-94-196 03.24 PM

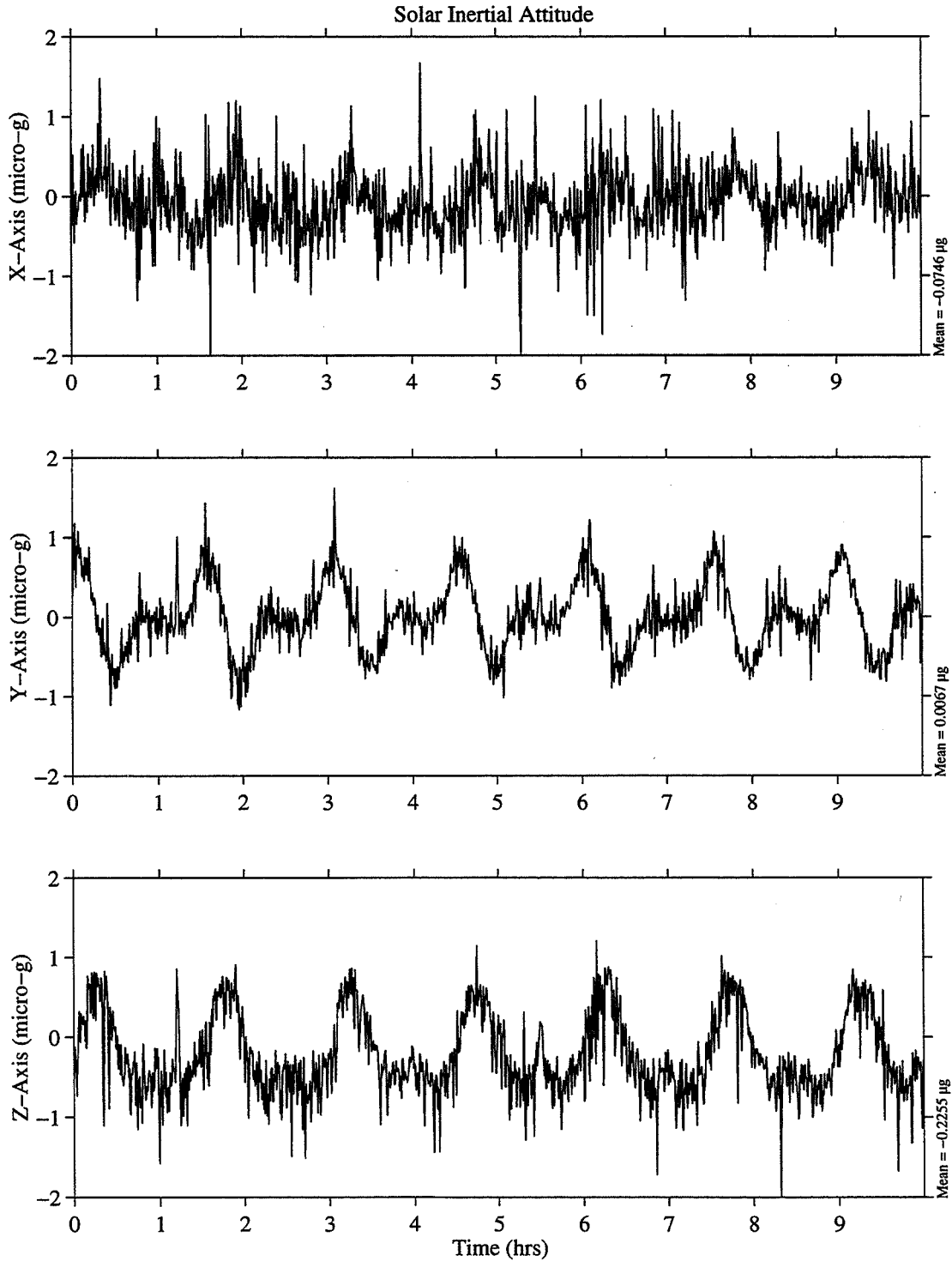
Figure 10: OARE TMF Data from LMS (STS-78)

*A Review of Microgravity Levels on Ten OARE Shuttle Missions*

OARE, Trimmed Mean Filtered  
OARE Location

MET Start at 010/18:00:16.920

Frame of Reference: Inertial  
USML-2  
Body Coordinates



MATLAB: 30-Aug-96 9:55 am

**Figure 11: OARE TMF Data During Solar Inertial Attitude from USML-2 (STS-73)**

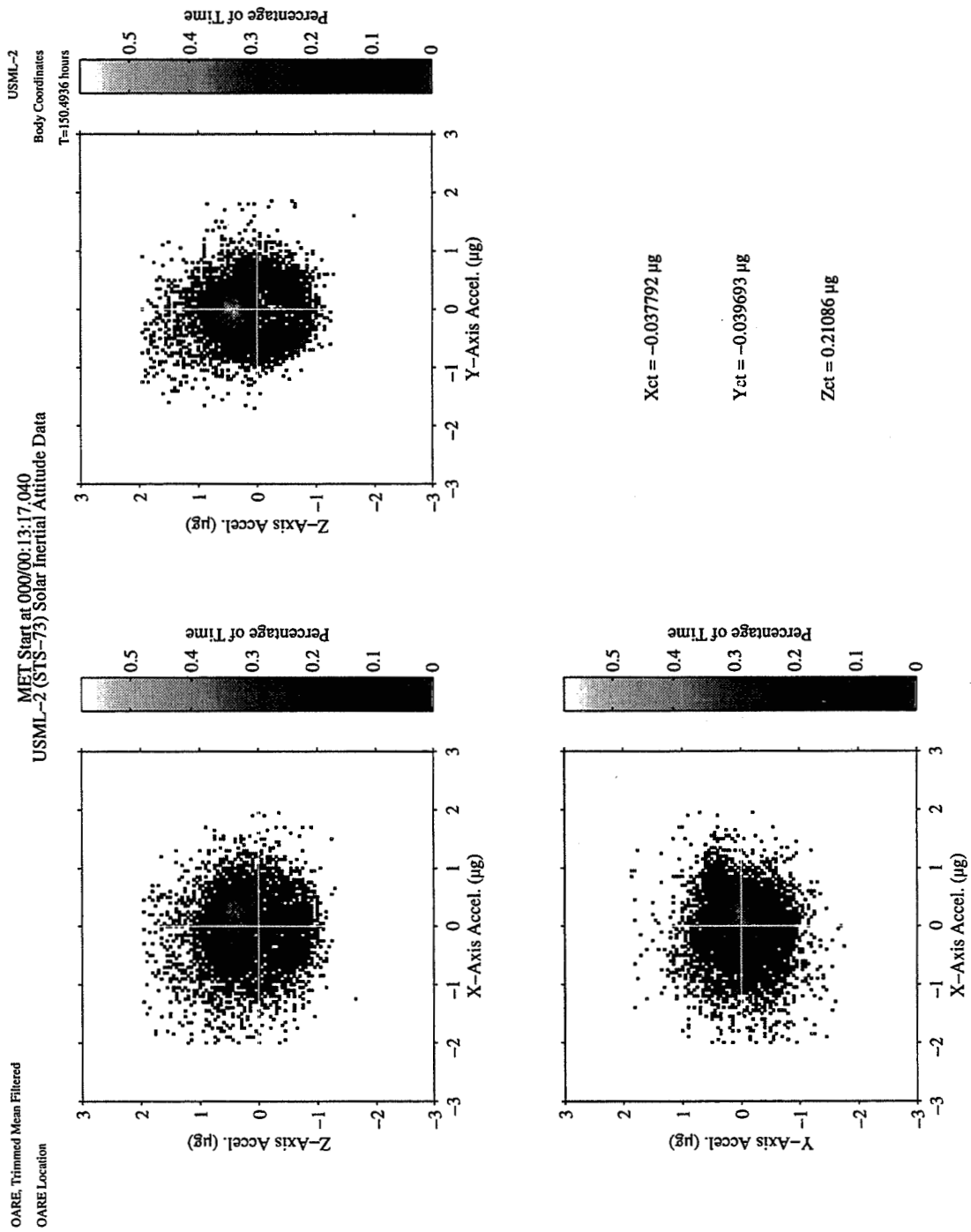


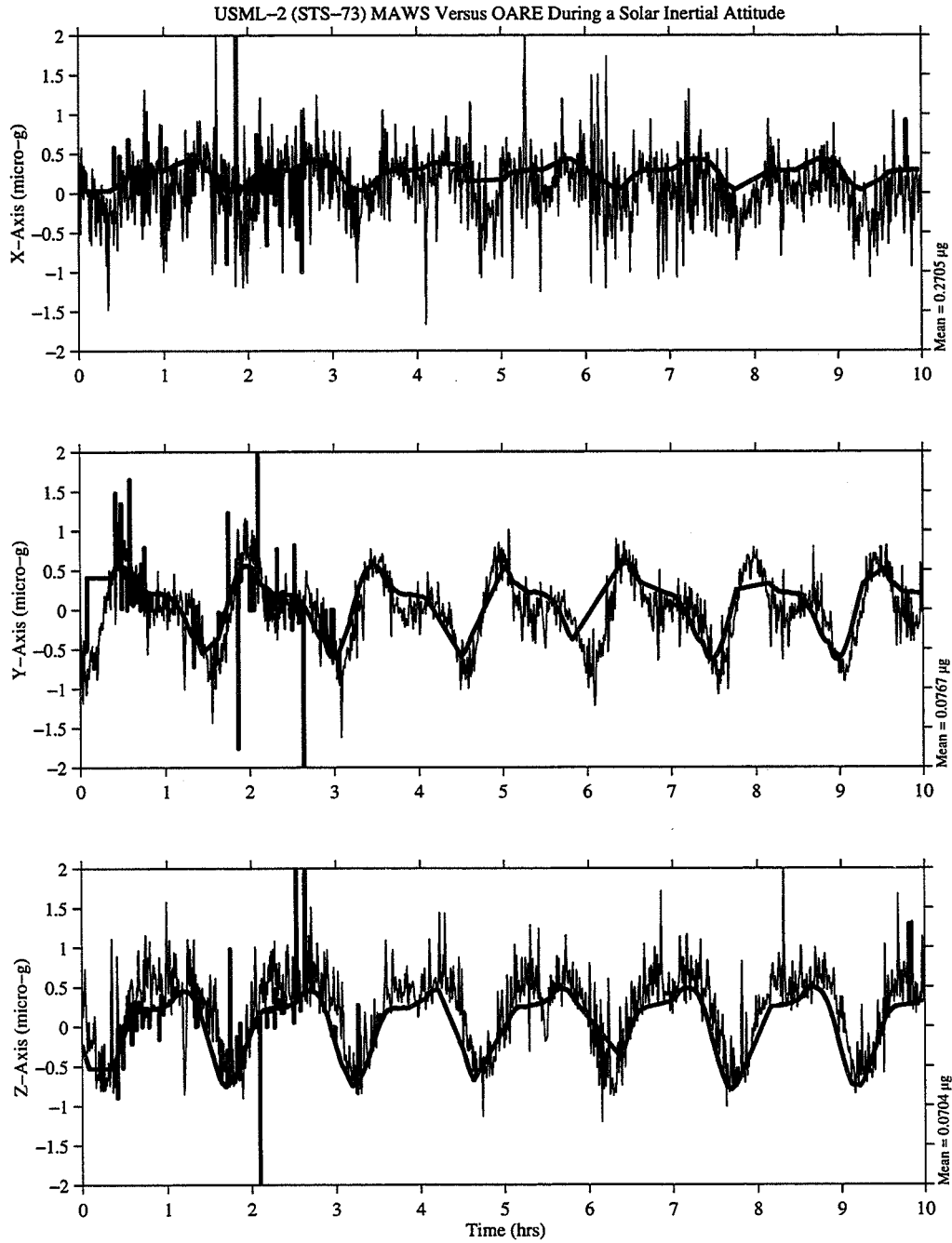
Figure 12: OARE TMF Data During Solar Inertial Attitude from USML-2 (STS-73)

*A Review of Microgravity Levels on Ten OARE Shuttle Missions*

OARE/MAWS Data  
OARE Location

MET Start at 010/18:00:16.920

Frame of Reference: Orbiter  
USML-2  
Body Coordinates



MATLAB: 24-Feb-1998 07:34 pm

**Figure 13: MAWS (Thick Line) Versus OARE TMF Data During Solar Inertial Attitude from USML-2 (STS-73)**

**Paper Number: 3**

# **Review Of MMA Measurements On Four Shuttle Missions**

---

Andreas Schütte, Daimler-Benz Aerospace AG, Bremen, Germany

## **Review Of MMA Measurements On Four Shuttle Missions**

Author:

A. Schütte, Daimler-Benz Aerospace, Bremen, Germany et alii

### **ABSTRACT**

The Microgravity Measurement Assembly (MMA) is a microgravity monitoring system capable of providing investigators and the on-board crew with real-time display of accelerations detected by up to seven sensor heads, five of which can be deployed in racks where microgravity-sensitive investigations are carried out. The MMA has been flown on four Spacelab missions in 1993, 1996 and 1997.

After the first mission a new sensor has been developed to extend the MMA sensitivity into the quasi-steady and low-frequency range. The resolution of this sensor allows the measurement of the residual effects of events with a frequency corresponding to an orbital period directly.

The first preliminary analyses indicate that the atmospheric drag measured corresponds to the theoretical predictions.

### **BACKGROUND**

In April/May 1993 it has been flown successfully on the German Spacelab D-2 mission. The D-2 mission triaxial sensor heads, called Microgravity Sensor Packages (MSPs), are based on capacitive micromechanical silicon-chip technology. They are sensitive to disturbances from  $10^{-5}$  g to  $10^{-2}$  g within the frequency range of 0.1 to 100 Hz. The MMA provided real-time acceleration data to the scientists of the various disciplines involved. Additionally an experiment was performed to determine the transfer function of the Spacelab structure. The excitation with an impulse hammer and the measuring of the responses of the six MSPs in the Spacelab formed the on-board part of this experiment. It complemented the ground reference measurements that had been performed a few months earlier on the fully integrated Spacelab configuration at the Kennedy Space Center.

For the reflight campaign on the LMS mission and the MSL-1/1R missions the MMA has been enhanced by the ASTRE accelerometer (Accéléromètre Spatial Triaxial Electrostatique), which was developed to extend the MMA sensitivity into the quasi-steady and low-frequency range. The ASTRE working principle is based on keeping a proof mass motionless in its nominal position and attitude by means of electrostatic suspension, such that the required electrostatic forces are a direct measure of the three acceleration components. The resolution achieved by ASTRE is  $10^{-9}$  g in the measurement bandwidth DC to 1 Hz.

On ground, the HRM data are continuously acquired and stored by the MMA Ground Station (GST), which complements the flight segment by providing MMA data-processing capabilities during both check-out and mission activities. In particular during the mission, the GST can perform on-line analysis of the measurement output, in both time and frequency domain, using either real-time or play-back data. The GST generates analog recordings from each microgravity sensor (axis by axis) and displays any of them as defined by the operator. In parallel, the GST can produce peak value plots which can be consulted by interested investigators. Using the play-back function, the GST can perform detailed data analysis offering a wealth of tools including zooming, windowing, 3-D displays, Fourier monitor, power-spectrum density, coherence functions.

During the LMS mission and the MSL-1/1R missions the processed MMA data were available to all interested parties via the World Wide Web in near real-time.

### **STATUS OF THE ANALYSES**

The real-time analyses of acceleration data synchronized with the on-board clock helped the scientists to promptly assess the measured vs. required microgravity environment, and to plan for possible corrective actions on their own experiments, like e.g. the repetition of experiment runs where the micro-g levels had been exceeded and the interruption of experiment runs during crew exercise periods. This finally lead to an optimization of experiment operation times and increased scientific results.

The analysis of the Spacelab D-2 Microdynamics Transfer Function Experiments has been performed under technical coordination of ESA and the final report of the Microgravity Dynamics Disturbance Study (MGDD-1) has been published in August 1995.

Currently the analysis of the ASTRE measurements which were recorded during the MSL-1 and MSL-1R mission is in progress, in order to extract the quasi-steady component and correlate them to the orbiter position and attitude data as well as theoretical predictions.

As a first step a data set from the MSL-1R mission from GMT 193/18:00 to 194/04:00 has been analyzed. The first fundamental frequency of this data set corresponds exactly to the orbital period of 90 minutes. The data have then been processed applying two Kalman filters with the first and the second fundamental frequency. The ASTRE x-axis pointed in the direction of the velocity vector since the orbiter attitude "-ZN45DEGROLL" was constant over the investigated period. Therefore the x-axis signal is a measure of the atmospheric drag, which is the perturbation of the highest order in this direction.

The top half of figure 1 shows the individual components of the first (ASTRE X ord1) and the second (ASTRE X ord2) fundamental. The bottom half represents the superimposed signal.

The maxima of the first fundamental and the superimposed signal appear at the local GMT 14:00 with an amplitude of ~0.5 micro-g as predicted, when the orbiter passes the bulge of the atmosphere.

The second fundamental indicates a modulation with a frequency even lower than once per orbit. An analysis correlating the measurements to orbiter position and attitude data as well as perturbation models is currently under progress.

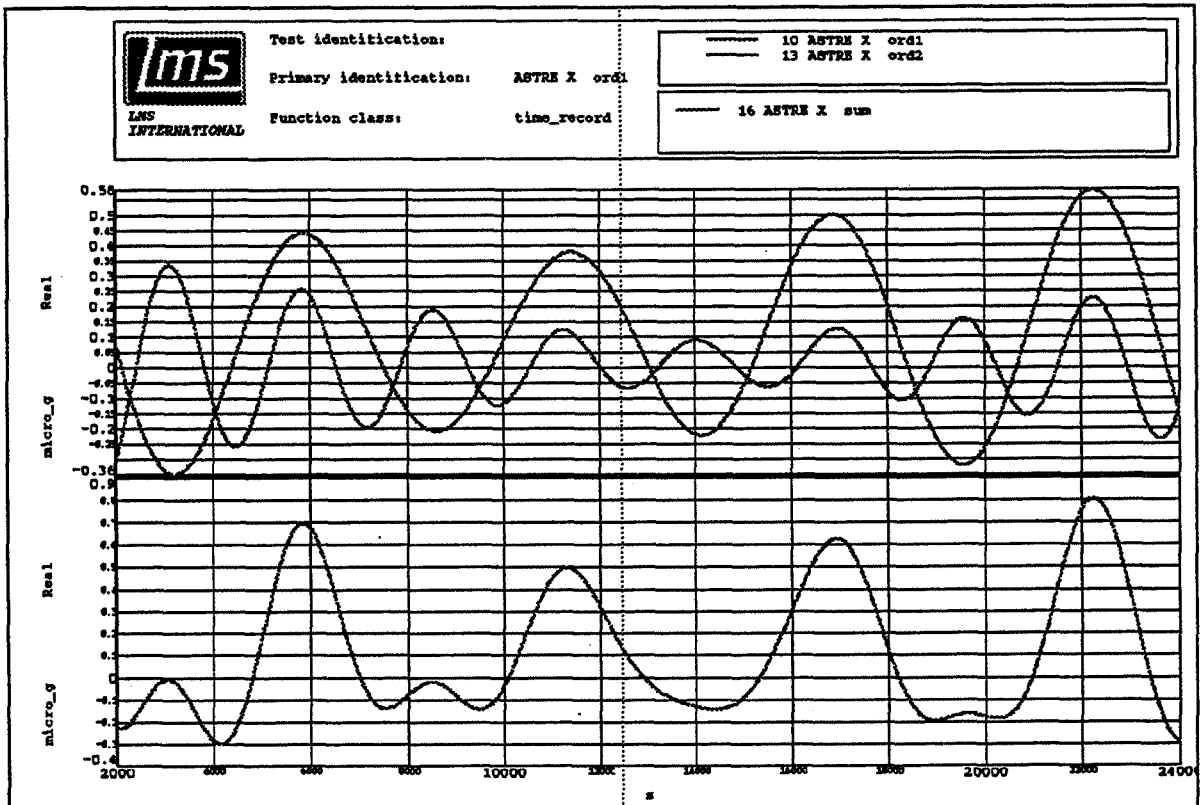


Figure 1: ASTRE x-axis Measurements from the MSL-1R Mission, Start Time: GMT 193/18:00

## **CONCLUSIONS**

Throughout the four missions the MMA provided a valuable and highly appreciated real-time service to the scientific community.

The extension of the sensitivity of the MMA into the quasi-steady and low-frequency range adds to the various possibilities for the utilization of the MMA.

The potential of MMA in view of the operation on the European Columbus Orbiting Facility is higher than exploited up to now.

**Paper Number: 4**

# **Firsthand Perspective on the Microgravity Environment**

---

Dr. Donald A. Thomas, Astronaut Office, NASA Johnson Space Center, Houston, Texas

## **Firsthand Perspective on the Microgravity Environment**

**Don Thomas  
Astronaut Office  
NASA Johnson Space Center**

Extended periods of microgravity simply cannot be created on Earth and rely on orbiting spacecraft in low earth orbit. These low microgravity levels are one of the most critical resources for most experiments being conducted aboard the space shuttle and those proposed for the International Space Station. A second critical resource for successfully conducting many of these experiments in space is the presence of human beings. Trained mission specialists and payload specialists become the eyes and ears of the scientists on the ground. In their function as in-flight technicians and "observers" they are important for reporting first hand the progress of the experiments, as well as being on call to trouble shoot malfunctioning equipment and make necessary repairs. Unfortunately, as important as astronauts are to the successful performance of many experiments, they can be in conflict with the first goal of achieving as pristine a microgravity environment as possible. A simple astronaut sneeze has been calculated to induce a perturbation of  $10^{-5}$  g which may adversely affect some of the more sensitive experiments.

A first hand perspective of what it is like to work in this environment and ways crewmembers can work more effectively to minimize disturbances will be discussed as well as ways that the ground can assist crewmembers to protect the microgravity environment.

### **INTRODUCTION**

In terms of the microgravity environment, there are basically two types of space shuttle missions that are flown. The first category include those missions in which the microgravity environment is of minimal importance. Examples of this type of mission include the Hubble Space Telescope servicing flights (STS-61, 82, 103), Radar Lab flights (STS-59, 68, 101), the International Space Station assembly flights (STS-92, 96, 97, 98, 99, 100) or satellite deploy flights such as the Tracking and Data Relay Satellite deploy flights (STS-6, 26, 29, 43, 54, 70) or the upcoming Advanced X-ray Astrophysics Satellite on STS-93. The primary mission objective of all these flights involve extensive crew activity servicing, assembling, or deploying hardware, and the microgravity environment is of little consequence. An EVA crewmember pounding on a piece of hardware in the payload bay may be considered a highly desirable activity !

The second category of missions are those dedicated exclusively to the microgravity sciences. These have typically consisted of the Spacelab module (Spacelab J, D, IML, LMS, MSL), Spacelab pallet (USMP series: STS-52, 62, 75, 87) and Spacehab flights (STS-57, 60, 63). For these missions the microgravity environment becomes one of the

most important parameters to be monitored and protected. These flights typically carry 4 or more different microgravity measurement devices to fully measure and record the exact microgravity environment, and have these data available to the numerous investigators for both real-time and post-flight analyses. A simple sneeze from one of the astronauts may be picked up by one of these onboard accelerometers, transmitted real-time to the ground, and cause a principal investigator to shudder.

Clearly it is important for the astronauts to make a distinction between these two categories of flights !

## **PROTECTING THE MICROGRAVITY ENVIRONMENT**

### **The Role of the Crew**

One of the most important things that microgravity scientists can do to help minimize crew disturbances and optimize the microgravity environment, is to educate the crew about the importance of low microgravity levels and increase their awareness of microgravity disturbances. And the earlier you can get to the astronauts the better. The ideal time to begin would be to brief new astronaut candidates during their first year of training. It is well worth the effort to plant the seed early that even extremely small disturbances can have a detrimental impact on many experiments. Short video clips showing the effects of normal crew activities such as crew exercise or orbiter burns on molten liquid zones or other free liquid surfaces are excellent ways to get the point across. Summarizing the disturbances measured aboard the space shuttle and Mir during various crew and orbiter activities also need to be reviewed and discussed. The basic goal is to eliminate the notion that there is "zero gravity" up in space and get the astronauts thinking in terms of microgravity disturbances and increase their awareness of what impact these disturbances may have on their primary mission objective, i.e., microgravity science.

Once crew members have become sensitized to the adverse effects of crew induced disturbances, they will typically do all they can to protect the microgravity environment, not only during the flight, but in many preflight planning sessions and reviews as well. For example, when looking at preliminary middeck locker layouts, well trained crew members will be looking at keeping microgravity sensitive payloads such as protein crystals as far away as possible from high traffic areas such as next to the galley, to help minimize crew induced disturbances. And during the mission itself, these same crewmembers will "police" the microgravity environment, and remind the other crew members during those periods of time when extra special care needs to be taken for some of the more sensitive experiments. Reminders in the crew procedures are useful and highly desirable, but on most occasions, a crew member will remind the others to be careful and to minimize disturbances on their own initiative. You might not see it written in the procedures or hear it on the air-to-ground calls, but protecting the microgravity environment becomes a top priority during microgravity science missions.

Once fully aware of the implications of crew induced disturbances, there are many simple things that crewmembers can do to help out. Simple activities like slowly and deliberately

closing a locker door instead of just slamming it shut, or slowly and cautiously transferring large heavy bulky items to keep them under control at all times become important factors in minimizing disturbances, especially given the frequency in which astronauts are required to open and close locker doors and other stowage containers. This will become even more critical during the early era of the International Space Station when crews will be transferring 1000-2000 pound racks from the shuttle to ISS !

One tool that has recently become available to some crews (STS-75 and STS-87) is the capability to view the Space Acceleration Measurement System (SAMS) data in near-real-time on orbit. This feature was used extensively on STS-75, and crew members reported that they could almost use the feedback from SAMS to get the g-levels to very low values. Again, increased awareness contributes directly to fewer disturbances and lower microgravity levels onboard orbiting spacecraft.

### **The Role of the Ground**

Besides the crew being more aware and sensitive to disturbances and working more cautiously and deliberately in space, there are a wide range of things the ground can do both in planning the mission preflight and during the mission itself, that can also contribute to minimizing the onboard disturbances. Based on the experiences of my two Spacelab flights (IML-2 and MSL-1), the one factor which most strongly influences the crew's ability to protect the microgravity environment is being overworked. When they get behind the timeline, crewmembers will always rush to try to catch up. And in the process of rushing around, the slow deliberate movements throughout the lab and slow and easy opening/closing of locker doors are some of the first things to go. When things must be done quickly at the expense of slow careful movements, the microgravity environment will usually suffer. Pushoff loads will always increase for crewmembers rushing around the lab. It would be interesting to compare the background levels observed during those times when crewmembers are being rushed and overworked with those during more relaxed nominal operations. My personal experience tells me there should be a big difference. So while overworking the crew may maximize the quantity of science returned from the mission, the quality of the science may suffer as a result of increased disturbances induced from crewmembers rushing around.

Another factor influencing crew induced disturbances that can be worked on the ground preflight is stowage. I have tried to open some overhead as well as locker drawers in the Spacelab that were so packed, that they were hard to get open and closed again. They required a firm "tug" when opening and an equally firm "shove" on closing. These drawers did not slide out smoothly, but required wrestling by the crew. Some stowage volumes have bulky latches that cannot be easily closed and require pounding and prying to open. Besides being hard on the hands, it can be detrimental to the microgravity environment. Combine these features with a crewmember who is behind the timeline and is rushing, and once again the microgravity environment will suffer even further. More effort in designing "microgravity friendly" stowage would be a large step forward.

Another factor which can affect the microgravity environment is the scheduling and performance of in-flight maintenance (IFM) activities. These off nominal procedures will frequently have crewmembers opening panels, twisting connectors, tightening valves, etc., not to mention pounding with a hammer, that cause unwanted disturbances. It may be desirable to delay the start of an IFM to fix one experiment, until the more sensitive experiments are through their most critical periods. It would be highly desirable to have IFMs coordinated and accounted for in managing the microgravity environment.

Another factor affecting the onboard crew disturbances are the availability of handrails and other crew translation aids. On MSL-1, we flew with an EXPRESS rack that did not have handrails because they were not available in time for flight. Without proper handrails, any protrusions become the default handrails, and these usually involve cables or other sensitive experiment hardware. Crewmember need to hold onto something in getting around, and if handrails aren't provided, the experiments themselves may be utilized to fill that void.

For the transfer of large, massive, bulky equipment, it is strongly desired to have at least two crewmembers scheduled to perform the task. Not only does this help in maintaining positive control of the free floating object, but the additional set of eyes are useful watching out for potential collisions.

## **SUMMARY**

In summary, early education of the astronauts and increased awareness of the detrimental effects of crew and orbiter induced disturbances on many microgravity experiments can have a dramatic influence on how crewmembers work and operate in space. In addition, there are many factors that the ground is in control of that likewise influence the amount of disturbances generated. As experiments are developed and flown that require even lower gravity levels, the recognition and management of the microgravity environment as a critical resource, the same as is done for oxygen or power, will become mandatory. Both crewmembers and the ground teams will need to continue working closely together to take full advantage of the microgravity environment.

# **Fifteen Years of European Experience in Microgravity Characterization-From Spacelab to the International Space Station**

---

Dr. Hans Hamacher, German Aerospace Center (DLR), Koeln, Germany

Hendrik Stark, European Space Agency (ESA), Noordwijk, The Netherlands

Reiner Jilg, ACSYS, Rimsting, Germany

# **Fifteen Years of European Experience in Microgravity Characterization-From Spacelab to the International Space Station**

Authors:

Hans Hamacher, German Aerospace Center (DLR), Koeln, Germany  
Hendrik Stark, European Space Agency (ESA), Noordwijk, The Netherlands  
Reiner Jilg, ACSYS, Rimsting, Germany

## **Abstract**

European activities to characterize the microgravity ( $\mu\text{g}$ -) environment of a space laboratory started with the first Spacelab flight SL-1 in 1983 and was continued until MSL-1 and the 11th mission of the Russian free flyer FOTON (both in 1997). Accordingly, the microgravity measurement technique required to meet the specific needs for onboard detection of the residual acceleration has been gradually developed. The Quasi-Steady Acceleration Measurement System (QSAM) and the Microgravity Measurement System (MMA) are complementary instruments capable for application the International Space Station (ISS).

## **Introduction**

Experimentation under microgravity conditions is a focal point in the European space utilization programs since the late seventies when NASA and ESA agreed to develop Spacelab and to fly it jointly in the first Mission SL-1 in 1983. About two third of the experiments carried out in SL-1 were investigations in materials science and fluid physics which made use of the microgravity environment. The German Spacelab missions D-1 and D-2 (1985 and 1993, respectively) were especially dedicated to microgravity experimentation. ESA designed the unmanned free flyer EURECA (European Retrievable Carrier) which was launched by the Space Shuttle in 1992 to stay in a 500 km orbit for about one year. EURECA-1 carried a nearly 100% microgravity payload. European scientists also participated with microgravity experiments in the IML flights, USML, USMP, LMS and MSL-1. They also contributed  $\mu\text{g}$ -experiments to the Russian space station Mir and to other flight opportunities like the Russian free flying capsule FOTON.

Almost all European microgravity investigations have been accompanied by efforts to measure the residual acceleration within the spacecraft. It started with a single measurement

device of the Materials Science Double Rack (MSDR) of SL-1. The payload of D-2, brought into orbit a decade later, was equipped with the centralized Microgravity Measurement Assembly (MMA) which comprised fixed installed as well as mobile sensors packages. It allowed to transmit real time acceleration data to ground during the mission enabling the experimenters to judge whether the experimental conditions had been reached. The special requirements to detect the low frequency part of the spectrum, most important to many physical phenomena, are met with the Quasi-Steady Acceleration Measurement System (QSAM).

It was recognized soon that microgravity analysis must be guided by the needs of the physical phenomena to be investigated. Like NASA, ESA and European national agencies supported studies to analyze the susceptibility of the physical phenomena to residual acceleration [1-5]. Chief results were sensitivity curves indicating the level of residual acceleration tolerated by experiments versus frequency. Recent investigations emphasis the significance of the direction of residual acceleration with respect to the relevant experiment axis [6]. In the following some of the microgravity measurement activities for Spacelab missions are described briefly.

## **Microgravity Measurement Activities**

### **SL-1 Mission (1983)**

The Material Science Double Rack (MSDR) was one of the very first payload elements to be equipped with an accelerometer system for monitoring the microgravity environment [7]. Even though operated in a peak detection mode to reduce the amount of data, the system provided valuable data for scientists as well as for design and system engineers. These early data revealed the order of magnitude of residual acceleration attainable in Spacelab experiment racks. Some results were truly unique. Owing to the fact that the Space Shuttle was equipped with extensive auxiliary measurement devices in its early flights, the MSDR-sensor data could be related to data of other instruments. For example, a thermally induced stick-slip event, monitored with a strain gauge at the Transfer Tunnel, could be correlated to a sharp spike in the  $\mu\text{g}$ -recording. This "thermal cracking" is an example of a stochastic event which cannot be recognized usually in  $\mu\text{g}$ -measurements. Thermal cracking is an important problem in the prediction of the ISS  $\mu\text{g}$ -environment. SL-1 also gave first valuable experience how to correlate acceleration data to operational disturbing sources. It turned out that continuous onboard video recordings are indispensable means for microgravity data interpretation.

### **D-1 Mission (1985)**

All microgravity payload racks of that mission carried at least one accelerometer [8, 9]. High frequency signal sampling ensured appropriate frequency bandwidth for the experiments and, in combination with extensive onboard video recording, data correlation to many onboard events. D-1 gave some novel insights into Spacelab's on-orbit dynamics and the spectral composition of its acceleration. The achievements effectively forwarded our knowledge to improve experiment hardware design and operation. It demonstrated Spacelab's excellent capability as a carrier for microgravity payloads.

### **D-2 Mission (1993)**

Despite these accomplishments, D-1 also indicated difficulties in the analysis of data which were detected by different autonomous systems. Various investigations, such as transfer function measurements for structural dynamics experiments, call for precise time correlation and accuracy of the data. It was for this and some other fundamental reasons that Spacelab D-2 was equipped with a centralized system, the MMA [10]. It comprised six tri-axial sensors, four of which permanently mounted to experiment racks and two mobile sensor packages for special measurements across the entire Spacelab module. The MMA made use of small size micro-mechanical accelerometers developed by CSEM (Centre Suisse d'Electronique et de Microtechnique S.A., Switzerland), under ESA contract [11]. This sensor allows installation close to the experiment. Another novel feature of the MMA was real-time data transfer capability to ground. During D-2, processed  $\mu\text{g}$ -data were available for the all experimenters in the Payload Operations Control Center in Oberpfaffenhofen, Germany to judge whether the experimental condition had been met. This principle is intended by ESA to be used in the Columbus Orbiting Facility (COF) for interactive experimentation. The MMA also comprised an impulse hammer to measure the structural transfer function under microgravity conditions [12, 13]. The D-2  $\mu\text{g}$ -characterization program included acceleration measurements on ground at the fully integrated Spacelab prior to mission during the Mission Sequence Test. The intention was to investigate the difference between the structural behavior on ground and in orbit, if any. The experiment revealed very interesting and novel results, first of all a higher structural damping in orbit compared to the data measured on ground. Details are given in Ref. [12]. The MMA was also flow on Spacelab missions LMS and MSL-1 [14].

### **Low Frequency Measurement.**

The lower detection limit of the MMA is 0.1 Hz. The measurement of components below this limit, including the d.c. components, requires additional on-orbit calibration to allow absolute acceleration measurement. The instrument QSAM (Quasi-Steady Acceleration Measurement) has been developed for this purpose. Continuous zero-offset elimination is

obtained by periodic signal modulation which is achieved by flipping the sensor sensitive axis. QSAM is a small instrument capable for rack installation. It was successfully flown on IML-2, MSL-1 and the Russian free flyer FOTON. (FOTON-11 mission). QSAM is presently under development for Space Station application [15].

## Conclusions and Outlook

Experimentation in Spacelab has shown that microgravity measurement is an indispensable tool to support scientific experimentation [16]. Spacelab missions have also demonstrated the effectiveness of  $\mu\text{g}$ -measurement in other important areas: to characterize the systems structural dynamics and the systems operational status. Future needs are dictated by the ISS and the needs of its scientific utilization. The measurements within the various ISS modules have to be coordinated and synchronized to obtain a complete picture of the ISS  $\mu\text{g}$ -characteristics. Recent investigations emphasize the particular importance of optimal experiment orientation with respect to the low frequency acceleration vector. Its local measurement is therefore an essential task.

The acceleration measurement systems developed for Spacelab are a solid basis for utilization on the ISS.

## References

- [1] *Langbein, D., Tiby, C.*, "Allowable g - levels for microgravity payloads", Final Report for ESA, Contract No. 5.504/83/F/FS(SC), Batelle Frankfurt, 1984, pp. 1 -24.
- [2] *Alexander, J. I. D.*, "Low gravity experiment sensitivity to residual acceleration: a review", *Microgravity Science and Technology*, 3, 1990, pp. 52 - 68
- [3] *Naumann, R.J.*, "Susceptibility of materials processing experiments to low-level accelerations", NASA CP 2199, 1981, pp. 63 - 68
- [4] *Monti, R., Langbein, D., Favier, J., J.*, "Influence of residual accelerations on fluid physics and materials science experiments", in: "Fluid Sciences and Materials Science in Space", H. U. Walter (ed.), Springer-Verlag, Berlin, 1987, pp. 637 - 680
- [5] *Feuerbacher, B., Hamacher, H., Jilg, R.*, "Compatibility of microgravity experiments with spacecraft disturbances", *ZfW* 12,1988, pp. 145 - 151

- [6] *Monti, R.*, "Microgravity sensitivity of typical fluid experiments", Seventeenth Microgravity Measurements Group meeting, March 24-26, 1998, Cleveland, Ohio
- [7] *Hamacher, H., Merbold, U.*, "The microgravity environment of the Material Science Double Rack During Spacelab-1", *J. Spacecraft & Rockets*, 24,1987, pp. 264 - 269
- [8] *Hamacher, H., Jilg, R., Merbold, U.*, "Analysis of microgravity measurements performed during D1", ESA SP-256, 1987, pp. 413-420
- [9] *Hamacher, H., Fitton, B., Kingdon, J.*, "The environment of earth-orbiting systems", in: "Fluid Sciences and Materials Science in Space", H. U. Walter (ed.), Springer-Verlag, Berlin, 1987, pp. 1 - 50
- [10] *Eilers, D., Gerhard, I., Hofer, B., Rudolf, F., Brungs, W.*, "Microgravity Measurement Assembly (MMA) for Spacelab Module missions", IAF-88-343, 1988, 8 pp.
- [11] *Rudolf, F., Jornod, A., Bergqvist, J., Leuthold, H.*, "Precision accelerometers with  $\mu\text{g}$  resolution", *Sensors and Actuators*, A21-A23, 1990, pp. 297-302
- [12] *Stark, H. R., Oery, H., Hamacher, H.*, "Investigation of structural dynamics under zero-gravity", IAF-97.1.2.08, 48th IAF Congress, 1997, 5 pp.
- [13] *Bluemel, U.*, "The microgravity environment of Spacelab and attempts for its improvement"(in German), DLR-Forschungsbericht 97-33, 1997, 137 pp.
- [14] *Schuette, A.*, "Review of MMA measurements on four Shuttle missions", Seventeenth Microgravity Measurements Group meeting, March 24-26, 1998, Cleveland, Ohio
- [15] *Hamacher, H., Jilg, R., Richter, H.-E.*, "An approach to detect low-frequency acceleration", 24th International Conf. on Environmental Systems and 5th European Symp. on Space Environmental Control Systems", Friedrichshafen, Germany, 1994, paper 941362, 5 pp.
- [16] *Hamacher, H.*, "Microgravity environment conditions - from Spacelab to the International Space Station", *Microgravity Science and Technology*, 11 (1996), 3, pp. 152 -157

**Session B**  
**SUMMARY OF MIR MICROGRAVITY**  
**ENVIRONMENT**

---

Chair: Julio C. Acevedo, NASA Lewis Research Center, Cleveland, Ohio

Paper Number: 6

# **Acceleration Disturbances in the Mir Microgravity Environment**

---

Milton E. Moskowitz, Tal-Cut Company, North Olmsted, Ohio

# **Acceleration Disturbances in the Mir Microgravity Environment**

Author:

Milton E. Moskowitz, Tal-Cut Company, North Olmsted, Ohio

## **Abstract**

The microgravity environment of an orbiting space laboratory (such as Mir) is a complex (and highly dynamic) phenomenon. NASA Lewis Research Center's Space Acceleration Measurement System (SAMS) has recorded approximately 50 GB (about 90 days worth) of acceleration data onboard Mir since its installation in 1994. A number of acceleration sources have been identified including experiment operations, life support systems, crew exercise, attitude control gyroscopes, altitude control thrusters, Shuttle docking/undocking events, and the docking of the Priroda module. Reduced disturbances in the microgravity environment have been noted during crew sleep/rest periods. This paper briefly discusses select disturbances, and the associated presentation shows plots of these data.

## **Accelerometer System Background**

The Space Acceleration Measurement System (SAMS) was developed at the NASA Lewis Research Center (in Cleveland, Ohio) to "provide an acceleration measurement and recording system capable of serving a wide variety of microgravity science and technology experiments." A SAMS unit consists of a main processing box, and up to three remote Triaxial Sensor Heads (TSHs), which may be separated from the main unit by as much as 20 feet [1].

A specially modified SAMS unit was flown to the Mir Space Station aboard the Progress 224 vehicle in late August of 1994. Since that time, SAMS has been used to record the acceleration environment, supporting a variety of U.S. and Russian microgravity experiments. The SAMS unit aboard Mir utilizes two TSHs, one with a cutoff frequency of 100 Hz (sampled at 500 samples per second), the other with a cutoff frequency of 10 Hz (sampled at 50 samples per second). The lower frequency limit of both of these sensors is approximately 0.01 Hz. The absolute value of low frequency (quasi-steady) accelerations are not accurately measured by

---

[1] SAMS Group. Space Acceleration Measurement System. Publication B-0339. Cleveland: NASA LeRC. 1991.

SAMS, and are discounted from further discussions. Shifts in the low-frequency environment are accurately measured, and two such examples will be used in this paper. As of January 1998, almost 50 GB of SAMS data have been recorded aboard Mir. Based upon the sampling rate of the SAMS unit, this correlates to about 90 days worth of recorded data.

## **Characterization of Accelerations**

The Principal Investigator Microgravity Services (PIMS) group at the NASA Lewis Research Center supports microgravity science investigators with acceleration data and interpretation as they evaluate the effects of the microgravity environment on their experiments. The PIMS group produces summary reports (as NASA Technical Memoranda) of the SAMS data recorded aboard Mir. These reports are distributed via the World Wide Web (WWW) and in hardcopy form. The SAMS unit aboard Mir has recorded acceleration disturbances from a wide range of sources. Select sources will be briefly discussed in this paper. For further information, see [2].

Disturbances related to the Mir station itself produce some of the most consistent acceleration sources. These include operations of the Vozdukh (BKV-3) dehumidifier, life support system fans, vehicle structural modes, and operations of the gyrodynes used for attitude control. The BKV-3 is characterized by a fundamental frequency around 24.2-24.4 Hz, and has measured accelerations in excess of  $1,700 \mu\text{g}_{\text{RMS}}$  (recorded in the Priroda module). The life support system fans in the Priroda module operate nominally in the 38-44 Hz region, and have been measured in excess of  $1,200 \mu\text{g}_{\text{RMS}}$ . The vehicle structural modes depend upon the physical configuration of Mir, but have generally been observed between 0.5 and 7.5 Hz. The gyrodynes, used for attitude control, operate at a nominal speed of 10,000 rpm ( $\sim 166.7$  Hz). Occasionally, they are spun-down (stopped) and spun-up (restarted). SAMS data recorded during these events show a slow (3-4 hour) ramp-up or ramp-down of an acceleration disturbance between 0 Hz (stopped), and 166.7 Hz (full speed).

The docking of Progress, Soyuz, Mir modules, and the Space Shuttle to the Mir Space Station have all been recorded by SAMS. In general, the larger the craft, the larger the effect to the microgravity environment. Docking and undocking activities of the Space Shuttle have shown not only a shift in vehicle structural modes, but also a transmission of acceleration disturbances (i.e. compressors, pumps, etc.) between the vehicles. While docked, the two vehicles form a single complex, this causing the shift in structural modes. A docking of the Priroda module caused a shift in structural modes, but no vibratory transfer was apparent since

---

[2] URL: <http://www.lerc.nasa.gov/www/MMAP/PIMS>

there were no powered-on experiments in the module at the time of docking. Docking of the Soyuz and Progress vehicles impart less of a microgravity impact, most likely due to their relatively small size.

A firing of a Progress vehicle's engine resulted in a 50 second duration acceleration of 2,300  $\mu\text{g}$ . Another Progress engine firing test was conducted, measuring 400  $\mu\text{g}$  for a 6.5 minute duration.

Crew exercise results in primary frequencies between 1 and 2.5 Hz, harmonics of the primary frequencies, and an increased excitation of structural modes. The magnitude of the primary excitations are varied based upon the crew member's exertion level, exercise type (treadmill or velo-ergometer), exercise location, and acceleration recording location, but will typically be in the 100-1000  $\mu\text{g}_{\text{RMS}}$  neighborhood.

Overall, about 70-75% of the ambient RMS acceleration magnitude (in the 0.01-100 Hz region) is caused by life-support systems (BKV-3, fans, etc.) [3].

During crew rest or sleep periods, reduced acceleration disturbances (in the region under about 10 Hz) have been noted. This reduction is presumably due to reduced crew activity (i.e. no push-offs, etc.), and reduced equipment activity (crew-run experiments are not run while the crew is sleeping).

## Summary

Since its installation in 1994, the Space Acceleration Measurement System (SAMS) has recorded about 50 GB of acceleration data from Mir. The SAMS aboard Mir utilizes two sensor heads to record accelerations in the 0.01-100 Hz and 0.01-10 Hz frequency regimes, at two (potentially) different recording locations. About 50 GB of data have been recorded by SAMS aboard Mir.

The PIMS group (at NASA Lewis Research Center) publishes NASA Technical Memoranda which contain summaries of the SAMS data recorded aboard Mir. Information regarding these reports may be obtained by contacting the PIMS Project manager via e-mail at "pims@lerc.nasa.gov".

A number of acceleration disturbance sources have been identified. These include operations of the Vozdukh dehumidifier (24.2-24.4 Hz), life support systems (38-44 Hz), vehicle structural modes (0.5-7.5 Hz), attitude control gyrodynes (166.7 Hz), vehicle docking

---

[3] Moskowitz, Milton E., Kenneth Hrovat, Robert Finkelstein, and Timothy Reckart. SAMS Acceleration Measurements on Mir from September 1996 to January 1997. Cleveland: NASA LeRC, December 1997. NASA TM 97-206320.

and undocking activities (changes in structural modes, transmission of vibrations), Progress vehicle engine firings (steady-state acceleration shifts), and crew exercise (1.0-2.5 Hz).

The vast majority of the microgravity disturbances aboard Mir are related to the operations of life-support systems, such as fans (to circulate air), and the Vozdukh BKV-3 compressor (a dehumidifier system).

The microgravity environment aboard Mir is highly dynamic. Many of these acceleration disturbances are unavoidable (i.e. life support systems). Some of these acceleration events may be avoided (i.e. crew exercise, gyrodyne spin-up/down, docking/undocking activities) if a proper timeline is adhered to.

For experiments which are sensitive to the microgravity environment, a measurement system (such as SAMS) provides the ability to record the acceleration environment to which the experiment was subjected. During the analysis of an experiment, these acceleration records may be used to correlate acceleration sources and disturbances with effects (if any) which were observed by the investigator. Such correlation may help to understand the phenomenon being studied, and may assist with future experiment preparations by helping the experimenter plan timelines, experiment locations, etc.

omit this  
page

Paper Number: 7

## Acceleration Measurements with MIM on Mir and Shuttle Mission STS-85

---

Bjarni V. Tryggvason, Canadian Space Agency, Montreal, Quebec, Canada

William Y. Stewart, Canadian Space Agency, Montreal, Quebec, Canada

Jean de Carufel, Canadian Space Agency, Montreal, Quebec, Canada

Lawrence Vezina, Canadian Space Agency, Montreal, Quebec, Canada

**PAPER NOT AVAILABLE**

57-29

Paper Number: 8

# **Gravitational Sensitivity Analysis of Microgravity Environment on Mir Space Station**

---

Prof. Vadim Polezhaev, Russian Academy of Sciences, Moscow, Russia

# **Gravitational Sensitivity Analysis of Microgravity Environment on Mir Space Station**

Author:

Prof. V. I. Polezhaev, The Institute for Problems in Mechanics,  
Russian Academy of Sciences, Moscow, Russia

## **ABSTRACT**

A comprehensive data of microgravity environment on MIR station are available now due to measurements with the use SAMS system during last years. The paper presents results of analysis convective processes in realistic microgravity environment on MIR orbital station using SAMS data during 1995-1997 missions on the basis of mathematical models for Boussinesq and non-Boussinesq media. A hierarchy of two dimensional and three dimensional unsteady models and numerical codes on the basis of Navier Stokes equations are developed for this goal.

Preparation of measurements of microacceleration data for the direct use in computer codes is developed. Comparisons of measurements and calculations of microaccelerations are done. Gravity gradient, rotation of spacecraft, and vibrations are take in account for these models. Low frequency and high frequency regimes are discussed. Two dimensional model is used for quick analysis and video presentation with the use of possibilities of computer system COMGA. Computer laboratory in microgravity on the basis of this system and it's possibility for analysis of gravitational sensitivity in future ISS projects are discussed.

Comparisons of the results using Mir and Shuttle microacceleration data are presented.

Spatial effects of concentration inhomogeneities for low and high frequency regimes are discussed. Impact of microacceleration environment on near-critical convection is discussed. Idea of convective sensor for benchmark of convection models in realistic microgravity environment is also discussed.

## **1. INTRODUCTION. GOALS AND GENERAL CONCEPT OF GRAVITATIONAL SENSITIVITY ANALYSIS**

General concept of microgravity research in the ISS Era should be formulated as "conquest of the Microgravity World". It means elimination a number of side effects of the low gravity, which appear in the field of fundamental physics, measurement of physical properties ("convective contamination") and material processing (macro- and microsegregation, induced by residual convection). Besides these problem benchmark of mathematical models in microgravity environment may be of interest, specifically for compressible nonboussinesq and near critical processes [1-6].

The paper presents results of analysis convective processes in realistic microgravity environment on MIR orbital station using SAMS data during 1995-1997 missions on the basis of mathematical models, following general conception of the research seminar on Microgravity Mechanics and Gravitationally Sensitive Systems by guidance of Prof. V.I. Polezhaev and Prof. V.V. Sazonov, started in September 1997, in the Institute for Problems in Mechanics, Russian Academy of Sciences for discussion statements of the problems with gravitationally - sensitive systems which have to be studied in space experiments, microaccelerations and certification of spacecraft, mathematical models, using realistic microgravity environment and tools for analyzing of spatially-temporal behavior of gravitationally-sensitive processes.

## **2. MICROGRAVITY ENVIRONMENT ON THE ORBITAL STATION "MIR".**

Comprehensive data of microgravity environment on MIR station provided by the measurements with the use SAMS system presented [7-10]. Comparisons of measurements and calculations of microaccelerations are done. Gravity gradient, rotation of spacecraft, and vibrations are taken in account for these models. Low frequency and high frequency regimes are discussed. Theoretical prediction of the quasistatic component and measurement data analysis for the use in computer fluid dynamics models. Preparation of measurements of microacceleration data for the direct use in computer codes is also done [8].

### **3. MODELS/CODES AND RESULTS OF GRAVITATIONAL SENSITIVITY ANALYSIS IN REALISTIC MICROGRAVITY ENVIRONMENT**

A hierarchy of two dimensional and three dimensional unsteady models and numerical codes on the basis of Navier Stokes equations for Boussinesq and non-Boussinesq media are developed for this goal. Two dimensional model is used for quick analysis and video presentation with the use of possibilities of computer system COMGA. Computer laboratory in microgravity on the basis of this system and it's possibility for analysis of gravitational sensitivity in future ISS projects are done. Comparisons of the results using MIR and SHUTTLE microacceleration data are presented in [5-6]. Spatial effects of concentration inhomogeneities for low and high frequency regimes are discussed. Impact of microacceleration environment on near critical convection convection is studied in space experiments [12]. Quick analysis of the "convective contamination" and video presentation on the basis of 2D models (effects of concentration inhomogeneities) presented in [9]. Most complicated model is developed on the basis of three dimensional unsteady Navier-Stokes equations for a model of microgravity system.

### **4. A SYSTEM FOR ANALYSIS AND CONTROL OF THE CONVECTIVE PROCESSES ABOARD OF SPACE STATION.**

Idea of convective sensor for benchmark of convection models in realistic microgravity environment is appeared many years ago in [2 ] and discussed in a number of our previous works[5,6,13]. Objectives of the system is benchmark of convection models in microgravity (three dimensional controlled initial and boundary conditions unsteady dependency, nonboussinesq effects, average convective motions etc.), prediction of gravitational three dimensional unsteady numerical simulation of convection in enclosure using spacecraft sensitivity in realistic microgravity environment (convective sensor), control of convection for accelerometer's data fundamental research and material processes during different flight regimes, evaluation of the low frequency microaccelerations and connection of the numerical simulation of convection in enclosure with the results of the measurements. New version of hardware Dakon is created [13].

Model of thermal convection in the convective cell under space flight microgravity environment three dimensional unsteady convection (Boussinesq approach) in cylindrical cell taken into account rotation, angle accelerations, gravity gradient, aerodynamic's drag and precise controlled temperature boundary conditions. Calculation of the thermal convection for

Dakon cell for the orbital station "MIR" flight is realized for low and high frequency components of accelerations for nondimensional temperature difference in crosssections of the cylinder. Time dependency of the isolines of the temperature difference between convective and diffusive regimes is presented in the Video.

## 5. CONCLUSIONS.

Conquest of the Mg World in the ISS Era needs scientific coordination support and efforts for measurement, documentation of the Mg environment, damping of vibration using isolation's platforms and more close interface between fluid flow computer models in realistic microgravity environment for benchmark and control.. Software for theoretical calculation and analysis of the microaccelerations data in the computer's readable form, an interface of the fluid flow computer models in realistic microgravity environment, two dimensional model for the compressible Navier -Stokes equations for near critical fluid, three dimensional model for realistic spatial/temporal behaviour of the convection in cylindrical enclosure are developed. "Dakon" hardware for measurement of the convection aboard Space Station and software for operative analysis, comparison and control of the temperature field is created. Calculations for realistic microgravity environment using theoretical models and measurements on Mir station are done.

## REFERENCES

1. Polezhaev V.I. and Fedyushkin A.I., *Izv. Akad. Nauk SSSR, Mekhan. Zhidk. i Gaza*, No.3, 1980,pp. 11-18, (in Russian).
2. Polezhaev V.I., et al, *Convective processes in microgravity*, Moscow, Nauka, 1991 (in Russian)
3. Alexander J.I.D, *J. Crystal Growth* 97, 1989, pp. 285-302.
4. Alexander J.I.D, *J. Crystal Growth* 113, 1991, pp., 21-38.
5. V.I.Polezhaev. *Microacceleration Regimes, Gravitational Sensitivity and Methods of Analyzing Technological Experiments in Microgravity*. A translation of *Izvestia Rossiiskoi Akademii Nauk - Mekhanika Zhidkosti i Gaza*, Vol.29, No.5, Sept.-Oct., 1994, Publications Fluid Dynamics, Plenum Publishing Corporation, New York, March, 1995, 608-619.
6. Polezhaev V.I. *Toward the quantitative analysis and control of convective processes in microgravity*. In: *Microgravity Quarterly*, 1994, vol. 4, N 4, "Highlights of the

- International Workshop on Non-Gravitational Mechanisms of Convection and Heat/Mass Transfer", p.241-246.
7. R. DeLombard, S.B. Ryabukha, K. Hrovat, M.Moskovitz Further analysis of the microgravity environment on Mir Space station during Mir-16. NASA Technical Memorandum 107239, June 1996
  8. V.V.Sazonov, M.M.Komarov, S.G.Zykov, M.Yu.Belyaev, V.M.Stazhkov. Evaluation of the quasi-state component of the acceleration on board the STS-60 orbiter. Microgravity Measurement Group Meeting, N 14, 21-23, March 1995, Meeting Minutes.
  9. V.V. Sazonov, M.M. Komarov, V.I.Polezhaev, S.A. Nikitin, M.K.Ermakov, V.M.Stazhkov, S.G.Zykov, S.B. Ryabukha, J.Acevedo, E.L.Liberman. Microaccelerations on board the Mir orbital station and quick analysis of the gravitational sensitivity of convective heat/mass transfer processes Keldysh Institute of Applied Mathematics RAS, Preprint N 50, 1997
  10. Sazonov V.V., Ermakov M.K., Ivanov A.I. Measurements of the microaccelerations on the "MIR" orbital station during experiments with the use of Alice-1 instrument (in Russian) "Kosmicheskie issledovaniya", 1997 (in press)
  11. Polezhaev V.I , Ermakov M.K., Griaznov V.L., Nikitin C.A.and Pavlovsky D.S. Computer laboratory on convective processes in Microgravity: Concepts, Current Results and Perspective, 46th Intern. Astron. Congress. Oct. 2-6, 1995, Oslo, Norway, IAF-95 - J.3.11, 9p.
  12. S.V.Avdeev, A.I.Ivanov, A.Kalmikov, A.A.Gorbunov, S.A.Nikitin, V.I.Polezhaev, G.F.Putin, A.V.Zuzgin, V.V.Sazonov, D.Beysens, Y.Garrabos, B.Zappoli, T.Frolich. Experiments in the far and near critical fluid aboard Mir Station with the use of the "Alice-1" instrument. Proc. Joint Xth Europ. and VIth Russian Symposium on Physical Sciences in Microgravity. St.Petersburg, Russia, 15-20 June 1997, Vol.1, 333-340.
  13. Bogatirev G.P., Putin G.F., Polezhaev V.I. A system for Measurement of convection aboard of Space Station, Proc. 3rd Microgravity Fluid Physics Conference, Cleveland, Ohio, July, 13-15, 1996, 813-818.

**Session C**  
**ISS MICROGRAVITY ENVIRONMENT**

---

Chair: Dr. Allen M. Karchmer, NASA Lewis Research Center, Cleveland, Ohio

58-29

Paper Number: 9

# **Introduction of International Microgravity Strategic Planning Group**

---

Robert Rhome, Code UG, NASA Headquarters, Washington, DC

# **Introduction of International Microgravity Strategic Planning Group**

Author:

Robert Rhome, Code UG, NASA Headquarters, Washington, DC

## **Summary**

Established in May 6, 1995, the purpose of this International Strategic Planning Group for Microgravity Science and Applications Research is to develop and update, at least on a biennial basis, an International Strategic Plan for Microgravity Science and Applications Research. The member space agencies have agreed to contribute to the development of a Strategic Plan, and seek the implementation of the cooperative programs defined in this Plan. The emphasis of this plan is the coordination of hardware construction and utilization within the various areas of research including biotechnology, combustion science, fluid physics, materials science and other special topics in physical sciences. We are meeting in Cleveland this week to complete the initial development of that plan.

The Microgravity Science and Applications International Strategic Plan is a joint effort by the present members - ASI, CNES, CSA, DLR, ESA, NASA, and NASDA. It represents the consensus from a series of discussions held within the International Microgravity Strategic Planning Group (IMSPG) In 1996 several space agencies initiated multilateral discussions on how to improve the effectiveness of international microgravity research during the upcoming Space Station era. These discussions led to a recognition of the need for a comprehensive strategic plan for international microgravity research that would provide a framework for co-operation between international agencies.

The Strategic Plan is intended to provide a basis for inter-agency co-ordination and co-operation in microgravity research in the environment of the International Space Station (ISS) era. This will be accomplished through analysis of the interests and goals of each participating agency and identification of mutual interests and program compatibilities. The Plan provides a framework for maximizing the productivity of space-based research for the benefit of our societies.

I am pleased to introduce to you the principal representatives of the member agencies of the IMSPG:

**Canadian Space Agency (CSA)**

Dr. Philip Gregory

Dr. Rodney Herring

**European Space Agency (ESA)**

Dr. Gunther Seibert

Dr. Hannes Walter (IMSPG Co-Chairman)

**French Space Agency (CNES)**

Dr. Bernard Zappoli

Mr. Gerard Cambon

**German Space Agency (DLR)**

Dr. Rainer Kuhl

**Italian Space Agency (ASI)**

Dr. Jean Sabbagh (ASI)

Dr. Carlo Mirra (MARS)

**National Space Development Agency of Japan (NASDA)**

Dr. Shinichi Yoda (NASDA)

Mr. Tai Nakamura (NASDA)

Mr. Makoto Natsuisaka (NASDA)

**National Aeronautics and Space Administration (NASA)**

Dr. Brad Carpenter (IMSPG Co-Chairman)

Dr. Mike Wargo

Ms. Judee Robey

Dr. Roger Crouch

We also are pleased to introduce representatives from three other international agencies/organizations who are participating in the IMPSG meetings as observers:

**National Space Agency Ukraine (NSAU)**

Dr. Oleg P. Fedorov

Dr. Victor F. Los

**National Institute for Space Research - Brazil (INPE)**

Dr. Irajá N. Bandeira

Dr. Demetrio B. Neto

**Institute for Problems in Mechanics - Russian Academy of Sciences (RAS)**

Dr. Vadim Polezhaev

59-29

Paper Number: 10

## Quasi-Steady State Microgravity Performance Assessment

---

Michael Laible, Boeing Company, Houston, Texas

# **Quasi-Steady State Microgravity Performance Assessment**

Author:

Michael Laible, Boeing Company, Houston, Texas

## **Background**

Quasi-steady state microgravity performance assessment was carried out for flights UF-1, 13A, 1JA and the Assembly Complete configuration of the Rev. C Assembly Sequence for the Design Analysis Cycle (DAC) 6. Results from this assessment (TDS 6.3-3) are used to evaluate Assembly Complete microgravity performance requirements compliance and assembly stage microgravity performance.

The Assembly Complete microgravity requirements are summarized as follows: In at least 50% of the International Standard Payload Rack locations, while in microgravity mode 1) the peak quasi-steady state ( $f \leq 0.01$  Hz.) acceleration must be less than or equal to  $1.0 \mu g$  and 2) the instantaneous acceleration component perpendicular to the orbit-average acceleration vector direction must be less than or equal to  $0.2 \mu g$ .

The system level quasi-steady microgravity requirements flow down to the segment specifications and PIDS as an allocation of  $0.02 \mu g$  on individual disturbances, excluding the effects of gravity gradient, and aerodynamic drag. The US LAB and HAB each have an allocation of  $0.04 \mu g$  for all of their combined quasi-steady microgravity disturbances. This assessment did not include the effects of individual disturbances. Individual disturbance results from DAC5 are still valid.

## **Discussion/Assumptions**

The quasi-steady state microgravity assessment was performed using multi-rigid-body dynamic simulation techniques which model the GN&C non-propulsive attitude control system and sun-tracking photovoltaic arrays. US solar arrays ideally tracked solar alpha and beta angles and RS SM and SPP solar arrays tracked solar alpha angle with continuous rotation at orbit rate. In reality, the SM joints step at  $26^\circ$  intervals. This “ratcheting” effect was not modeled since the torque commands are small compared to the pitch gravity gradient torque

derivatives, and would also be considered transient. The SPP has a “zeta” joint to allow for out of plane sun tracking, but at low solar beta angles, this joint is locked with the solar arrays parallel to the truss. Finally, the Thermal Radiator Rotary Joint was not modeled since it is considered to be a transient disturbance and was placed at 0 degrees. These assumptions are consistent with the GN&C simulations and capture the dominant aerodynamic effects.

The Assembly Complete configuration included the ESA Columbus Orbital Facility (COF), the Centrifuge module, and the JEM-PM. For micro-g compliance assessment quasi-steady accelerations and stability were calculated at the center of each International Standard Payload Rack (ISPR) location within the U.S. Lab, NASDA JEM-PM, and ESA-COF. Additional quasi-steady accelerations were obtained at the JEM-EF payload locations, two CAM positions, and attached payload locations for S1 and P1 System level quasi-steady microgravity requirements do not apply to payloads within the Russian Segment; hence, performance metrics do not include any of those locations. The NASDA JEM-PM and COF ISPRs were moved in the station X direction 4.27 feet to accommodate for the ISA Node 2 extension.

In accordance with SSP50036A, “Microgravity Control Plan,” the analysis conditions were based on the manifested rendezvous altitude and date of the stage following AC, assuming a 51.6° orbit inclination and 0° solar beta angle. The NASA maximum solar flux and geomagnetic index and most likely solar cycle 23 start date were used for each case. The specific operating condition was that of a 2ATV launch date since that was the end of the first microgravity period greater than 30 days. In addition, two mature operations scenarios were assessed with operating conditions at 24LF and 13 HTV. These cases were analyzed because of the positions with respect to the altitude profile and the minimum micro-g altitude curve, and provide an envelope of expected quasi-steady acceleration levels over the 10 year mature operational life of ISS. The minimum micro-g altitude curve is a constant density curve while varying solar flux and plotting altitude. Atmospheric density was calculated using the Marshall Engineering Thermospheric (MET) density model, and the aerodynamic model assumed a 60% diffuse – 40% specular reflection of particles per the GN&C AIT aerodynamic assumptions.

## **Analytical Models**

The mass properties for the Assembly Complete assessment were based on the DAC6, Rev C Assembly Sequence. These mass properties and geometries were delivered by Lockheed in the form of IDEAS solid models, per Technical Task Agreement JT-33, Assembly Configuration Modeling.

The NASA maximum atmosphere statistics are documented in SSP30425 Rev. B, “Space Station Program Natural Environment Definition for Design,” with dates shifted minus 13 months to reflect the most likely start date of the solar cycle.

The analysis tool used for this assessment was the Space Station Multi- Rigid-Body Simulator (SSMRBS), Vb1.8. The McDonnell Douglas Space Station Attitude Control System was modeled in this simulation tool, and the attitude controller gains were provided by the GN&C AIT.

The microgravity simulations modeled the US solar arrays to be perfectly sun-tracking and the RS SPP and Service Module arrays to be solar alpha angle tracking at 360° per orbit. The SPP zeta joint was not modeled, and the SM/FGB “ratcheting” effect was not modeled.

## Summary of Results

The baseline DAC6 Assembly Complete configuration was found to be non-compliant with the quasi-steady state microgravity performance requirements with only 14 ISPR locations (44%) meeting both the magnitude and stability criteria simultaneously. The 50% ISPR threshold was achieved for the combined criteria of 1.2  $\mu\text{g}$  magnitude and 0.2  $\mu\text{g}$  stability. 27 ISPR locations, (84%) were found to meet this 1.5  $\mu\text{g}$  level. Stability performance was not an issue since the post-assembly complete altitude strategy was defined to support microgravity stability performance. The following list summarizes the quasi-steady magnitude performance within each partner laboratory at Assembly Complete:

- US LAB: 12 ISPRs  $\leq$  1.0  $\mu\text{g}$
- JEM-PM: 0 ISPRs  $\leq$  1.0  $\mu\text{g}$ , 1 ISPRs  $\leq$  1.3  $\mu\text{g}$ , 10 ISPRs  $<$  1.7  $\mu\text{g}$
- ESA-COF: 2 ISPRs  $\leq$  1.0  $\mu\text{g}$ , 3 ISPRs  $\leq$  1.3  $\mu\text{g}$ , 10 ISPRs  $<$  1.7  $\mu\text{g}$

The two mature operation assessments (24LF and 13 HTV) were assessed for comparison. The 24LF case was picked because it was at the minimum micro-g altitude and the 13 HTV was deemed to be worse case because it was the furthest under the minimum micro-g altitude (Note, that there is an approximate three year period when the microgravity altitude cannot be achieved due to Russian altitude constraints, and hence during which degraded quasi-steady performance is expected.). The 24LF case showed to have comparable performance as the AC case. The 13 HTV case proved to be significantly degraded performance, as would be expected. This case should capture worse case conditions expected during mature operations. The following list summarizes the quasi-steady magnitude performance within each partner laboratory at the worse

case conditions, 13HTV:

- US LAB: 10 ISPRs  $\leq 1.0 \mu\text{g}$ , 12 ISPRs  $\leq 1.1 \mu\text{g}$
- JEM-PM: 0 ISPRs  $\leq 1.0 \mu\text{g}$ , 1 ISPRs  $\leq 1.3 \mu\text{g}$ , 10 ISPRs  $< 1.8 \mu\text{g}$
- ESA-COF: 0 ISPRs  $\leq 1.0 \mu\text{g}$ , 2 ISPRs  $\leq 1.3 \mu\text{g}$ , 10 ISPRs  $< 1.8 \mu\text{g}$

The DAC6 Assembly Complete performance was better compared to DAC5, where 10 ISPRs met the quasi-steady microgravity requirements. It should be noted that two of the COF ISPRs are not ARIS compatible.

## **Conclusions and Issues**

Results from this assessment indicate that the Assembly Complete configuration of the International Space Station remains non-compliant with the quasi-steady microgravity specifications. This issue remains open since DAC2, and the resolution plan is unchanged (RDMA #3175). Rev C performance is slightly better than Rev B performance due to mass distribution and delayed assembly complete timeframe. A parametric study will be performed to assess the ability to meet the Quasi-steady requirement with the current configuration. The quasi-steady performance is highly dependent on torque equilibrium attitude which is a function of configuration/mass properties, gravity gradient torques, and aerodynamic parameters. Such parameters as mass, Ballistic number, and ISPR locations will be assessed to quantify the ability to meet the quasi-steady requirements. Otherwise configuration modification or requirements change will be needed for compliance resolution. Final recommendations will be submitted to the appropriate teams.

510-29

**Paper Number: 11**

# **Review of DAC-6 Microgravity Environment**

---

Sreekumar K. Thampi, Boeing Company, Houston, Texas

## **Review of DAC-6 Microgravity Environment**

Author:

Sree Thampi, Boeing Company, Houston, Texas

### **Background**

The Microgravity “vibratory” performance assessment of the International Space Station (ISS) is comprised of a structural dynamic and a vibroacoustic analysis of the ISS Assembly Complete (AC) vehicle configuration. This paper summarizes the structural dynamic analysis which was performed for Design Analysis Cycle No.6 (DAC-6). The analysis predicts the acceleration response at the internal user payload locations due to disturbances occurring during the microgravity mode of operation. The response attenuation provided by the Active Rack Isolation System (ARIS) is reflected in these predictions.

The acceleration responses are assessed against the various segment and overall system requirements (SSP 41162D and SSP 41000D) that specify the allowable acceleration environment at the internal user payload locations. Two microgravity vibratory specifications are used here as metrics. The first requirement applies to the total root-mean-square (RMS) acceleration magnitude which is produced at the internal payload structural mounting interfaces by a set of disturbance sources occurring simultaneously within any 100 second time window. The acceleration response limit of the various Product Groups (PG) and International Partners (IP) depends on their sub-allocation of the System allowable which is apportioned on a root-sum-square basis. The second requirement is a transient acceleration limit for individual transient disturbances which is comprised of two components: an instantaneous magnitude limit of 1000  $\mu\text{g}$  per axis, and an integrated acceleration limit of 10  $\mu\text{g}$  -seconds over any 10-second interval.

### **Discussions/Assumptions**

Finite element model simulations are used to calculate the acceleration responses at the internal user payload locations due to vibratory force and moment inputs throughout the ISS. These disturbance inputs are provided by various PG’s and IP’s based on analytical studies or test measurements of their respective disturbance sources. Disturbance sources considered for DAC-6 analysis are the

“tall poles” identified in the previous DAC-4 analysis. This includes all DAC-4 disturbances contributing 20% or more to the system vibratory power in each 1/3 octave band between 0.01 to 50 Hz. Following is a list of disturbances considered for DAC-6 analysis.

#### **Transient Disturbances:**

1. Lab Vacuum Exhaust T-Vent: The disturbance from a vent blowdown event is modeled as an exponential decay with a time constant of 6 seconds and initial force of 4 lbs.
2. Airlock Solenoid Valves: The disturbance from solenoid valve operation is modeled as a positive rectangular pulse, 7.5 lb in magnitude, 0.1 second duration followed by a negative pulse, - 75.0 lb. magnitude and 0.01 second duration.
3. Airlock Relief Valves: The disturbance from relief valve operation is modeled as a positive rectangular pulse, 7.5 lb in magnitude, 0.2 second duration, and followed by a negative pulse, -75.0 lb. in magnitude and 0.02 second duration.
4. Science Power Platform (SPP) Solar Array: The disturbance due to the SPP Solar Array operation is modeled by a series of rectangular pulses of 0.1 second duration and 1 second spacing. The magnitude of pulses representing rotation about SPP is 2390 in. lb. and rotation of arrays is 885 in.lb.
5. SPP Radiator: The disturbance due to SPP Radiator operation is modeled by a series of rectangular pulses, 347 in. lb. magnitude, 0.1 second duration and 5 second spacing.
6. Thermal Radiator Rotary Joint (TRRJ) Slew: The thermal radiators periodically perform a 180° slew to prevent them from rotating through a complete circle during normal tracking and a large slew, up to 90° , to reorient themselves towards Earth to prevent freezing after the ISS goes into Earth’s shadow. The transient disturbance due to this slew motion was evaluated considering a baseline slew rate of 0.75 %/sec. and an acceleration rate of 0.01%/sec<sup>2</sup>.

#### **Steady State Disturbances:**

1. KU Band Antenna: The disturbances due to KU Band antenna operation in its slew, search, and tracking modes are determined through analytical simulations. The base forces and moments were provided in 1/3 octave band format and represent the envelope of six disturbance cases covering the various operational modes. The disturbances represent the combined output of both upper and lower gimbals.
2. Control Moment Gyros: The disturbances from CMG operation are primarily due to rotor imbalance and are based on test data. The measurements were made for nominal CMG operating speed of 6600 rpm. The base forces and moments were provided in 1/3 octave band format.
3. Ergometer: . There are two ergometers in the manifest - an isolated ergometer in the US Lab, and a non-isolated ergometer in the Russian Service Module (SM). The disturbance from ergometer operation is modeled by curve-fitting KC-135 measurement data. The model provides amplitude and phase for three harmonic force inputs at 0.5, 1, and 2 times the operating frequency. The worst-case operating frequency of 3.9 Hz. (SM ergometer) and 4.7 Hz. (Lab Ergometer) were determined through a parametric study. An isolation factor of 0.1

was considered for the Lab ergometer disturbances.

4. Treadmill: The treadmill is located in the Russian Service Module. The disturbance from treadmill operation is modeled by curve-fitting KC-135 measurement data. The model provides amplitude and phase for five harmonic force inputs at 0.5, 1, 1.5, 2, and 3 times the operating frequency. The worst-case operating frequency of 1.5 Hz. for walking and 2.0 Hz. for jogging exercises were determined through a parametric study. Isolation factors ranging from 0.001 to 0.015, depending on the disturbance frequency and direction, were considered for the SM treadmill.
5. Solar Array Rotary Joint (SARJ) / Thermal Radiator Rotary Joint (TRRJ): Disturbances due to resolver error and torque (bearing friction, torque ripple, gear train) were considered.
6. Coldplates: The broad-band disturbance from the operation of coldplates distributed throughout the ISS (4 in the Airlock, 48 in the US Hab module and 33 in the US Lab module) was considered.

The transient disturbances are analyzed in the time domain. Simulations are performed, and peak and 10 second integrated response are determined from the response time histories. Response power spectra are then developed from the time histories and integrated in one-third octave bands to get the corresponding RMS values. The steady state disturbances are analyzed in the frequency domain. Frequency response functions (FRFs) are developed between the disturbance source and response locations for this purpose. Response power spectra for the broad-band disturbances and response amplitudes of the narrow-band (monochromatic) disturbances are computed, and RMS values in each one-third octave band are determined. A number of key assumptions are incorporated into the analysis. The most significant ones are:

- The acceleration response environment due to a typical disturbance is represented by the envelope of 33 grid point responses. These consist of 24 ARIS ISPR interface locations in the U.S. Lab and 8 in the ESA-COF module, and one geometric center location in JEM PM.
- Acceleration responses from multiple disturbance sources are combined on a root-sum-square basis.
- Constant modal critical damping ratio of 0.25% is assumed throughout the frequency regime.
- There is no ARIS simulation in the finite element model. ARIS attenuation is applied to the acceleration responses during post-processing using a fifth order filter which emulates the ARIS attenuation. The attenuation factors are a function of frequency and are assumed at 50% of the ARIS specification values to primarily account for ARIS performance variability as a function of payload mass and stiffness characteristics.
- No source isolation was considered for the SM ergometer. As mentioned earlier, source isolation was considered for the US Lab ergometer and SM treadmill.
- All disturbances, except SARJ/TRRJ, were analyzed with the SARJ/TRRJ controller joints locked. For the SARJ/TRRJ disturbances, the rotary joint controller models were incorporated in the DAC-6 ISS finite element model. Responses were calculated with the disturbed joints

active (i.e. closed loop) while the non-disturbed joints remained open-loop.

## Analytical Models

The finite element models used to perform this analysis are based on the ISS Rev C assembly sequence manifest and are analyzed using the MSC/NASTRAN finite element code. The basic model of the assembly-complete ISS configuration was provided by the Loads & Dynamics AIT. Several modifications were made to this baseline model in order to perform the structural dynamic microgravity assessments.

- Modal content was increased from 30 to 100 Hz. for all component models except Node 2, Node 3, Hab, Airlock, and Passive CBMs.
- Component models of Node 1 and FGB were replaced with test-verified versions. The reduced Node 1 model retained frequency content up to 100 Hz. and included the internal structure dynamics. The reduced FGB model retained frequency content up to 66 Hz.
- The eight Photovoltaic Array (PV) models delivered, which retain modal content up to 5.7 Hz, were replaced with higher fidelity PV Array models which capture modal content up to 25 Hz. This increased fidelity is due to a refined PV mast.
- The U.S. Lab and ESA-COF module models delivered were replaced with more detailed microgravity versions which include standoff dynamics and appropriate acceleration recovery locations. Twelve ARIS ISPRs in the US Lab module and four in the ESA COF were removed in order to improve the ARIS simulation. The remaining system racks were modeled as concentrated masses.
- The mass properties of the CAM model were updated.

## Summary of Results

The combined acceleration responses due to the various segment disturbance sources are compared against their respective allocations. These vibratory response allocations correspond to a 100 second averaged, RMS magnitude limit which is defined at the center frequency of each of the one-third octave bands which span the 0.01 Hz to 50 range. All results presented herein include the ARIS attenuation factors.

- Combined acceleration responses due to PG-1 (Boeing, Huntington Beach) disturbances are compliant with the PG-1 vibratory allocation. The PG-1 “tall poles” are primarily due to the SARJ and TRRJ torque disturbances.
- Combined acceleration responses due to PG-2 (Boeing Canoga Park) disturbances are non-compliant with the PG-2 vibratory allocation due to the KU Band antenna force disturbances. They exceed allocation by a factor of 0.7 at 0.16 Hz. 1/3 octave band and by a factor of 0.6 at 5 Hz. 1/3 octave band.
- Combined acceleration responses due to PG-3 (Boeing, Huntsville) disturbances are compliant

with the PG-3 vibratory allocation. Note that an isolation factor of 0.1 is applied to the U.S. Lab ergometer disturbance.

- Combining the PG-1, PG-2, and PG-3 acceleration responses on a root-sum-square basis results in the USOS acceleration response. This combined response was found to be compliant with the USOS vibratory allocation.
- Combined acceleration responses due to Russian Segment (RS) disturbances are non-compliant with the RS vibratory allocation due to the SM ergometer operation. At the worst-case operating speed of 3.9 Hz., the non-isolated SM ergometer exceeds the RS vibratory allocation by a factor of 3.2 at 2.0 Hz 1/3 octave band and by a factor of 5.5 at 4.0 Hz 1/3 octave band.
- Combining the PG-1, PG-2, PG-3, and RS acceleration responses on a root-sum-square basis results in the overall System acceleration response (Fig.1). Note that this only includes contributions from disturbances considered for DAC-6 which are the tall-pole disturbances identified in DAC-4. This response was found to be compliant with the System allocation with the exception of the SM ergometer. The SM ergometer exceeds the System allocation by a factor of 1.4 at 2.0 Hz 1/3 octave band and by a factor of 2.4 at 4.0 Hz 1/3 octave band.
- All transient disturbances considered were found to be compliant with the individual transient disturbance requirements. The largest peak response of 12.0  $\mu\text{g}$  was due to RSA SPP Solar Array disturbance and the largest 10 second integrated response of 9.2  $\mu\text{g}$ -seconds was due to the US Lab Vacuum Exhaust T-vent disturbance.

## Conclusions

The DAC-6 microgravity assessment has identified segment-level non-compliances from KU-band antenna slew motion and SM ergometer operation and system-level non-compliances from SM ergometer operation. Further analysis has been performed by the responsible contracting organization to develop a more refined set of disturbances for the KU-band antenna. The ergometer disturbance forcing functions will also be updated to include force and moment data based on upcoming CHeCS ground tests at the Johnson Space Center and KC-135 flight tests. The SM ergometer and KU-band antenna non-compliances will be re-evaluated as part of the upcoming Verification Analysis Cycle -2 (VAC-2) effort.

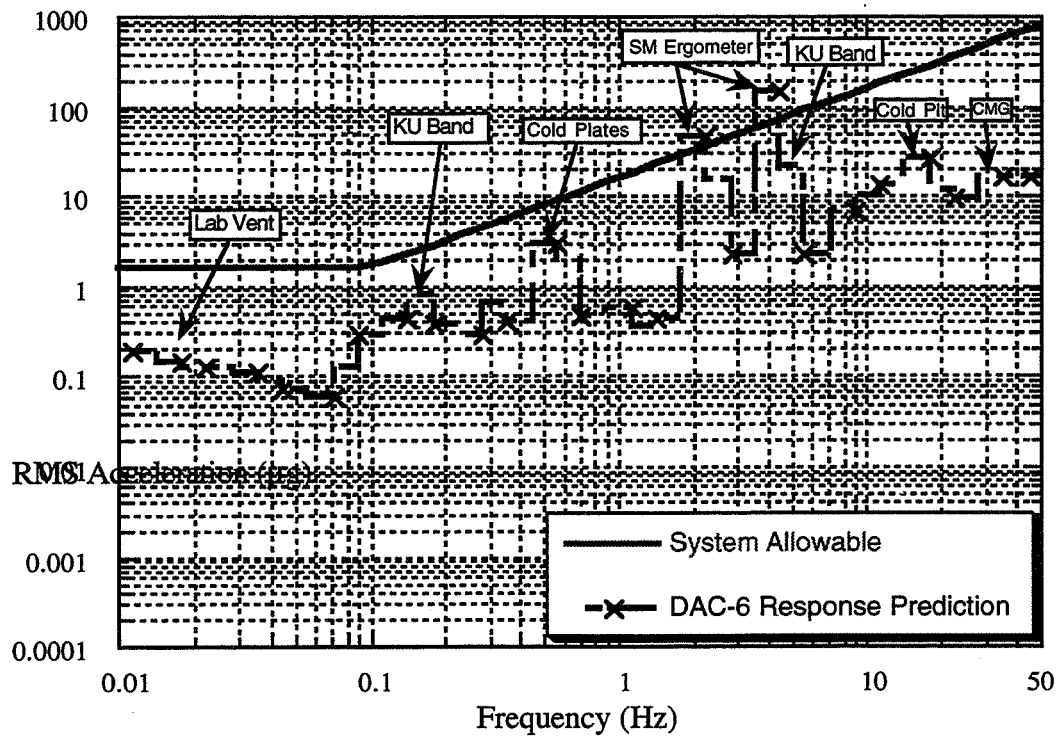


Fig 1. DAC-6 Microgravity Response Prediction

511-29

**Paper Number: 12**

## **ARIS Final Design and Flight Test Results**

---

Glenn Bushnell, Boeing Company, Seattle, Washington

Paper used with permission of the Boeing Company.

# ACTIVE RACK ISOLATION SYSTEM DEVELOPMENT FOR THE INTERNATIONAL SPACE STATION

Glenn S. Bushnell  
Tyler M. Anderson  
Marc D. Becraft  
A. Dean Jacot

Boeing Defense and Space Group  
Kent, Washington

## ABSTRACT

The design development of a microgravity active rack isolation system (ARIS) used to isolate a Space Station International Standard Payload Rack (ISPR) from Space Station disturbances is presented. Acceleration requirements down to the microgravity level at frequencies below 10 Hz have been levied by users for particular classes of payloads, and have been incorporated into the International Space Station (ISS) system specification at the rack locations. However, Space Station vibration estimates and space shuttle acceleration measurements show that disturbances from crew motion and other mechanical disturbers can cause exceedance of the microgravity acceleration requirements. The primary purpose of ARIS for the ISPR is to provide a microgravity environment by isolating the payload from these low frequency off-board disturbances.

The ARIS control concept is to actively cancel payload umbilical disturbance forces based on sensed payload inertial acceleration. Accelerations are sensed using low noise linear accelerometers, and control forces are generated using highly linear, rotary type, voice coil actuators. A digital computer is utilized for real time control and decouples the isolator system

Copyright © 1997 by the Boeing Company. Published by NASA Lewis Research Center with permission.

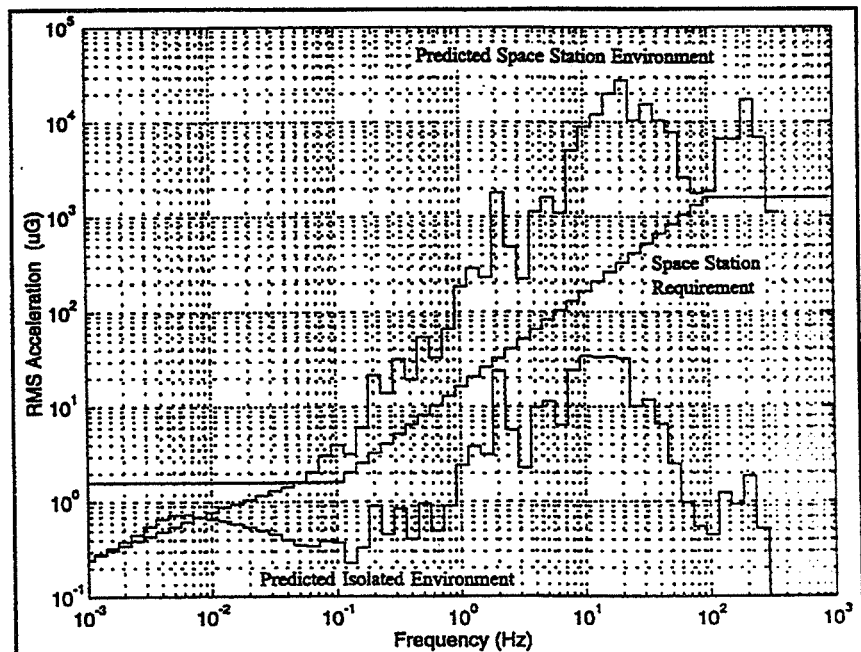
(which is highly coupled due to the mechanical configuration). Design and performance feasibility is shown by ground and flight test results. ARIS was flown on a shuttle mission to the Russian MIR Space Station (STS-79) in September of 1996. Flight testing was necessary due to ground test limitations on microgravity measurement, suspension, and control.

## Introduction

One of the primary objectives of the Space Station is to provide an acceleration environment suitable for microgravity class science experiments. Microgravity experiments include many materials science payloads as well as some protein crystal growth and fluid experiments. The maximum acceleration level considered acceptable for most classes of microgravity experiments is specified in the Space Station requirement [1] and is shown in Figure 1. This requirement constrains the root-mean-square (rms) acceleration level per one-third octave bandwidths. As can be seen in the figure, a 1.0  $\mu\text{g}$  acceleration level is required below 0.1 Hz. Higher levels of accelerations are allowed with increasing frequency and plateaus above 100 Hz.

Figure 1 also includes an estimate of the Space Station

FIGURE 1 - SPACE STATION  $\mu\text{G}$  REQUIREMENT & PREDICTED ENVIRONMENT WITH AND WITHOUT ISOLATION



acceleration environment [2]. The estimate is based on both quantified and assumed disturbances. The US Segment, Russian Segment, and crew input disturbance acceleration response predictions were computed using quantified forcing functions with finite element models for the lower frequency range and with statistical energy analysis procedures for the high frequency range [3]. The European Space Agency Columbus Attached Pressurized Module (APM) and the Japanese Experiment Module (JEM) and payload disturbances were modeled using the US Airlock/Hab/Lab environments which were assumed similar for each element until the quantified disturbance data becomes available.

As can be seen, the predicted environment peaks are an order of 10 higher on average than the requirement. These exceedances are caused by major component mechanical disturbers such as the solar and thermal radiator rotary joint mechanisms (TRRJ & SARJ) and control moment gyros (CMG), crew motion, and "housekeeping" equipment such as pumps and fans.

These estimates indicate that more severe requirements would need to be levied on the allowable disturbance levels of the ISS hardware. However, due to the cost and complexity of either actively controlling or passively isolating the disturbance sources, it was determined that addition of active isolation at the science payload was essential to meet the microgravity requirement. The benefit of active isolation can be seen in Figure 1 which shows the predicted isolated payload response (952 lb payload) to the predicted space station environment. As can be seen, the isolated response meets the requirement. Active payload isolation is also advantageous because it provides assurance that acceptable microgravity environments will be achievable even with uncertainty in crew motion and hundreds of other small but contributory disturbance sources. The active isolation decision was made after completion of the ISPR design and publication of the ISPR interfaces, and consequently, the ISPR had no interface provisions for active isolation.

The active isolation design approach chosen for payload isolation incorporates Boeing's Active Rack Isolation System (ARIS) and is described below.

#### ARIS Design Approach

#### System Isolation Configuration Trades

For the Space Station, the science payloads are mounted in ISPR's located in the US lab, APM, and

JEM modules. The ISPR's were designed to maximize the payload available weight and volume and provide standard science payload resource utilities (vacuum, power, data, video, cooling). Maintaining the as designed science payload resources are paramount to the design of the active isolator. The following summarizes some of the key trades in selecting the type of active vibration isolator.

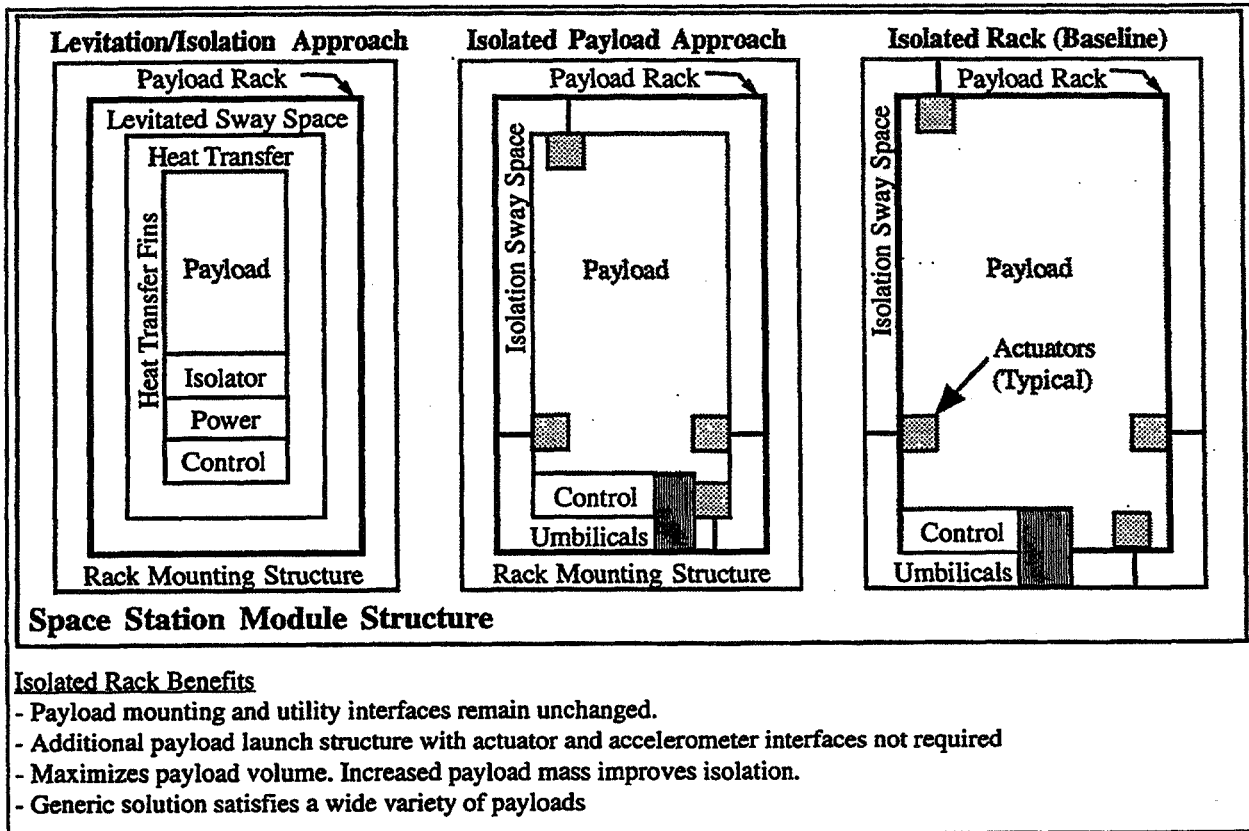
#### Cancellation vs. Levitation

System isolation configuration trades resulted in the selection of an umbilical cancellation approach instead of a levitation approach. The levitation concept insures a microgravity environment by essentially eliminating the primary source of the disturbance by adding large utility support equipment such as power transformers, data couplers, and cooling fins. The isolation via cancellation concept has sensors on the payload that sense these disturbances and control actuators that provide forces and torque's that oppose (or cancel) the disturbances. The left part of Figure 2 illustrates this concept. While it is significantly easier to achieve a  $\mu\text{G}$  environment with the levitation approach, the impact to the user payload volume is severe. In addition, for high power payloads, the aero coupling across the fins reduces the "purity" of this approach as ESA supported rack isolation studies have shown, as does the active feedback necessary to linearize and control most types of non-contact actuators. For the ISS program, where a wide variety of payloads will be used, a generic isolator that allows payload services via an umbilical is needed, and leads to the selection of the cancellation approach.

#### Rack vs. Locker

Another key trade is isolation at the rack (integrated payload) vs. the locker (just the  $\mu\text{G}$  sensitive part of the payload). The dominant isolation issue is at the ISS fundamental structural frequencies, which are slightly below 0.1 Hz. The frequencies are easily excited by crew motion, rotating joints (i.e., solar arrays), and movement of external payloads, etc. Passive isolation at this low a frequency is virtually impossible with attached utilities. The uncontrolled payload natural frequency is the square root of disturbance path stiffness divided by the payload mass. For typical rack size payloads and standard umbilicals, this is a few tenths of a Hz, near the ISS natural frequency. The cancellation approach essentially augments the mass of the payload by a couple orders of magnitude to drop this frequency to a few hundredths of a Hz, well below

FIGURE 2 - PAYLOAD ISOLATION CONCEPTS



the ISS critical frequencies. Accomplishing this with small lightweight (locker size) payloads can be very difficult. With many payloads the  $\mu\text{G}$  sensitive part of the payload is also the large power/cooling consumer, and thus needs a good part of umbilical services (which raises the natural frequencies and provides paths for disturbance sources). Therefore, there is an isolation benefit by isolating the entire heavier integrated payload.

The other major consideration leading to the rack level isolation is to develop a single generic isolator solution that satisfies a variety of payloads. Since payloads will be constantly changing over the life of the ISS, this is an important cost consideration.

#### Rack in a Rack vs. Floated Rack

The ISPR is a very stiff and strong Graphite Epoxy (GrEp) structure in which the payload components are mounted and integrated. They are then taken up to the ISS in a separate carrier flight; mounted in the US, European or Japanese laboratory module; and returned

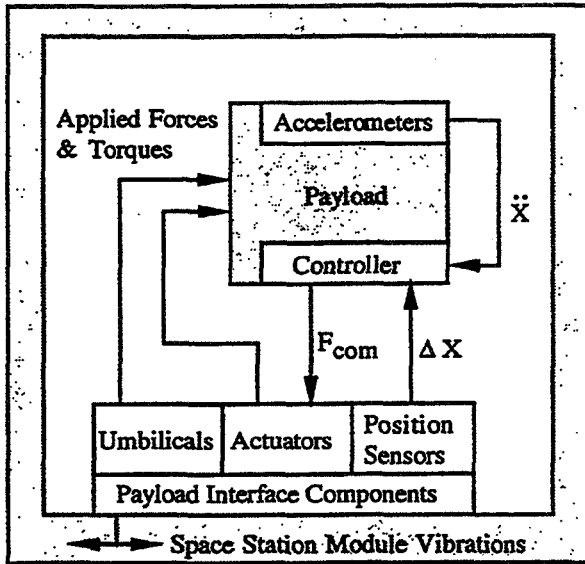
after the experiment is completed. The ISPR provides the necessary boost load capability for payloads with first frequency above 25 Hz and avoids the necessity of vibration testing each payload/ISPR before launch. Since the ISPR was designed to be rigidly attached to the vibrating ISS module, a concept of a floated rack within the ISPR to mount the payloads had been widely studied and is illustrated as a rack in the center illustration of figure 2. The problem is the inner rack needs sufficient volume and weight to be stiff to support high performance vibration isolation, and the high stiffness of the outer rack is of little value. An alternative concept, titled "Floated Rack" is to take advantage of the stiff GrEp ISPR by floating and isolating the entire payload/ISPR as shown at the right of figure 2. Either concept requires attachment of the payload for boost loads (the crew removes attachments after launch and installation) and a sufficient gap or sway space around the entire outer envelope of the payload rack. By floating the ISPR, the volume and mass of the inner rack is avoided, standardized interfaces to the payload community are provided, and the investment in developing the ISPR is preserved.

Isolation via cancellation and floating the entire payload/ISPR is the selected approach.

Isolation by Acceleration Cancellation

The active payload isolation by acceleration cancellation approach used by ARIS is thus illustrated in Figure 3.

**FIGURE 3 - ACCELERATION ISOLATION FUNCTIONAL CONCEPT**



Unwanted payload accelerations are induced by disturbance forces and torques transmitted to the payload through the utility and actuator interfaces. Payload translational and angular accelerations are sensed by a set of linear accelerometers and are canceled by appropriate actuator commanded forces. The reaction forces are inertially based and in effect increase the mass and damping of the payload. This increase in apparent mass/damping lowers the passive utility-spring/payload-mass break frequency and improves isolation. Reducing the utility stiffness is also an effective way to improve the isolation performance. The overall passive system stiffness is partially reduced using positive position feedback to cancel umbilical forces. The payload position is also used to close a low-authority feedback loop to avoid payload drift resulting in impact with the off-board structure.

Utility Interface Design

To support the varying science payload functions, the

ISPR has incorporated a utility interface panel at the front bottom section of the ISPR as shown in Figure 4. To improve isolation performance the utilities are looped to reduce stiffness and unwinding bias forces.

A standard umbilical assembly (SUA) interface was selected for ISS production and includes power, thermal control, vacuum, & data lines required for typical microgravity experiments. Two subsets of the ISS configuration were selected for ground and flight testing, a "partial set" with 13 umbilicals similar to the ISS set and a "minimum set" with 7 umbilicals for increased isolation performance. The ISS production and flight experiment umbilical sets are listed in Table 2. As can be seen, the resources require sizable utilities. Flight utility stiffness tests were conducted and results are listed in Table 1.

**FIGURE 4 - INTERNATIONAL STANDARD PAYLOAD RACK (ISPR) AND UTILITY INTERFACE**

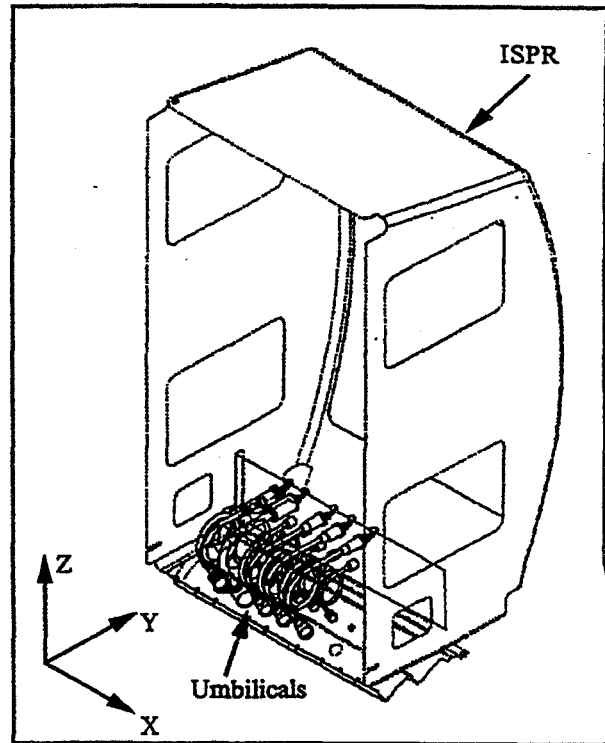


**TABLE 1 - MEASURED UMBILICAL STIFFNESS**

| (lbs/ft) | X   | Y  | Z  |
|----------|-----|----|----|
| Minimum  | 65  | 55 | 50 |
| Partial  | 102 | 82 | 82 |

TABLE 2 - SPACE STATION AND FLIGHT EXPERIMENT UTILITY ARRANGEMENTS

| Function                                      | Quantity : Wire Type  | ISS Production | RME1313 Min. Set | RME1313 Partial Set |
|---|---|----------------|------------------|---------------------|
| Main Power                                    | 2 : 4 Gauge Wire<br>1 : 8 Gauge Wire  | X              | X                | X                   |
| Auxiliary Power                               | 2 : 4 Gauge Wire  | X              | X                | X                   |
| 1553 A  | 19 : 75 Ohm twisted shielded pair   | X              |                  |                     |
| 1553 B  | 19 : 75 Ohm twisted shielded pair   | X              |                  | X                   |
| High Rate Data, Fiber Optic                   | 4 : 16 gauge wire   | X              |                  | X                   |
| Video (RME1313 Laptop Interface)              | 2 : 22 gauge twisted shielded triplet<br>3 : 22 gauge twisted shielded pair | X              | X                | X                   |
| Maintenance (RME1313 pump and off-board fans) | 6 : 22 gauge twisted shielded pair<br>5 : 22 gauge twisted pair             | X              | X                | X                   |
| Ethernet                                      | 7 : 100 ohm twisted shielded pair   | X              |                  | X                   |
| Ethernet                                      | 7 : 100 ohm twisted shielded pair   | X              |                  | X                   |
| RME1313 Off-board Electronics                 | 10 : 100 ohm twisted shielded pair<br>3 : 22 gauge twisted shielded triplet |                | X                | X                   |
| Vacuum Resource                               | ½ inch flexible hose  | X              |                  | X                   |
| Vacuum Exhaust                                | ½ inch flexible hose  | X              |                  |                     |
| TCS Inlet                                     | ½ inch flexible hose  | X              | X                | X                   |
| TCS Return                                    | ½ inch flexible hose  | X              | X                | X                   |
| Gaseous Nitrogen                              | 3/8 inch flexible hose  | X              |                  | X                   |

The minimum set stiffness results in uncontrolled passive natural frequencies in the 0.2 Hz region (952 pound flight payload, typical microgravity payloads weigh from 1000 to 1800 lbs). It is shown that active isolation can lower the system natural frequency by more than a factor of 10 to obtain critical isolation in the tenth of a Hz region. To improve isolation performance, the Boeing ARIS product group has a design goal to reduce the stiffness of the ISS set down to the minimum set values. Methods to reduce the stiffness of the ISS set have been found by material selection, and the effort is ongoing.

**Risk Mitigation Experiment**

As a proof-of-concept, ARIS was flown on the Space Shuttle Mission STS-79 to MIR as an International Space Station Risk Mitigation Experiment (RME-1313). The primary RME-1313 mission objective was to mitigate Space Station ARIS hardware design, performance, and operation risks. Design risks were mitigated by taking into consideration Space Station production requirements. Performance and operation risks were mitigated by flight testing in zero-G which was necessary to characterize 6-DOF low frequency µG isolation behavior. The mission to MIR also provided an excellent opportunity to test in a manned Space

Station acceleration environment. The design, development, and testing of the RME-1313 hardware and software is presented here.

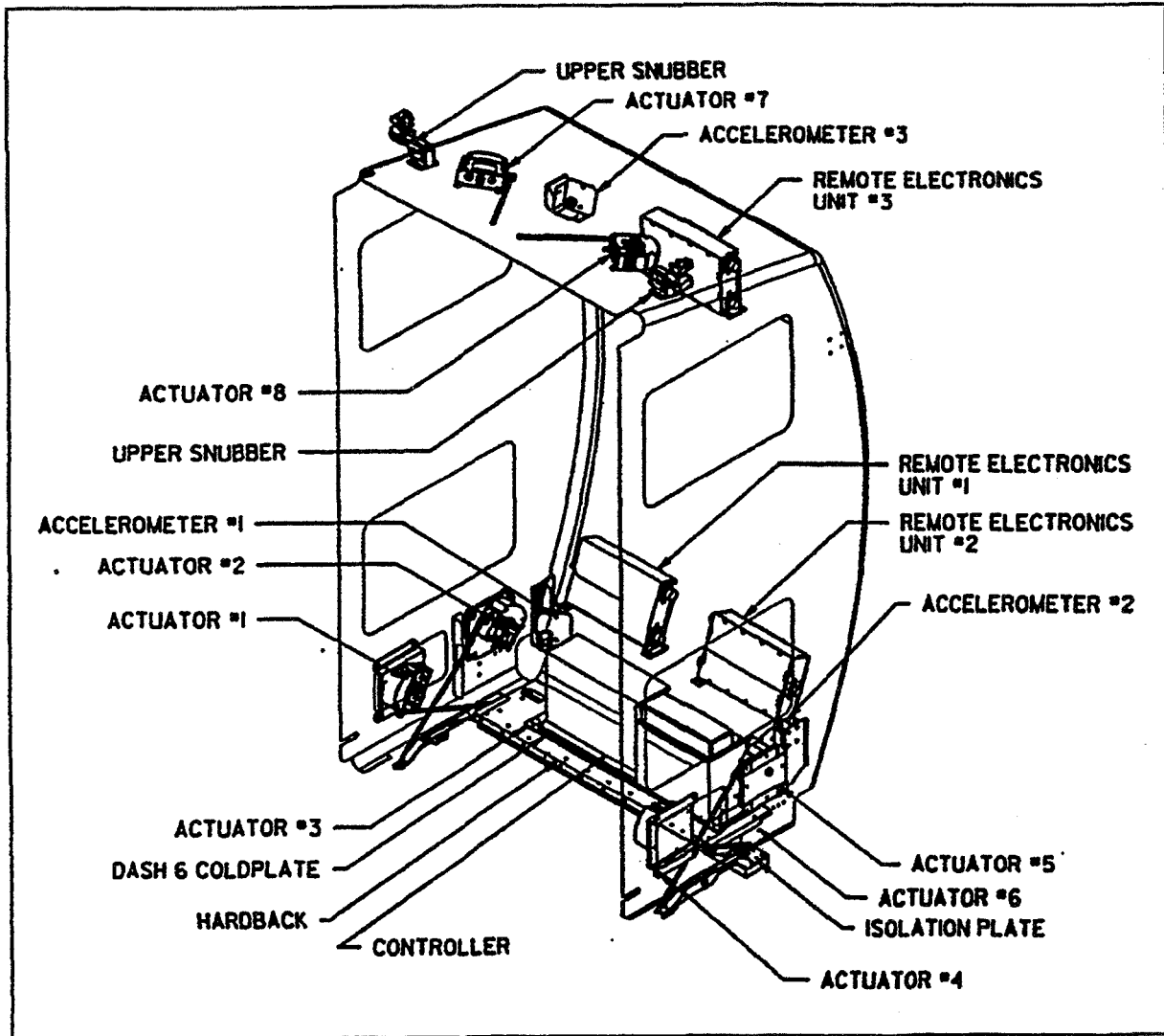
**ARIS System Configuration**

The ARIS control system consists of a digital controller, 8 linear accelerometers, 8 linear position sensors, 8 linear force actuators, 8 pulse width modulators (PWM) actuator drivers and multiple 16-bit analog-to-digital and digital-to-analog converters to provide I/O for the controller.

The digital controller approach has many advantages, one of which is the ability to resolve and decouple actuator and accelerometer control signals. Decoupling capability is important because it allows valuable flexibility in the placement of actuators and accelerometers. With this advantage, the ARIS actuators and accelerometers were mounted in the nooks and crannies of the ISPR, behind posts and in corners, and outside the primary payload volume. The ARIS component placements can be seen in Figure 5.

Six actuators are placed in the bottom section of the rack to counter utility disturbance forces and two are placed on top of the rack to provide better torque authority. Actuators were oriented to minimize power

FIGURE 5 - ISPR INTEGRATED WITH ARIS COMPONENTS



and provide single failure redundancy, but configuration choices were constrained due to ISPR and ISS packaging interference constraints. Of particular concern for actuator placement is the resulting power required to drive the actuators to counteract utility bias and stiffness forces. The total power required to counteract a 3.0 lb bias force acting at the center of the utility panel is shown in Table 3. In comparison, a single actuator at 3.0 lb would require 13.5 watts, and eight actuators at 3/8 lb. each would require 1.7 watts total (Actuator power is proportional to the square of the actuator force).

Accelerometer heads were placed in three opposite corners of the rack to increase sensitivity to angular

TABLE 3 - POWER REQUIRED TO COUNTERACT A 3.0 LB BIAS FORCE ACTING AT THE CENTER OF THE UTILITY PANEL

| 3 lb Bias Direction     | X    | Y    | Z    |
|-------------------------|------|------|------|
| Actuation Power (Watts) | 6.0  | 5.0  | 10.2 |
| Single Failure Power    | 11.5 | 12.9 | 17.3 |

accelerations, and near ISPR posts away from local ISPR panel flexible modes. The bottom two heads each have an orthogonal set of linear accelerometers. The top head has two orthogonal accelerometers for a total of eight. The head axes were oriented to increase single and double failure redundancy, but complete double failure redundancy was not obtainable due to the limitation of 3 head locations and 8 accelerometers.

The top two accelerometers were aligned such that if one failed the other would provide redundancy in the double failure singular direction. The bottom two were then skewed with respect to each location to increase redundancy.

Position of the payload is determined from measurements of the stroke of each actuator. The position sensors are integrated into each actuator housing.

**Control System Architecture Description**

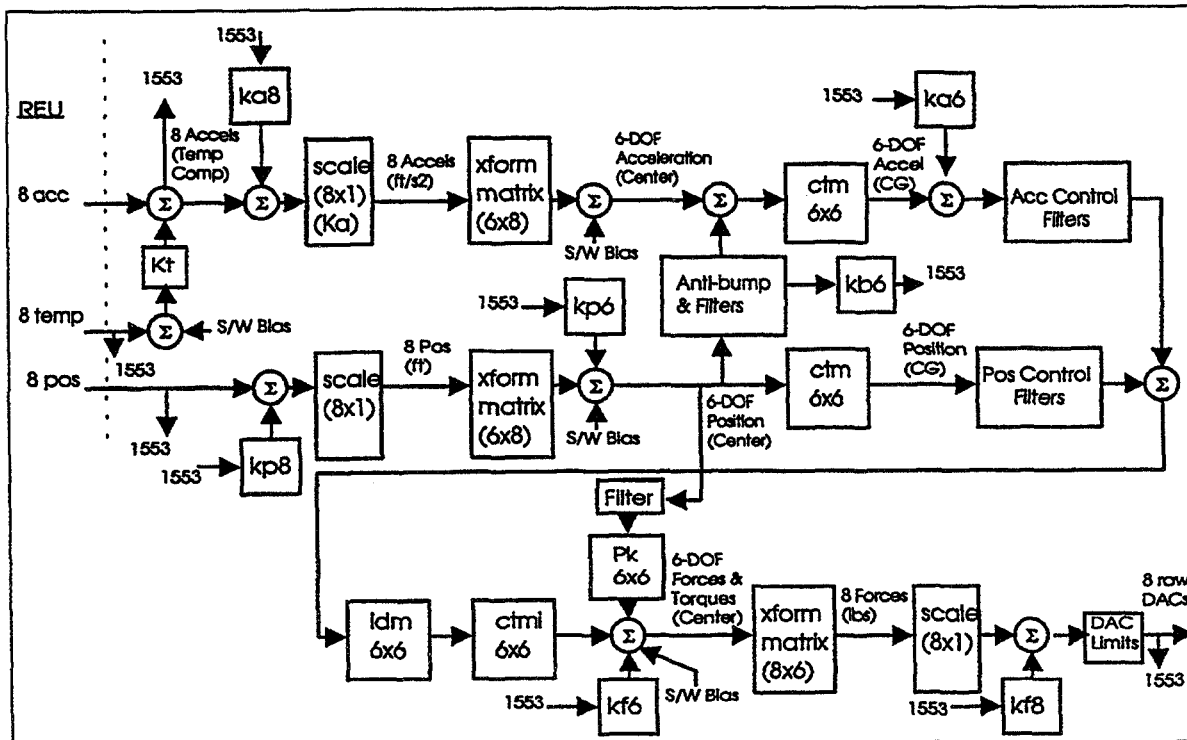
The control system feedback architecture is shown in the block diagram in Figure 6. Acceleration and position control filters and gains operate on signals resolved about the payload center of gravity (CG) in 6 independent loops (signals labeled "6-DOF Accel (CG)" and "6-DOF Position (CG)"). Transformation matrices are used to compute 6-DOF measurements from the eight acceleration and eight position sensor measurements. The 6-DOF control force and torque commands are resolved back into individual actuator commands using a pseudo-inverse of the forcing matrix. The pseudo-inverse method minimizes power usage.

Control compensation required to stabilize the system is simplified by decoupling the plant dynamics using stiffness shaping feedback (see block labeled "Pk 6X6") and the inertia decoupling transformations (see blocks labeled "ctm", "idm", & "ctmi"). Decoupling the plant allows each loop compensator to be designed independently. Stiffness shaping is also used to improve isolation performance by partially canceling umbilical stiffness.

The digital acceleration filters implement three 2<sup>nd</sup> order filters and one 1<sup>st</sup> order filter. The first order filter is used for rigid body stability, and the second order filters are used for either structural mode stabilization (notch filters) or for response shaping to improve isolation performance. The position filters consist of a PID compensator with low pass filtering of the position and derivative terms. They are used to close a low bandwidth position loop to center the rack. This allows ARIS to operate in the presence of larger off-board motions without exceeding its 1.0 inch hard-stopped sway space range limitation.

A nonlinear anti-bump feedback algorithm was also implemented as a secondary means to prevent the ISPR

**FIGURE 6 - DIGITAL CONTROL BLOCK DIAGRAM**



from bumping into hardstops. This is done by computing deceleration commands that will stop the ISPR at a prescribed boundary. If the computed command exceeds a prescribed limit (typically 15  $\mu\text{G}$  for translation) then the limit is commanded. The deceleration command is computed for each controlled axis (see "6-DOF Acceleration (Center)" summing junction) based on the position and velocity of the center of the rack. The anti-bump algorithm is illustrated in Figure 7.

### Control System Hardware

#### Controller

The ARIS controller consists of a dual 33 MHz TMS 320C30 floating-point digital signal processor (DSP) board, an analog I/O board and a power supply. Each DSP executes code independent of the other and communicates with the other via dual port RAM. Sensor data is retrieved from the REUs over a common high speed (2 Mbps) serial digital bus. Sensor data is shared with outside computer systems via a MIL-STD 1553 bus. ARIS control parameters and mode commands are also loaded via the 1553 bus.

The primary control DSP is an "Input/Output Processor" (IOP) and handles all 1553, sensor, and terminal communications. The IOP processor retrieves sensor measurements from the REUs every 2 milliseconds and shares it with the Control Processor via dual port RAM and with external computers, such as a payload processor, via the MIL-STD 1553 bus. The IOP is also responsible for monitoring system health. A terminal interface is also available for stand-

alone testing.

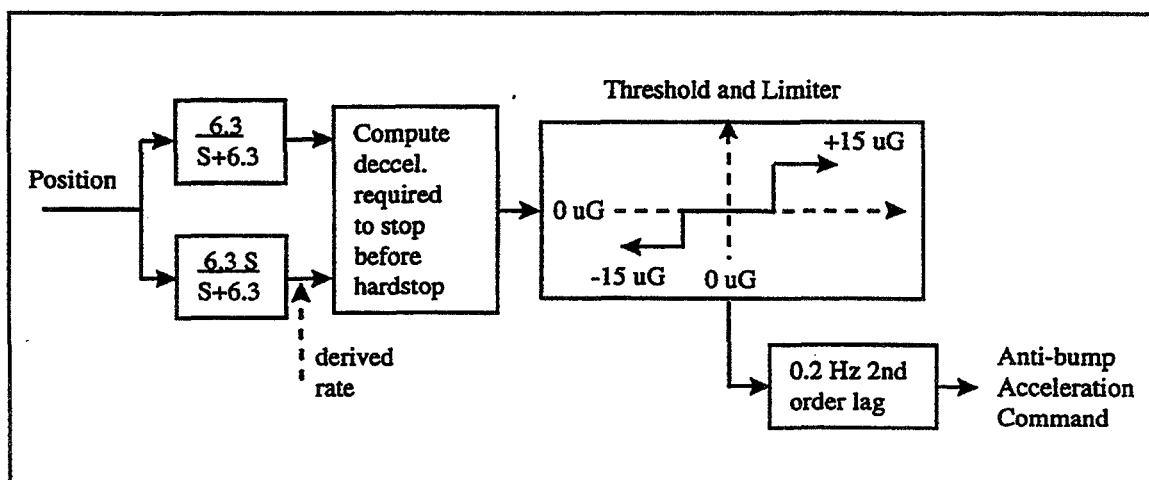
The second controller DSP is the Control Processor (CP) and performs all the sensor decoupling, control law filters, algorithms and actuator force command generation. All computations are performed using 32-bit floating-point math. Digital force commands are updated and sent to digital-to-analog converters every 2 milliseconds, creating voltages which command the PWM modules. The PWMs generate currents in the voice coil-type actuators proportional to the voltage commands. Voice coil currents can also be sensed, for health monitoring purposes via analog-to-digital converters.

The controller is housed in a chassis which has provisions for four circuit cards/modules, including the CPU circuit card, the PWM interface card, a spare card slot and the power supply module. The entire chassis is conductively cooled, and heat is transferred to a coldplate which is attached in the bottom back section of the rack as shown in Figure 4.

#### Remote Electronics Units

To reduce parts and cables, the signal conditioning electronics for 3 position sensors and 3 accelerometers were combined into a single package as remote electronic units (REU's). The RME1313 experiment system consists of three onboard ARIS REUs and three offboard REUs. The offboard REUs were used to measure offboard accelerations so that ARIS performance could be assessed.

FIGURE 7 - ANTI-BUMP ALGORITHM BLOCK DIAGRAM



All REUs are identical and are built around a TMS320C30 DSP (same as controller). The DSP communicates with the controller over a high speed 2 Mbps serial bus and controls the analog-to-digital conversion process for all sensors. In addition, it controls the gain settings of the accelerometers, sets the corner frequency of the digitally controlled analog 2nd order filters on each accelerometer signal and removes accelerometer biases via 16-bit digital-to-analog converters which inject a bias-canceling signal into the accelerometer signal. The REU's are mounted near the sensors to provide analog-to-digital conversion near the sensors, minimizing noise on the sensor readings. Each REU also takes measurements of accelerometer and motor housing temperatures.

There are two acceleration sensing channels incorporated into each REU, a "control" channel and an "Acceleration Measurement Sensing (AMS)" channel. The control channel is used for active isolation feedback and the AMS channel is used to measure high frequency accelerations. Very high resolution measurements may be obtained on the accelerometers (0.02  $\mu$ G) using two digitally adjustable analog gain stages per channel, fixed and adjustable filtering, and a 16-bit ADC. A block diagram of the accelerometer electronics is shown in Figure 8.

Dividing the overall accelerometer gain into two stages permits higher sensor resolutions to be achieved. The first stage converts the sensor signal into a voltage which

is then filtered to remove high amplitude high frequency components which tend to cause saturation. With the high frequency components of the signal removed, the second stage gain amplifies the signal further without saturation.

In addition to removing high frequency components to prevent saturation, the software-adjustable 2<sup>nd</sup>-order filter is also used to provide stability margins for high frequency flexible modes in the acceleration control loop.

### Acceleration Sensors

Microgravity isolation requires a high resolution acceleration measurement system with low measurement noise. Tests showed that 2 kHz bandwidth inertial grade servo force balance accelerometers, and appropriate signal conditioning, would provide the necessary performance. Correlated and uncorrelated noise levels were determined by adding or subtracting the signals of back-to-back and parallel mounted accelerometers (respectively) to remove the true sensed acceleration component. Tests showed that the uncorrelated noise was significantly less than the correlated noise.

Figure 9 shows the correlated electronic noise levels computed from back-to-back accelerometer tests with resolution set at .02  $\mu$ G/bit. (Multiple data runs superimposed). The upper dashed line is the derived acceleration measurement accuracy requirement. This requirement was based on the flight experiment measurement accuracy requirement and on impacts that measurement errors or noise have on control jitter and payload position drift. The derived jitter based requirement was set at 10% of the maximum allowable on-board ISS levels, and was equal to the flight accuracy requirement. The drift based requirement was based on the position response of the rack to low frequency white noise, which can cause the ISPR to bump into the hardstops if too high. The white noise maximum derived level was determined by constraining the position response to have less than a 1% chance of exceeding 0.05 inches in 30 days. The jitter and drift based constraints were combined into a single minimum constraint. The lower dashed line is the envelope of accelerometer noise as published by the accelerometer vendor [4].

**FIGURE 8 - ACCELEROMETER SIGNAL CONDITIONING ELECTRONICS BLOCK DIAGRAM**

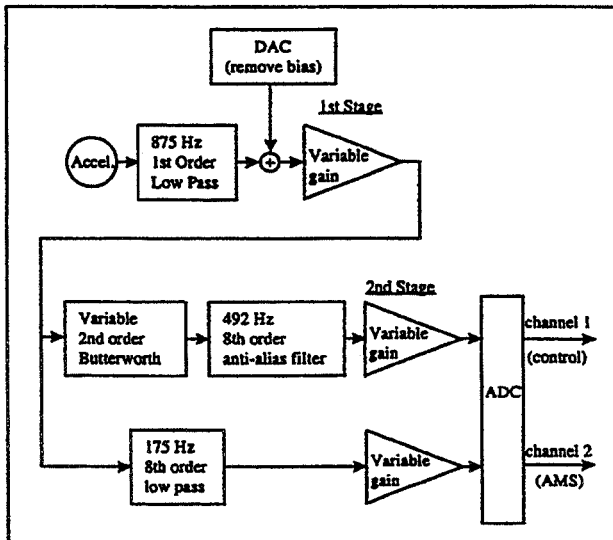
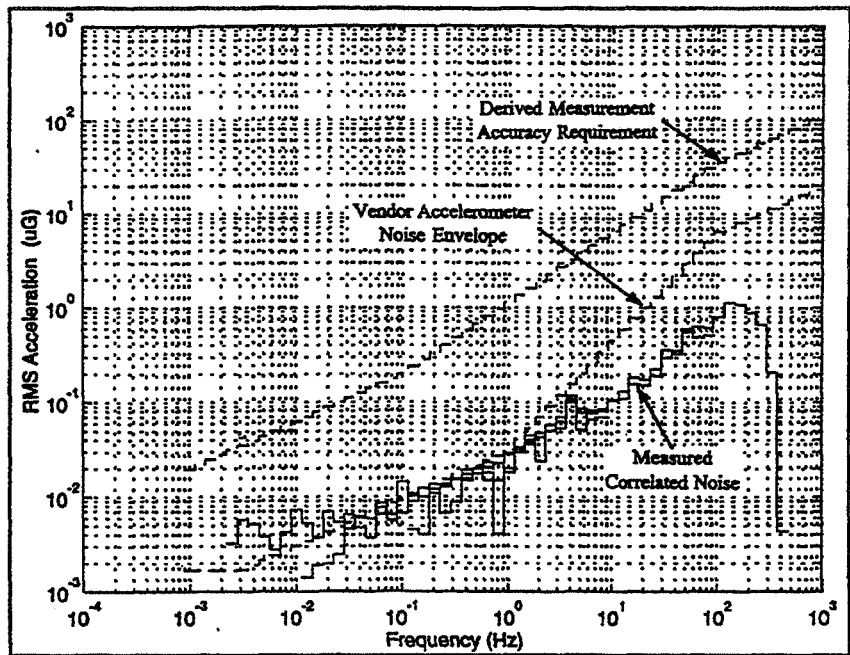


**FIGURE 9 - CORRELATED ACCELEROMETER NOISE RESULTS**

Note in Figure 9 that the sensor electronic noise is well below the derived requirement.

**Actuation**

Microgravity control requires a few pounds of actuation capability with large stroke, low stiffness actuation, and negligible friction or hysteresis. Noncontact magnetic actuation can solve this problem, but the large stroke requirement means a substantial increase in power or size. For this reason, a light-weight/low-power voice coil actuator with direct contact actuation was chosen. The actuator applies forces to the ISPR via a flexure hinged pushrod linkage. The direct contact linkage design was challenging because the flexure hinges must be very soft for isolation purposes.



The actuator mechanism design is shown in Figure 10. The actuator is a rotary-type and consists of a light weight voice coil which is free to pivot within the actuator magnetic gap. Incorporation of a rotary actuator (instead of a linear type) reduces the mechanism size because a compact 1 DOF hinge joint can be used to suspend the coil. This hinge is a cross flexure type joint with two 0.003 inch thick flexure plates. The cross configuration provides the stiffness required in the off rotation axis directions to prevent the coil from physically interfering with the magnets. The gap between the coil and magnets is only 0.020 inches, and improves power consumption, coil thermal dissipation, and reduces the overall actuator size. The actuator characteristics are listed in Table 3.

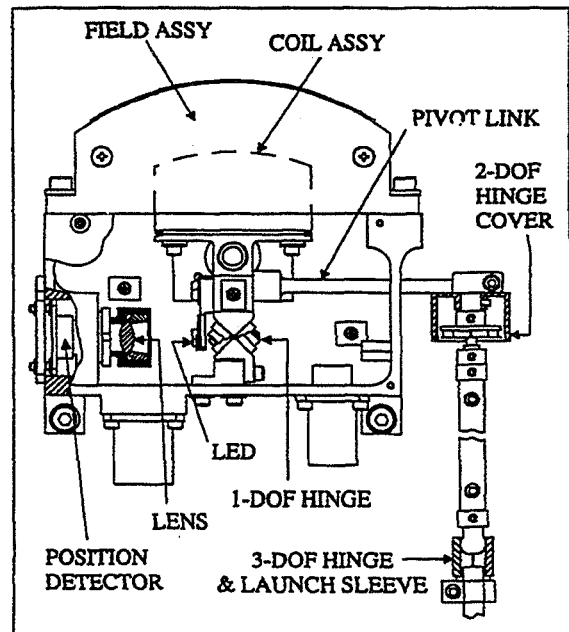
hinge is located on a three inch lever arm to provide the necessary stroke capability (which can be easily increased by extension of the lever arm). The 2-DOF hinge travel range is 26 degrees, 20 degrees for actuator pivot motion and 6 degrees for perpendicular rack

**Table 3 - ACTUATOR CHARACTERISTICS**

|            |                        |
|------------|------------------------|
| Stroke     | 1.0 inches             |
| Peak Force | 6.2 lbs                |
| Power      | 1.8 lbs/amps, R=5 ohms |
| Stiffness  | 0.2 lbs/inch           |
| Weight     | 3.3 lbs                |

The pushrod is attached to the coil linkage by a 2-DOF hinge. The 2-DOF hinge is a single wire which runs collinear with the center axis of the pushrod and through the center of a flat circular disc shim. The wire sustains axial actuation forces and the disc shim provides radial reinforcement to prevent buckling. The

**FIGURE 10 - ACTUATOR ASSEMBLY**



motion. The pushrod far end joint has 3 DOF to allow complete 6-DOF rack motion. It can bend in two directions as well as twist because the hinge is a single wire without a disc shim. The shim was not required because the 3-DOF hinge range of travel is only 6 degrees.

#### Position Sensor

The coil position sensor is mounted in the actuator housing as shown in Figure 10. The position sensor consists of an LED mounted to the actuator coil support linkage and a single axis lateral effect photo detector and optics mounted off the linkage. The photodetector senses the location of the LED which moves laterally as the coil rotates. Test data showed that the translation of the pushrod end position (at the 3-DOF hinge) could be measured linearly to within 1%.

Table 4 - RME1313 ARIS Component Characteristics

| Item                        | Size (in <sup>3</sup> ) | Power (Watts) | Weight (lbs) |
|-----------------------------|-------------------------|---------------|--------------|
| Actuator Assembly (8)       | 325                     | (see PWM)     | 26.4         |
| Controller & Power Supply   | 580                     | 28            | 17.1         |
| Power Supply Inefficiency   |                         | 30            |              |
| PWM (8 Actuator Drivers)    | 604                     | 13            | 22.3         |
| Remote Electronic Units (3) | 669                     | 44            | 18           |
| Accelerometer Package (3)   | 108                     | 3             | 3.9          |
| Cables                      |                         |               | 20.6         |
| Totals                      | 1.33 ft <sup>3</sup>    | 118           | 108          |

#### Component Resource Requirements

The RME1313 ARIS component characteristics are listed in Table 4.

#### ARIS Performance

##### Isolation Performance

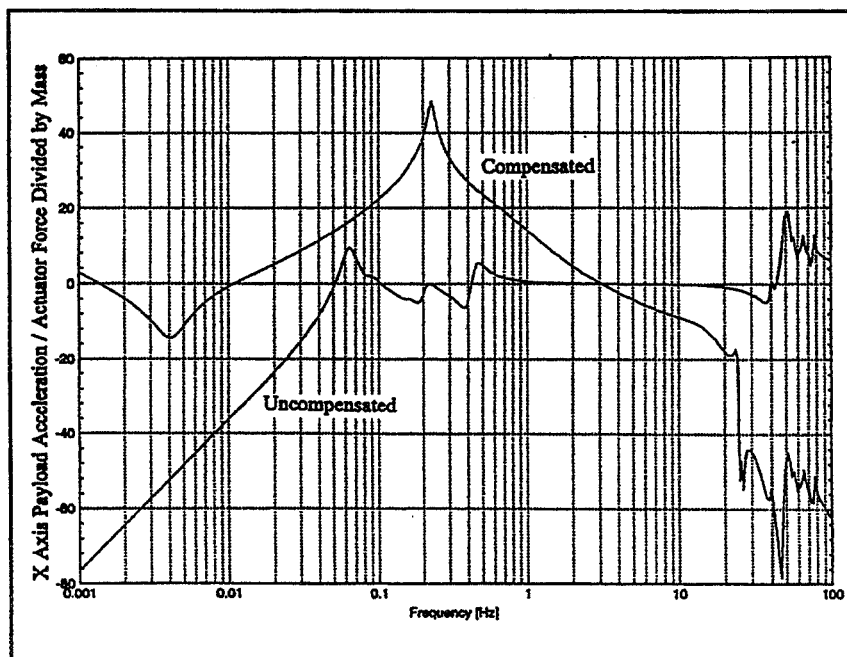
##### Predicted Open Loop Response

The uncompensated and compensated open loop acceleration payload responses to actuator commands are shown in Figure 11. A stable isolator is designed by integrating acceleration and crossing over in the frequency region below the structural modes, as shown in the compensated response.

Isolation is improved by increasing the acceleration loop gain, but is ultimately limited either by system stability, saturation, or low frequency accelerometer drift errors resulting in violation of the sway space (feedback will counter false accelerations errors with real payload acceleration). Off-board rigid body motion also limits achievable isolation, since the payload must either follow the

space module or risk bumping surrounding structure. For this reason, the Space Station microgravity environment approach is two pronged. First, the space station provides smooth attitude and rigid body translation control below 0.01 Hz, and secondly, active isolation provides attenuation of residual vibratory and momentum disturbances above 0.01 Hz.

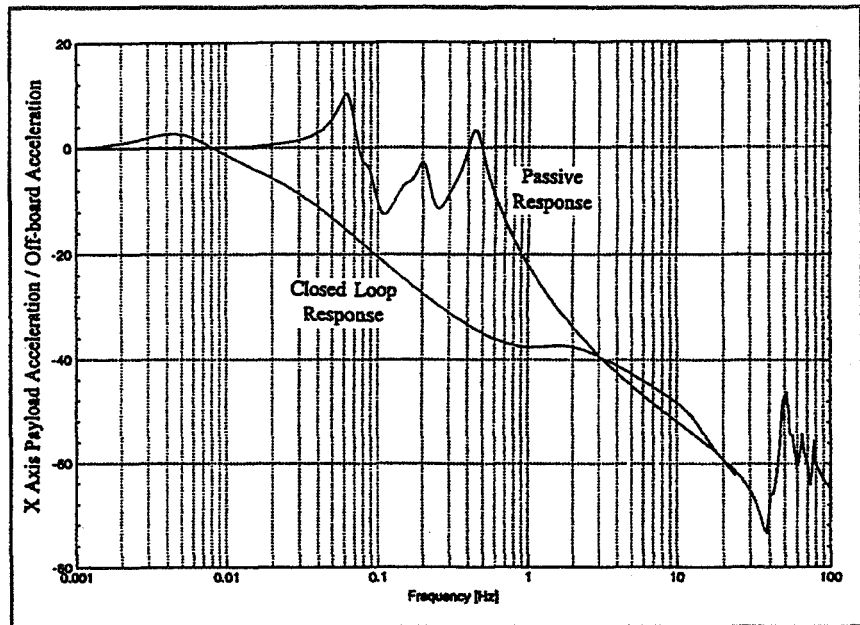
FIGURE 11 - OPEN LOOP UNCOMPENSATED AND COMPENSATED ACCELERATION RESPONSE



### Predicted Isolation Responses

The predicted x-axis payload passive response to space station acceleration is shown in Figure 12. It can be seen that the system is highly coupled with several of the utility-payload modes being excited. It also can be seen that the passive system only begins to isolate at 0.4 Hz, and is insufficient to attenuate ISS structural disturbance vibrations near and below the same frequency. The predicted closed loop payload response to off-board acceleration is also shown in the figure. The closed loop response has increased damping and begins isolating at 0.01 Hz.

**FIGURE 12 - PREDICTED PASSIVE AND ACTIVE ISOLATION RESPONSE**



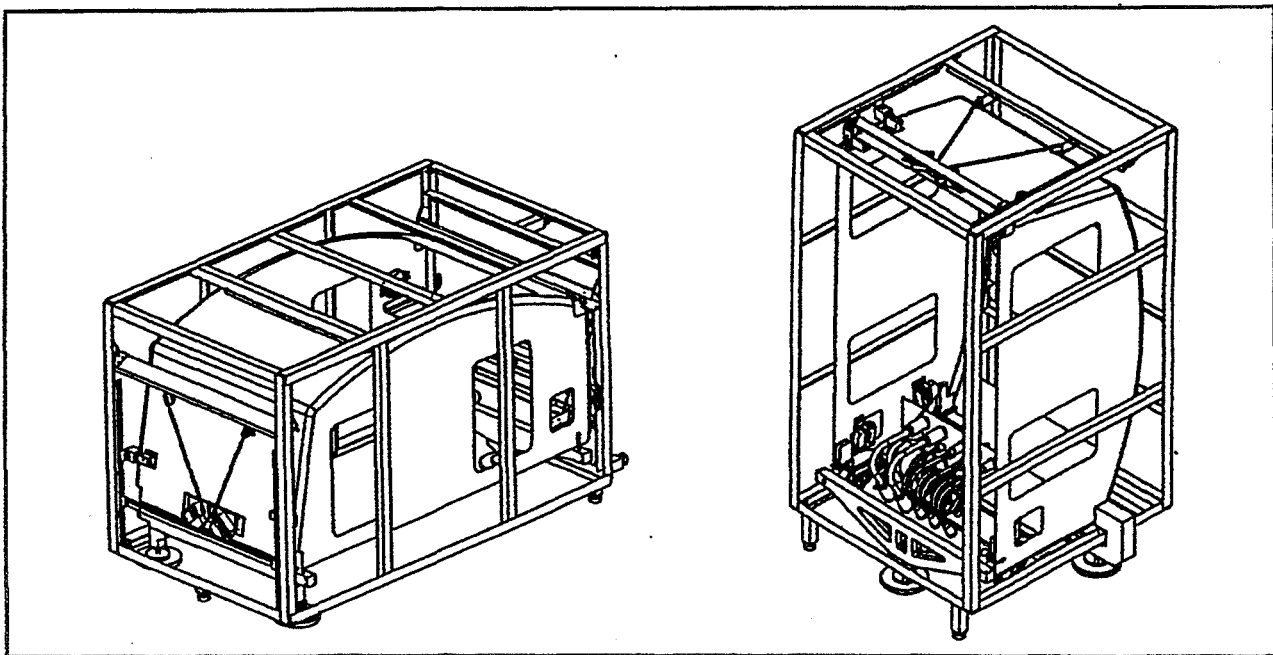
### Ground & Flight Test Results

#### Ground Tests

Isolation tests on the ground were performed by floating two racks on airpads on a flat surface; an on-board rack (ISPR) and an off-board rack representing

the space station. Both the inner and outer racks are constrained to 3 degrees-of-freedom planar motion as illustrated in Figure 13.

**FIGURE 13 - 3 DEGREE-OF-FREEDOM UPRIGHT & FACEDOWN FLOATING DEVELOPMENT TEST SETUP CONFIGURATIONS**



Simulated space station accelerations were induced by shaking the off-board rack at a discrete frequency in a single direction. Accelerometers mounted off-board were used to measure the disturbance. Isolation was then derived at the shake frequency from the off-board and on-board ARIS acceleration measurements.

**Test issues**

Ground testing was compromised by 1-G coupling. This is because the earth's gravity cannot be distinguished from true accelerations, and tilting of the rack mounted accelerometers can cause large, false sensed accelerations. Small amplitude low frequency motions were of most concern because they may result in large translations of the isolated payload. For example, if the accelerometers tilt 10 micro-radians, the active isolator will accelerate the payload to zero out the false acceleration error. This constant acceleration produces 5 inches translation in one minute.

There are many sources of tilting including ground motion, test table motion, and rack structural bending. Each of these were partially addressed by modifications to the testbed or test approach. Changes of table tilt due to movement of the heavy rack on a flexible test table were effectively minimized by use of a granite table with granite legs. The granite table also had a very flat surface which eliminated problems of the rack tilting as it moved on the surface of the table.

Local tilt in the concrete floor would occur as a person walked by the test table resulting in changes of acceleration around 5  $\mu$ G's. Therefore, the test table was placed on a concrete slab which was isolated from the rest of the laboratory's concrete floor.

In the upright test configuration the ISPR was found to bend when pushed by the top ARIS actuators. This effect was reduced by setting the software parameters to minimize usage of the top actuators (This did not cause a problem because of the redundancy of the 8

actuator system in controlling the 3-DOF motion). The facedown configuration was modified to use four airpad/legs instead of three to reduce the effect of flexibility in the rack/airpad interface structure.

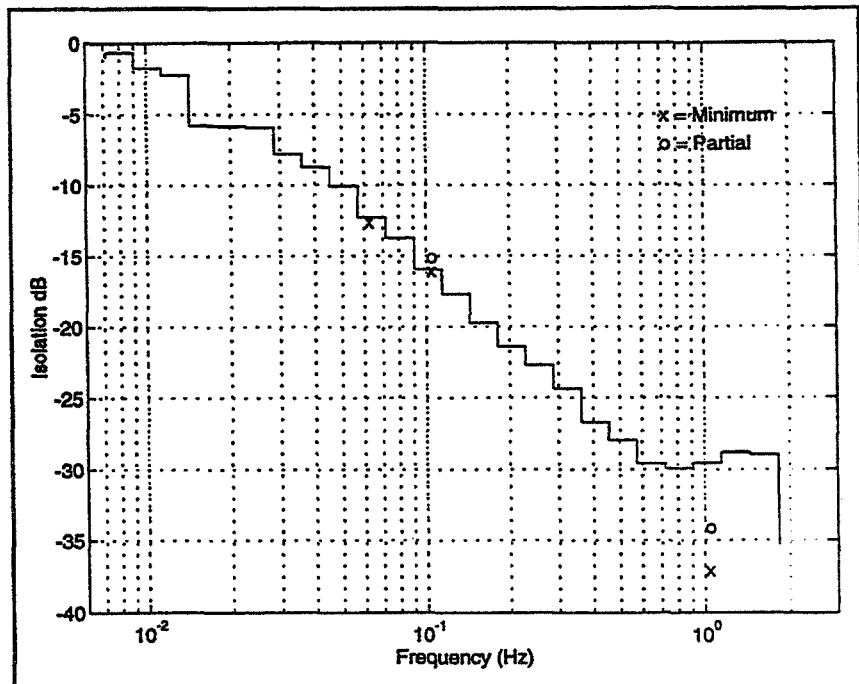
A secondary 1-G coupling issue was electronic noise induced by non-flight electronics used to remove 1-G coupling biases from each accelerometer (accelerometers skewed with projections along the gravity vector). The noisy bias increased the noise by a factor of 10 below 0.2 Hz. Although desirable, improvements to the non-flight bias electronics were not made.

Finally, the position loop gains were increased and the acceleration loop gains decreased to prevent unacceptable ISPR motion due to 1-G coupling. It was eventually possible to obtain a large enough gain to obtain significant isolation over short time duration's and verify ARIS performance.

**Test results**

Figure 14 shows ground test results from X axis isolation tests with the ISPR in the facedown configuration. The ground test isolation data was evaluated at 0.06, 0.1, and 1.0 Hz and is shown by X's and O's corresponding to data taken with the minimum

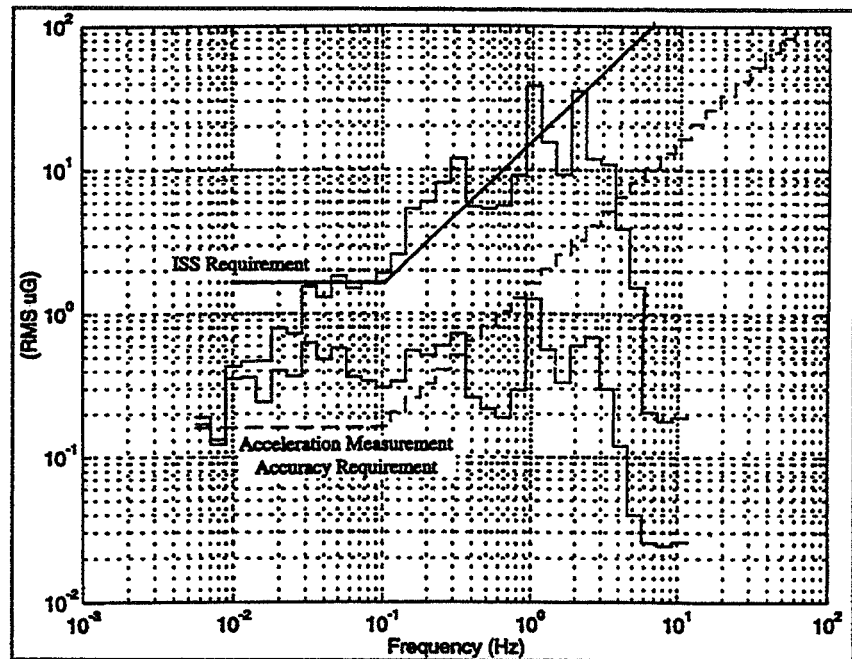
**FIGURE 14 - GROUND AND FLIGHT ISOLATION TEST RESULTS**



and partial umbilical sets installed respectively. Stiffness cancellation compensation was used to reduce the stiffness of the partial set down to the stiffness of the minimum set. Figure 14 also includes flight test data from a 14 minute test conducted during crew MIR treadmill exercise. The flight data shows isolation evaluated over 1/3 octave bands with accelerations resolved at the ISPR CG.

The corresponding on and off-board flight accelerations are shown in Figure 15. Off-board accelerations exceed the ISS requirement while isolated on-board levels remain well below the requirement. The accelerations are attenuated at the higher frequencies because the data was post-processed decimated and filtered with a 3.5 Hz 8<sup>th</sup> order filter. Below .006 Hz it was found that the off-board acceleration levels were too small to overcome measurement noise.

**FIGURE 15 - ISOLATED AND NON-ISOLATED FLIGHT 1/3 OCTAVE BAND ACCELERATION TEST RESULTS (14 MINUTE TEST RUN)**



organizations and NASA Shuttle, Russian MIR, and McDonnell Douglas SpaceHab flight teams.

### Concluding Discussion

Isolation of an entire space station rack with large standard space station rack utilities was successfully demonstrated. This proved that acceleration cancellation with direct contact actuation, skewed control components, and system decoupling is a viable microgravity solution. Increasing performance by increasing acceleration feedback gain was limited in ground testing by 1-G coupling effects. The acceleration feedback gain was increased significantly in zero-G flight tests, but time constraints prevented further gain increases (by changing digital filter parameters) to find the system limitation. Utility design improvements to reduce stiffness will improve isolation performance and are under development. Updates to flight verified utility models are also underway to increase the fidelity of the ARIS simulation.

### Acknowledgment

The Boeing ARIS development and flight experiment was a cooperative team effort including participation from NASA Space Station Prime, Phase 1, and Code U

### References

1. Boeing Defense & Space Group Missiles & Space Division, "System Specification for the International Space Station", Specification #41000D, Nov. 1<sup>st</sup>, 1995
2. Rombado, Gabriel, "DAC-4 ARIS Off-board Acceleration Environment", Station Prime Microgravity Memo #059 (SSP-MG96-059), Jan. 10<sup>th</sup>, 1997
3. DelBasso, S., "The Space Station Freedom Microgravity Environment", AIAA Paper 93-0831, Jan. 1993
4. Peters, Rex. B., "Noise PSD Measurement of a High-Performance Accelerometer with Motion Cancellation", Sundstrand Data Control, Inc Technical Paper.

**Session D**  
**SUMMARY OF FREE FLYER MICROGRAVITY**  
**ENVIRONMENT**

---

Chair: Kevin M. McPherson, NASA Lewis Research Center, Cleveland, Ohio

# **Terrier-Black Brant Sounding Rocket Microacceleration Environment**

---

Thomas J. Kacpura, Aerospace Design & Fabrication, Brook Park, Ohio

Julio C. Acevedo, NASA Lewis Research Center, Cleveland, Ohio

## **Terrier-Black Brant Sounding Rocket Microacceleration Environment**

**Authors:**

Thomas Kacpura, Aerospace Design & Fabrication, Brook Park, OH  
Thomas.J.Kacpura@lerc.nasa.gov  
Julio Acevedo, NASA Lewis Research Center, Cleveland, OH  
Julio.C.Acevedo@lerc.nasa.gov  
<http://www.lerc.nasa.gov/WWW/MMAP/SAMSFF/>

### **ABSTRACT**

On September 10, 1997 a Terrier-Black Brant Sounding Rocket was launched to support the Lewis Research Center DARTFire combustion experiment at the White Sands Missile Range in New Mexico. The sounding rocket also carried two microacceleration measurement systems to support the DARTFire experiment by measuring the microacceleration environment. The SAMS-FF system and a SAMS-type triaxial sensor head (TSH) were flown. The SAMS-FF system consisted of a variable frequency, digital output TSH and a roll rate sensor. Data from the two systems were analyzed and compared. Data will be presented from both systems in order to characterize the sounding rocket microacceleration environment.

The data collected demonstrated that a sounding rocket is a viable vehicle for conducting space experiments that require a quiet, dedicated microacceleration environment.

### **BACKGROUND**

The SAMS-FF  $\mu\text{g}$  measurement system consisted of a Control and Data Acquisition Unit (CDU), and two external sensors. The CDU was used to control operation, and provide data storage. A digital output Triaxial Sensor Head (TSH) was used to record accelerations. A Fiber Optical Gyroscope (FOG) was used to record the residual roll of the spacecraft. The SAMS-FF presentation at the 16<sup>th</sup> MGMG meeting gave further details on the hardware design.

### **DARTFire MISSION OBJECTIVES**

This initial test demonstration flight was scheduled on a sounding rocket. This mission was in support of the 4<sup>th</sup> DARTFire flight. The mission objectives were:

1. Provide a checkout of the SAMS-FF hardware in an actual flight environment, and exercise the flight team from integration through post-flight data processing.
2. Characterize the sounding rocket environment.

3. Redundantly support the collection of  $\mu\text{g}$  data to support DARTFire in its compliance with science requirement for  $\mu\text{g}$  environment. (DARTFire flew a 5 Hz analog SAMS TSH connected to the DARTFire onboard control computer).

## **MISSION INTEGRATION**

The requirements for integration mandated that it be non-intrusive on the DARTFire payload. The aft bulkhead, which housed a shockbox for recording launch and landing shock loads, temperature and pressure measurements, was extended in height from 3.5 to 5.5". The increased weight of adding SAMS-FF to the DARTFire payload was approximately 15 pounds.

The CDU and roll rate sensor were mounted on an aluminum plate, which was insulated from the bulkhead using a G10 spacer. The TSH was the only component mounted inside the DARTFire payload, on top of one of the combustion tunnels on a bracket using existing holes. Also, SAMS-FF was operated using experiment power starting at T+55 seconds and ending shortly before impact.

The software for this mission was designed to run a script file that controlled recording status, FOG synchronization, and TSH commanding temperature and RMS interleave, and bandwidth. This script file initiated whenever the unit was powered.

## **TSH DATA**

Five bandwidth changes were made during the flight, to exercise the capabilities of the TSH and to better capture the  $\mu\text{g}$  environment. A higher rate of 400S/sec (104.8 Hz) was used at the beginning and the end of the mission, where the  $\mu\text{g}$  environment was not as low and the rocket and the experiment create disturbances. A rate of 25 S/sec (6.5 Hz) was used from the time the rocket officially entered the " $\mu\text{g}$ " portion of the flight at 100 miles altitude to just after the apogee. The sampling rate was raised to 200 S/sec (52.4 Hz) for a brief period after the apogee to record the difference in noise as the bandwidth was increased. The rate was chosen at 50 S/sec (13.1 Hz) for the descent, double the 25 S/sec rate during ascent. Both of these two relatively low rates allowed low noise, high quality  $\mu\text{g}$  data collection.

The data collected is of higher quality than originally expected. A summary sheet in the paper lists the average and RMS  $\mu\text{g}$  values of each of the bandwidth collection periods, for each axis. For the lowest bandwidth, the RMS value is less than 10  $\mu\text{g}$ . In addition, time domain plots and the associated power spectral density calculations are shown for each axis in the same period. DARTFire personnel identified disturbances at two frequencies from the imaging system filter wheels. An infrared camera filter rotated at 1 Hz, and the filter wheel for the visible / ultraviolet camera that rotated at 5 Hz. These are clearly seen in the power spectral density plots.

## **SAMS-FF VERSUS DARTFire SAMS TSH COMPARISON**

A comparison of data was performed between the SAMS-FF TSH data and the analog SAMS 5 Hz TSH data. The SAMS TSH had been used to collect data for the three previous DARTFire flights and was flown again for a baseline comparison to the SAMS-FF TSH. The SAMS TSH used QA2000 accelerometers, and the sensor current output from each axis was converted to a voltage with a 7.5 k $\Omega$  resistor, in parallel with a 3.5  $\mu$ F capacitor. This was filtered through a 2 pole Sallen-Key filter into a 12-bit A/D converter, and stored with the rest of the DARTFire experiment data.

The original DARTFire SAMS TSH was designed merely to verify compliance with the DARTFire  $\mu$ g requirement of 100  $\mu$ g, and does not provide as nearly as good quality data as the SAMS-FF hardware, as plots in the presentation illustrate. The SAMS-FF data quality, as compared to the SAMS data, is greatly improved in terms of noise level, filtering / aliasing, resolution, and accuracy.

This conclusion is supported by comparing the power spectral density information of the of the SAMS TSH with the 25 S/sec data (Bandwidth = 6.5 Hz) of the SAMS-FF TSH. The base noise floor level of the SAMS TSH is approximately  $10^{-10}$  ( $g^2 / \text{Hz}$ ), but the SAMS-FF TSH is better than 3 orders of magnitude lower. Events can be clearly seen in the SAMS-FF plots, and these are attributed to specific equipment in the payload. None of these events can be seen in the SAMS plots, since the  $\mu$ g environment is lower than the SAMS TSH (and associated A/D conversion circuitry) noise floor.

## **ROLL RATE DATA**

The roll rate sensor data collection began immediately after the CDU was booted, after the despin of the rocket was completed. (The rocket is spin stabilized during ascent and descent.) The despin is considered complete when the spin is less than 0.2 $^\circ$ /sec, in each of the three axes. The despin system is then turned off.

The roll axis is initially stabilized to less than 0.02  $^\circ$ /sec. Residual forces caused the roll to accelerate, to a maximum of 0.4 $^\circ$ /sec. With a payload diameter of 17", the contribution from this centripetal acceleration is small, less than 0.5  $\mu$ g. The roll during the  $\mu$ g period is approximately 100 $^\circ$ , which is slightly more than  $\frac{1}{4}$  turn.

The pitch and yaw rates are on the same order as the roll rate. Both are stabilized to less than 0.2 $^\circ$ /sec, and the maximum rates are 0.4 $^\circ$ /sec and -0.6 $^\circ$ /sec, respectively. This corresponds to a roll of  $\sim$ 100 $^\circ$  for the pitch axis, and  $\sim$ 200 $^\circ$  for the yaw axis. This is more disturbing to the  $\mu$ g environment, due to the larger distance from the c.g., but is still relatively small ( $< 10 \mu$ g) for these levels. As a result, the payload is slowly tumbling in space about all three axes.

## **SYSTEM SUMMARY & CONCLUSIONS**

1. Flexible, modular system was adapted & integrated to platform in very short time.
2. The digital TSH using 24-bit  $\Delta\Sigma$  ADCs was exercised through varied bandwidth, which has common design elements to the SAMS-II design.
3. The TSH successfully measured  $\mu\text{g}$  levels.
4. Successfully flew state-of-the-art Fiber Optics Gyro.
5. Software-based GSE and Labview interface developed for both sensors and CDU.
6. Prepared TSH performance report, which is available from the team.

## **MISSION SUMMARY & CONCLUSIONS**

1. Exercised the project team from design & development, integration & mission, to data analysis.
2. Successful integration & operation were completed.
3. Characterized high quality microgravity environment for sounding rocket for DARTFire payload.
4. Data correlated w/ DARTFire hardware.
5. Prepared mission data results report, which is available from the team.

## **FUTURE FLIGHTS**

Since this mission, the SAMS-FF TSH has been used connected to a laptop through a serial port to support the LeRC  $\mu\text{SEG}$  experiment flying on the NASA KC-135 airplane performing parabolic maneuvers. In addition, another unit has been prepared in hermetic enclosures for use in the Space Shuttle cargo bay. This system, consisting of a CDU and two TSHs, will record acceleration data in support of HOST payload on STS-95. The HOST payload is a shuttle test demonstration of a cryogenic cooler designed for the Hubble Space Telescope. Other flight possibilities are available and presently being investigated.

## **ACKNOWLEDGEMENTS**

The SAMS-FF team includes: Bruce Johnson, David Miller, Dale Mortensen, Dan Bloom, Bruce Smith, John Merry, John Bowen, Leon Rasberry, Gregory Fedor, Kevin McPherson, Julio Acevedo, and Thomas Kacpura.

5/3-29

Paper Number: 14

## **Review of 3-DMA Measurements on Six Shuttle Missions and Nine Suborbital Flights**

---

Jan A. Bijvoet, CMDS, University of Alabama in Huntsville, Huntsville, Alabama

Philip D. Nerren, CMDS, University of Alabama in Huntsville, Huntsville, Alabama

## **Review of 3-DMA Measurements on Six Shuttle Missions and Nine Suborbital Flights**

Authors:

Jan A. Bijvoet and Philip D. Nerren

Consortium for Materials Development in Space, The University of Alabama in Huntsville,  
Huntsville, Alabama

### **ABSTRACT**

In the period 1989 to 1998, different configurations of the 3-DMA (3-Dimensional Microgravity Accelerometer) have flown on nine sounding rocket and six space shuttle missions.

In addition to providing Principal Investigators with information on the acceleration environment, a principal purpose of the 3-DMA continuous development program is the introduction and validation of improved technologies for the measurement of the microgravity environment.

A particular interest of the Consortium for Materials Development in Space (CMDS), as one of the Commercial Space Centers, is achieving an instrumentation with low development and low operations costs.

In particular sounding rocket flights give excellent design, development and validation opportunities. Sounding rocket missions have the potential of very low microgravity disturbance levels, permit upgrading hardware and procedures until shortly before launch and have a short turn around time for the data.

This paper will review the technology improvements introduced.

The low microgravity disturbance environment achievable and the high instrument sensitivities will be shown by representative data plots.

The space shuttle missions included several SPACEHAB missions and a Spacelab mission.

New developments for these missions will be reviewed and representative time and frequency data plots shown.

### **ADVANTAGE OF SOUNDING ROCKET FLIGHTS**

Sounding rocket flights have very low-g levels and have a clean microgravity environment. These flights have a low cost per pound. The six minutes of microgravity environment is

sufficient for validating new microgravity measurement instrumentation. The data and hardware are immediately available after recovery of the vehicle. The hardware may be updated up until the launch date. There is minimal documentation and safety compliance costs compared with space shuttle missions. In the pre-launch phase, a realistic mission sequence test is possible.

### **3-DMA TECHNOLOGIES VALIDATED**

These technologies were validated in the various 3-DMA missions.

1. Three simultaneous frequency bands for each accelerometer
2. Hard disk drive viability
3. Fully automatic data recording
4. True real-time acceleration data to ground on USML-2
5. Invertable accelerometer
6. High-G ascent and microgravity on orbit with same instrument (CONQUEST 4/96)
7. A small and autonomous "Free-Flyer" Unit, using PC-104 processor technology, was developed and flown (CONQUEST, April '96)
8. No suppression of "DC" component
9. Very low noise level
10. Sensitivity increase and bias control
11. Novel panoramic data display
12. Pre-mission microgravity mission sequence test

### **MEETING CMDS COST REDUCTION REQUIREMENTS**

These features were incorporated to meet CMDS cost reduction requirements.

1. Off the shelf hardware was utilized where possible
2. Automatic operation for on orbit operation which minimized crew involvement
3. No supplementary stowage of disks or cables
4. Real-time microgravity data was supplied to the ground operations centers
5. Data supplied directly to the PI's
6. "Free-flyer" PC-104 system was utilized
7. Pre-mission microgravity tests were performed
8. Low-cost invertable accelerometer was developed
9. Low mass of 3-DMA for low launch cost
10. Low-power which also reduced cooling requirements (no liquid or air cooling)
11. Precursor sounding rocket flights were used before shuttle missions

### 3-DMA supported missions

#### 1. Space shuttle missions

|                                |               |
|--------------------------------|---------------|
| CONCAP III, Tether             | STS-46, 8/92  |
| SPACEHAB 01                    | STS-57, 6/93  |
| SPACEHAB 02                    | STS-60, 2/94  |
| SPACEHAB 03                    | STS-63, 2/95  |
| Spacelab, USML-02              | STS-73, 10/95 |
| SPACEHAB 05, ETTF, MACEK, ARIS | STS-79, 8/96  |

#### 2. Suborbital missions

|                 |         |
|-----------------|---------|
| CONSORT 1, 2, 3 | 89 - 90 |
| JOUST           | 91      |
| CONSORT 4, 5, 6 | 91 - 93 |
| METEOR          | 10/95   |
| CONQUEST - 1    | 4/96    |

*omit this  
page*

**Paper Number: 15**

**First Microgravity Measurement Results  
of FOTON-11 by QSAM**

---

Dr. Hans Hamacher, German Aerospace Center (DLR), Koeln, Germany

H.E. Richter, German Aerospace Center (DLR), Koeln, Germany

**PAPER NOT AVAILABLE**

514-29

Paper Number: 16

**Some Results of Measuring Microgravity in the Process  
of "FOTON no. 11" Microgravitational Space Platform  
Flight**

---

Valentin F. Agarkov, Central Specialized Design Bureau, Samara, Russia

Vladimir D. Kozlov, Central Specialized Design Bureau, Samara, Russia

# **Some Results of Measuring Microgravity in the Process of “FOTON no. 11” Microgravitational Space Platform Flight**

Authors:

Valentin F. Agarkov, Central Specialized Design Bureau, Samara, Russia

Vladimir D. Kozlov, Central Specialized Design Bureau, Samara, Russia

## **ABSTRACT**

The microgravity measurement system SINUS-6 was operated during the Foton-11 mission in October 1997. Measurement results from two periods of operation, each approximately twenty-four hour duration, will be presented.

## **FOTON no. 11 MICROGRAVITY ENVIRONMENT**

In the process of “FOTON no. 11” microgravitational platform flight during October 9 to 23, 1997 microgravity was measured using “Sinus-6” system.

“Sinus-6” system comprises 2 three-axis accelerometers, which measure quasiconstant microgravity component in the range between 0.1 and 0.000001  $g/g_0$  with an accuracy of 10% and better. Accuracy is worse outside the specified range.

The system enables to make a spectral analysis of microacceleration transducer signals, direct control of the signal values and their statistical processing. On-board memory size is up to 720,000 16-digit words.

Microgravity platform flight pattern envisaged a attitude-hold mode in orbital coordinates after orbiting and launch vehicle separation. It resulted in decreasing angular velocities of the platform with respect to centre of mass to values of max 0.05 degrees per second.

Then attitude control was disengaged and the platform was in free flight up to the end and descent vehicle recovery. Besides, all on-board mechanical assemblies were disengaged but for thermal control systems assemblies, maintaining specified thermal conditions in leak-proof space platform modules.

According to pre-set programme, scientific hardware from Russia, ESA, CNES, DARA was switched on and off in flight.

Measuring hardware was switched on in flight twice for large intervals of time in order to measure disturbances during various on-board and scientific hardware operation. Tables 1 and 2 partially show results of measuring linear (or quasiconstant) component of microgravity.

Table 1 shows measurements during activation on October 16, 1997, starting since 13:19:25 (h:m:s). Table 1 shows measurements during activation on October 22, 1997, starting since 10:57:16 (h:m:s).

Designations: the right column shows time, specifying hours, minutes, seconds of measurement, according to Moscow time.

X1, Y1, Z1 - first accelerometer measurements;

X2, Y2, Z2 - second accelerometer measurements.

A preliminary measurement result analysis enables to make the following conclusions:

1. Quasiconstant component values did not exceed values in minus 5th power throughout "Foton" space platform flight.
2. Measurements have indicated that microgravity values measured by accelerometers were continuously changing.
3. Difference in indications of two accelerometers placed from each other at a distance of a little more than a meter was of an order and more.
4. Generally, measurement results confirm the authors' theoretical conclusions concerning the existence of continuously changing microgravity fields, specified in the report.

## LITERATURE

1. V. Agarkov, V. Kozlov, Y. Gorelov, S. Danilov: The Basics of Methodology of Space Automatic Microgravity Platform Design - Mathematical Simulation of Microgravity Fields, Microgravity Measurements Group Meeting #15, April 30 - May 2, 1996.

**Table 1: Sample of data from Sinus-6 accelerometer on October 16, 1997**

| Time     | X1       | Y1       | Z1      | X2       | Y2       | Z2       |
|----------|----------|----------|---------|----------|----------|----------|
| 13:19:25 | -4.93E-5 | -1.22E-5 | 4.39E-5 | -9.69E-6 | -1.51E-5 | -4.68E-5 |
| 13:24:25 | -1.65E-5 | -9.89E-6 | 3.41E-5 | -1.03E-6 | -2.23E-5 | -4.20E-5 |
| 13:29:25 | -1.34E-5 | -2.51E-6 | 2.98E-5 | -1.67E-5 | -3.98E-5 | -3.03E-5 |
| 13:34:25 | -1.57E-5 | -1.19E-5 | 2.23E-5 | 1.78E-5  | -8.81E-6 | -1.84E-7 |

**Table 2: Sample of data from Sinus-6 accelerometer on October 22, 1997**

| Time     | X1       | Y1       | Z1       | X2       | Y2       | Z2      |
|----------|----------|----------|----------|----------|----------|---------|
| 10:57:16 | 3.68E-6  | -1.04E-6 | 1.18E-6  | 6.13E-6  | -7.21E-6 | 7.34E-7 |
| 11:02:16 | -7.86E-7 | -1.32E-5 | -3.98E-6 | -2.34E-6 | -2.09E-5 | 4.69E-6 |
| 11:07:16 | 7.32E-6  | -2.21E-6 | -3.76E-6 | -1.15E-6 | -3.92E-6 | 4.55E-6 |
| 11:12:16 | 1.04E-5  | -7.28E-6 | -8.85E-8 | 4.20E-6  | 7.34E-6  | 6.52E-7 |

**Results of Synchro Experiment on Simultaneous  
Measurement and Estimation using Digital Model of  
Microgravity in places of Accelerometer Installation  
during "FOTON no. 11" Flight for Digital Model  
Accuracy Assessment**

---

Valentin F. Agarkov, Central Specialized Design Bureau, Samara, Russia

Vladimir D. Kozlov, Central Specialized Design Bureau, Samara, Russia

# **Results of Synchro Experiment on Simultaneous Measurement and Estimation using Digital Model of Microgravity in places of Accelerometer Installation during “FOTON no. 11” Flight for Digital Model Accuracy Assessment**

Authors:

Valentin F. Agarkov, Central Specialized Design Bureau, Samara, Russia

Vladimir D. Kozlov, Central Specialized Design Bureau, Samara, Russia

## **ABSTRACT**

The results of concurrent measurements and estimations using a mathematical model of microgravity at the accelerometer locations during the Foton-11 free flyer mission will be presented. The goal of this work is to verify the mathematical model.

At this time, only results from the quasi-steady model are presented. The results show that the quasi-steady environment was mainly in the  $10^{-6}$  g range.

Preliminary discussions about the vibratory regime will be made.

## **FOTON no. 11 MICROGRAVITY ESTIMATION**

The object of this work was to assess accuracy of mathematical digital model for estimating microgravity values in any point of descent vehicle of specialized “Foton N11” space microgravity platform.

The task in question is to give microgravity experiment customers microgravity values directly in the research zone: in melting furnace, bioreactor, active zone of electrophoretic facilities, in liquid or melt under examination etc. There is no possibility of placing microgravity measuring accelerometers directly in these active points.

As have been shown in report (I) and confirmed by measurements, difference in microgravity values in two points with a distance between each other of approximately 1 meter, measured at the same point of time can reach one order.

Thus microgravity values in operational zones of scientific hardware can be estimated only

by calculations. Principally, it is possible by mathematical modeling and digital models, as has been shown in (I). However these models can be used only if their accuracy is estimated and is within permissible levels. Mathematical modeling has indicated that estimation accuracy can be essentially increased if microgravity values in flight are measured simultaneously in several points and these measurements are used for estimating microgravity values in specified points.

Thus a combination of measurements and digital models shall increase authenticity of knowledge of microgravity values in operational zones of experimental facilities.

Mathematical analysis has shown that the best results can be achieved using simultaneous indications of four three-axis accelerometers in specified estimated points.

Development and manufacture of "Sinus 15" second generation microgravity measuring system with 5 three-axis accelerometers are based on the results of theoretical research data. Indications of any 4 accelerometers out of 5 can be used for estimations.

"A synchro experiment method" combining theoretical and experimental methods has been developed for practical realization of the above offers. The method presupposes microacceleration estimation of the Earth using mathematical digital models simultaneously with flight measurements by four accelerometers through the whole flight.

In-flight measurements are downlinked by radio channel. They are used to correct digital model errors and to estimate microgravity values in any point of scientific hardware.

Thus the above method requires:

1. Assessment of mathematical digital model accuracy and thus to prove its availability for realization of "synchro experiment" method;
2. Creating a microgravity measuring system with four three-axis accelerometers;
3. Developing a mathematical digital model, enabling to estimate microgravity in any point of scientific hardware using measurements of 4 accelerometers.

Experiment during "Foton N 11" flight is intended for "Synchro experiment" method development and digital mathematical model error estimation.

The first experiment is not literally a synchro one because measurements were not immediately downlinked by radio channel but were stored in memory. For that reason estimations and comparisons with in-flight measurements were made after "Foton N11" return capsule recovery. General view of "Foton N 11" space microgravity platform, system of coordinates and stabilization planes are shown in figure 1. Flight direction is shown for the time of SC stabilization after space vehicle separation.

Inside reentry capsule there is Russian, ESA, CNES and DARA scientific hardware and Russian measuring hardware "Sinus 6".

Foton N 11 SC was launched from Plesetsk cosmodrome on October 9, 1997 at 22-00 Moscow time and the reentry capsule landed on October 23 at 11:52 Moscow time. After orbiting SC was transferred into orbital attitude-hold mode. Attitude hold mode lasted for 70 minutes, which was followed by attitude control system disengagement and SC free non-oriented flight. Residual angular SC velocities in all three axes did not exceed 0.02 to 0.05 degree/sec.

Considering comparatively small changes in ballistic parameters and heliophysical situation in the course of the flighty, estimations were based on ballistic measurements during two revolutions, characterizing the flight sufficiently well.

1. October 14, 1997, 75th revolution

|                                 |             |
|---------------------------------|-------------|
| Inclination:                    | I = 62.8.   |
| Perigee altitude:               | 227.06 km.  |
| Apogee altitude:                | 391.17 km.  |
| Orbit ascending node longitude: | W = 220 27. |
| Pericenter argument:            | 105 19.     |
| Argument of latitude:           | 0.          |
| Solar activity index:           | F = 100.    |
| Geomagnetic disturbance factor: | fT = 12.    |

2. October 22, 1997, 203rd revolution

|                                 |             |
|---------------------------------|-------------|
| Orbital plane inclination:      | I = 62.8.   |
| Perigee altitude:               | 225.7 km.   |
| Apogee altitude:                | 384.9 km.   |
| Orbit ascending node longitude: | W = 189 11. |
| Pericenter argument:            | 105 28.     |
| Argument of latitude:           | 0.          |
| Solar activity index:           | F = 100.    |

Attitude control system was activated and atmospheric attitude control 10N thrust jets started operating 24 hours before the end of the flight.

Two three-axis "Sinus 6" system accelerometers were accommodated in the hermetic descent vehicle and returned to the Earth after the end of the flight. Accelerometer layout with respect to reentry capsule 0, X, Y, Z axes of coordinates is shown in figure 2.

Accelerometer N1: X = -978; Y = 0; Z = 0:

Accelerometer N2: X = 342; Y = -496, Z = -585.

Dimensions are given in mm.

Direction of accelerometer axes of coordinates coincides with descent vehicle 0, X, Y, Z

axes of coordinates.

Comparison of measurements and estimated values in points of accelerometer installation for the same time is given in Table 1.

Table designations:

2xE-6 corresponds to  $2 \times 10^{-6}$  g/go.

Comparison results show:

1. Estimated values based on theoretical digital models have a good convergence. An absolute error does not go beyond the limits of a measurement order.
2. Mathematical digital models can be used in ground synchro experiments during "Foton" microgravity platform flights.

## CONCLUSIONS

1. "A method of synchro experiment" enabling to estimate microgravity during space platform flight in zones, non-available for accelerometer installation (in material melting zone, chemical and biological reactor zone, active zones of electrophoretic facilities) on the Earth with a sufficiently high accuracy. High estimation accuracy is achieved by periodic correction of digital model based on direct in-flight accelerometer measurement results.
2. "A method of synchro experiment" enables to offer a higher servicing to commercial customers of "Foton: S/C experiments; they can continuously observe and document microgravity change pattern inside their experimental facilities from the Earth, which is problematic today by any other methods.
3. "A method of synchro experiment" can be fully used together with "Sinus-15" measuring system, incorporating five three-axis accelerometers and a telemetry downlink for a part of information.
4. The results of work have indicated that specifying statistical characteristics of digital model errors requires processing of the whole measurement array, which is a time-taking task to be fulfilled in 1998.
5. "Sinus-6" measurements show that microgravity values did not go beyond the limits of the fifth order during "Foton no. 11" flight.

## LITERATURE

1. V. Agarkov, V. Kozlov, Y. Gorelov, S. Danilov: The Basics of Methodology of Space Automatic Microgravity Platform Design - Mathematical Simulation of Microgravity Fields, Microgravity Measurements Group Meeting #15, April 30 - May 2, 1996.

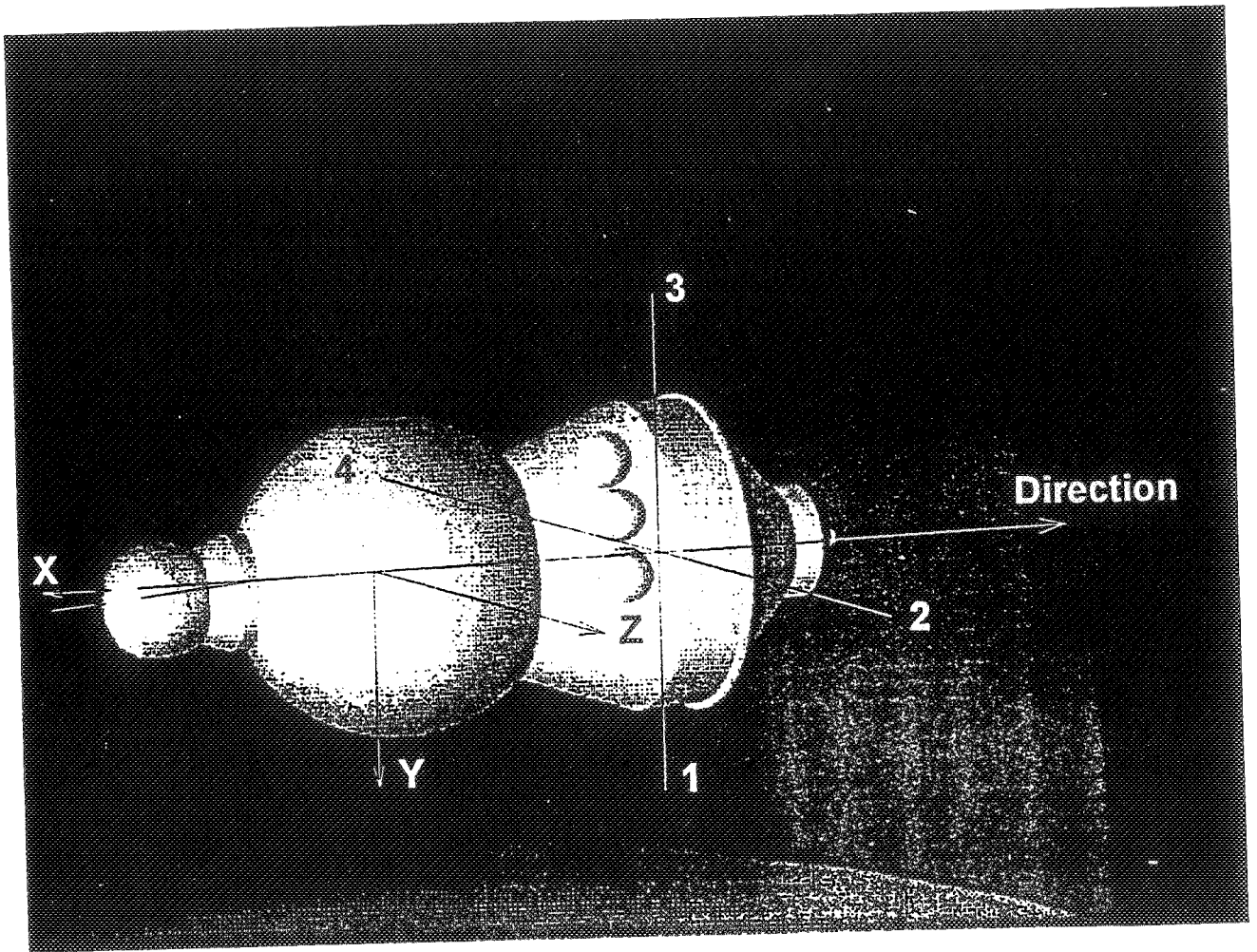


Fig 1

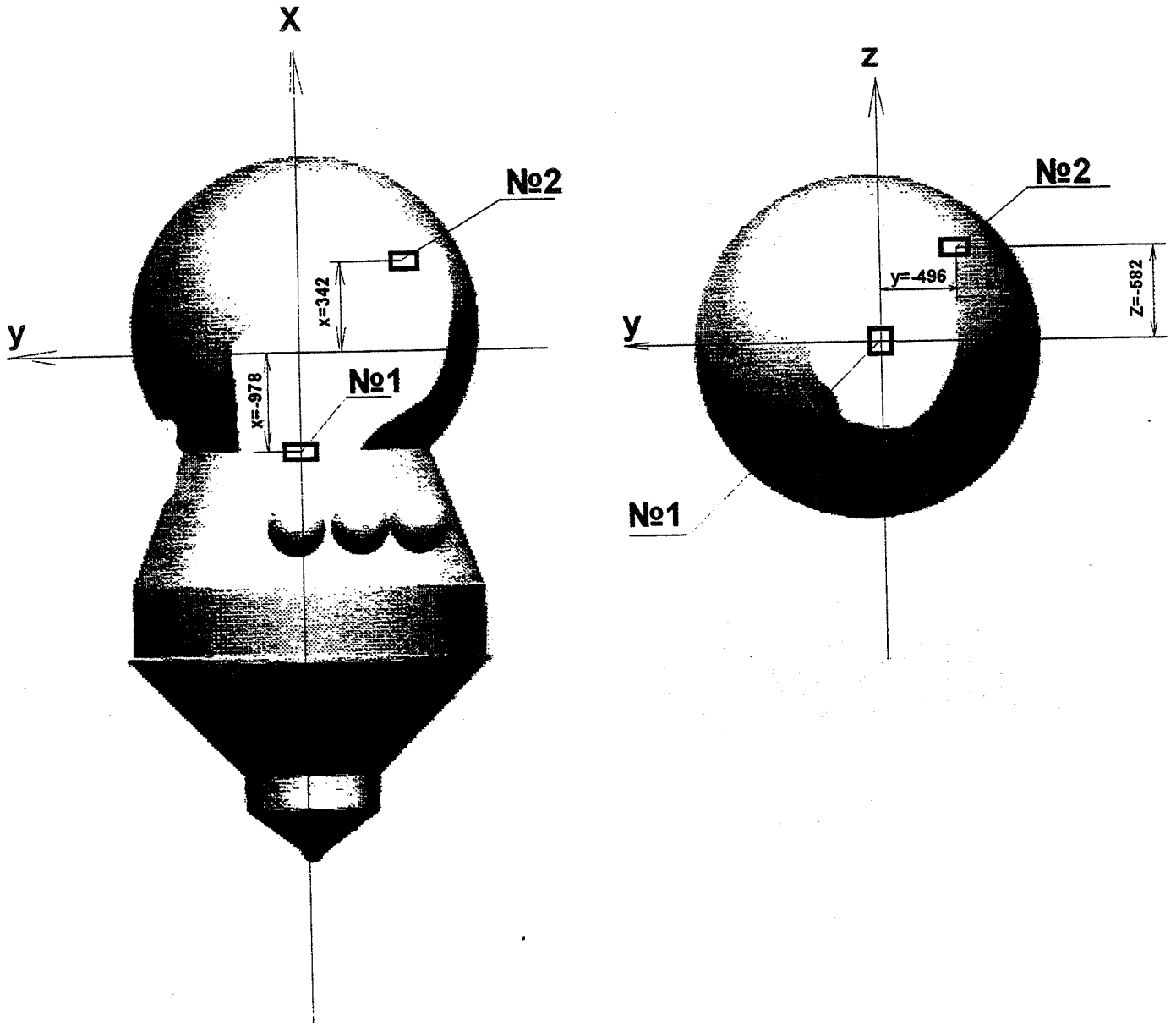


Fig. 2

| Time     | X <sub>1</sub> | Y <sub>1</sub> | Z <sub>1</sub> | X <sub>2</sub> | Y <sub>2</sub> | Z <sub>2</sub> |
|----------|----------------|----------------|----------------|----------------|----------------|----------------|
| 13:59:25 | 1.45E-6        | 1.71E-6        | 7.18E-6        | -9.46E-6       | 5.38E-6        | -1.00E-5       |
|          | 1.00E-6        | 2.00E-6        | 9.00E-6        | -6.20E-6       | 3.10E-6        | -9.00E-6       |
|          | measurement    | 9.1E-6         |                | measurement    | 1.0E-5         |                |
|          | estimated      | 9.9E-6         |                | estimated      | 1.1E-5         |                |
| 14:34:25 | -2.37E-6       | 7.42E-6        | 2.17E-6        | 3.35E-6        | 7.25E-6        | -1.4E-6        |
|          | -1.80E-6       | 5.30E-6        | 4.20E-6        | 4.50E-6        | 4.60E-6        | -3.0E-6        |
|          | measurement    | 8.0E-6         |                | measurement    | 8.1E-6         |                |
|          | estimated      | 6.9E-6         |                | estimated      | 7.7E-6         |                |
| 15:39:25 | 1.79E-5        | 2.60E-6        | -2.28E-6       | 1.21E-6        | -6.75E-6       | 5.37E-7        |
|          | 1.20E-5        | 1.80E-6        | -1.90E-6       | 1.60E-6        | -7.20E-6       | 7.20E-7        |
|          | measurement    | 3.9E-6         |                | measurement    | 8.8E-6         |                |
|          | estimated      | 1.2E-5         |                | estimated      | 5.7E-6         |                |
| 17:24:25 | -2.60E-5       | -7.53E-6       | -1.21E-6       | 9.49E-6        | -1.01E-5       | -2.14E-5       |
|          | -3.60E-5       | -1.00E-6       | -4.00E-6       | 1.10E-5        | -2.20E-5       | -2.60E-5       |
|          | measurement    | 1.19E-6        |                | measurement    | 2.50E-5        |                |
|          | estimated      | 6.30E-6        |                | estimated      | 3.50E-5        |                |
| 17:59:25 | -8.47E-6       | 4.81E-6        | -2.63E-6       | 7.97E-6        | -1.48E-6       | 3.10E-6        |
|          | -6.00E-6       | 5.60E-6        | -6.40E-6       | 6.40E-6        | -1.20E-6       | 2.60E-6        |
|          | measurement    | 9.80E-6        |                | measurement    | 8.50E-6        |                |
|          | estimated      | 1.03E-5        |                | estimated      | 7.00E-6        |                |
| 19:24:25 | -2.09E-5       | 5.39E-6        | -2.77E-6       | 7.04E-6        | -3.15E-6       | 3.57E-6        |
|          | -2.30E-5       | -6.10E-6       | -3.20E-6       | 8.20E-6        | 4.30E-6        | 4.10E-6        |
|          | measurement    | 6.70E-6        |                | measurement    | 5.90E-6        |                |
|          | estimated      | 7.23E-6        |                | estimated      | 1.00E-5        |                |
| 20:24:25 | 2.15E-5        | -8.15E-6       | 4.26E-7        | 1.08E-6        | 3.18E-6        | 9.69E-7        |
|          | 2.30E-5        | -7.60E-6       | 4.60E-7        | 2.20E-6        | 3.30E-6        | 8.90E-7        |
|          | measurement    | 8.30E-6        |                | measurement    | 3.20E-6        |                |
|          | estimated      | 8.00E-6        |                | estimated      | 9.70E-6        |                |
| 22:29:26 | -3.45E-6       | -2.71E-6       | 6.84E-7        | -3.34E-6       | -6.15E-6       | 3.32E-6        |
|          | -3.20E-6       | -2.90E-6       | 5.10E-7        | -2.10E-6       | -5.20E-6       | 4.10E-6        |
|          | measurement    | 4.40E-6        |                | measurement    | 7.40E-6        |                |
|          | estimated      | 4.30E-6        |                | estimated      | 6.80E-6        |                |
| 23:29:26 | 1.57E-5        | 2.09E-6        | -2.91E-7       | -2.70E-6       | -4.08E-6       | -1.05E-6       |
|          | 2.10E-5        | 3.50E-6        | -3.20E-7       | -2.10E-6       | -4.40E-6       | -2.10E-6       |
|          | measurement    | 2.50E-6        |                | measurement    | 4.80E-6        |                |
|          | estimated      | 4.00E-6        |                | estimated      | 5.20E-6        |                |
| 25:59:26 | -7.11E-6       | 3.68E-6        | 5.17E-6        | -5.55E-6       | 2.55E-6        | 3.33E-6        |
|          | 6.50E-6        | 3.10E-6        | 4.90E-6        | -5.30E-6       | 2.60E-6        | 3.50E-6        |
|          | measurement    | 9.50E-6        |                | measurement    | 6.50E-6        |                |
|          | estimated      | 8.60E-6        |                | estimated      | 6.60E-6        |                |

OMIT  
THIS  
PAGE

**Session E**  
**SCIENCE AFFECTED BY MICROGRAVITY**  
**ENVIRONMENT**

---

Chair: Melissa J. B. Rogers, National Center for Microgravity Research on Fluids and Combustion, Cleveland, Ohio

## **Fluids and Materials Science Studies Utilizing the Microgravity-vibration Isolation Mount (MIM)**

---

Rodney Herring, Canadian Space Agency, Montreal, Quebec, Canada

Bjarni V. Tryggvason, Canadian Space Agency, Montreal, Quebec, Canada

Walter M. Duval, NASA Lewis Research Center, Cleveland, Ohio

# **Fluids and Materials Science Studies Utilizing the Microgravity-vibration Isolation Mount (MIM)**

Authors:

Rodney Herring, Bjarni Tryggvason\* and Walter Duval\*\*

Microgravity Sciences Program, Canadian Space Agency, St. Hubert, PQ, J3Y 8Y9

\*Canadian Astronaut Program, Canadian Space Agency, St. Hubert, PQ, J3Y 8Y9

\*\*NASA Lewis Research Center, Cleveland OH 44135

## **Introduction**

Canada's Microgravity Sciences Program (MSP) is the smallest program of the ISS partners and so can participate in only a few, highly focused projects in order to make a scientific and technological impact. One focused project involves determining the effect of accelerations (g-jitter) on scientific measurements in a microgravity environment utilizing the Microgravity-vibration Isolation Mount (MIM).

Many experiments share the common characteristic of having a fluid stage in their process. The quality of the experimental measurements have been expected to be affected by g-jitters which has lead the ISS program to include specifications to limit the level of acceleration allowed on a subset of experimental racks. From finite element analysis (FEM), the ISS structure will not be able to meet the acceleration specifications. Therefore, isolation systems are necessary.

## **Experimental Measurements**

Recent accelerations measurements of Mir and the Space Shuttle [1] are less than the specified ISS requirements, i.e., the acceleration on the Mir and Space Shuttle are already better than those expected for the isolated regions meeting the ISS requirements. FEM analysis also shows that the racks not isolated will suffer degradation in the acceleration levels compared to those expected from the station by itself.

Experiments which may have sensitivity to g-jitter have been performed using Mir and the Space Shuttle as the reference condition. It should be noted that if the acceleration environment on Mir and the Space Shuttle are not good enough for experimental measurements then those

measurements taken on platforms which just meet the station requirements or are non-isolated will also not be good enough. There is a need to know the acceleration levels necessary for various types of experiments, i.e., what quality of gravity is necessary to make good measurements of fundamental material properties and enable some types of materials processing?

Experiments having their platform either isolated or non-isolated or having induced g-pulses were performed using the Microgravity-vibration Isolation Mount (MIM) [1]. These experiments included the QUELD furnace on MIM operating in Mir in the STS-Priroda missions where ~250 materials samples have been processed to date which include 1) measurements of intrinsic metal diffusion, 2) measurements of Soret coefficients and the Ostwald ripening phenomenon and, 3) processing of semiconductor materials and glasses. Other measurements were taken on the STS-85 flight where 5 fluid science experiments were performed, which included 1) the generation of resonance patterns experiments, 2) wave maker experiments, 3) bubble motion experiments, 4) liquid diffusion experiments and, 5) Brownian motion of small particles. More recent measurements include the growth of protein crystals on/off MIM which were returned from Mir on STS-89, January, 1998.

While the results of these experiments are still being analyzed, several of these indicate a clearly observable difference between isolated and non-isolated conditions. The results are significant since they predict significantly greater sensitivity to g-jitter than the current ISS vibratory specification for ARIS isolated racks assumes. They are contentious in that they contradict the results of many analytic and numerical studies conducted over the years to predict the g-jitter sensitivity.

If the results seen thus far are accurate predictors of the sensitivity for experiments planned for the ISS then the various experimental facilities being developed for the ISS and not mounted in an ARIS will need to incorporate provision for isolation systems. These results have raised interest and concerns of facility developers in Canada, Europe and Japan. While any decision to incorporate isolation systems as integral components of facilities implies additional costs, it will be far more cost effective to do this as part of the facility development, rather than to try to fix facilities once they are on orbit in the ISS.

## **Implications**

For the ISS as a whole, the current vibratory specification is inadequate by a large margin which has even greater cost implications. The ARIS is being designed to provide the currently

defined vibratory environment in those racks that will incorporate the ARIS. However if the current requirement is in fact not stringent enough then experiments conducted in an ARIS supported rack may still be degraded by g-jitter.

There have been numerous questions raised about the experiments listed above. The questions raised have been entirely appropriate. The experiments were designed as first looks at the g-jitter issue. Much of the hardware was developed on very short time scales in order to meet Phase 1 schedules for the Mir operation, and in order to meet schedules for flight of the second system on STS-85. There are grounds for questioning the solidity of some of the results. However, with similar indications from several independent experiments, the overall finding is that many experiments on the ISS will need an environment that is much cleaner than the current specification, and the cost implications for this is on a strong footing.

### **Summary**

Fluid science results and materials science results show significant sensitivity to g-jitter. The work done to date should be viewed only as a first look at the issue of g-jitter sensitivity. The work should continue with high priority such that the international science community and the ISS program can address the requirement and settle on an agreed to overall approach as soon as possible.

### **Reference**

- 1) B. Tryggvason: Acceleration levels and operation of the Microgravity Vibration Isolation Mount (MIM) on the Shuttle and the Mir space station, Proceedings of the 17th MGMTG, March 24-26, 1998, Cleveland, Ohio.

# Fundamental Physics Microgravity Sensitivity

---

Ulf Israelsson, Jet Propulsion Laboratory, Pasadena, California

Roger Williamson, Stanford University,

Robert V. Duncan, University of New Mexico,

# Fundamental Physics Microgravity Sensitivity

Author:

Ulf E. Israelsson, Jet Propulsion Laboratory

## ABSTRACT

An introduction followed by a brief discussion about the sensitivity to microgravity environment disturbances for some recent and planned experiments in microgravity fundamental physics will be presented. In particular, correlation between gravity disturbances and the quality of science data sets measured by the Confined Helium Experiment (CHeX) during ground testing and during the November 1997 USMP-4 flight will be described.

## INTRODUCTION

The fundamental physics program is managed for NASA by the Jet Propulsion Laboratory (JPL) and aims at studying far-reaching physics questions that are obscured by gravity on the Earth. In the early eighties the program consisted of a small community of investigators supported by NASA's Physics And Chemistry Experiments Program (PACE). This community expanded in the late eighties and early nineties to involve many major Universities. Currently NASA is funding over 50 investigators (10 for potential flight) in the fundamental physics area. 34 of the investigations are in the low temperature and condensed matter physics area, 14 investigations are in the laser cooling and atomic physics area, and 6 investigations are in the relativity and gravitational physics area. Historically, the program has focused on research in the condensed matter physics area, primarily on critical point studies, although significant growth has occurred recently in the other research areas.

In 1985 the Superfluid Helium Experiment, developed by the Jet Propulsion Laboratory, demonstrated the containment and control of liquid helium aboard the space shuttle and the feasibility of supporting a science instrument insert within a liquid helium dewar. Containment using the fountain pressure was accomplished by pumping with space vacuum on the helium through a porous plug. The porous plug and vent plumbing must be precisely adapted to the expected operating conditions for containment to occur.

In 1992 the Lambda-Point Experiment (LPE), developed by Stanford University, JPL and Ball Aerospace, added nanokelvin high resolution thermometry to this capability which allowed a precise test of the Nobel Prize winning Renormalization Group (RG) theory of

critical phenomena to be performed. The LPE demonstrated that the superfluid transition in  $^4\text{He}$  is sharp to within about one nanokelvin. This represented two orders of magnitude improvement in the approach to a critical point than possible in a ground experiment. LPE demonstrated that advanced technology, high-resolution experiments could be made to survive the shock associated with launch and can operate flawlessly in the hostile space environment. Subsequent flight projects, including the plans for experimentation aboard the space station relies heavily on the pioneering work developed for the LPE flight.

In November 1997, the Confined Helium Experiment (CHeX) used the unique properties of liquid helium to perform a high-resolution test of the theory of finite size effects. CHeX investigated the shape of the heat capacity curve very near the lambda transition of a sample confined in one of the dimensions to about 57 microns thickness. Confinement is accomplished by stacking nearly 400 4-cm diameter 50-micron thick Silicon wafers on top of each other with a 57-micron spacer between.

Other low temperature experiments will be flown aboard the International Space Station early in the next century. Plans are also underway to develop hardware to allow LCAP and GRP experimenters access to a microgravity environment. Due to space and time limitations, the discussion on acceleration sensitivity will be limited to some recent experience from the CHeX flight.

## **LOW FREQUENCY ACCELERATION ENVIRONMENT SENSITIVITY**

Experiments near the lambda transition are mainly disturbed by a DC acceleration environment due to hydrostatic pressure induced effects. The dependence of the lambda transition temperature on pressure in a one-g environment is roughly 1.27 microdegrees per cm height of helium sample. This dependence scales in a linear way with the gravity environment. A 0.1-cm tall helium sample on the ground would thus show gravity smearing within about 127 nK of the superfluid transition. For a typical experiment size of 3 cm and a thermometry resolution of 1 nK, an experiment would thus be sensitive to DC disturbances larger than about 3 mg. This number is consistent with the sensitivity of the LPE and CHeX experiments and is easily achievable in a Shuttle environment. Other experiments may have more stringent requirements in this area depending on the specifics of their investigation.

## **G-JITTER SENSITIVITY – GROUND TESTING**

The acceleration environment at higher frequencies is usually more of a concern in low

temperature physics experiments. This is mainly due to time varying vibration heating effects that may occur and introduce hard to quantify error sources in the scientific data. Of particular concern has been the 17 Hz Ku band antenna dither on the Shuttle and harmonics thereof, especially the 51 Hz harmonics. Our LPE and CHeX instruments had a known resonance near 55 Hz. Figure 1 shows the effect of sweeping a low level vibration signal mechanically attached to the CHeX instrument while monitoring the effective instrument heating rate. As can be seen the resonance is located at 55.15 Hz and has a linewidth of about 0.3 Hz. The concern during the flight was if any Shuttle vibration sources would overlap with this band of sensitivity.

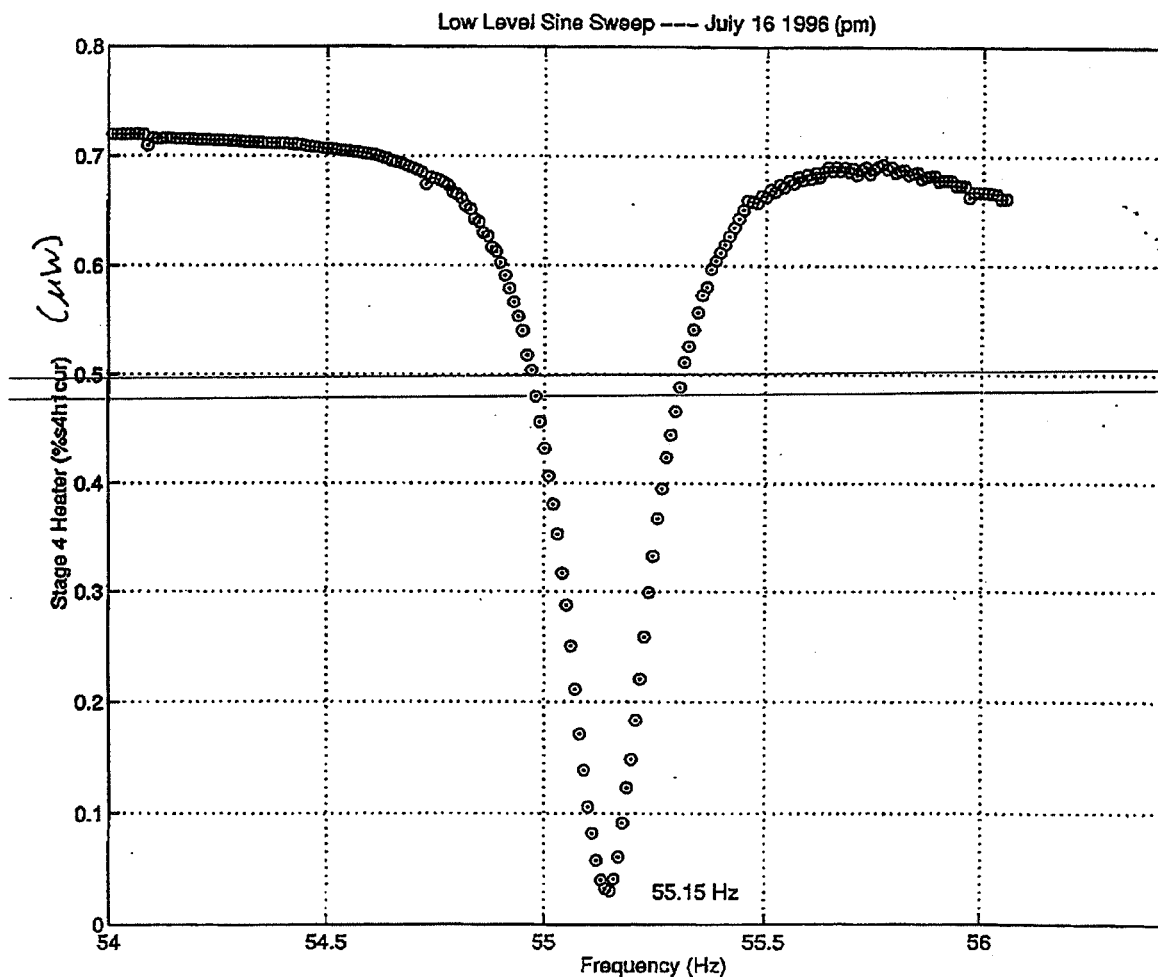
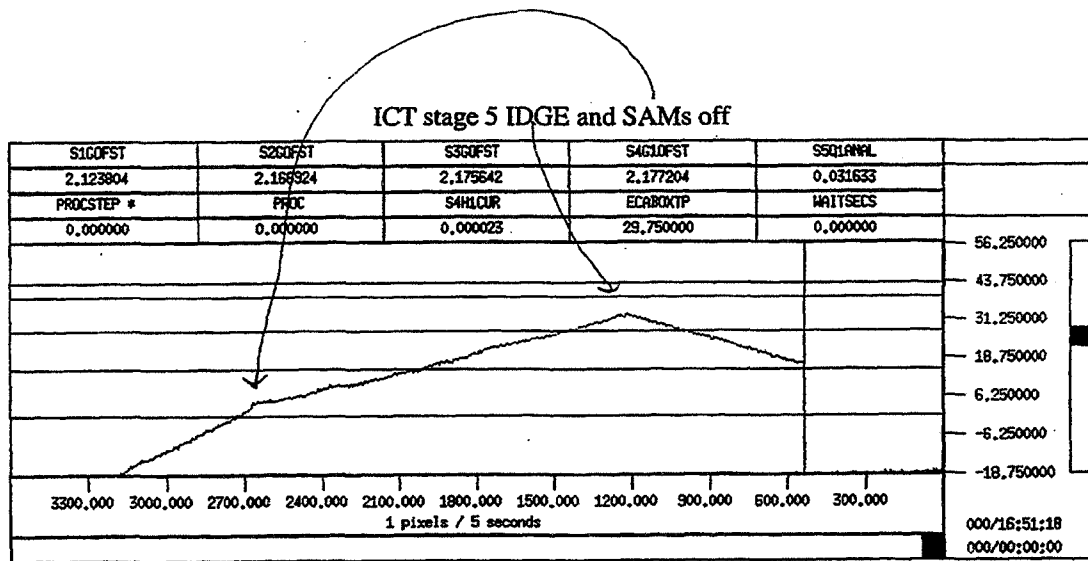


Figure 1. CHeX instrument resonance at 55.15 Hz.

During testing of a fully integrated system at KSC (Mission Sequence Testing) prior to the CHeX flight some anomalous sensitivities were detected when the SAMS instrument and the IDGE instrument were turned on. We were unable to trace down the exact cause of

the disturbances but it was thought to arise either from EMI disturbances or mechanical disturbances from fans operating in the instrument electronics. Figure 2. Shows the CHeX instrument slowing down in its warm-up rate when SAMS and IDGE is turned off. The vertical axis is high-resolution thermometer output and the horizontal axis is time.



**Figure 2.** Reduction in CHeX instrument warm-up rate when IDGE and SAMS are turned off recorded during ground testing at KSC.

## G-JITTER SENSITIVITY – FLIGHT

During the CHeX flight, there were some difficulties with deploying the SPARTAN satellite. To conserve fuel and allow for additional SPARTAN deploy attempts, there were extra periods of time where the Shuttle was maneuvered using primary thrusters instead of the regularly used vernier thrusters in microgravity flights. This mode of Shuttle alignment was called ‘ALT-DAP’ mode and it severely impacted the CHeX data. Fortunately ALT-DAP was only used for limited periods of time and CHeX was able to fully meet its science objectives. Figure 3 shows CHeX data during ALT-DAP operation and an insert of a typical high-resolution trace. The heat capacity steps in the insert are about 9 nK. It is clear that no useful data could be gathered during ALT-DAP operations. During ALT DAP spurious heating events of up to 30 nK was seen.

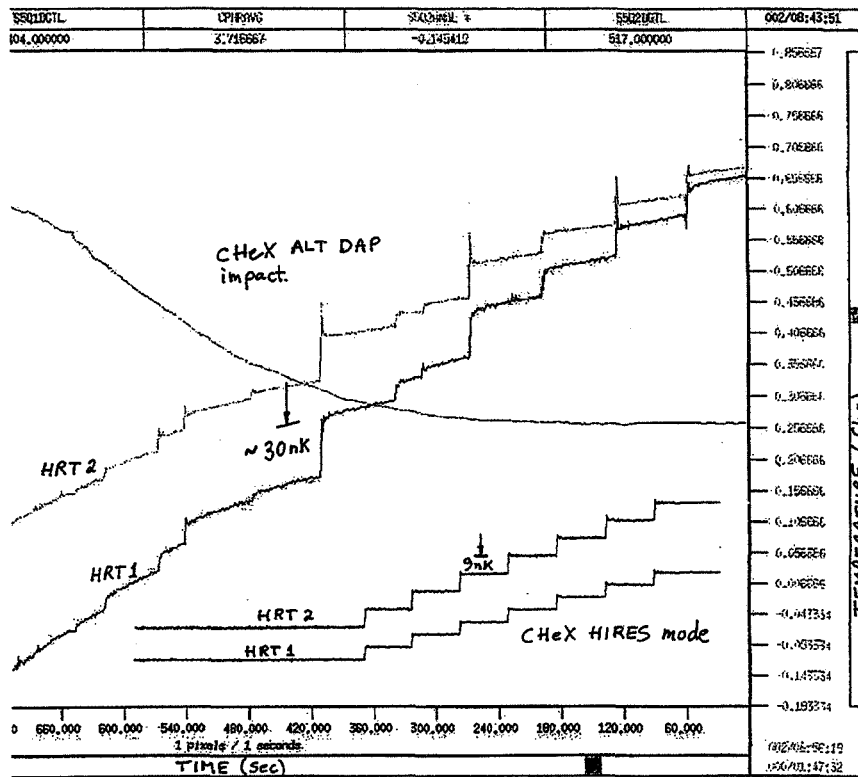


**Figure 3.** Impact to CHEX from ALT DAP operation with primary thrusters. Insert shows regular CHEX data gathering mode called HIRES.

During the CHEX flight we also noticed a vibration signal near 56 Hz when the IDGE instrument was turned on early in the mission. To search for a correlation with the spurious events observed at KSC we turned the SAMS instrument off briefly during the flight. The data is captured in figure 4. It is clear that the SAMS unit does generate spurious heating in the CHEX instrument. Some research revealed that there are some muffin fans that are used to keep electronic components cold that operate unregulated near about 56 Hz. The same fans are used in the IDGE instrument. It is likely that these fans are the source of heating seen in the CHEX instrument. LeRC personnel are planning to study these potential effects closely using actual flight units and report on the out come later on.

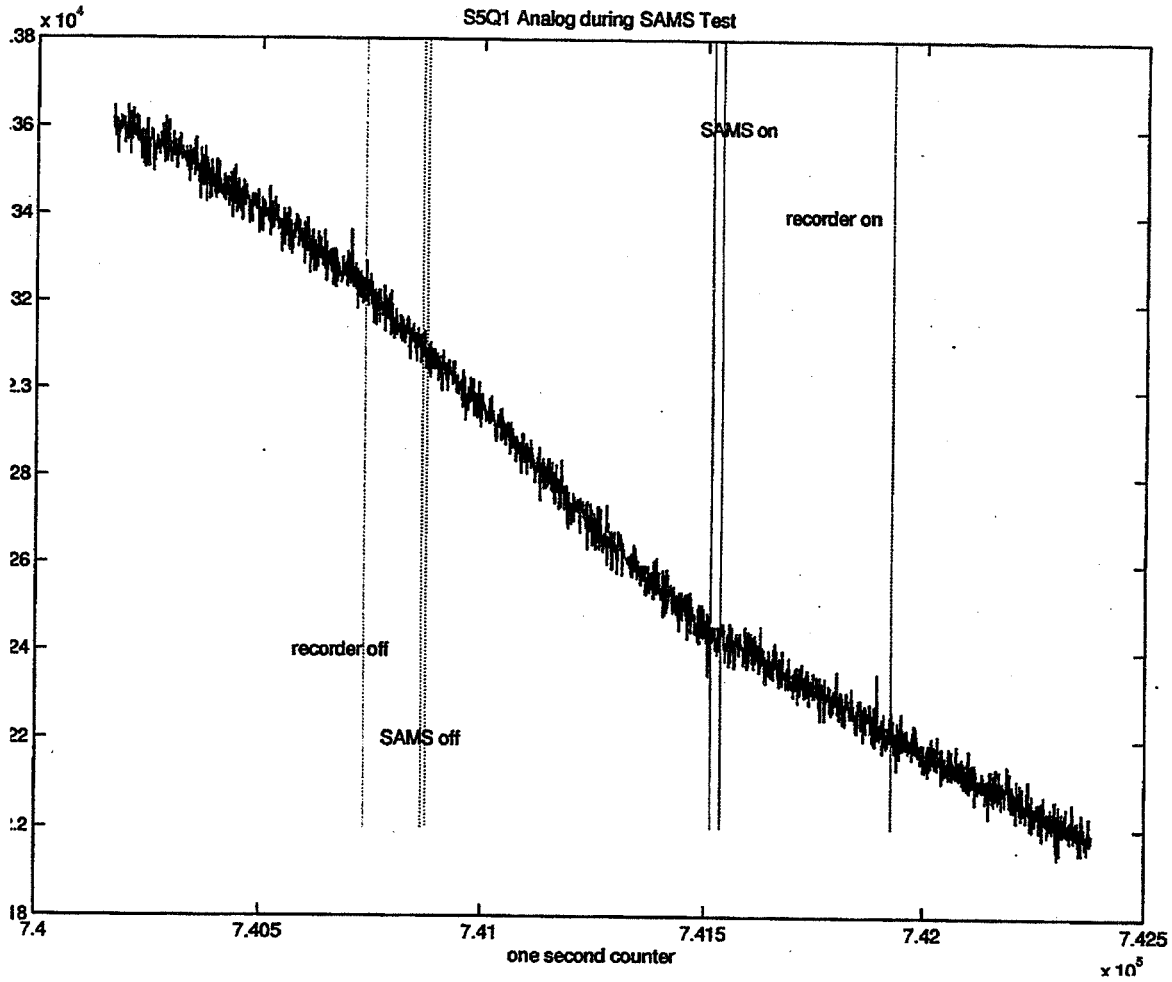


Figure 4. Reduced heating observed in the CHeX instrument when the SAMS unit was turned off.

## CONCLUSIONS

The primary acceleration environment sensitivity of low temperature experiments is from heating at high frequencies. The CHeX instrument resonance was at 55.1 Hz, with smaller resonance's occurring all the way up to a few hundred Hertz. Unfortunately, during the CHeX flight some overlap with this resonance was discovered. The overlap was weak enough to only marginally affect CHeX data, but was clearly seen as coming from both the SAMS and IDGE instruments.

## **Materials Science Experiments Microgravity Sensitivity**

---

Dr. J. Iwan D. Alexander, National Center for Microgravity Research on Fluids and Combustion & Department of Mechanical Engineering, Case Western Reserve University, Cleveland, Ohio

Dr. Donald C. Gillies, NASA Marshall Space Flight Center, Huntsville, Alabama

**PAPER NOT AVAILABLE**

Paper Number: 21

## **A Short Collation of G-Jitter Effects on Combustion Experiments in Microgravity**

---

Dr. Howard D. Ross, NASA Lewis Research Center, Cleveland, Ohio

## **A SHORT COLLATION OF G-JITTER EFFECTS ON COMBUSTION EXPERIMENTS IN MICROGRAVITY**

Author:

Howard D. Ross, Microgravity Science Division, NASA Lewis Research Center

### **ABSTRACT**

Variations in g level and direction are often apparent on low gravity *aircraft* and affect the flame behavior. A few examples – droplet, candle and jet diffusion flames are cited – which indicate a significant phase lag in flame response, and in changing the flame shape, color, and sooting propensity.

In general, the frequencies of sources of g-jitter on *spacecraft* are sufficiently high that combustion systems are unresponsive, despite the seemingly large amplitude of the accelerations. Sounding rocket experiments in flame spread across liquid pools are cited as an example of this. Impulsive accelerations are rare events that may create a momentary increase of buoyant flow, as demonstrated in the SOFBALL experiments on STS-83 and STS-94.

### **BACKGROUND**

Although gravity has a major effect on laminar and turbulent combustion processes, relatively little study has been performed on the effects of unsteady accelerations such as 'g-jitter' and momentary impulsive accelerations that may also influence microgravity combustion experiments. G-jitter herein is a time-dependent and repetitious acceleration that originates with vibrations of equipment on an aircraft, spacecraft or drop rig. These vibrations are transmitted through the structure of the aircraft, spacecraft and/or rig, unless means are provided for isolation. Examples of sources of vibration include fans on experiments or spacecraft, astronauts' exercise equipment such as rowing or cycling machines, and dithering of the spacecraft antennae to maintain communications. Impulsive accelerations are single or rare events that may create a momentary increase of buoyant flow. Examples include overboard venting of waste; bumping of or pushing off from the spacecraft's structure by an astronaut; and thruster firings for maintenance of attitude and/or altitude. These cause momentary acceleration levels of the order of  $10^{-3} g_e$ , and as such may affect briefly the combustion experiment in space. Another type of variation in g level and direction is often apparent on low gravity aircraft because the changes in air density and wind

velocity (both speed and direction) with altitude affect the pilots' ability to null all confounding accelerations. The direction of the residual acceleration is variable, and affects the flame behavior.

## EXAMPLES

### Low-G Aircraft: Effect Of Variable Residual Acceleration Vector

Anyone who has flown an experiment on low-g aircraft has observed the effect of the time-varying residual acceleration on the flame shape, color, size, and direction. While there are moments on the order of a second when the residual acceleration is small enough to emulate drop tower behavior, these moments are rare, and the flame response is subject to the previous moment's residual acceleration vector. Premixed gas flames, such as flame ball experiments, having no inertia per se, show a response in the flame position as a function of time. The SOFBALL experiments[1] flown on the aircraft and twice on the Shuttle involved the combustion of hydrogen and air in a mixture concentration very near the fuel-lean flammability limit, i.e. with a lesser fuel concentration, the mixture could not be ignited. Near the limit, the flame(s) that are produced are spherical and stationary in a microgravity environment. The flame balls themselves are very robust and appear not to change shape when the residual g vector of the aircraft changes, but their position inside a combustion chamber correlates well with the direction of the residual acceleration vector. The variable g vector may also induce the formation of flame cylinders, a.k.a. flame strings when the fuel concentration in the unburned premixed gas is raised.

As the inherent momentum of the combustion system increases, one would expect the effects of variations in g to diminish, as expressed by a Froude number,  $Fr=U^2/gL$ , where U is the forced velocity and L is a characteristic length. Candle and droplet flames, being very low-momentum systems (the only "forced flow" is the evaporative mass flux from the condensed-phase fuel) are still, however, subject to low-frequency g jitter at the levels apparent on the aircraft. This is because the forced velocity diminishes with distance from the droplet or wick surface, i.e. U is proportional to  $1/r$ , where r is the radius from the droplet center. Near the droplet or candle surface, U is large, but near and outside the flame, U is small such that  $Fr = O(1)$  or less at the residual acceleration levels on aircraft. As such, burning rates which depend on evaporative flux may be relatively insensitive to g jitter, but flame shape and position may be sensitive. An excellent example of variable g effects is shown in **figure 1**, as well as a video clip on the Internet at <http://zeta.lerc.nasa.gov/expr3/combust.htm>, displaying the burning of fuel wetting a 5 mm diameter porous sphere in an ambient of 15% oxygen, 85% nitrogen at a total pressure of 0.05 MPa[2]. This configuration simulates a very large droplet burning in microgravity. The layer of liquid in the film coating the sphere is held constant by an operator. The line in the figure is the

acceleration vector originating at the center of the porous sphere; each circle represents an acceleration magnitude of  $0.01 g_E$ . Time between photos is 0.2 seconds and progresses from the upper left as shown by the arrows. Note that there is a phase lag between a change in the residual acceleration vector and the direction of the flame tail. Note also that the flame lacks spherical symmetry due to the magnitude of the residual acceleration, except the lower left picture which is unrelated to the previous sequence; this last picture was taken when the  $g$ -level was small for a few seconds. Candle flames behave similarly[3], as do flames spreading[4] across thin solid fuels at partial gravity.

Experiments at larger Froude number involve laminar gas jet flames. These involve fuel issuing from a nozzle into a quiescent environment. Oxidizer from the environment is entrained in the jet. At the exit of the fuel nozzle, velocities are sufficiently high that the Froude number is between 10 and 1000, rendering gravitational effects small. While the total momentum of the system is constant, the local momentum in the jet diminishes with distance from the fuel nozzle. Thus at some distance from the nozzle, e.g. near the flame tip, the Froude number may be small enough for gravitational effects to be manifest even if the residual acceleration vector is aligned with the jet's axis. Furthermore, when the residual acceleration vector is orthogonal to the jet's principal axis, the transverse velocity of the entrained air or fuel is likely small relative to the  $g$ -induced velocity. In this case, the flame will bend and lose its axisymmetry. This indeed is what is observed {Urban, personal communication}.

Low-frequency  $g$ -jitter, emulating aircraft behavior but with the direction of the oscillation constrained, has been analyzed based on computational results for a laminar, ethylene-air, jet diffusion flame[5]. These were the first attempts to predict soot concentrations in a transient code with variable  $g$  level and radiative heat loss from the flame. These predict, consistent with drop tower experiments, enhanced soot production at  $10^{-5} g_E$ , owed to longer (by Order(10)) residence times in the flame, but also lower flame temperatures due to radiative loss. At intermediate levels of residual acceleration associated with aircraft environments, the results are, as expected, intermediate to those at microgravity and earth's gravity. At  $-0.01 g_E$ , the flame becomes nearly flat just above the nozzle, with the hot products swept away by buoyancy.  $G$ -jitter simulations were conducted by varying the gravitational field from  $+0.01 g_E$  through  $0 g_E$  to  $-0.01 g_E$  with a 1 Hz sine wave frequency. Simulations were conducted through 4 sinusoidal cycles, with the initial condition being the flame shape at  $+0.01 g_E$ . As the  $g$  level was reduced, the flame height shrunk. There was sufficient phase lag, however, that the flame never reached the shape that matched the  $-0.01 g_E$  flame, even when the  $g$  level reached this magnitude. The flame height showed a slight oscillation, but always remained between the heights of the steady flame heights seen at constant  $+0.01 g_E$  and  $-0.01 g_E$ .

The previous simulation was by Kaplan et al. Another simulation by Long et al [6] showed different results for a co-flow of air. When a co-flow of air was simulated in a methane-air system (general simulation of similar complexity, but no soot prediction), no effect of g-jitter at the same magnitude and frequency was seen on the combustion system: the flame looked exactly like the 0g flame. This suggests again that the local momentum near the flame tip is higher than in the case when air is viscously entrained.

### **G-jitter on Spacecraft**

In general, the frequencies of the sources of g-jitter on spacecraft are sufficiently high that combustion systems are unresponsive, despite the seemingly large amplitude of the accelerations. Sounding rocket experiments in flame spread across liquid pools will be cited as an example of this [7]. Buoyant forces can affect both the liquid-phase and gas-phase convective fields and consequently the rate of liquid preheating, the fuel-air mixing, and the rate of chemical reaction. Gas-phase buoyant flow transports oxidizer to the flame zone and hot products away from the flame zone. Liquid-phase convection, due to both thermocapillarity and buoyancy, transports heated liquid ahead of the leading edge of the flame. This liquid flow distinguishes flame spread across liquids from the more well-studied flame spread across solids, and causes much faster flame spread. These experiments used an array of non-intrusive diagnostic instrumentation that detect flame position, shape, and color, liquid surface and subsurface temperatures and gas and liquid phase flow patterns. A 30 cm long x 2 cm wide x 2.5 cm deep fuel tray was located inside a 10 cm x 10 cm cross-sectional area flow duct to provide a laminar, forced-air flow, ranging from 5 cm/s to 30 cm/s in the freestream over the fuel tray. The values of opposed, forced-air flow velocity were selected to be on the same order or less than that which occurs due to buoyancy in 1g experiments of this scale. The experiments were conducted with dry air at 1 atm and the temperature of the butanol fuel tray was between 20 and 21 C (depending on the test) at the time of ignition; these conditions are well into the pulsating spread regime for 1-butanol.

G-jitter effects would be manifest, in addition to the effects cited above for the flame, in the formation of waves along the liquid pool and potential spilling of fuel. The very large pool dimensions create a large Bond number ( $\rho_L g L / \sigma$ , where  $\rho_L$  is the liquid density,  $L$  is the liquid's characteristic length, and  $\sigma$  is the surface tension), making it unusually susceptible to g variations. None was observed. Also a seemingly small change -- the use of a different fan to provide the forced air flow -- resulted in a considerable increase in the amplitude of the g-jitter levels; these however also had no apparent effect on the observed behavior of the flame or liquid pool.

This experiment and many other types of experiments that have flown on the Space Shuttle have not shown a *known* response to the g-jitter levels on that spacecraft. Simulations of flame

behavior however have not attempted to predict g-jitter effects for any of these experiments, to this author's knowledge. Thus there may be an effect on flame behavior that is presently masked by expectation, neglect, or ignorance. Simulations are badly needed to verify these observations.

### **Impulsive acceleration on spacecraft**

Impulsive events on spacecraft cause momentary acceleration levels of the order of  $10^{-3} g_e$ , and as such may affect briefly the combustion experiment in space. One example from space experiments is provided: SOFBALL experiments on STS-83 and STS-94; a second example, Candle Flame experiments on STS-50, has previously been described [3].

When the SOFBALL experiments were performed on the Shuttle, they produced the weakest flames ever burned, either on the ground or in space, as may be seen in video form in the SOFBALL experiment description at <http://zeta.lerc.nasa.gov/expr3/combust.htm>. Flame ball powers as low as one watt were measured. By comparison, a birthday candle is about 50 watts. The drift of the flame ball(s) was much less than what was expected by scaling and extrapolation from aircraft results; this is because the scaling of the drift velocity on the aircraft balanced buoyancy and inertia, while at the lesser g levels on the Shuttle, the correct scaling should be between buoyancy and viscous shear forces {Ronney, personal communication}. As such, the flame ball survived indefinitely rather than drifting, as expected, into the wall of the combustion chamber after 10 minutes or so. Impulsive acceleration did affect the flame position, however, as detected by radiometers. When a flame ball moves closer to a radiometer, the irradiation on the sensor increases. **Figure 2** shows the 4 radiometric signals and the measured acceleration level as a function of time in the shuttle tests. They appear to be reaching an asymptotic value prior to GMT 1:25:00. When the Shuttle's vernier thrusters (VRCS) were energized, there was a momentary rise in the residual acceleration level to around 70 micro g's as noted on the figure. This was followed by a long-term effect in signal level at the radiometers. This effect was seen repeatedly whenever the thrusters were fired during the SOFBALL experiment. To prevent this, subsequent experiments were conducted in periods of "free drift" when impulsive accelerations were precluded by spacecraft operators.

## **CONCLUSIONS**

1. G jitter at the levels found on spacecraft does not apparently affect combustion experiments performed to date. Simulations are badly needed, however, to verify this conclusion.
2. Impulsive accelerations found on spacecraft, however, do affect combustion experiments that have particularly low momentum, e.g. premixed gas, droplet, and candle flame experiments.

3. The accelerations on aircraft are sufficiently high and variable in direction that combustion experiments are clearly affected and data must be carefully analyzed to draw conclusions, especially as they might be applied to an eventual space-based experiment. Those experiments with high Froude number do better in this extrapolation.

#### References

1. Ronney, P.D., *Structure of Flame Balls at Low Lewis-number (SOFBALL)*, in *3rd International Microgravity Combustion Workshop*, NASA Lewis Research: Cleveland, OH. p. pp. 439-444.
2. Struk, P.M., Dietrich, D. L., and T'ien, J. S., *Large Droplet Combustion Experiment Using Porous Spheres Conducted in Reduced Gravity Aboard an Aircraft -- Extinction and the Effects of g-jitter*. *Microgravity sci. technol.*, 1996. **IX**(2): p. 106-116.
3. Dietrich, D.L., H.D. Ross, and J.S. T'ien, *Candle Flames In Non-Buoyant And Weakly Buoyant Atmospheres*, in *32nd Aerospace Sciences Meeting & Exhibit*, AIAA: Washington, DC. p. pp. 1-18.
4. Sacksteder, K.R. and J.S. T'ien, *A New Formulation of Damkohler Number for Studying Opposed Flow Flame Spread and Extinction*, in *33rd Aerospace Sciences Meeting and Exhibit*, AIAA: Washington, DC. p. pp. 1-6.
5. Kaplan, C.R., Oran, E. S., Kailasanath, K., and Ross, H. D. *Gravitational Effects on Sooting Diffusion Flames*. in *26th International Combustion Symposium*. 1996. Naples, Italy: Elsevier Press.
6. Long, M., K. Walsh, and M.D. Smooke, *Computational and Experimental Study of Laminar Diffusion Flames in a Microgravity Environment*, in *Fourth International Microgravity Combustion Workshop*, NASA Lewis Research: Cleveland, OH. p. pp. 123-128.
7. Ross, H.D., *et al.*, *Flame Spread Across Liquids*, in *3rd International Microgravity Combustion Workshop*, NASA Lewis Research: Cleveland, OH. p. pp. 47-54.

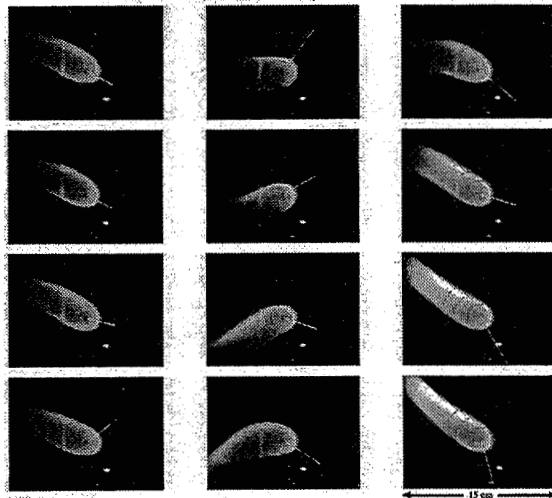


Figure 1: Reprinted from Struk et al. – see text for description

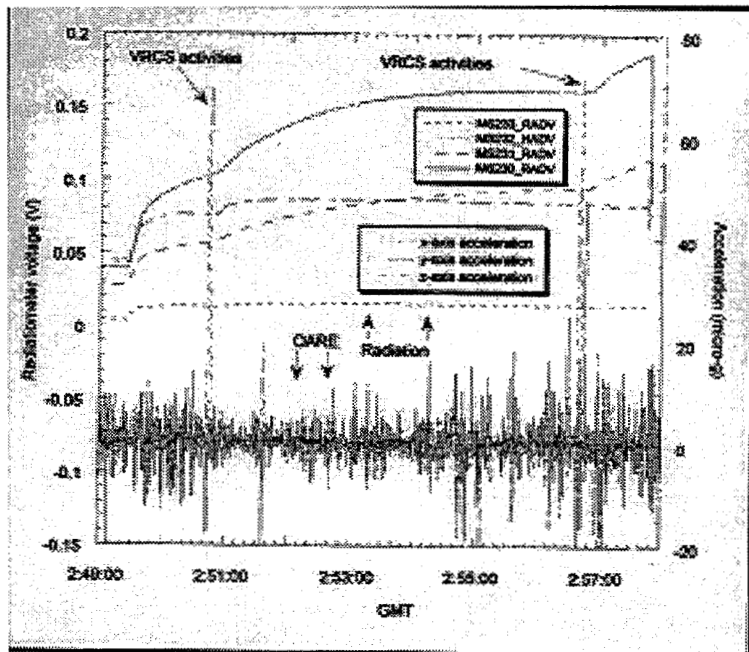


Figure 2: Reprinted from Ronney et al.

Paper Number: 22

# **NASA's Microgravity Fluid Physics Program - Tolerability to Residual Accelerations**

---

J. Raymond Skarda, NASA Lewis Research Center, Cleveland, Ohio

## NASA's Microgravity Fluid Physics Program - Tolerability to Residual Accelerations

J. Raymond Skarda, NASA Lewis Research Center, Cleveland, OH

### **Abstract**

An overview of the NASA microgravity fluid physics program is presented. The necessary quality of a reduced-gravity environment in terms of tolerable residual acceleration or g levels is a concern that is inevitably raised for each new microgravity experiment. Methodologies have been reported in the literature that provide guidance in obtaining reasonable estimates of residual acceleration sensitivity for a broad range of fluid physics phenomena. Furthermore, a relatively large and growing database of microgravity experiments that have successfully been performed in terrestrial reduced gravity facilities and orbiting platforms exists. Similarity of experimental conditions and hardware, in some cases, lead to new experiments adopting prior experiments g-requirements. Rationale applied to other experiments can, in principle, be a valuable guide to assist new Principal Investigators, PIs, in determining the residual acceleration tolerability of their flight experiments. The availability of g-requirements rationale from prior  $\mu$ g experiments is discussed. An example of establishing g tolerability requirements is demonstrated, using a current microgravity fluid physics flight experiment.

The Fluids and Combustion Facility (FCF) which is currently manifested on the US Laboratory of the International Space Station (ISS) will provide opportunities for fluid physics and combustion experiments throughout the life of the ISS. Although the FCF is not intended to accommodate all fluid physics experiments, it is expected to meet the science requirements of approximately 80% of the new PIs that enter the microgravity fluid physics program. The residual acceleration requirements for the FCF fluid physics experiments are based on a set of fourteen reference fluid physics experiments which are discussed.

### **Introduction**

In 1957, the Soviet satellite, Sputnik was successfully launched into orbit capturing attention worldwide. One impact was that it prompted some to consider the effect of reduced gravity on physical phenomena that are typically studied while influenced by their terrestrial (1-g) environment. A NASA Lewis researcher contemplated how one might simulate low-g conditions to study heat transfer phenomena, and in 1958 built the first modern day drop tower shown in Fig. 1. Low gravity boiling heat transfer was studied in the short free fall time of 0.7 seconds, and results of that investigation (see Fig. 2) were published shortly afterwards (Siegel and Usiskin, 1959).

The prediction and control of liquid propellants within storage tanks is important to the design of reliable liquid propellant systems for space vehicles. However, the wetting nature of liquid propellants creates difficulties in predicting liquid-vapor interfaces in the fuel storage tanks (Petrash, et. al. 1963). A proposed method of controlling the liquid location was to use surface tension or capillary forces by installing baffles in the fuel storage tank. This led to the earliest reported manned space flight experiment of interfacial phenomena that was flown onboard Mercury-Atlas 7 on May 24, 1962. The experiment was situated just above and behind the Astronaut, Scott Carpenter. Results of the experiment are shown in Fig. 3. They indicated that the only effect of orbital maneuvers was an occasional slosh of the liquid outside the base of the standpipe which occurred during pitch maneuvers, yielding residual accelerations of approximately  $10^{-2}g_0$  (Petrash, et. al. 1963). Fluid control of the surface tension baffle was lost at approximately  $0.3g_0$  during reentry.

Low gravity fluid physics phenomena such as capillarity, wetting, and reorientation phenomena were also investigated in drop towers (Salzman 1967, Masica 1968, Labus 1969). Many of these early studies stimulated development of appropriate theoretical models, validated analytical solutions, and provided empirical correlations where theory and analytical solution were nonexistent. Other terrestrial low-g facilities have been constructed worldwide, and aircraft and space flight experiments were also initiated in the early 1960's (Siegel 1967). At NASA LeRC, a 2.2 second drop tower which currently handles as many as 12 drops a day has been in operation since the mid 60's, while a 5 second drop tower initiated operation in 1966 (Lekan, et. al. 1996). The early reduced-gravity heat transfer work is reviewed by Siegel, 1967 while advances in low gravity fluid flow phenomena through 1966 are presented and discussed in detail by Abramson (1966). More recent summaries and discussions of low gravity fluid physics and transport phenomena can be found in Ostrach (1982), Koster and Sani (1990), Antar and Nuotio-Antar (1993), and Singh (1996). Although boiling, capillary, wetting, and liquid reorientation phenomena remain very active topics of study, other phenomena under investigation in NASA's current microgravity fluid physics program include thermocapillary and granular media flow phenomena (see Figs. 4-9).

In this paper, an overview of the current NASA microgravity fluid physics program is given with the question of g-level and g-jitter sensitivity in mind. Next, methodologies for assessing g-tolerability of various fluid physics phenomena are identified. The application of these methodologies to establish credible g-requirements for space flight experiments is then briefly discussed. A case study for estimating free surface related g-requirements is presented using a  $\mu g$  experiment currently under development. Finally, the current g-level and g-jitter requirements set forth in the FCF Science Requirements Envelope Document for fluid physics experiments are presented.

## **Brief Overview of the NASA's Microgravity Fluid Physics Program**

NASA's Microgravity Research Program is comprised of five program disciplines: biotechnology, combustion science, fluid physics, fundamental physics, and materials science. The purpose of the program is "to use the microgravity environment of space as a tool to advance knowledge; to use space as a laboratory to explore the nature of physical phenomena, contributing to progress in science and technology on Earth; and to study the role of gravity in technological processes, building a scientific foundation for understanding the consequences of gravitational environments beyond Earth's boundaries," (Rhome, 1998).

Often, a broad range of fluid physics phenomena have been studied with remarkable success using existing low-g facilities and platforms. This has contributed to the growth of the microgravity fluid physics program as observed in Fig. 10 which shows the participation in both the fluids and combustion microgravity programs from 1988 to 1996. Fig. 10 also shows that roughly  $\frac{1}{4}$  of the proposals submitted to the 1996 NASA Research Announcement (NRA) were funded. Approximately 125 principal investigators (PI's) currently participate in the microgravity fluid physics program and perform research related to one or more of the subdisciplines shown in Fig. 4. The benefits from improved understanding of these phenomena are also shown in Fig. 4 and further illustrated in Figs. 5 through 9. For example, greater understanding of thermocapillary flows leading to suppression of oscillatory flows could result in improved crystal growth processes. A better understanding of multiphase flow phenomena can lead to more efficient terrestrial and space based power generation/heat rejection systems.

Of the 125 PI's, 102 are in the ground program and 23 are in the flight program. Some such as the Extensional Rheology Experiment<sup>†</sup>, are manifested on a near term missions that are scheduled for flight in approximately 1999-2000. Others such as Coarsening in Solid-Liquid Mixtures are re-flights, while some experiments such as the Microscale Hydrodynamics Near Moving Contact Lines and Constrained Vapor Bubble Flight Experiments are developing science and engineering requirements for missions after 2000. One hopes that the rationale developed to establish g-tolerability requirements and post flight analysis of these experiments will be sufficiently documented to assist future investigators needing to assess g-tolerability of their microgravity experiments.

A comprehensive definition of g-tolerability is given by Monti et. al. (1987). For this paper however, we define g-tolerability as the maximum tolerable g-level above which the residual accelerations severely compromise a proposed low-gravity investigation. Residual acceleration tolerance, residual acceleration sensitivity, and g-sensitivity are also used synonymously with g-tolerability in the literature. In the current fluid physics program, g-tolerability is typically specified in terms of a steady g-level, and an unsteady but oscillatory requirement defined by disturbance amplitude and frequency. The principle investigator must also consider the vector nature, hence the

---

<sup>†</sup> The Extensional Rheology Experiment is scheduled as a sounding rocket payload in 1999.

orientation of the residual accelerations. The steady or quasi-steady acceleration level of terrestrial or orbiting low-g facilities is often referred to as the steady residual acceleration or g-level (Ostrach 1982, Monti et. al. 1987, Nelson, 1994). Steady g-level for the space shuttle is  $10^{-3}g_0$  to  $10^{-4}g_0$ , while values of  $10^{-5}g_0$  to  $10^{-6}g_0$  are anticipated on the International Space Station (ISS), where  $g_0$  is the terrestrial gravitational constant,  $g_0=9.81 \text{ m/s}^2$ . In the broadest sense, the unsteady or transient accelerations, referred to as g-jitter, are stochastic in nature. However they are often treated as either single impulse or periodic for analysis purposes. Periodic residual accelerations applied at a single frequency are typically used to establish g-jitter requirements of proposed microgravity experiments.

Although some analysis of impulse-like disturbances and their effects on heat transfer and fluid physics phenomena have been performed, current practice is to schedule experiments around infrequent but large disturbance events such as thruster firings. Impulse-like transients events can have significant effect on the fluid physics experiments (see Alexander 1990, and Nelson 1994). Sources of such accelerations include primary thruster firings,  $O(10^{-2}g_0)$ , venier thruster firings  $10^{-3}$  to  $10^{-4}g_0$ , and crew motion,  $10^{-2}$  to  $10^{-3}g_0$  (Nelson 1994). The effect of a thruster firing during the microgravity experiment, "A Study of the Effects of G-jitter on Brownian Motion and Diffusion," was recently and unexpectedly recorded. This experiment examined diffusion process across the interface of two miscible fluids. During one run of this investigation the well defined interface catastrophically deteriorates at the time of the thruster firing resulting in significant mixing at the interface. The event is captured on video tape (Duval, 1998). In another experiment, "Surface Tension Driven Convection II Experiment," residual accelerations from a fan associated with the Glovebox Facility affected free surface measurements. Free surface deformations of a liquid surface were measured using a Ronchi system. During some of the tests, disturbances on the free surface due to residual acceleration obscured the measurements of small surface deflections. The temporary solution was to use coarser diffraction gratings and measure deflections larger than the background noise. The source of the disturbance, was eventually identified and test runs were performed with the glovebox fan turned off, eliminating the free surface noise (Kamotani 1998, Delombard 1997).

### **Options For Assessing g-Tolerability: Analysis and Comparison to Previous Experiments**

In this section we identify the microgravity experiment(s) databases and note the methodologies that are available for determining or estimating residual acceleration effects. The references cited in this section also reflect the current state of knowledge concerning the residual acceleration effects on fluid physics phenomena.

The potential benefits from improved understanding of interfacial, thermocapillary/solutal capillary, multiphase flow, complex fluids, and granular media phenomena to applications such as processing, liquid management, space thermal control,

power generation, and other applications shown in Figs. 4 to 9 have contributed to growth in microgravity research. Not all processes are equally affected by residual acceleration levels and g-jitter characteristics. This is clearly demonstrated in Fig. 16 for diffusion processes where thermo-diffusion (Soret effect) processes are approximately two orders of magnitude more sensitive to g-levels than self-diffusion processes. The stochastic nature of g-jitter and its effects on complex of fluid-thermal processes such as crystal growth processes and critical point phenomena warrants continued examination of steady residual accelerations and g-jitter effects on fluid flow processes (Nelson, 1994, Singh, 1996, Monti and Savino, 1996). Nevertheless an extensive number of experiments have successfully been performed in low-g environments. Various methodologies for determining or estimating g-tolerability have been developed.

Methodologies for determining the effects of residual accelerations on fluid physics phenomena include: scaling or order of magnitude analyses (OMA), stability analysis, direct numerical simulations, and correlations developed from terrestrial reduced gravity experiments. With regard to microgravity fluid physics, OMA techniques are typically described with buoyancy and surface tension driven flows in mind, in part because successful exploitation of OMA has contributed to proper experimental design and physical insight related to such flow processes. A rigorous but pragmatic scaling analysis is described in detail by Ostrach (1982), for buoyancy and surface tension driven flows, paying careful attention to defining characteristic or reference values.

Stability analyses have had their greatest engineering and design impact on interfacial phenomena thus far. For example, stability maps for plane, cylindrical, annular, spherical, and other axisymmetric interfaces are reported in Abramson (1966). These maps are typically given as functions of the Bond number,  $Bo$ , contact angle, and free surface characteristic length as shown in Figs. 11a and 11b. Stability analyses of liquid bridges have been successfully performed for crystal growth processes as reported in Alexander (1990), in addition to analyses of stabilization techniques such as acoustic or electrodynamic stabilization of liquid bridges (Marr-Lyon et. al. 1997, Sankaran and Saville 1993).

Numerical analysis in support of both design and analysis of microgravity experiments has become widely accepted. Commercially available computational fluid dynamics (CFD) software such as FIDAP and FLOW3D have successfully modelled a broad spectrum of complex fluid flow problems such as surface tension drive flows, crystal growth processes, fluid management processes, and multicomponent flows<sup>‡</sup>. With appropriate training, equipment, and experience, meaningful results can be obtained for relatively complex fluid flow problems using the commercially, or otherwise available CFD software.

Comprehensive summaries exist that describe the above methodologies, analysis tools, and their effectiveness for determining residual acceleration effects on fluid physics

---

<sup>‡</sup> FLOW 3-D Theory Manual, 1996, and FIDAP Users Manual, 1993

phenomena (Ostrach, 1982, Monti, et. al., 1987, Alexander, 1990, Langbein, 1990). Although not specifically addressed it is expected that these analyses are applicable or in due course can be adapted to establish g-requirements for flow phenomena such as granular flows, colloids, and complex fluids. Such inclusive reviews can greatly aid investigators new to microgravity, engineers and designers of future space flight hardware, and reviewers or evaluators of microgravity initiatives in assessing g-requirements. As an example, the g-requirements of a microgravity experiment currently under development are established in the next section using some of the approaches identified above.

The growing number of microgravity fluid physics experiments also provides a database that can benefit the design, construction, and establishment of science requirements for future space flight experiments (Singh, 1996). A list of 49  $\mu\text{g}$  fluid physics flight experiments is given in Appendix A. Various microgravity databases that identify both completed and proposed space flight experiments are also found on the internet, some of which are given in Appendix B. Such databases might also benefit new microgravity investigators by providing specific examples of g-requirements as well as documenting the rationale applied to establish these and other science requirements. If residual acceleration measurements are available for experiments from the above databases, the rationale used to determine g-requirements could then be evaluated. However, in preparing the cursory flight experiments summary provided in Appendix A, it was this author's experience that g-tolerability rationale was generally not documented with the science requirements. In some cases, both steady residual acceleration and g-jitter values, themselves, were not found (documented as part of the science requirements). The allowable quasi-steady g-level requirements are shown in Fig. 12 for experiments listed in Appendix A.<sup>§</sup> Because the g-jitter and frequency requirements were scarce, no attempt was made to summarize this information.

The above resources are perhaps underutilized as evidenced by the g-rationale (or lack of) presented in fluid physics science requirements documents. Improved dissemination of the relevant residual acceleration papers cited above, to new PIs entering the microgravity program could improve the situation. A summary of g-requirements, their rationale, and post flight assessment of the requirements from several flight experiments would also improve the reliability of g-tolerability predictions.

### **Selected Case Studies: Estimation of g-level and g-Jitter Tolerability**

In this section, we demonstrate estimation of g-tolerability that might be a minimum level of justification used to initially establish residual acceleration science requirements. First a detailed example is worked for a microgravity flight experiment currently under development. Then we present diffusion and thermocapillary scaling analyses because these problems are frequently encountered in the program. It is hoped

---

<sup>§</sup> Missing values also occurred because the author was not in possession of some (SRD)'s before this Meeting

that these examples illustrate how g-sensitivity analyses can be used by a microgravity investigator to estimate g-requirements a priori to flight and by reviewers or evaluators to quickly assess g-requirements of proposed experiments.

The estimation of interfacial related g-requirements (tolerability) is demonstrated using the Microscale Hydrodynamics Near Moving Contact Line Flight Experiment as an example. The experiment will rigorously test fundamental theory of interface shapes and flow fields in the vicinity of the (moving) contact line, as well as examine a flow property (geometry free independence) associated with the theory (Garoff and Weislogel, 1997). For purposes herein, the discussion is confined to the simplified configuration shown in Fig. 13. One fluid that will be used in the moving contact line flight experiment is 200cSt Silicone Oil, with density,  $\rho=.970\text{g/cm}^3$ , and surface tension,  $\sigma=.02\text{ N/m}$ . The inner radius,  $r_i$ , is 2 cm and the outer cylinder radius,  $r_o$ , is 4 cm. Microgravity platforms such as the space shuttle or space station can orbit in various orientations. In the event that such platforms are in an earth viewing orbit, the maximum component of the aligned-g vector, would be in the direction shown in Fig. 13. In this orientation, the static interface is an inverted annular meniscus that can become unstable at sufficiently large steady residual g-values. The meniscus stability can be investigated with the aid of the stability diagram in Fig. 11a. The “worst case” contact angle,  $\theta$ , in terms of stable interface is  $\theta=0$ , which is also a  $\theta$  value for several test runs. In Fig. 11a for  $r_i/r_o=0.5$ , the interface is stable for Bond number, Bo, less than 1.4, where  $Bo = \frac{g\rho r_o^2}{\sigma}$ . Using the above property values and dimensions,  $Bo=.00761$  for a steady g-level of  $10^{-5}g_o$  well below the static instability threshold. On the other hand, in  $1g_o$ ,  $Bo=761$ , indicating an unstable interface, in agreement with terrestrial observations that the oil runs to the other side of the container.

To estimate the g-jitter\*\* tolerability both amplitude and frequency of residual accelerations need to be considered. The natural frequency of this system can be computed using the empirical correlation given below in equation (1) (Labus, 1969). The correlation was developed for fluids in annular cylinders with “near” zero contact angles and is valid for  $h/(r_o - r_i) > 2$ , where h,  $r_o$ , and  $r_i$  are defined in Fig. 13.

$$\Omega^2 = Bo f_1(r_i / r_o) + f_2(r_i / r_o) \quad (1)$$

The annular natural frequency parameter  $\Omega$ , is defined as  $\Omega^2 = \frac{\rho\omega_A^2 r_o^3}{\sigma}$ , and values for parameters,  $f_1$  and  $f_2$ , are tabulated in Labus (1969). For  $r_i/r_o=.5$ ,  $f_1 = 1.35468$  and  $f_2 = 1.6$ . Substituting the above properties and dimensions into equation (1) leads to Bond numbers, dimensionless natural frequencies,  $\Omega$ , and dimensional natural frequencies,  $\omega_n$ , given in Table 1. Thus to avoid resonance in a  $10^{-5}g_o$  environment, residual acceleration disturbances near a frequency of .1146 Hz should be eliminate or minimized.

---

\*\* Here, g-jitter is assumed in the context of oscillatory residual accelerations.

The next step might be to investigate in a terrestrial low g-facility, the free surface response (deflection) to residual acceleration disturbances,  $g_{rms}$ , values near the natural frequency, where  $g_{rms}$  is the root mean square acceleration value about the mean residual acceleration. In fact tolerable g-jitter values,  $g_{rms}$ , in the SCR were estimated by adapting the resonant frequency results of cylinders of Kamotani and Ostrach (1987), to an annular configuration (Garoff and Weislogel, 1997). The fluid properties and dimensions for this example vary slightly from those reported in Science Requirements Document (SCR)<sup>††</sup>. Finally the maximum  $g_{rms}$  (ISS Requirement) for the International Space Station Fluids and Combustion Facility (ISS-FCF) can be obtained from Fig. 14, at the resonant frequency. For  $\omega_n = .11$  Hz, Fig. 14 indicates a maximum allowable  $g_{rms}$  value of  $10^{-6} g_0$  suggesting that ISS-FCF requirement is adequate for our example problem.

Table 1 natural frequency for annular cylinder from Labus, (1960) correlation

| $g/g_0^*$ | Bo     | $\Omega^2$ | $\omega_n$ (Hz) |
|-----------|--------|------------|-----------------|
| 1         | 761    | 1033       | 2.9             |
| $10^{-5}$ | .00761 | 1.601      | .1146           |

\* $g_0 = 9.81 \text{ m/s}^2$

Sloshing and damping studies have been performed for several other simple geometries such as , cylinders, squares, spheres (Reynolds, et. al., 1964, Abramson,1966, Salzman and Masica, 1969 and Salzman et. al, 1967, Kamotani and Ostrach, 1987, Chao, et. al., 1992, and Kamotani, et. al., 1995). Expressions, tabulated data and graphical results for computing  $\omega_n$ , damping coefficients, and surface deflections near resonance are reported in these references.

The usefulness of OMA is demonstrated by the g-level tolerability graphs for diffusion experiments shown in Fig. 16 (taken from Langbein, 1990). Estimates of g-tolerability for specific diffusion processes in terms of accelerations and frequencies can be computed directly from equation (2).

$$g_{tol} = Ra_{tol} \frac{D_{eff} v_{eff}}{\epsilon_p L_c^3} \quad (2)$$

where  $\epsilon_p = \Delta\rho / \rho$ ,  $v_{eff} = \sqrt{v^2 + (\omega L_c^2)^2}$ , and  $D_{eff} = \sqrt{D^2 + (\omega L_c^2)^2}$

For heat and mass transport by conduction to be much greater than that by the convection due to the unsteady inertial acceleration, a tolerable Rayleigh number,  $Ra_{tol}$ , must be  $Ra_{tol} \ll 1$ . By setting desired  $Ra_{tol}$  value, to say .01,  $g_{rms}$  can then be computed for a specific system, defined by the values of characteristic length,  $L_c$ , the kinematic viscosity,

<sup>††</sup> SCR properties and dimensions were carefully chosen to ensure conservatism various g-requirements

$\nu$ , diffusivity<sup>‡‡</sup>,  $D$ , and density variation,  $\Delta\rho / \rho$ . When the Boussinesq Approximation applies,  $\Delta\rho / \rho$  can be replaced with  $\beta_s \Delta S$ , where  $\Delta S$  is the characteristic temperature or concentration difference and  $\beta_s$  is the corresponding expansion coefficient. The development of the appropriate reference values for velocity, temperature, and concentration yielding definitions for  $\nu_{\text{eff}}$  and  $D_{\text{eff}}$  is treated in Monti et. al., (1987), Langbein (1990), and Alexander (1990). Several g-tolerability maps for specific crystal growth, thermo-diffusion, semiconductor, and solidification experiments are shown in Monti et. al. (1987).

Using scaling arguments of Ostrach (1982), Alexander (1990) has generated several g-tolerability maps for thermocapillary systems over a wide range of parameter values. As in the case of diffusion experiments, this provides a methodical approach and perhaps a “minimum rationale” that should be used to estimate g-jitter requirements of relevant thermocapillary flight experiments. The relative importance of buoyancy and thermocapillary forces in a flight experiment, studying freeze/thaw characteristics of thermal energy storage materials, was also estimated using Ostrach’s scaling criteria (Skarda et. al., 1991).

Estimates of characteristic time constants such as the characteristic diffusion times for momentum,  $(L^2 / \nu)$ , temperature,  $(L^2 / \kappa)$ <sup>§§</sup>, and concentration,  $(L^2 / D)$ , can aid in determining the necessary duration of low-g. Typical reduced gravity times for facility such as drop tower, low-gravity aircraft, sounding rockets, or space station are indicated in Fig. 13. An interesting example is the estimation of the characteristic time of a drop deployed into a reduced gravity environment from a one g environment (Becker, Hiller, Kowalewski, 1994 originally cited by Rosenberger, 1993). For the fundamental mode ( $n=2$ ), a drop with radius,  $L$ , the time to achieve a steady shape is  $\tau_v = O(L^2 / 5\nu)$ . Therefore a drop of 200 cSt Silicone oil of  $L=0.5\text{mm}$  and has a relaxation time of approximately 0.1s after release.

Orbiting platforms such as the space shuttle, the Russian Mir station, and the International Space Station provide opportunities to study these and other fluid phenomena that require longer periods of reduced gravity. The International Space Station (ISS) provides the longest duration of reduced-gravity of the facilities shown in Fig. 15. The fluid physics (science) g- requirements for the ISS Fluids and Combustion Facility (FCF) and rationale in determining these requirements are discussed in the following section.

### **Residual Acceleration Requirements for the International Space Station Fluids and Combustion Facility**

---

<sup>‡‡</sup>  $D$  represents either the thermal, concentration, or cross-diffusivity values (Incropera and DeWitt 1985, Cussler 1995).

<sup>§§</sup>  $\kappa$  is defined as the thermal diffusivity

The Fluids and Combustion Facility (FCF) is currently manifested in the US Laboratory of the International Space Station (ISS). Opportunities for fluid physics experimentation will also be available via the Expedite The Processing of Experiments to Space Station) EXPRESS racks also manifested throughout the ISS laboratories (Rhatigan, 1998). The FCF is designed with specific microgravity acceleration requirements based on the reference set of microgravity experiments discussed below. The current design of the ISS provides for standard thirty day microgravity periods, planned during times of reduced onboard operational activities. The FCF reference experiments generally fall within the bounds of capability for steady g-levels and g-jitter as shown in both Figs. 12 and 14, respectively. Both the FCF and four of the eight EXPRESS racks will be equipped with ISS-provided Active Rack Isolation Systems (ARIS). The ARIS is designed to isolate a payload rack from the normal quiescent environment of the ISS as well as from transient disturbances.

A set of “reference experiments” for the FCF were chosen to represent the broad range of fluid physics subdisciplines shown in Fig. 4. The specific choice of the fourteen reference experiments were based on the feedback received from Principal Investigators (PIs) in the flight and ground-based Fluid Physics program, the Fluids Discipline Working Group (DWG), and the external science community. The Science Requirement Envelope Document (SRED) was developed based on the information collected from science requirements from past and present flight experiments’ Science Requirements Documents (SRDs) as well as science requirements from experiments proposed to the NASA Research Announcements (NRAs). The first fourteen experiments in Table A of Appendix A are the reference experiments. Typical quasi-steady residual accelerations in Fig. 12 fall between  $10^{-5} g_0$  and  $10^{-3} g_0$ . Some experiments such as those involving bubbles and drops, and thermocapillary or double diffusive convection require quasi-steady accelerations on the order of the minimum expected background acceleration for ISS,  $10^{-6} g_0$ . In Fig. 14 two experiments fall below the “ISS requirement” suggesting that further vibration isolation would be necessary to minimize deleterious effects of g-jitter for these two cases.

## **Conclusions**

Residual accelerations can significantly affect  $\mu\text{g}$  fluid physics experiments. There is little disagreement in the literature that continued development of models and tools is necessary to better determine residual accelerations effects, and perhaps predict the conditions that could compromise a proposed fluids experiment. This view is shared by many of the individuals who must determine or assist in the determination of g-requirements for proposed  $\mu\text{g}$  flight experiments.

Tools and methodologies that have been reported in the literature are available for estimating g-tolerability. The use of one or more of these methodologies might provide

and acceptable rationale for determining the actual g-requirement values. Such values are typically required before an experiment is approved for flight. The applicability and limitations of the current methodologies such as scaling or stability analyses, could be assessed using actual results from (many) previously flown experiments. A collective assessment from flown  $\mu\text{g}$  experiments might promote the use of various g-tolerability methodologies as engineering tools where appropriate.

The ISS-FCF reference experiments are representative of the experiments currently performed within the fluid physics program. Of the g-levels reported, the ISS requirement should meet the g-requirements for many classes and types of fluids experiments. Vibration isolation will likely be necessary (and is planned) for some proposed experiments. As the residual acceleration environment and its effects on fluid phenomena are better understood, it is clearly possible that stricter g-requirements could be necessary for some experiment(s) while less stringent requirements might arise in other cases.

#### **Acknowledgments**

The input and comments received from the following people was of great help and is sincerely appreciated: J. Allen, N. Hall, M. Hill, A. Karchmer, H. Lee, J. Rhatigan, S. Sankaran, B. Singh, and R.A. Wilkinson. This work was supported by the National Aeronautics and Space Administration's, Microgravity Science Division.

#### **References**

Antar, B.N., and Nuotio-Antar, V.S., Fundamentals of Low Gravity Fluid Dynamics and Heat Transfer, CRC Press, 1993.

Abramson, H.N., The Dynamic Behavior of Liquids in Moving Containers. With Applications to Space Vehicle Technology, NASA SP-106, 1966.

Alexander, J.I.D., "Low-Gravity Experiment Sensitivity to Residual Acceleration: A Review," *Microgravity Science Technology*, Vol. 3, pp. 52-68, 1990.

Becker, E., Hiller, W.J., Kowalewski, T.A., "Nonlinear Dynamics of Viscous Droplets," *Journal of Fluid Mechanics*, Vol. 258, pp. 191-216, 1994.

Benjamin, T.B. and Ursell, F., "The stability of the plane free surface of a liquid in vertical periodic motion," pp. 505-515, 1954.

Chao, L., Kamotani, Y., Ostrach, S., "G-Jitter Effects on the Capillary Surface Motion in an Open Container Under Weightless Condition," *Fluid Mechanics in Microgravity*, AMD-Vol. 154, pp. 133-143, 1992.

Crowley, C.J., Iannello, V., Wallis, G.B., "Literature Review and Discussion of Microgravity Two-Phase Flow and Heat Transfer," Creare Technical Memorandum, TM-1186, September, 1987.

Cussler, E.L., Diffusion Mass Transfer in Fluid Systems, Cambridge-University Press, 1995.

Delombard, Richard, "Baseline Microgravity Requirements for Scientific Research on the International Space Station," Draft Report, February 10, 1997.

Duval, W. Presentation at Microgravity Measurements Group Meeting #17, March 24-26, 1998.

FIDAP Users Manual, FIDAP 7.0, Fluid Dynamics International, Inc., Evanston, IL, 1993.

FLOW 3-D Theory Manual, Flow Science, Inc, Los Alamos, NM, 1996.

Garoff, S., and Weislogel, M., "Microscale Hydrodynamics Near Moving Contact Lines," Microgravity Fluid Physics Science Requirement Document - Draft, NASA's Microgravity Sciences Program, October, 1997.

Incropera, F.P., and DeWitt, D.P., Fundamentals of Heat and Mass Transfer, John Wiley and Sons, NY, 1985.

Koster, J.N. and Sani, R.L., eds., Low-Gravity Fluid Dynamics and Transport, Volume 30, Progress in Astronautics and Aeronautics, AIAA, 1990.

Kamotani, Y., Chao, L., Ostrach, S., Zhang, H., "Effects of g-Jitter on Free-Surface Motion in a Cavity," Journal of Spacecraft and Rockets, Vol. 32, No. 1, pp. 177-183, 1995.

Kamotani, Y., and Ostrach, S., "Design of a Thermocapillary Flow Experiment in Reduced Gravity," Journal of Thermophysics, Vol. 1, No. 1, pp. 83-89, January 1987

Kamotani, Y., Personal Communication, February, 1998.

Labus, T.L., "Natural Frequency of Liquids in Annular Cylinders Under Low Gravitational Conditions," NASA TN D-5412, 1969.

Langbein, D., "Quality Requirements for Microgravity Experiments," Microgravity Science Technology, Vol. 3, pp. 138-142, 1990.

Lekan, J., Gotti, D.J., Jenkins, A.J., Owens, J.C., Johnston, M.R., "Users Guide for the 2.2 Second Drop Tower of the NASA Lewis Research Center," NASA TM 107090, April, 1996.

Marr-Lyon, M.J., Thiessen, D.B., and Marston, P.L., "Stabilization of cylindrical capillary bridge far beyond the Rayleigh-Plateau limit using acoustic radiation pressure and active feedback," *Journal of Fluid Mechanics*, Vol. 351, pp. 345-357.

Monti, R., Langbein, D., Favier, J.J., "Influence of Residual Accelerations on Fluid Physics and Materials Science Experiments," in *Fluid Sciences and Materials Science in Space, a European Perspective*, ed. Walter, H.U., Springer Berlin, pp. 637-680, 1987.

Monti, R., "Gravity Jitters: Effects on Typical Fluid Science Experiments," in Low-Gravity Fluid Dynamics and Transport Phenomena, ed. J. Koster and R. Sani, 1990.

Monti, R., and Savino, R., "Microgravity Experiment Acceleration Tolerability, on Space Orbiting Laboratories," *Journal of Spacecraft and Rockets*, Vol. 33, No. 5, 1996.

NASA SP-8009, "Propellant Slosh Loads", NASA Space Vehicle Design Criteria (structures), August 1968.

Nelson, E., "An Examination of Anticipated g-Jitter on Space Station and its Effects on Materials Processes," NASA TM-103775, May 1991.

Ostrach, S., "Low-Gravity Fluid Flows," *Annual Review of Fluid Mechanics*, Vol. 14, pp. 313-345, 1982.

Petrash, D.A., Nussle, R.C., and Otto, E.W., "Effect of the Acceleration Disturbances Encountered in the MA-7 Spacecraft on the Liquid-Vapor Interface in a Baffled Tank," NASA TN D-1577, 1963.

Reynolds, W.C., Saad, M.A., and Satterlee, H.M., "Capillary Hydrostatics and Hydrodynamics at Low g," Technical Report No. LG-3, Stanford University, September, 1964.

Rhatigan, J., Personal Communication, February, 1998.

Rhome, R., Microgravity Strategic Planning Meeting, Jan. 7, 1998.

Rosenberger, F., "Short-Duration Low-Gravity Experiments," *Microgravity Science Technology*, VI/3, pp. 142-148, 1993.

Salzman, J.A., Labus, T.L., and Masica, W.J., "An Experimental Investigation of the Frequency and Viscous Damping of Liquids During Weightlessness," NASA TN D-4132, August 1967.

Salzman, J.A., Masica, W.J., "Lateral Sloshing in Cylinders Under Low-Gravity Conditions," NASA TN D-5058, February 1969.

Sankaran, S., and Saville, D.A., "The Stability of a Fluid Cylinder in Axial Electric Field", Physics of Fluids A, Vol. 5, No. 4, pp. 1081-1083, April 1993.

Seebold, J.G., Hollister, M.P., and Satterlee, H.M. "Capillary Hydrostatics in Annular Tanks," Journal of Spacecraft, Vol. 4, no. 1, pp. 101-105, January 1967.

Siegel, R. And Usiskin, C., "A Photographic Study of Boiling in the Absence of Gravity," Transactions of ASME, pp. 230-236, August, 1959.

Siegel, R., "Effects of Reduced Gravity on Heat Transfer," in Advances In Heat Transfer, Vol. 4, Academic Press, 1967.

Singh, B., "Third Microgravity Fluid Physics Conference," NASA Conference Publication 3338, July, 1996.

Skarda, J.R.L., Namkoong, D., Darling, D., "Scaling Analysis Applied to the NORVEX Code Development and Thermal Energy Flight Experiment," NASA TM 1044462/AIAA-91-1420, 1991.

Science Requirements Envelope Document for the Space Station Fluids and Combustion Facility (FCF), Draft #3, NASA Lewis Research Center, Cleveland, OH, July, 31, 1996.

Appendix A Microgravity Flight Experiments Summary

(\* Denotes FCF Fluid Physics Reference Experiment)

| ID # | Flight Experiment   | Principal Investigators | Mission | Date   |
|------|---|-------------------------|---------|--------|
| 1*   | Thin Film Fluid Flows at Menisci                                    | Hallinan                |         |        |
| 2*   | MicroScale Moving Contact Line                                      | Garoff                  |         | 2002   |
| 3*   | Extension Rheology Experiment                                       | McKinley                |         |        |
| 4*   | Physics of Hard Spheres   | Chaikin                 | USML-2  | Oct-95 |
| 5*   | Colloid Physics in Microgravity                                     | Weitz                   |         |        |
| 6*   | Electrohydrodynamics of Liquid Bridges                              | Saville                 | LMS     | Jun-96 |
| 7*   | Nucleation and Growth of Microporous Crystals                       |                         |         |        |
| 8*   | T.C. Migr.of Bubbles and Drops                                      | Subramanian             | IML-2   | Jul-94 |
| 9*   | Thermocapillary Motion of Bubbles and Drops (Population of Bubbles) | Sangani                 |         |        |
| 10*  | Interfacial Transport and Micellar Solubilization Processes         |                         |         |        |
| 11*  | Thermocapillary and Double Diffusive Phenomena                      |                         |         |        |
| 12*  | Critical Point Phenomena  | Berg/Ferrell            |         |        |
| 13*  | Multiphase Flow/No Phase Change                                     | Favier/McQuillen        |         |        |
| 14*  | Boiling Heat Transfer   | Merte                   |         |        |
| 15*  | Mechanics of Granular Media   |                         |         |        |
| 16   | STDC - a  | Ostrach                 | USML-1  | Jun-92 |
| 17   | STDC - b  | Ostrach                 | USML-2  | Oct-95 |
| 18   | TES   | Namkoong                |         |        |
| 19   | Drop Dynamics - a   | Wang                    | USML-1  | Jun-92 |
| 20   | Drop Dynamics - a   | Wang                    | USML-2  | Oct-95 |
| 21   | ZENO - a  | Gammon                  | USMP-2  | Mar-94 |
| 22   | ZENO - b  | Gammon                  | USMP-3  | Feb-96 |
| 23   | Interface Configuration   | Concus                  | USML-1  | Jun-92 |
| 24   | Interface Configuration   | Concus                  | USML-2  | Oct-95 |
| 25   | Bubble Behavior under Low Gravity                                   | Viviani                 | IML-2   | Jul-94 |
| 26   | Thermal Equilibrium in a One-Comp Fluid                             | Ferrell                 | IML-2   | Jul-94 |
| 27   | Static and Dynamic Behavior of Liq. in Corners and Edges ...        | Langbein                | IML-2   | Jun-94 |
| 28   | Science and Technology of Surface-Controlled phen                   | Apfel                   | USML-1  | Jun-92 |
| 29   | Science and Technology of Surface-Controlled phen                   | Apfel                   | USML-2  | Oct-95 |
| 30   | Oscillatory Thermocapillary Flow Experiment                         | Kamotani                | USML-2  | Oct-95 |
| 31   | Bubbles & Drops Interaction With Solid Fronts                       | Monti                   | IML-2   | Jun-94 |
| 32   | Nonlinear Surface Tension Bubble Migration                          | Viviani                 | IML-2   | Jun-94 |
| 33   | Oscillatory Marangoni Instability                                   | Legros                  | LMS     | Jun-96 |
| 34   | ThermoCapillary in a 3-Layer System                                 | Legros                  | IML-2   | Jul-94 |
| 35   | Interface Configuration Experiment - Mir                            | Concus                  | MIR     | Apr-96 |

Appendix A Microgravity Flight Experiments Summary

(\* Denotes FCF Fluid Physics Reference Experiment)

|    |   |           |        |        |
|----|---|-----------|--------|--------|
| 36 | Technological Evaluation of MIM Expr                              | Allen     | MIR    | Apr-96 |
| 37 | Investigation of the Thermal Eq Dynamics of SF(6) Near ...        | Wilkinson | IML-1  | Jan-92 |
| 38 | Measurement of Liq-Liq Interfacial Tension and Role of g ...      | Weinberg  | USML-1 | Jun-92 |
| 39 | Solid Surface Wetting -Glovebox                                   | Trinh     | USML-1 | Jun-92 |
| 40 | Osc. Dyn. of Single Bubbles and Agglomeration in Ultrasonic-Glov. | Marston   | USML-1 | Jun-92 |
| 41 | Osc. Dyn. of Single Bubbles and Agglomeration in Ultrasonic-Glov. | Marston   | USML-2 | Oct-95 |
| 42 | Partical Dispersion Experiment -Glov                              | Marshall  | SL-J   | Sep-92 |
| 43 | Drop Dynamics in Space and Interference with Acoustic Field       | Yamanaka  | SL-J   | Sep-92 |
| 44 | Study of Bubble Behavior  | Azuma     | SL-J   | Sep-92 |
| 45 | Interfacial Phenomena in a Multilayered Fluid System              | Koster    | IML-2  | Jul-94 |
| 46 | GMSF Growth & Morphology, Boiling and Critical Fluc..             | Hegseth   |        |        |
| 47 | Liq. Motion In Rotating Tanks                                     | Dodge     |        |        |
| 48 | Meas. of Viscosity Near the Liquid-Vapor..                        | Berg      |        | Aug-97 |
| 49 | Constrained Vapor Bubble  | Wayner    |        | 2002   |

## **Appendix B Helpful Microgravity Internet Addresses (URL's)**

Relevant microgravity internet URL's are given below:

Microgravity Research Division (NASA-HQ)  
<http://microgravity.msad.hq.nasa.gov/>

Microgravity Research Program (NASA)  
<http://microgravity.msfc.nasa.gov/fame/>

Microgravity Fluid Physics (NASA)  
<http://zeta.lerc.nasa.gov/expr3/fluid.htm>

The National Center For Microgravity Research  
<http://www.microgravity.com/ncmr.html>

Funding Opportunities - NASA Research Announcements (NASA)  
[http://peer1.idi.usra.edu/peer\\_review/nra/nra.html](http://peer1.idi.usra.edu/peer_review/nra/nra.html)

Microgravity Research Experiments Database (NASA)  
<http://samson2.msfc.nasa.gov/fame/Fame.html>

Space Station Microgravity Fluids (NASA)  
<http://station.nasa.gov/science/disciplines/microgravity/fluid>

Microgravity Database (ESA)  
<http://www.esrin.esa.it/mgdb/mgdbhome.html>

Japan Society of Microgravity Application (JASMA)  
<http://moses.agnes.aoyama.ac.jp/~denjiman/gakkai/English.html>

Spacelink- Aeronautics & Space Education Resource (NASA)  
<http://spacelink.nasa.gov/NASA.Projects/Scientific.Research.Projects/Microgravity.Science.and.Applications>

Microgravity News (internet magazine) (NASA)  
<http://mgnwww.larc.nasa.gov>

Microgravity Research - National Academy of Sciences & Engineering  
<http://www.nas.edu/ssb/cmgrl.html>

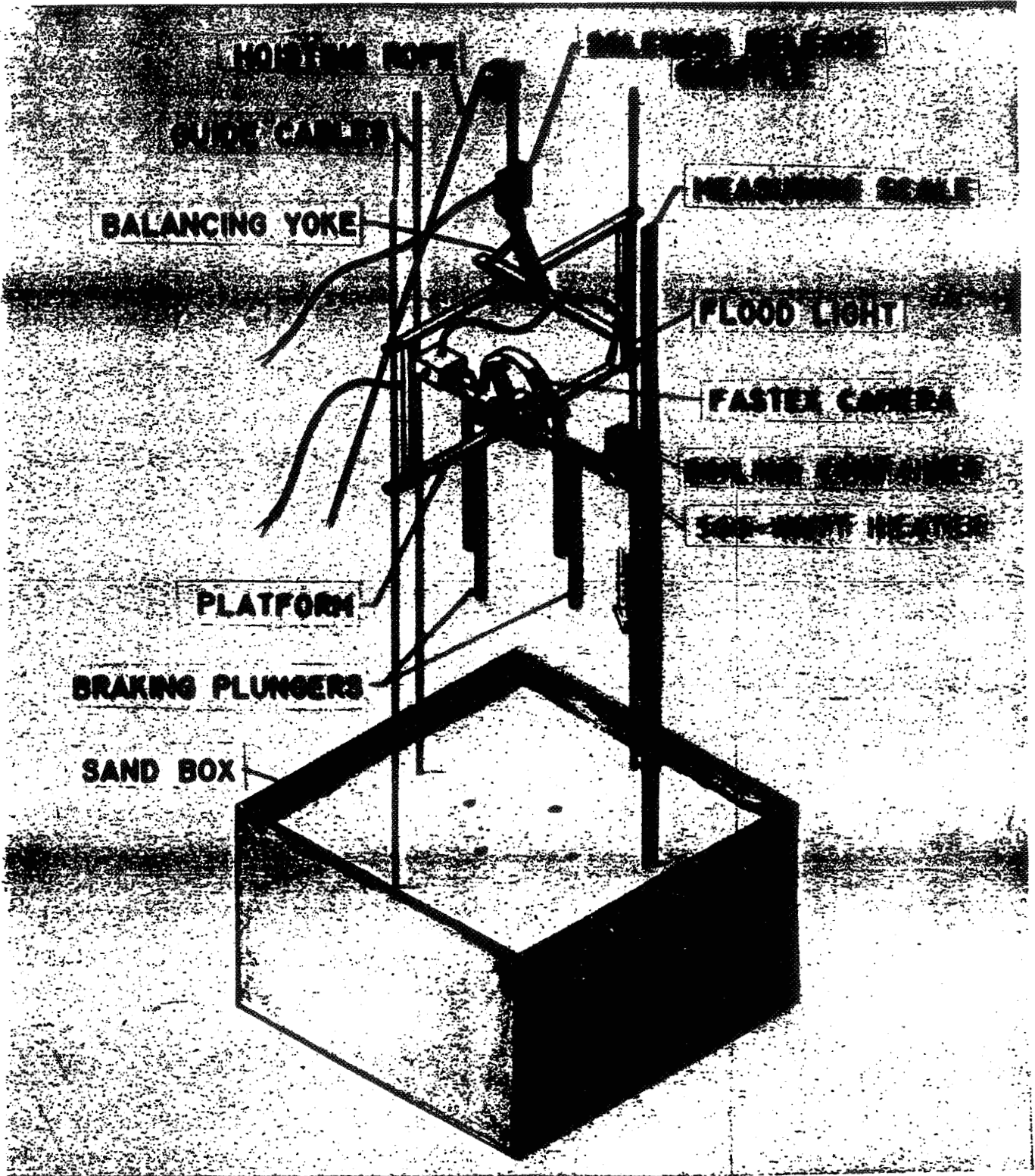


Figure 1 0.7 Second Drop Tower  
Built 1958, NASA LeRC

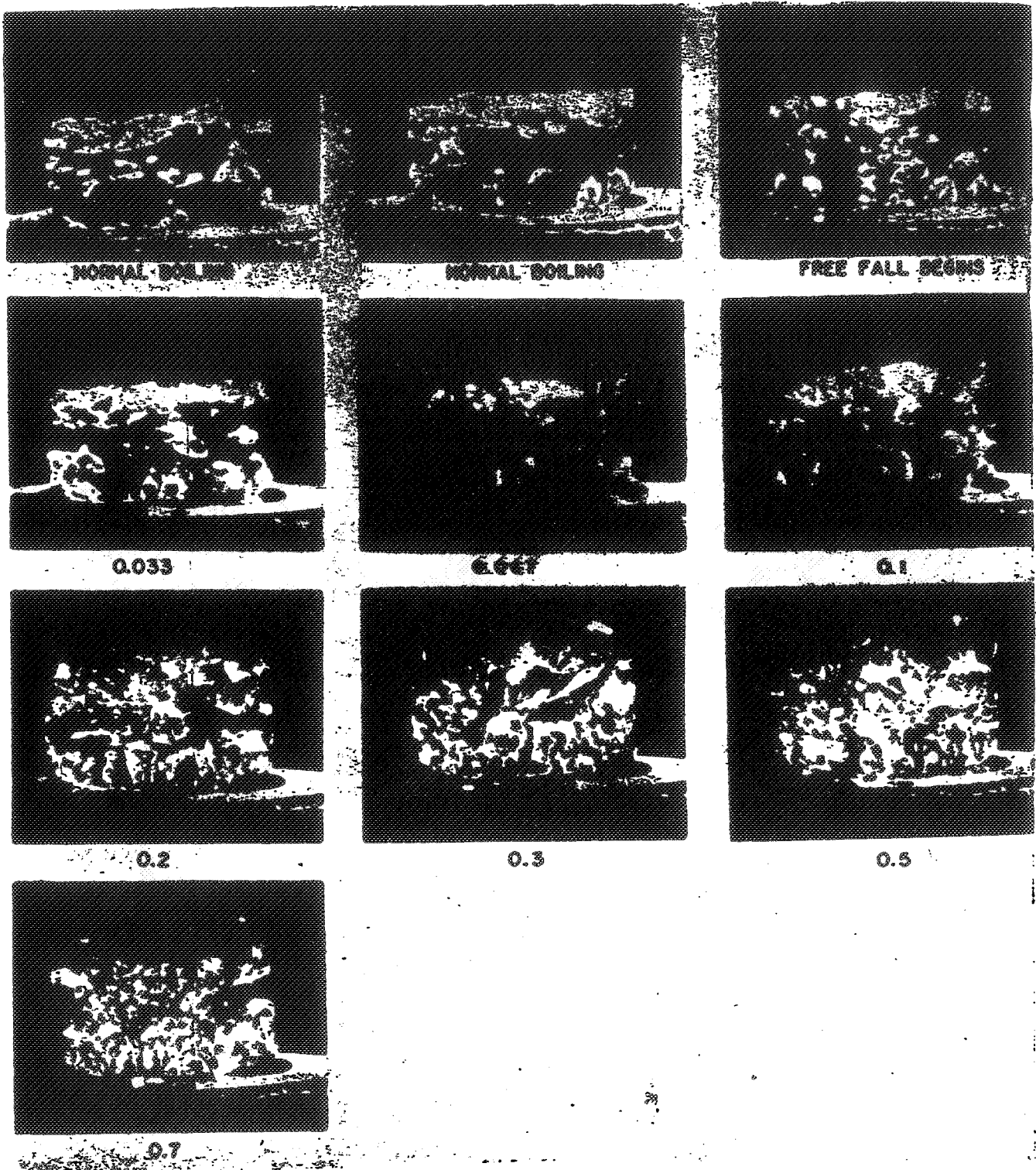
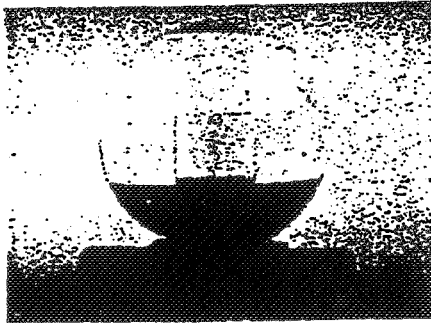
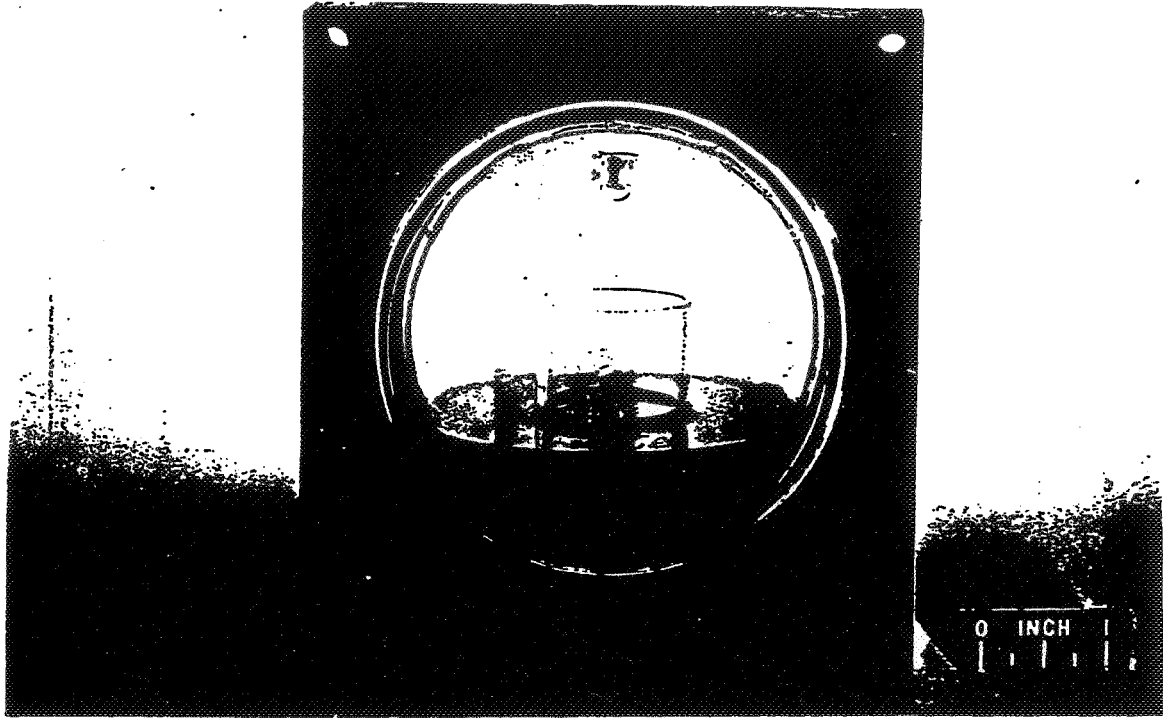


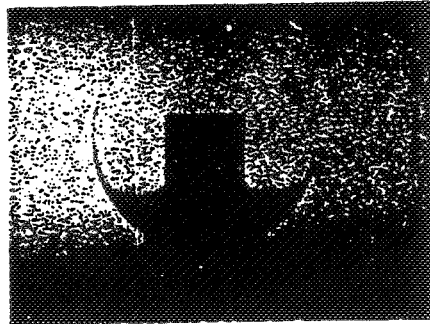
Figure 2 Pool Boiling From the Bottom of a Glass Beaker  
 R. Siegel and C. Usiskin 1959

Figure 3

# Free Surface Behavior of Baffled Tanks In Low Gravity

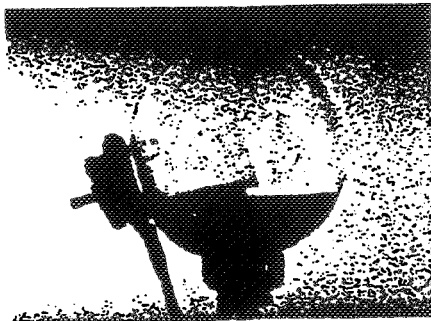


1-g configuration

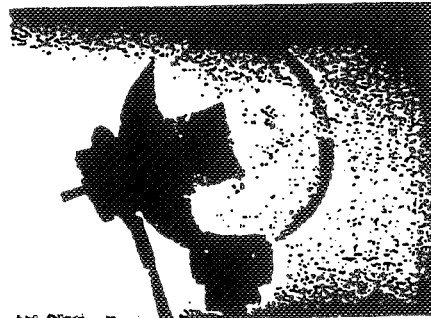


Zero-g configuration

(a) Initial mounting angle,  $0^\circ$ .



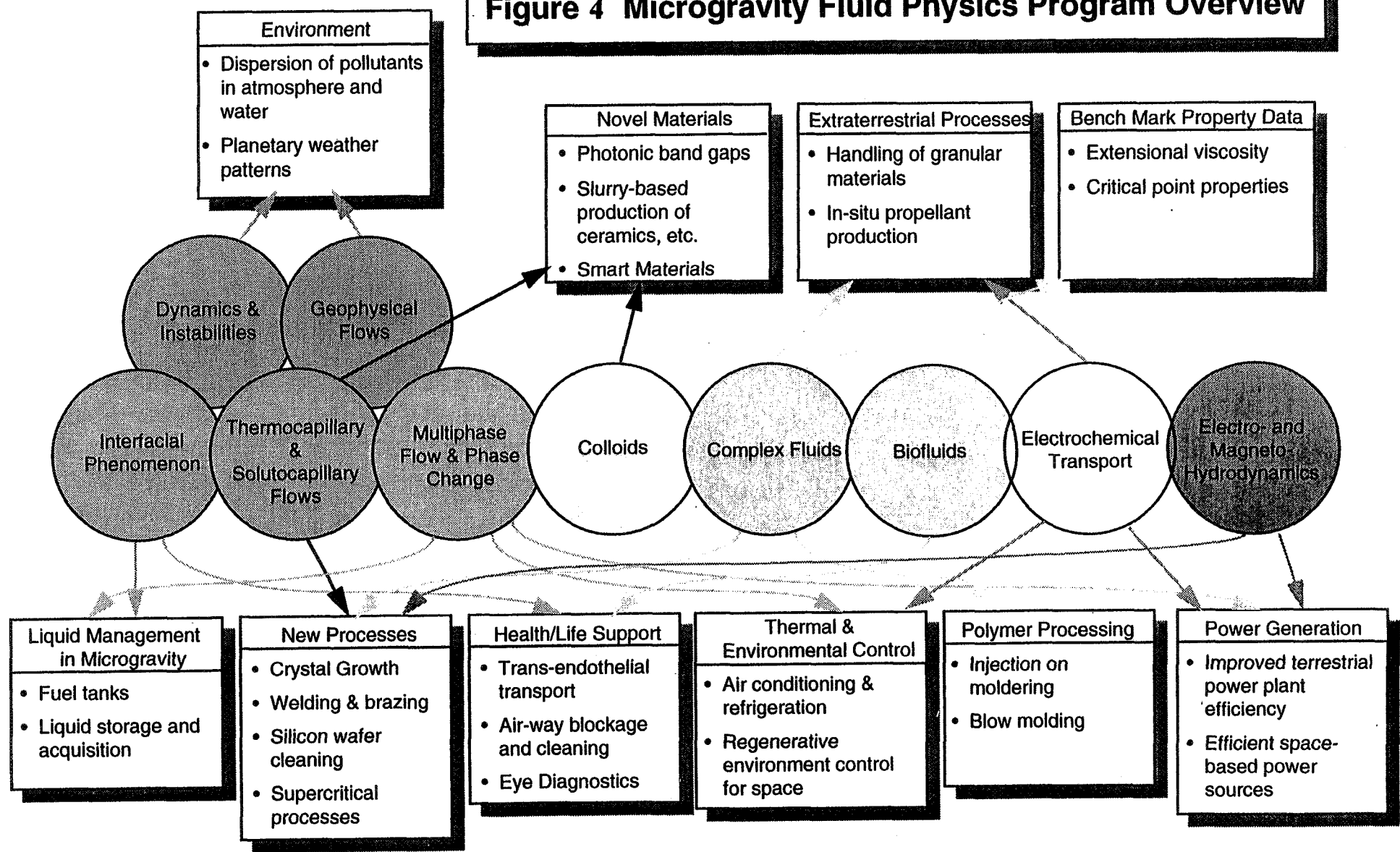
1-g configuration



Zero-g configuration

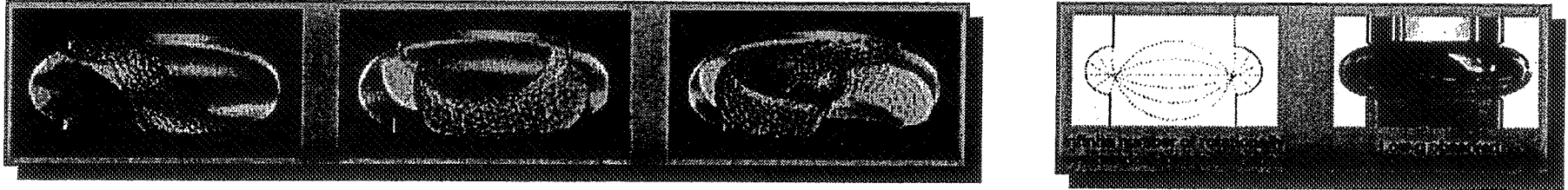
(c) Initial mounting angle,  $75^\circ$ .

**Figure 4 Microgravity Fluid Physics Program Overview**



Microgravity nearly eliminates buoyancy, sedimentation and hydrostatic pressure effects revealing phenomena masked by gravity. Affords better understanding of certain physical processes as well as leads to identification of new phenomena by allowing variation in g-levels.

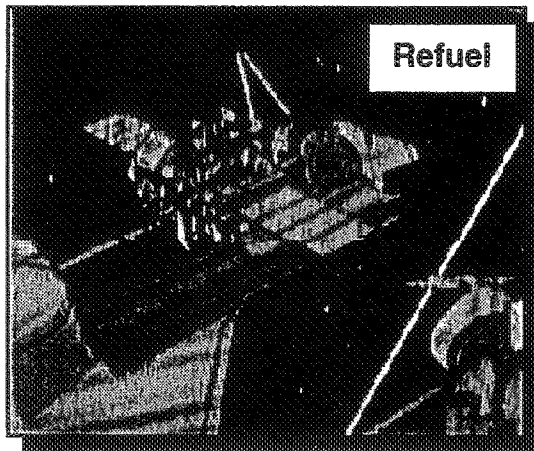
## Figure 5 Capillary and Interfacial Phenomena



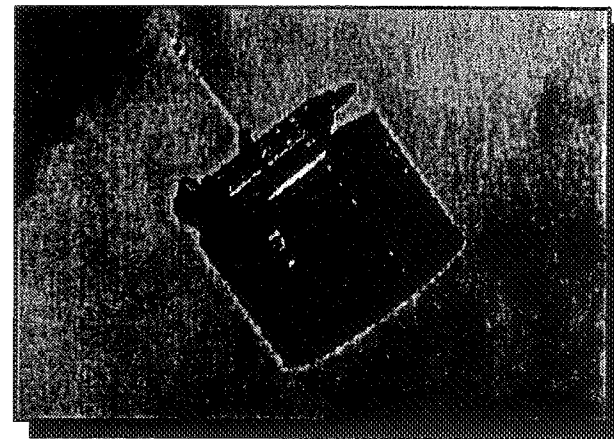
### Interfacial Configuration Experiment (ICE)

#### Objectives:

- To test the validity of mathematical results
- To indicate the role of contact line, resistance forces, surface roughness, vessel inaccuracies and other non-ideal conditions that are not accounted for by the current theory.
- To identify higher modal asymmetric interfaces.

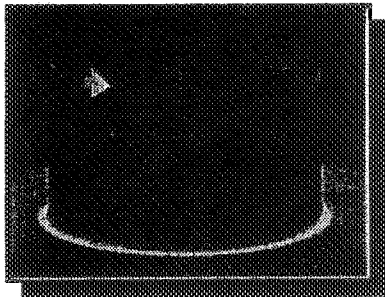
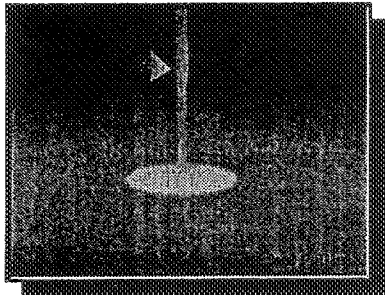
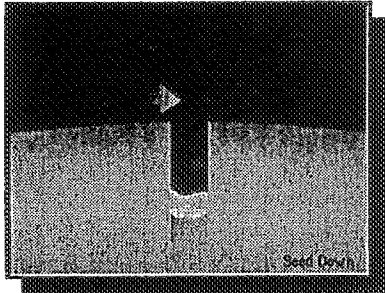


Artists concept depicting a typical satellite servicing activity.



View of the Syncom IV (Leasat-2) satellite in orbit over the earth.

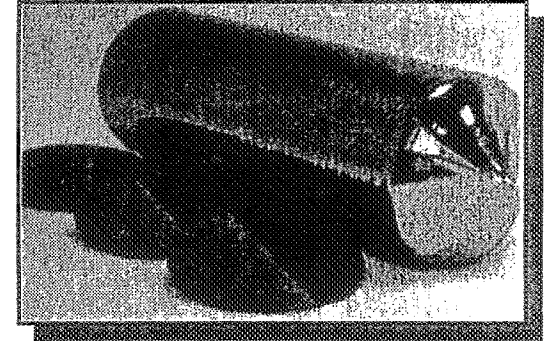
## Figure 6 Thermocapillarity & Solutocapillary Flows



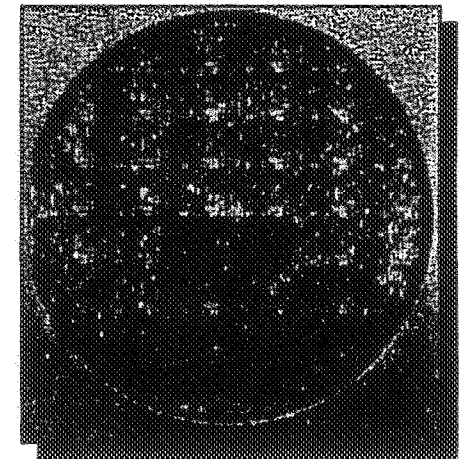
Crystal pulling (growing)



Welding processes

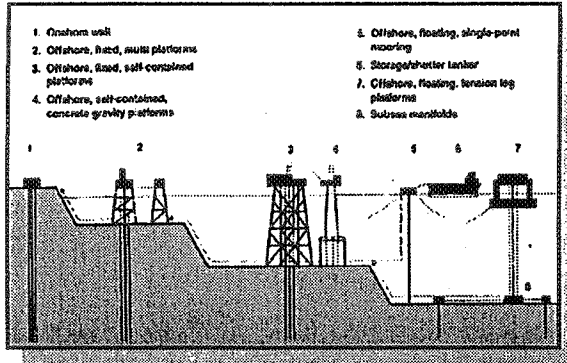


Silicon crystal & wafers

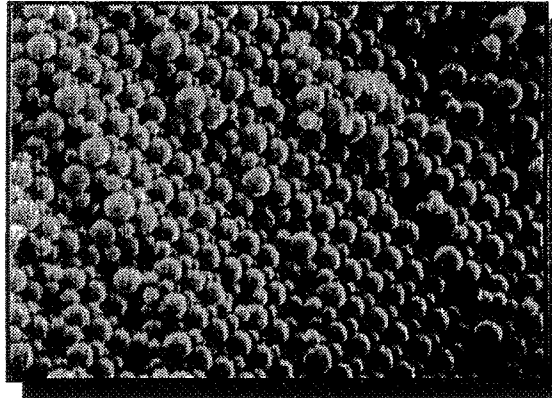


An integrated circuit wafer

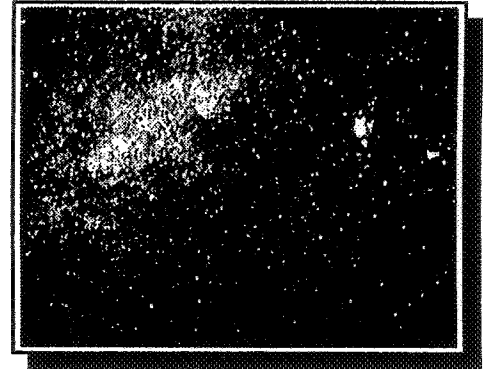
# Figure 7 Colloids



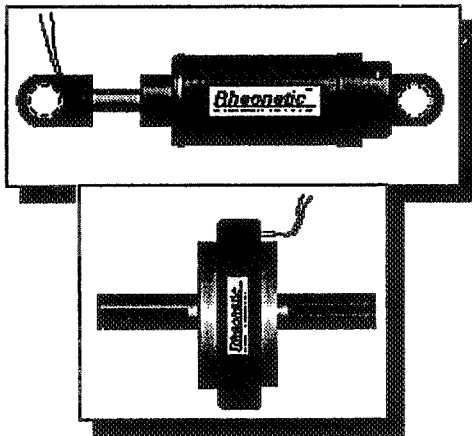
**Oil recovery**



**Colloidal crystals/  
new materials**



**Formation of galaxies**



**Rheologically controllable dampers and brakes.**

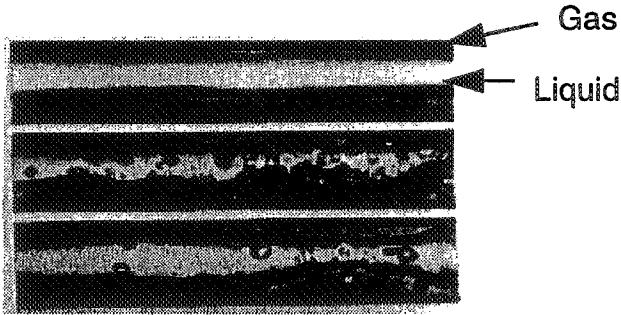


**Food products**

## Figure 8 Multiphase Flow, and Phase Change

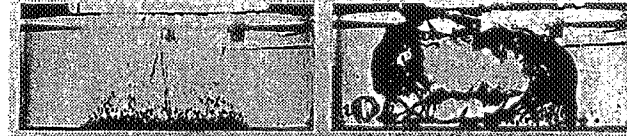
### Effect of G-Level on Multiphase Flow

**Stratified Flow**  
 Normal Gravity  
 ~ 1.0 g  
**Stratified Wavy Flow**  
 Lunar gravity  
 ~ 0.17 g  
**Slug-Annular Flow**  
 Microgravity  
 <0.01 g



Air-Water in 1.27 cm ID Tubes  
 Superficial Gas Velocity ~ 2.1 m/s  
 Superficial Liquid Velocity ~ 0.07 m/s

### Comparison of Normal- and Low-gravity Pool Boiling from the Lewis Zero Gravity Facility 11/28/89



**Fluid: Freon-113**  
**Side View**

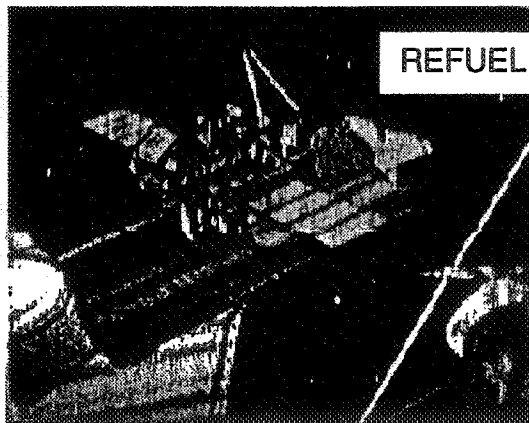
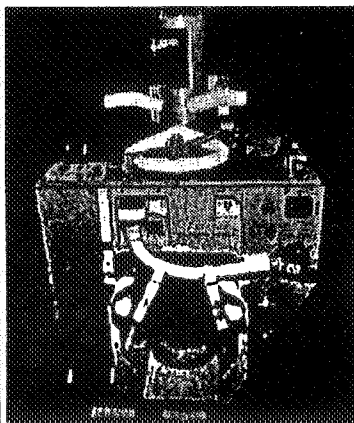
Normal Gravity (1.0 g)  
 Pressure = 22.5 psia  
 Temp (sat) = 142° F  
 Heat Flux = 8 W/cm<sup>2</sup>  
 Subcooling = 5° F

**Fluid: Freon-113**  
**Side View**

Low-gravity (10<sup>-6</sup> g)  
 Pressure = 16 psia  
 Temp (sat) = 122° F  
 Heat Flux = 8 W/cm<sup>2</sup>  
 Subcooling = 5° F

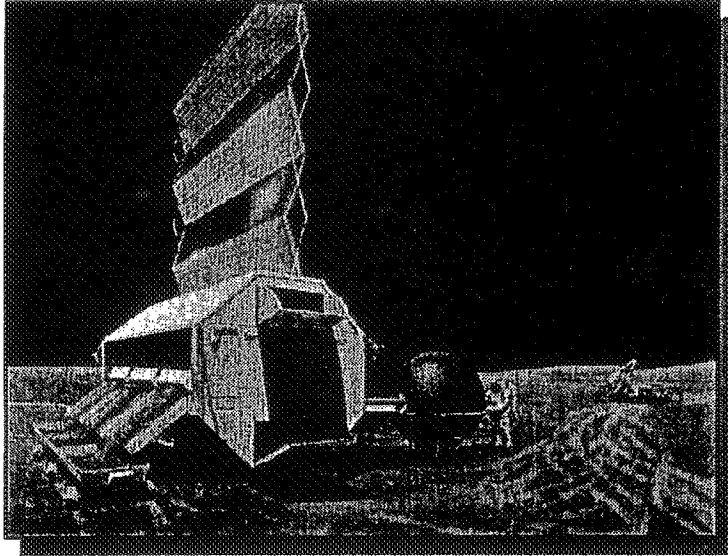
Gravity Level Strongly affects the nature of boiling

22-25

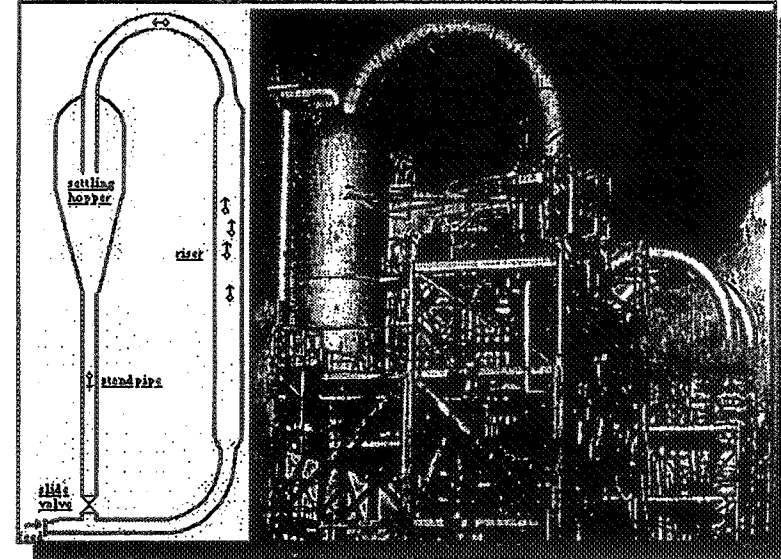


- \* Fluid flow in life support systems
- \* Fluid flow in Waste Collector Systems
- \* μ-g air-conditioning, refrigeration
- \* Fuel/liquid storage, transfer
- \* Cooling/heat-removal from equipment

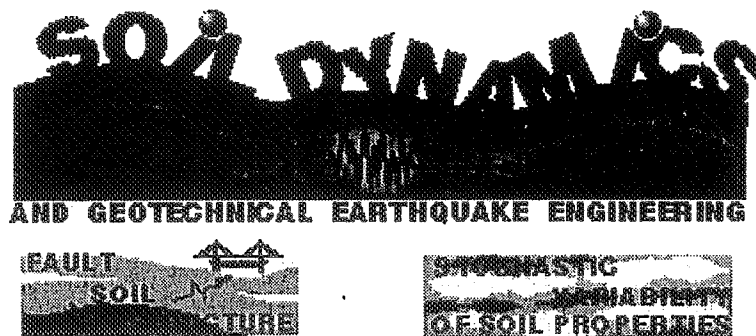
## Figure 9 Granular Media



Space mining, material processing

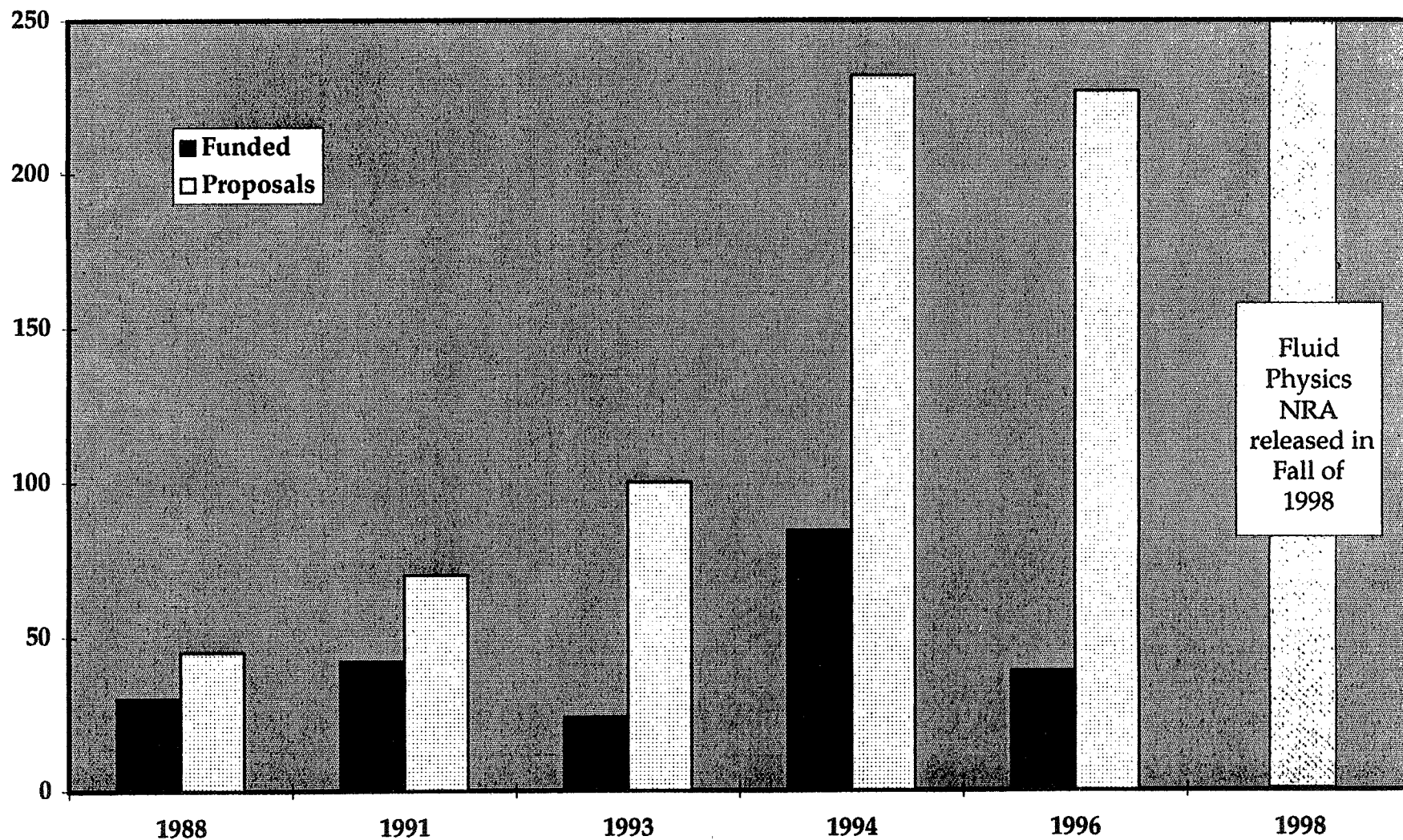


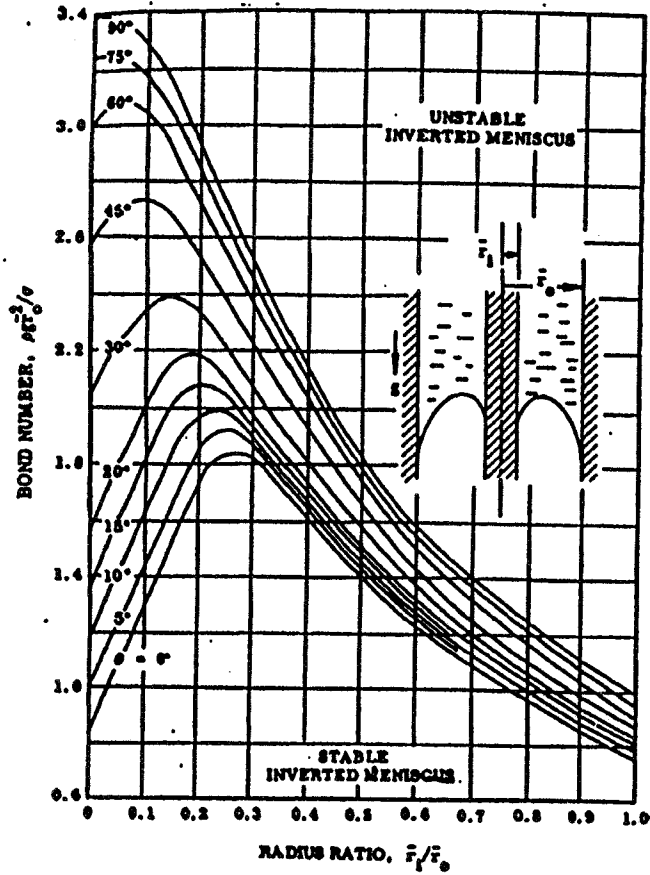
Granular flow in 'risers',  
and fluidized beds.



- \* Ceramics,
- \* Powder processing,
- \* Foundry, etc.

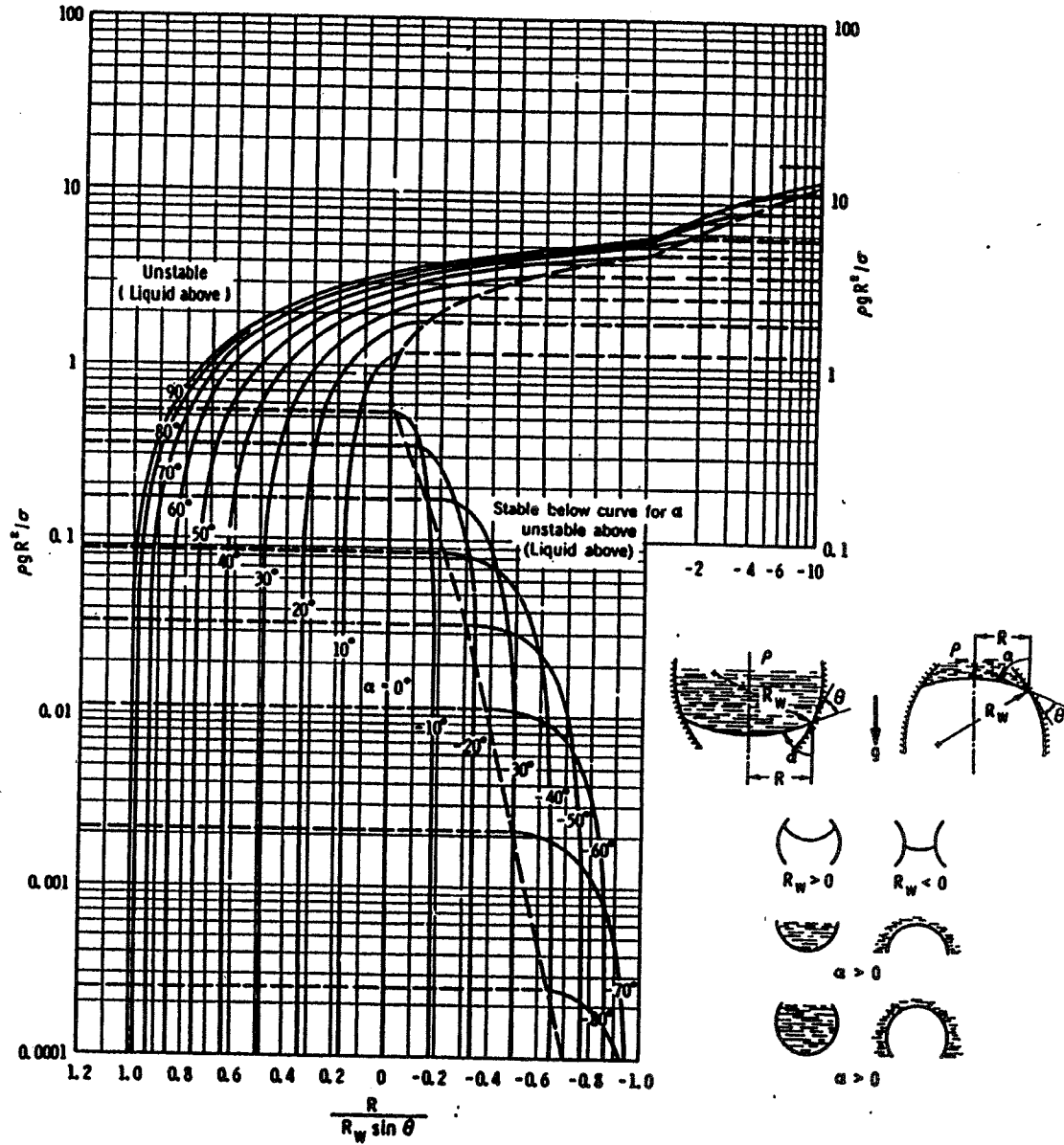
**Figure 10 Participation in the Fluid Physics Program**





(From Seebold, et. al., 1967)

Figure 11a Neutral Stability of an Inverted Annular Meniscus



(From Abramson, 1966, NASA SP-106)

Figure 11b Neutral Stability For Axisymmetric Menisci

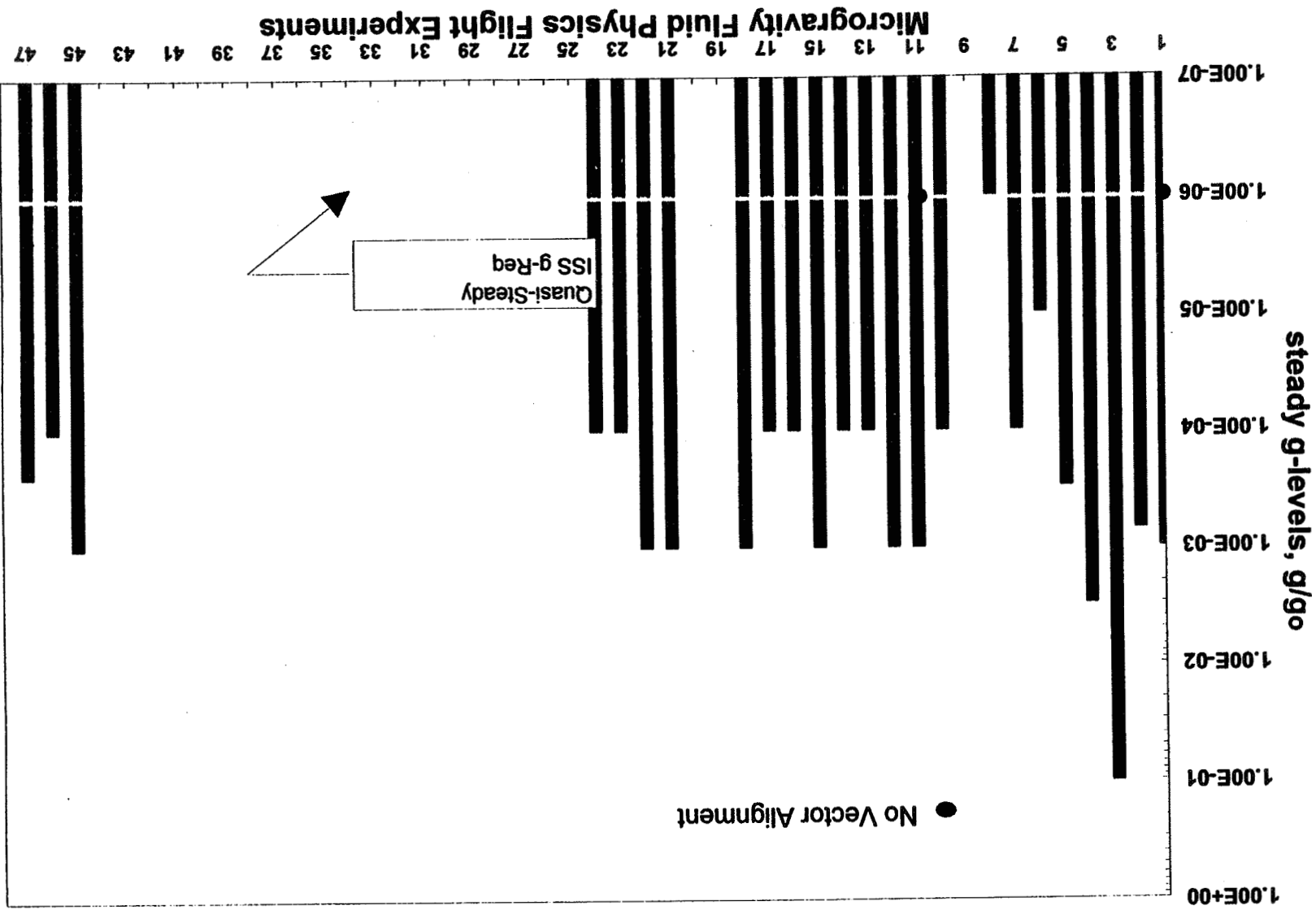


Figure 12 Maximum Allowable Background g-levels

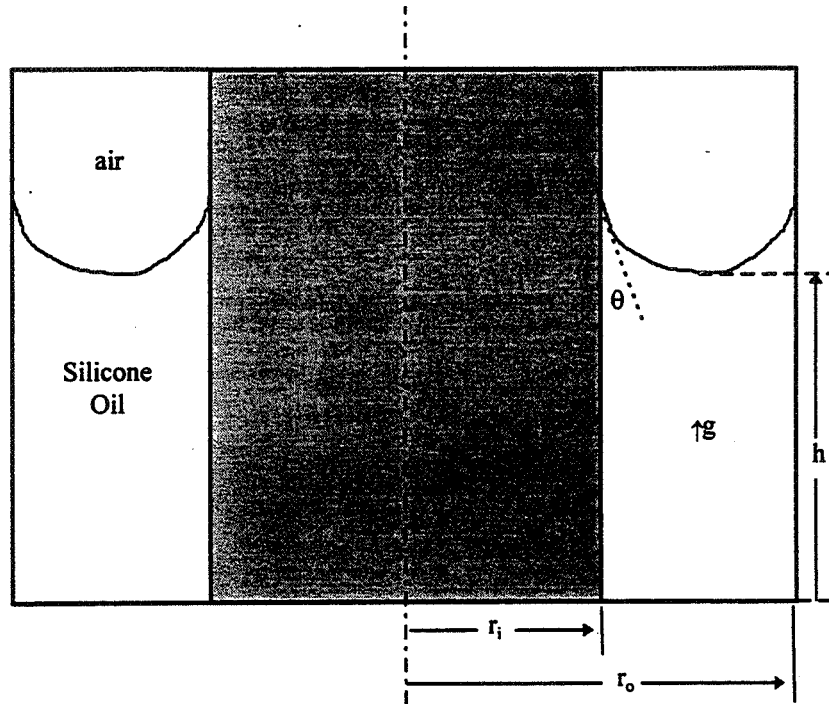


Figure 13 Microscale Hydrodynamics Near Moving Contact Lines Flight Experiment

$$\theta=0^\circ \text{ (wetting), } r_i=2 \text{ cm, } r_o=4 \text{ cm, } \frac{r_i}{r_o} = .5,$$

$$g = 10^{-5} g_o \Rightarrow Bo = .0076 \text{ \& } g = g_o \Rightarrow Bo = 761.$$

$$\text{where } Bo_o = \frac{\rho g r_o^2}{\sigma} \text{ and } g_o = 9.81 \text{ m/s}^2$$

# Spacelab, and Space Station Environments, and g-Jitter Requirements

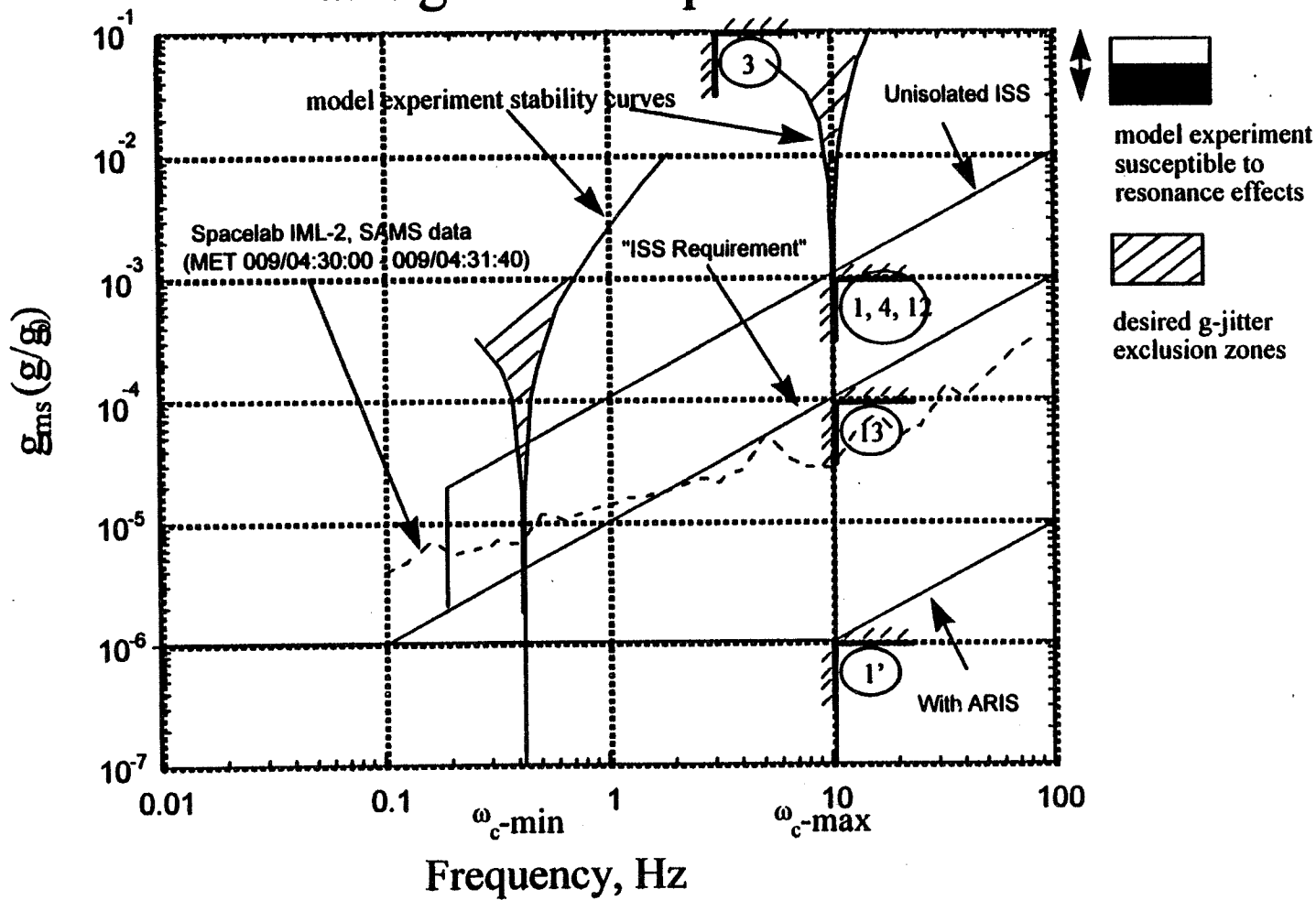
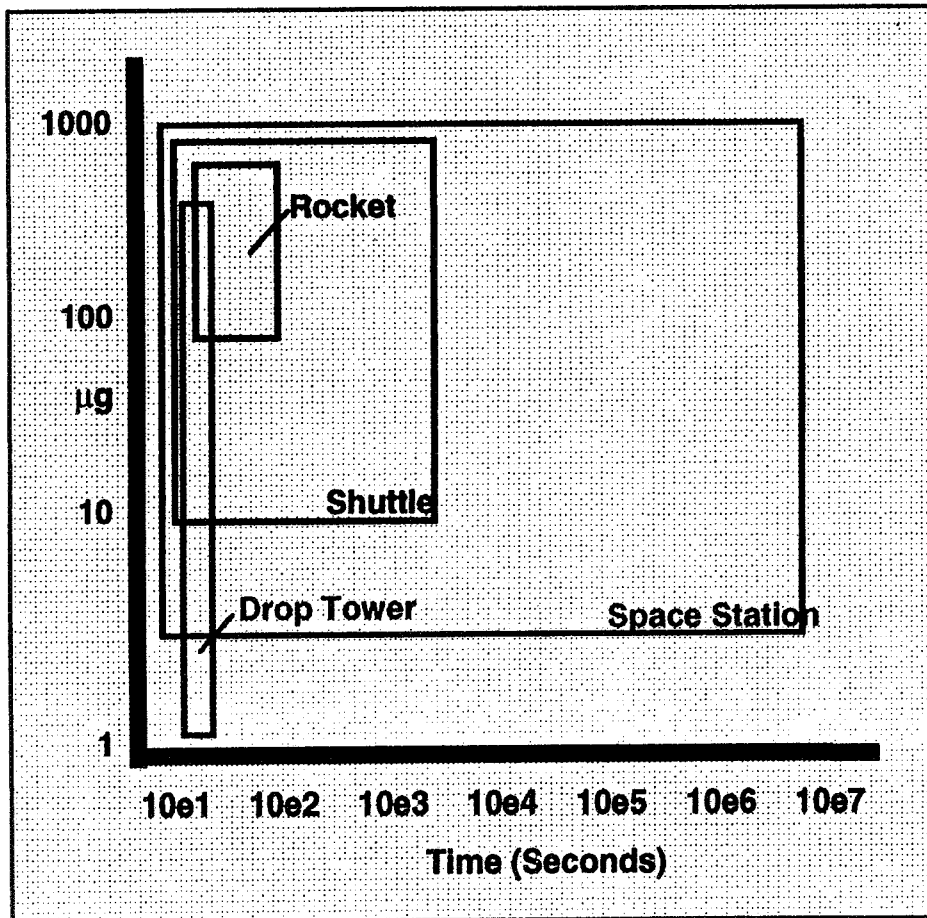


Figure 14 Requirements for ISS and Fourteen Fluid Physics Experiments  
(From ISS Fluids and Combustion Facility - Science Requirements Envelope Document)

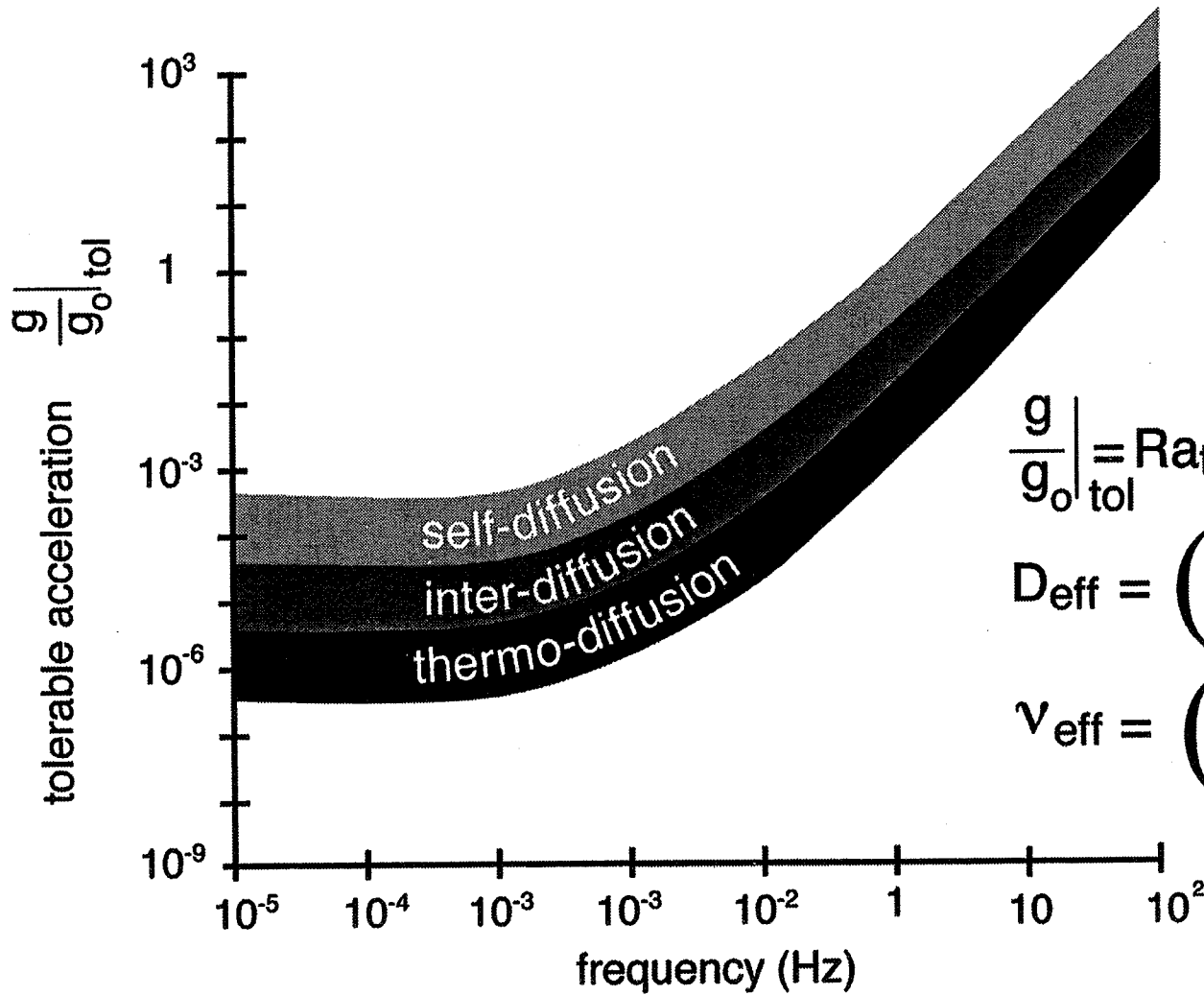
Figure 15

## Accessible Microgravity Times



| Facility              | Duration (Seconds) | g-Level ( $g_0$ )   |
|-----------------------|--------------------|---------------------|
| 2.2 Second Drop Tower | 2.2                | $10^{-5}$           |
| 5 Second Drop Tower   | 5                  | $<10^{-5}$          |
| KC-135                | 18 - 20            | .01                 |
| Sounding Rocket       | 90                 | $10^{-3} - 10^{-4}$ |
| Shuttle               | 5000               | $10^{-3} - 10^{-5}$ |
| Space Station         | $10^7$             | $10^{-3} - 10^{-6}$ |

# Figure 16 Residual Acceleration Tolerability For Diffusion Processes



$$\left. \frac{g}{g_0} \right|_{\text{tol}} = Ra_{\text{tol}} \frac{D_{\text{eff}} \nu_{\text{eff}}}{\beta_s \Delta S L_c^3}$$

$$D_{\text{eff}} = \left( D + (\omega L^2)^2 \right)^{1/2}$$

$$\nu_{\text{eff}} = \left( \nu + (\omega L^2)^2 \right)^{1/2}$$

$(g_0 = 9.81 \text{ m/s}^2)$

(Langbein, 1990)

# Microgravity Sensitivity of Typical Fluid Physics Experiment

---

Prof. Rodolfo Monti, Department of Science and Space Engineering 'L.G. Napolitano',  
Naples, Italy

Dr. Raffaele Savino, Department of Science and Space Engineering 'L.G. Napolitano',  
Naples, Italy

Dr. Marcello Lappa, Department of Science and Space Engineering 'L.G. Napolitano',  
Naples, Italy

## Microgravity sensitivity of typical fluid physics experiment

Rodolfo Monti, Raffaele Savino, Marcello Lappa

Dept. of Science and Space Engineering 'L.G. Napolitano', Naples, Italy

### ABSTRACT

This report summarizes a number of numerical results concerning the g-jitter sensitivity and the performances of Isolation Mounts for a typical Fluid Physics experiment in the Fluid Science Laboratory of the ISS. The results corresponding to the ideal (zero-g) purely diffusive situation are compared with the real case of residual-g superimposed to g-jitters, in the presence or in the absence of ARIS. The investigated cases correspond to the predicted accelerations on the ISS according to the NASA Design Analysis Cycles (DAC3 and DAC4), and to the worst situation, in which residual-g and g-jitters are supposed to be both perpendicular to the density gradient. In this situation buoyancy effects, induced by residual-g, and thermovibrational effects, induced by high frequency periodic oscillations, are concurrent and produce the maximum disturbances of the temperature and/or of the concentration fields, compared to the ideal diffusive (zero-g) situation.

The report addresses the following relevant points that help to take decisions on the suitability of implementing an isolation mount on the ISS for these categories of experiments.

- a) The exact knowledge of the real ISS microgravity environments. At the moment a number of analyses (Dynamic Analysis Cycles, DAC) are being refined according to the most recent data on the operation and on the H/W existing on board the ISS. For instance the last DACs (DAC-3 and DAC-4) present completely different scenarios for the ISS microgravity environment so much that DAC-3 would justify the introduction of the ARIS that, conversely, is not justified by DAC-4 (at least for the Columbus Orbital Facility, COF) because of the marginal improvements that could be achieved.
- b) The equivalence criterion between the convective disturbances caused by the residual-g existing at different locations of the ISS (mainly due to gravity gradients and to aerodynamic drag) and the relatively high frequency g-jitter caused by on board machinery and crew operations. Establishing an equivalence between these two kinds of perturbations could allow an evaluation of the relative importance of the residual-g and of the g-jitter and may provide a clear picture of the improvements that one can expect from ARIS.
- c) The benefits that one could expect from the orientation of the experiment cell with respect to the residual-g and to the g-jitter. In fact properly orienting the cell may result in benefits larger than killing all the high frequency g-jitter (by ARIS) that are likely to be present on the ISS.
- d) The possibility of taking advantage of the presence of the residual-g also to simulate on ground ISS experiments. In fact one is able to reproduce on ground the same convective effects that prevail in orbit due to both residual-g and g-jitters, by means of model liquids and appropriate dimensions. Experiments on ground and on the ISS have been identified that should exhibit similar behaviour.

### INTRODUCTION

Over the past two years, the University of Naples has carried out for ESA a series of studies on the numerical modelling of g-jitter effects in microgravity experiments with fluid phases and densities non uniformities. The numerical simulation is performed using three-dimensional codes. Two methods for g-jitter analysis are considered: a) numerical solution of the full non-linear and time-dependent Navier-Stokes equations with a time-dependent body force that give the instantaneous time-dependent flow; b) solutions of the time-averaged field equations for the thermovibrational

convection problem, obtained under the assumption of sufficiently small amplitudes and sufficiently large frequencies of the g-jitter. These studies have indicated that vibrations in fluid systems with density gradients (induced by temperature or concentration gradients), produce an average thermovibrational force that is responsible for steady convective flows that in turn produce steady distortions of the temperature distribution, compared to the purely diffusive distribution [1-6]. These effects could be important during fluid and material science microgravity experimentation on the International Space Station (ISS), where the residual gravity is reduced by several orders of magnitude and high frequency g-jitter may be sources of disturbances. In particular, a number of computations for different study cases pointed out that the velocity field  $V$ , induced by periodic  $\underline{g}$  is made up by an average value  $\bar{V}$  plus a periodic oscillation of amplitude  $V'$  ( $V = \bar{V} + V'$ , see Fig. 1a). As a result of this convective field a thermal (or concentration) distortion is induced (also formed by an averaged and an oscillatory part ( $\varepsilon_T = \bar{\varepsilon}_T + \varepsilon_T'$ , see Fig. 1b). The thermal distortion  $\varepsilon_T$  can be taken to be the difference of the total heat flow through a fluid cell ( $Q$ ) and the total heat flow in a purely diffusive condition ( $Q_D = k \frac{\Delta T}{L} S$ ). In terms of the Nusselt number ( $Nu = Q/Q_D$ ),  $\Delta Nu = Nu - 1 = (Q - Q_D)/Q_D$  represents the percentage increase of the heat flow due to the convective motions induced by the non-zero environment. Fig. 1b shows, for a typical microgravity experiment, that the relative value of  $\frac{\varepsilon_T'}{\varepsilon_T}$  (or equivalently of  $\frac{Nu'}{Nu}$ ) is sufficiently small. More specifically, in the frequency range of the ISS ( $f > 0.1$  Hz) the average thermal (or concentration) distortion is typically much higher than the oscillatory one ( $\frac{\varepsilon_T'}{\varepsilon_T} \ll 1$ ).

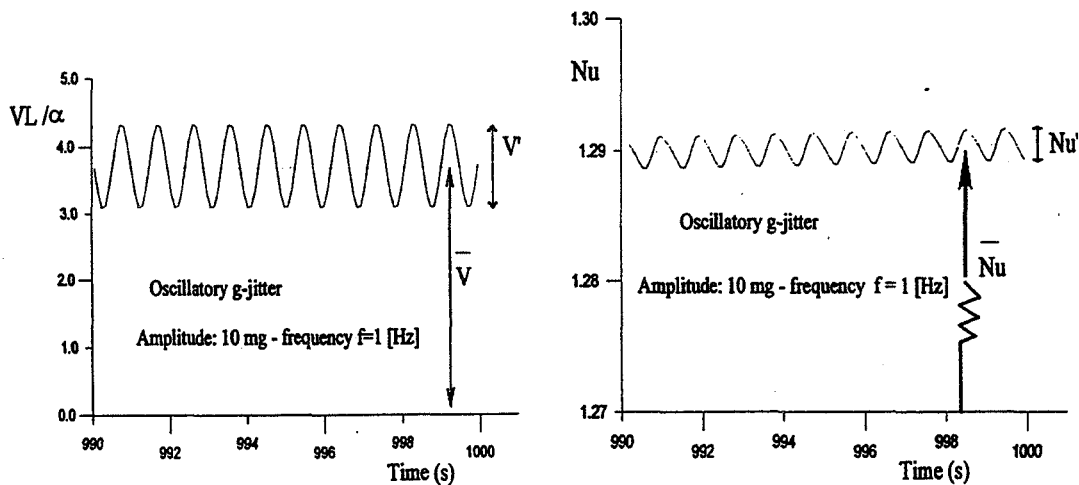


Fig. 1. Oscillatory and time-averaged distortions for a typical study case

The presence of the unavoidable residual-g on the International Space Station (ISS), that depends on the distance from the center of mass of the ISS (gravity gradient and centrifugal acceleration), may have a large impact on microgravity experiment sensitivity. In particular, the tolerability curves for g-jitter  $g(f)$ , that are based upon the assumption of a reference zero-g state and of a single-frequency periodic oscillation, might be of no use if the residual-g effects are not negligible. Based on these considerations one could ask if Isolation Mounts, like ARIS, are the best solution to mitigate acceleration effects during microgravity experiments on the International Space Station (ISS). As a matter of fact, one should consider that: 1) the g-jitter-induced disturbances depend, apart on the frequency and on the amplitude of the vibration, also on the relative directions of the

residual-g vector, of the vibration and of the density gradient; 2) for the European module COF there is a relatively large residual-g (between 1 and 2  $\mu\text{g}$ ) and Isolation Mounts can reduce only oscillatory g-jitters with relatively large frequency, but they reduce neither quasi-steady acceleration (due to gravity gradient and aerodynamic drag) nor large g-pulses (due e.g. to docking, meteorite impacts, ISS attitude control, etc.). This implies that the solution for COF may be not necessarily similar for the US Lab that is located rather close to the centre of mass of the ISS.

### STUDY CASE FOR A TYPICAL FLUID SCIENCE EXPERIMENT

When selecting a microgravity experiment to evaluate the effects of g-jitter of the kinds that are likely to occur on the Space Station one must keep in mind the following requirements:

1) The experiment must exhibit a very high sensitivity to g-jitter (typically this occurs when the liquid medium is quiescent at 0-g); 2) Very simple experiments must be identified for which the zero-g conditions are clearly computed and for which the differences between the disturbed and undisturbed conditions are clearly quantified; 3) Easy experimental measurements of the internal TFD (e.g. two dimensional velocity and refraction index distribution) must be possible.

To fulfill the above requirements: a) the liquid must exhibit a very low value of the diffusivity to achieve Peclet number sufficiently high (even with small values of the velocities); b) a single driving force should be present (i.e. isothermal with variable concentration or single component with variable temperature); c) a one dimensional temperature or concentration distribution should be established and g-jitter direction oriented either along or orthogonal to the temperature or concentration gradients to obtain a quasi 2-D TFD field in the fluid cell.

The choice between energy and species transport experiments depends mainly on the fact that in the first case it is easy to control the boundary conditions at the hot and cold side of the cell (e.g. constant temperature walls) but it is difficult to ensure a truly adiabatic conditions at the lateral walls. Conversely, truly impermeable conditions at lateral walls conditions can be achieved in the second case, however the concentration conditions at the solid liquid interface is not easily established. Typically, in the case of species diffusion, only unsteady experimentation could be performed.

The study case extensively analyzed within the ESA contract [1, 2] deals with a fluid cell with a single-component liquid in the presence of thermal gradients (Fig. 2).

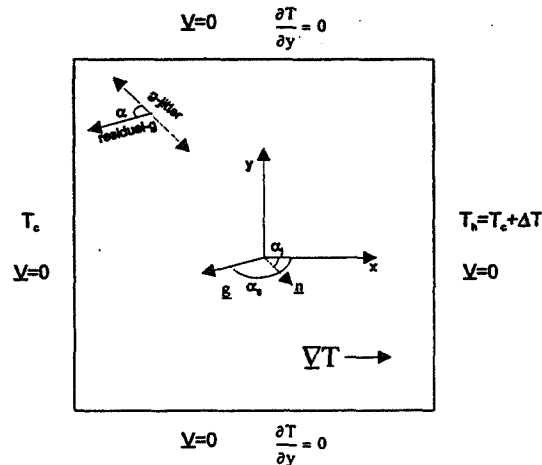


Fig. 2. Geometry of the problem and boundary conditions

A test cell with square section of side  $L$  in the plane  $xy$  is filled with a homogeneous Newtonian liquid. All the boundaries of the cavity are solid walls. The walls at  $x=0$  and  $x=L$  are maintained at constant temperatures  $T_c$  and  $T_h=T_c+\Delta T$ ; the other boundaries are adiabatic. A quasi-steady residual acceleration vector is present (denoted by  $\underline{g}$ ) and, in addition, a high frequency, periodic,

oscillatory acceleration is characterized by magnitude  $g_j$  and direction  $\underline{n}$ . In general, different relative orientations of the vibration and of the residual-g with respect to the x-axis can be considered, characterized by the angles  $\alpha_j$  and  $\alpha_g$ , respectively (see Fig. 2). The relative orientation between residual-g and g-jitter is characterized by the angle ( $\alpha = \alpha_g - \alpha_j$ ). The cases  $\alpha_g=0$  and  $\alpha_g=\pi$  correspond to  $\underline{g}$  parallel or anti-parallel to the temperature gradient; the case  $\alpha_g=\pi/2$  corresponds  $\underline{g}$  perpendicular to the temperature gradient. In the case  $\alpha=0$  residual-g and g-jitter are concurrent, whereas for  $\alpha=\pi/2$  the directions of  $\underline{g}$  and  $\underline{n}$  are perpendicular.

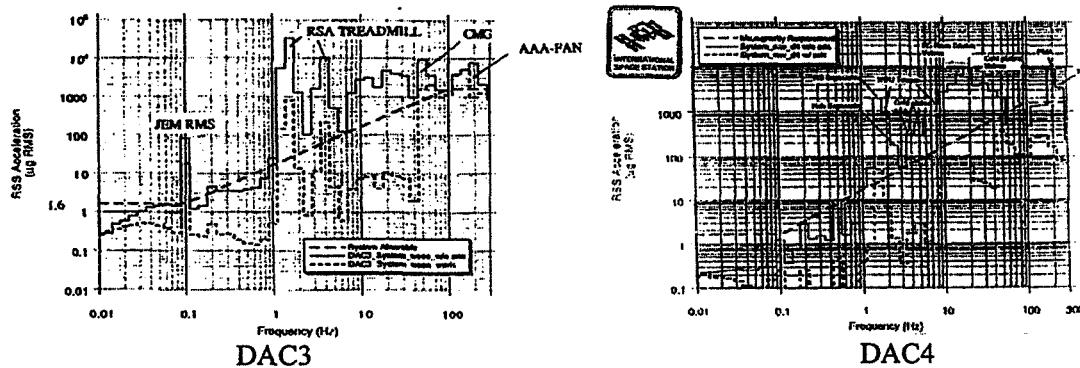
### MICROGRAVITY ENVIRONMENT OF THE ISS

The expected disturbances on the International Space Station are:

- 1) Steady (or quasi-steady) (residual-g). These include aerodynamic drag ( $1-3 \cdot 10^{-7} g_0$ ) . radiation pressure ( $10^{-8} g_0$ ), micrometeorites impacts ( $10^{-9} g_0$ ) and, for points distant from the center of mass, gravity gradient and rotation periodic with the orbit ( $1.1 \times 10^{-7} g_0/[m]$  along x, y  $-3.3 \times 10^{-7} g_0/[m]$  along z);
- 2) Pulse-like (single or compensating), due to thruster firings ( $10^{-4} g_0$ ), crew activities ( $10^{-3}-10^{-2} g_0$ ) or external forces (docking/berthing, of the order of  $10^{-4} g_0$ );
- 3) periodic, high frequency, due to on board machineries and natural frequencies excited by external forces ( $10^{-6} < g/g_0 < 10^{-2}$ ,  $0.1 [Hz] < f < 300 [Hz]$ ).

The predicted residual-g is of the order of magnitude of  $0.3 \mu g$ , for the US Lab, between 1 and  $1.8 \mu g$ , for the European COF, and about  $2 \mu g$ , for the Japanese module. The predicted high frequency g-jitter are usually reported in a plot of acceleration amplitudes vs. frequencies and compared with the System Allowable (so called «ISS requirements curve», see Figs. 3).

An extensive numerical experimentation has been carried out in terms of TFD distortions on the selected microgravity experiment. The computations have been performed for the ideal (zero-g) purely diffusive case and for the worst situation, in which residual-g and g-jitters are both perpendicular to density gradient ( $\alpha_g=\pi/2$  and  $\alpha=0$ ), on the basis of the outputs of the NASA Design Analysis Cycles (DAC3 and DAC4, see Figs. 3).



Figs. 3: DAC3 and DAC4 results

All the numerical calculations correspond to steady solutions and are obtained for a Prandtl number ( $Pr=15$ ) corresponding to a silicone oil with kinematic viscosity  $\nu=1$  [cs]. In the absence of acceleration disturbances (i.e. in the ideal zero-g conditions) a purely diffusive temperature

distribution would be obtained at the steady state, with isotherms stratified and parallel to the walls at different temperatures. In the presence of a steady residual-g field, orthogonal to the temperature gradient, buoyancy effects induced by density differences give rise to convective flows. Fig. 4 shows the computed stream-lines and isotherms for a typical value ( $Ra_g=800$ ) of the relevant gravitational Rayleigh number, defined as:

$$Ra_g = \frac{g\beta_T\Delta TL^3}{\nu\alpha}$$

where  $g$  is the quasi-steady acceleration,  $\beta_T$  the thermal expansion coefficient,  $\Delta T$  the temperature difference,  $L$  the characteristic length,  $\nu$  the kinematic viscosity and  $\alpha$  the thermal diffusivity. This value corresponds, for the considered study case, to a quasi-steady acceleration of about  $1 \mu g$ .

Fig. 5 and 6 show the stream-lines and the isotherms in the case of zero residual-g (corresponding to the ideal case of negligible aerodynamic drag for an experiment located in the center of mass of the Space Station), in the presence of high frequency g-jitters corresponding to the DAC3 and DAC4 predictions, respectively. The relevant dimensionless parameter in this case is the vibrational Rayleigh number defined by:

$$Ra_v = \frac{(b\omega\beta_T\Delta TL)^2}{2\nu\alpha}$$

where  $b$  is the displacement and  $\omega$  the angular frequency.

The real cases of residual-g superimposed to g-jitters, in the presence or in the absence of ARIS, are shown in Figs. 7, 8 and 9.

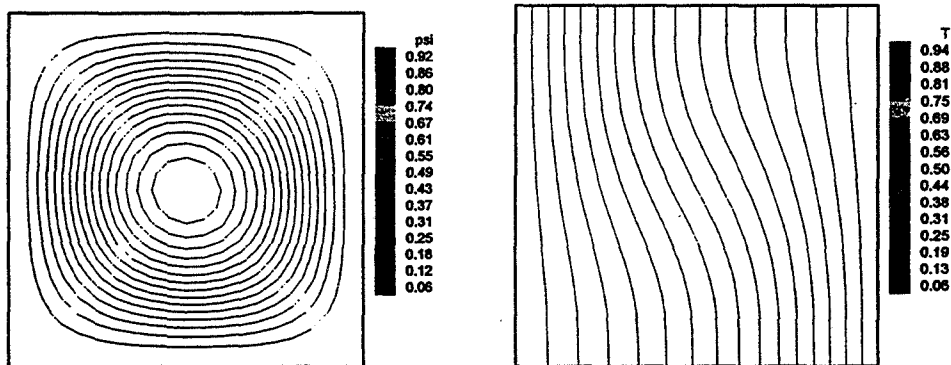


Fig. 4 Streamlines and isotherms for residual-g only ( $Ra_g = 800, Ra_v=0$ )

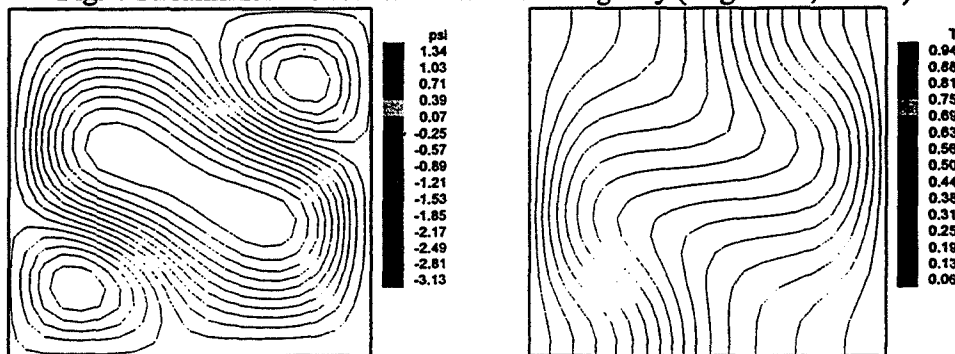


Fig.5 Streamlines and isotherms for g-jitter only, corresponding to DAC3 ( $Ra_v = 50000$ )

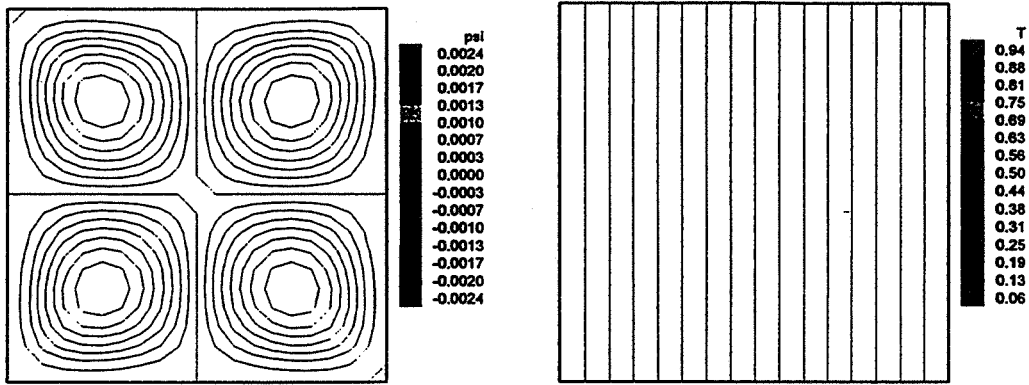


Fig. 6 Streamlines and isotherms for g-jitter only, corresponding to DAC4 ( $R_{av} = 80$ )

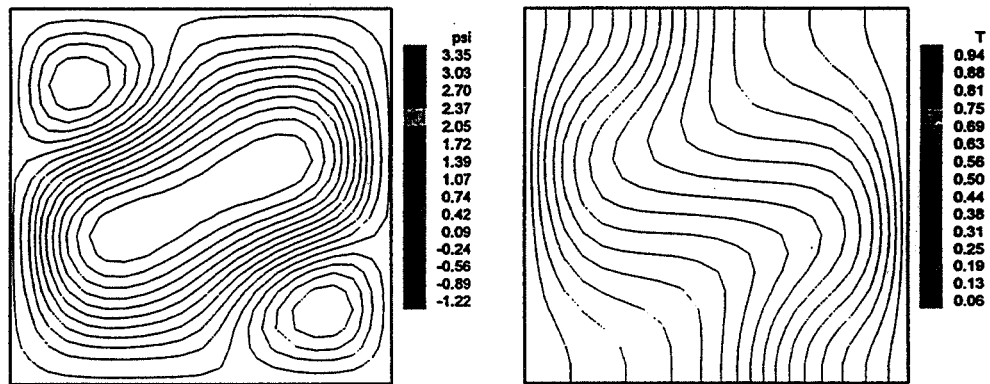


Fig. 7 Streamlines and isotherms for residual-g plus g-jitter, corresponding to DAC3 ( $R_{ag} = 800$   $R_{av} = 50000$ )

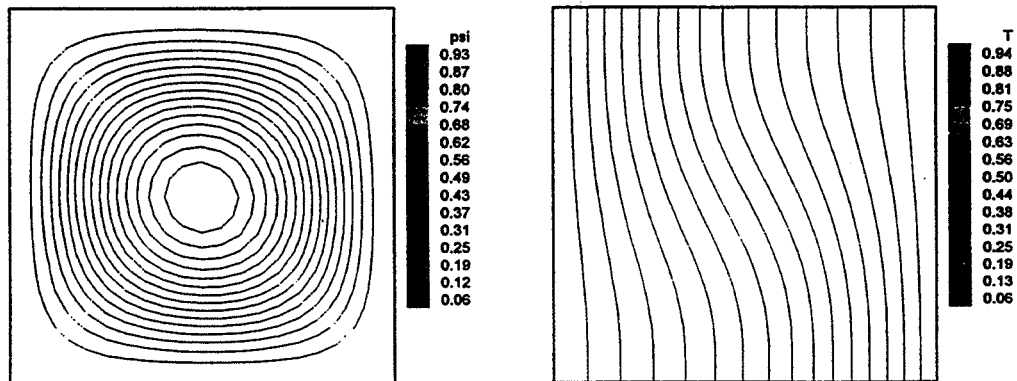


Fig. 8 Streamlines and isotherms for residual-g plus g-jitter, corresponding to DAC4 ( $R_{ag} = 800$   $R_{av} = 80$ )

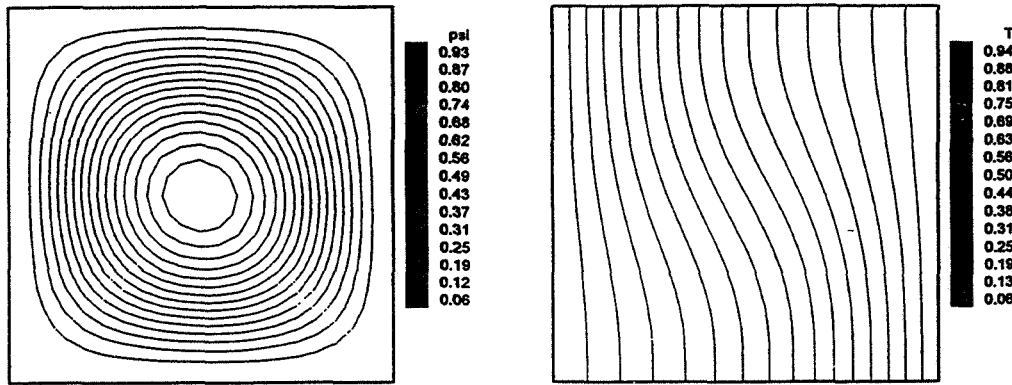


Fig. 9 Streamlines and isotherms for residual-g plus g-jitter filtered by ARIS ( $R_{ag}=800$   $R_{av}=0$ )

Fig. 10 summarizes the computed TFD distortions, expressed in terms of differences of the computed Nusselt numbers ( $\Delta Nu$ ), corresponding to different g-fields. This allows: 1) to check the microgravity relevance, for the selected experiment; 2) to evaluate the distortions due to residual-g only or to g-jitter only; 3) to assess the efficiency of the ARIS Isolation Mount. For this particular case the computations show that the experiment sensitivity to g-jitter strongly depends on the vibrational accelerations predicted for the ISS. In particular, Isolation Mounts seem to be necessary if the g-jitter will be those predicted by DAC-3, but for the DAC-4 predictions g-jitter effects are negligible compared to residual-g disturbances.

| Computed Field                                    |                     | TFD differences ( $\Delta Nu$ ) |                                | Comments  |
|---|---------------------|---------------------------------|--------------------------------|---|
| Ideal 0-g   | $Nu_0=1$            | $\Delta Nu=0$ ( $Nu=1$ )        |                                | Purely Diffusive Processes                              |
| Ground 1-g  | $Nu_G=11.2$         | $\Delta Nu_{G0} = 10.2$         |                                | Highly ideal MG relevant                                |
| Ideal MGE residual g                              | $Nu_R=1.092$        | $\Delta Nu_{R0} = 0.092$        |                                | ISS is a Suitable MG platform                           |
| DAC3 results                                      | DAC4 results        | DAC3 results                    | DAC4 results                   |   |
| Only G-jitter due to RS ergometer<br>$Nu_j=2.002$ | $Nu_j=1.001$        | $\Delta Nu_{j0}=1.002$          | $\Delta Nu_{j0}=0.001$         | Experiment sensitive to G-jitter only for DAC3          |
| Filtered G-jitter<br>$Nu_{Fj} \approx 1$          | $Nu_{Fj} \approx 1$ | $\Delta Nu_{Fj} = 1.002$        | $\Delta Nu_{Fj} \approx 0.001$ | ARIS needed for DAC3                                    |
| Actual MGE residual + g-jitter<br>$Nu_A=2.098$    | $Nu_A=1.092$        | $\Delta Nu_{AR}=1.006$          | $\Delta Nu_{AR} \approx 0$     | The experiment needs ARIS in presence of special events |
|   |                     | $\Delta Nu_{GA}=9.1$            | $\Delta Nu_{GA}=10.1$          | High actual MG relevance                                |
| Actual on ARIS<br>$Nu_I=1.092$                    | $Nu_I=1.092$        | $\Delta Nu_{IA} \approx 1$      | $\Delta Nu_{IA} \approx 0$     | ARIS needed for special events                          |

Fig. 10 Summary of the numerical results

## EQUIVALENCE CRITERION

Fig. 1 shows how, at relatively high frequencies (say  $f > 0.1$  [Hz]), the g-jitter induce an average velocity and a periodic velocity at the same frequency of the g-jitter. It is therefore very important to "compare" high frequency g-jitter effects (that could be reduced) with those induced by residual steady state g (that exist in any case on the ISS, independent of ARIS). This comparison shows the benefits that one can expect with the use of Isolation Mounts. There are two ways in which one can make this assessment: 1) an order of magnitude analysis by looking at the time averaged of the momentum equation where the source terms are respectively of the order of the residual-g Rayleigh number ( $R_{ag}$ ) and of the vibrational (thermal) Rayleigh number ( $R_{av}$ ); 2) numerical simulations, for different values of the  $R_{ag}$  and  $R_{av}$  parameters, that allow one to evaluate the thermo-fluid-dynamic distortions in terms of  $\Delta Nu = Nu - 1$  (see above discussion).

Fig. 11 summarizes the results of a numerical parametric analysis for the case considered in the present study. For each value of the residual-g, reported on the y-axis (and corresponding to a specific value of the residual-g Rayleigh number,  $R_{ag}$ ), the corresponding value on the x-axis gives the "equivalent" velocity of the g-jitter  $g(\omega)/\omega$  (proportional to the vibrational Rayleigh number,  $R_{av}$ ) that induces the same thermal distortion (i.e. the same value of  $\Delta Nu$ ). In particular Fig. 11 shows that a quasi-steady acceleration of  $1 \mu g$  (that corresponds to a value of  $\Delta Nu$  of about 0.13) is equivalent to a periodic g-jitter with  $g(\omega)/\omega = 1.5 [mg \times s]$ . This value is below the peak corresponding to the RS Treadmill in the DAC3 ( $g(\omega)/\omega = 3.3 mg \times s$ ) but well above the typical values of the high frequency g-jitter corresponding to the DAC4 predictions ( $g(\omega)/\omega = 0.4 mg \times s$ ). Therefore, the equivalence criterion confirms the results of the computations discussed above and shows that the distortions induced by high frequency g-jitter (that could be reduced by Isolation Mounts) are of the same order of magnitude or larger than those induced by residual-g only for the accelerations predicted by DAC-3; more specifically DAC-4 g-jitters are equivalent to a residual-g of about  $0.1 \mu g$  and DAC3 correspond to a residual-g of about  $5.5 \mu g$ .

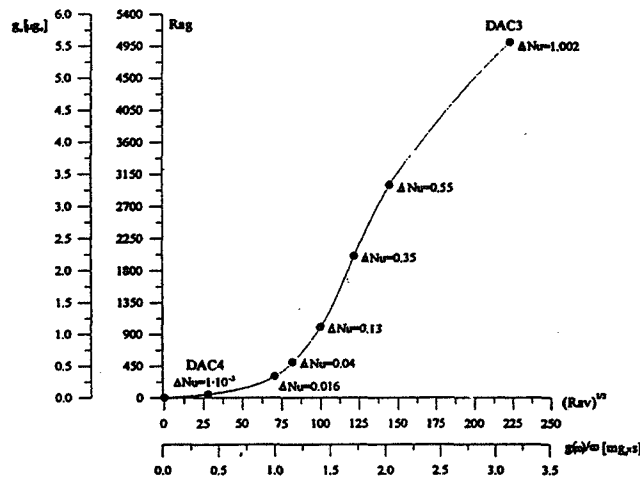


Fig. 11 Equivalence between residual-g and high frequency g-jitter

## FACILITY ORIENTATION

Many authors pointed out that convection due to quasi-steady residual acceleration during microgravity experiments could be minimized by suitable alignment of the residual-g vector with the direction of the density gradient (e.g. with the direction of the ampoule centerline for directional solidification experiments). Recent numerical studies have shown that quasi-steady residual-g and oscillatory g-jitter may be beneficial to approach pure diffusion conditions, if density gradients are

in the same direction of the acceleration direction [3]. The effect of high frequency vibrations, like that of quasi-steady acceleration, strongly depends on the direction of the vibration relative to the density gradient. In particular, it was pointed out in [6] that vibrations parallel to the density gradient tend to stabilize the purely diffusive regime, damping any residual convection due, e.g., to a destabilizing residual-gravity vector orthogonal to  $\nabla\rho$ . The above considerations suggest to focus the attention on possible experiment orientation, in order to minimize thermo-fluid-dynamic distortions due both to residual-g and g-jitters on the Space Station.

The effect of the facility orientation has been investigated for the same study case considered in the previous Section, consisting in a test cell bounded by rigid walls, completely filled with liquid, in the presence of a prescribed temperature difference. Although the quantitative results presented here are restricted to this particular study case, conclusions could be extended to different classes of microgravity experiments (e.g. Bridgman crystal growth, directional solidification, diffusion or thermodiffusion measurements experiments) in which the temperature or the concentration gradient direction is well defined, and for which the facility orientation can be properly changed to reduce undesirable convection disturbances.

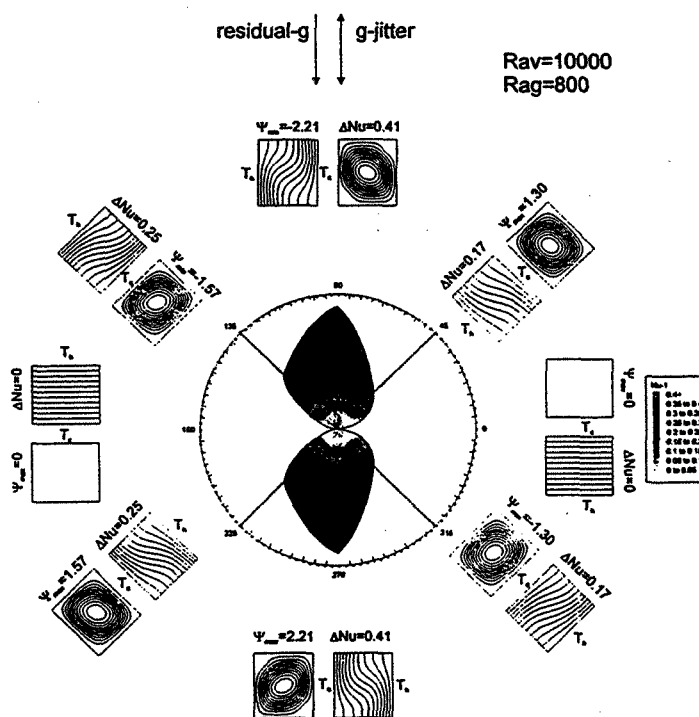


Fig. 12 Numerical results obtained changing the facility orientation.

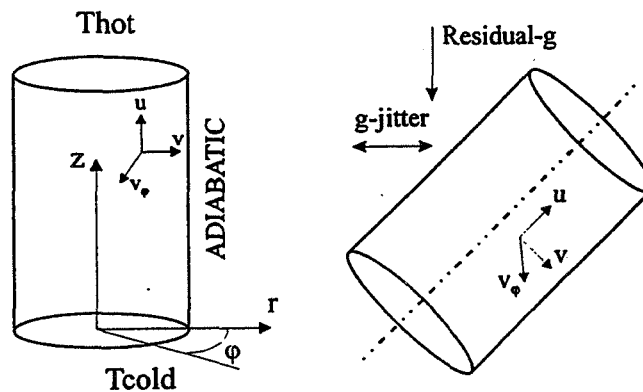
The results of an extensive numerical experimentation obtained for all possible orientations of the residual-g and g-jitter, with respect to the density gradient, are reported in [6] (see e.g. Fig. 12, relative to the case of residual-g and g-jitter both acting along the same direction). In particular, the numerical computations show that, in the absence of g-jitter, when the residual-g is opposite to  $\nabla\rho$  the residual-g has no effect (does not induce convective flows) for any value of its magnitude; when the residual-g is concurrent to  $\nabla\rho$  then TFD distortions arise only if the critical conditions for the onset of convection are exceeded (i.e. if the Rayleigh number is larger than the critical one, so that instability sets in). Finally, when the residual-g is orthogonal to  $\nabla\rho$  then TFD distortions arise for any value of the residual-g (and are somehow proportional to the Rayleigh number).

Similarly, the effect of high frequency vibrations strongly depends on the direction of the vibration relative to the density gradient. In particular, vibrations parallel to the density gradient tend to stabilize the purely diffusive regime, damping any residual convection due, e.g., to a destabilizing residual-gravity vector orthogonal to  $\nabla\rho$ . The above considerations suggest to change the facility orientation as a solution alternative to passive or active isolation devices, in order to minimize g-disturbances during microgravity experiments. In particular, for the typical study case considered in the present study, the numerical results indicate that, for the different possible configurations, corresponding to different relative orientations between residual-g and g-jitter, one should be able to properly orient the experiment to minimize the convection disturbances.

### NUMERICAL AND EXPERIMENTAL STUDY FOR THE COMPARISON BETWEEN ARIS AND FACILITY ORIENTATION

The presence of a fixed residual-g axis on the ISS allows a possible simulation on ground (i.e. in the presence of the gravity field) of the ISS conditions by scaling laws. Two experiments on the ISS and on ground have been designed for the evaluation of residual-g and g-jitter effects and for the study of the facility orientation. The two experiments are characterized by the same "steady acceleration" Rayleigh number and by the same "periodic disturbances" vibrational Rayleigh number. For the ISS microgravity experiment a cylindrical enclosure having length equal to the diameter ( $L=D=10[\text{cm}]$ ) is considered (see Figs.13). The liquid employed is silicone oil having viscosity  $1 [\text{cs}]$ . The applied temperature difference is  $\Delta T=50 [\text{K}]$ , for the residual g a typical value of  $g/g_0=1.6 \times 10^{-6}$  is considered, corresponding to the averaged value of the quasi-steady acceleration in the European COF. This corresponds to a value of the gravitational Rayleigh number of  $Ra_g=12000$ . For the g-jitter the typical amplitudes and frequencies corresponding to the NASA DAC-4 predictions are considered, giving a corresponding vibrational rayleigh number  $Ra_v=300$ .

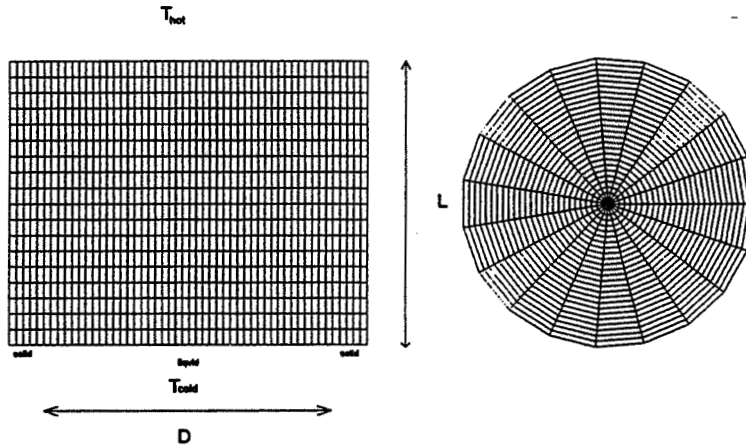
For the on ground experiment ( $g=g_0$ ) scaling laws have been applied in order to realize the same gravitational and vibrational Rayleigh numbers of the ISS experiment. The length and diameter are  $L= D= 2 [\text{cm}]$ , the viscosity of the silicone oil is  $1000 [\text{cs}]$  and  $\Delta T=10 [\text{K}]$ .



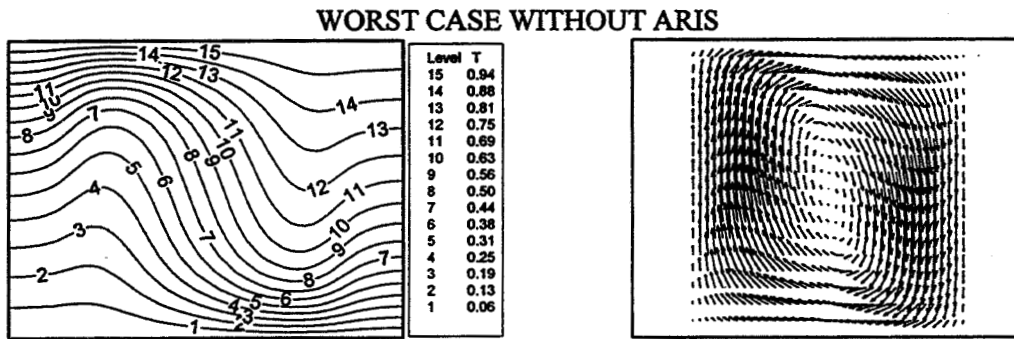
Figs. 13. Sketch of the cylindrical enclosure and of the "driving forces"

Preliminary three-dimensional numerical simulations of these experiments have been performed. Figs. 14 show the computational grids used for the numerical computations.

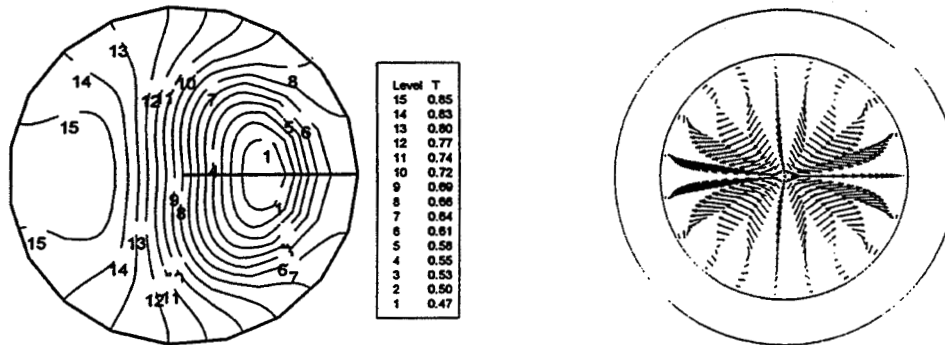
Figs. 15, 16 and 17 show the numerical results for the ISS experiment corresponding to the “worst case” (i.e. residual  $g$  and the  $g$ -jitter both orthogonal to the density gradient). Fig. 15 shows that the temperature field is strongly deformed, with respect to the diffusive situation (i.e. absence of convective driving forces), due to the convective cell arising in the meridian section  $\varphi=0$  (where the gravity vector and the  $g$ -jitter apply) (Fig. 15b).



Figs. 14. Computational grid employed for the 3D numerical computations



Figs. 15. Temperature and velocity field in the section  $\varphi=0$



Figs. 16. Temperature and velocity field in the section  $z=0.75$ , for the case of Fig. 15.

Fig. 17 illustrates the distribution of the local Nusselt number on the hot disk. In the purely diffusive situation this parameter would be, by definition,  $Nu=1$ .

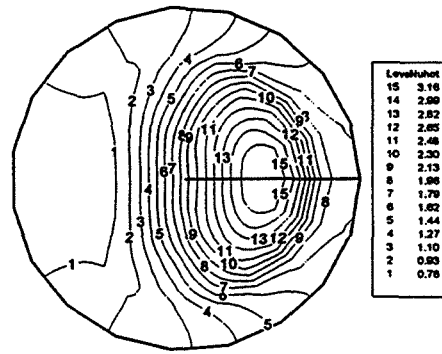


Fig. 17. Distribution of the Nusselt number on the hot disk, for the case of Fig. 15.

Due to the presence of the buoyancy and thermovibrational convection induced by the residual  $g$  and by the  $g$ -jitter the Nusselt number is locally increased or decreased. When the facility is properly oriented with the density gradient parallel to the residual- $g$  vector and the ARIS is applied (Figs. 18-21) the thermo-fluid-dynamic field is very close to the diffusive situation. ARIS in fact reduces the  $g$ -jitter whereas residual  $g$  is stabilizing by the facility orientation (fluid cell heated from above). Other situation have been considered, e.g. the facility properly oriented without ARIS, and the  $g$ -jitter reduced by ARIS without facility orientation. The results obtained in the different situation are summarized in Figs. 21.

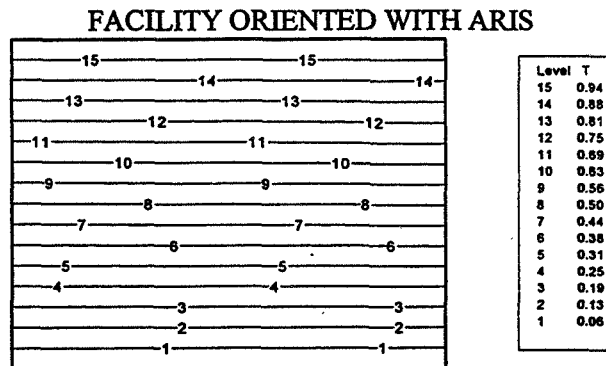
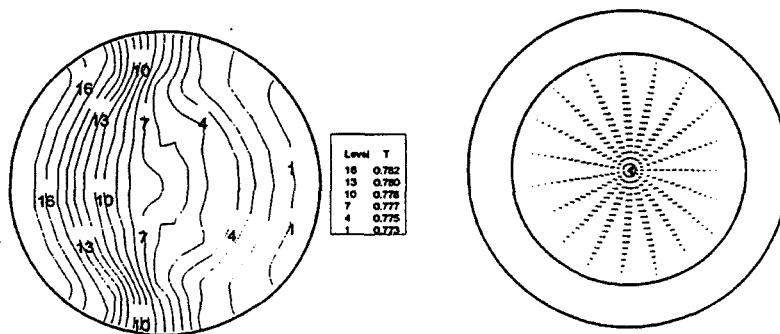


Fig. 18. Temperature field in the section  $\phi=0$



Figs. 19. Temperature and velocity field in the section  $z=0.75$ , for the case of Fig. 18.

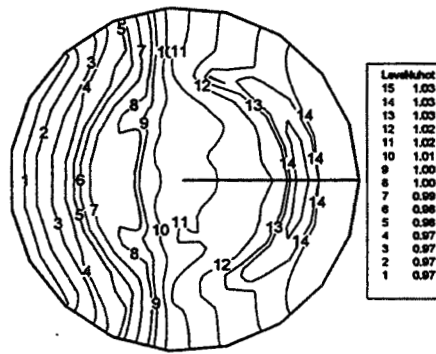
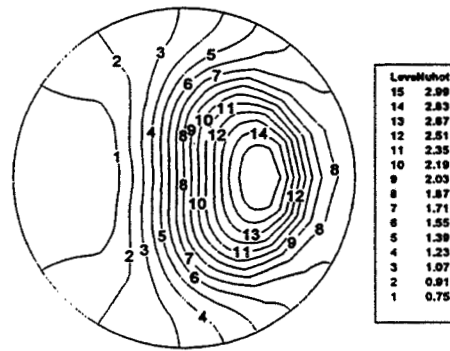
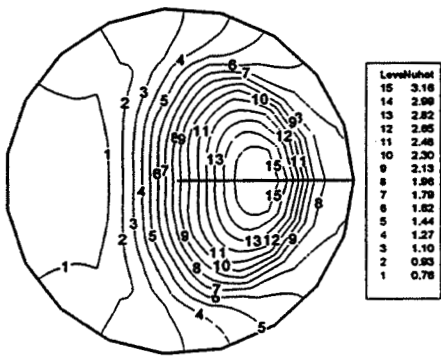
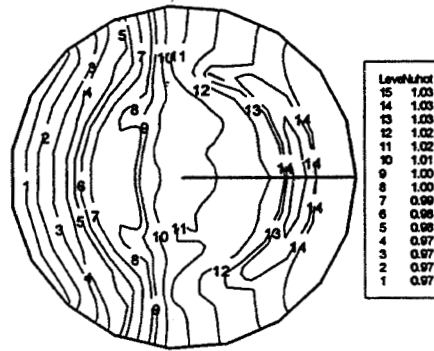
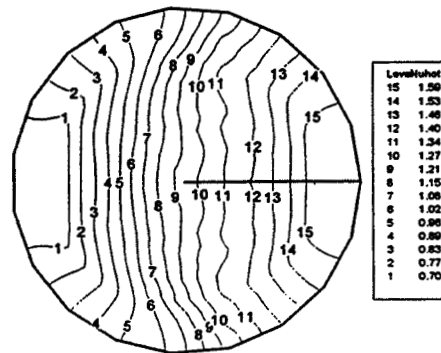


Fig. 20. Distribution of the Nusselt number on the hot disk, for the case of Fig. 18.



WORST CASE WITHOUT ARIS

WORST CASE WITH ARIS



BEST CASE (FACILITY ORIENTED)  
WITHOUT ARIS

BEST CASE (FACILITY ORIENTED)  
WITH ARIS

Fig. 21. Nusselt number on the hot disk for different situations

## CONCLUSIONS

The overall conclusions from the above presented numerical experimentations are summarized in Fig. 22. To give an idea of the transition times between different steady state microgravity conditions Fig. 22 shows the value of the Nusselt number time profile on the hot disk starting from the worst case conditions in the absence of any g-jitter (worst case with ARIS) at which the value of  $Nu=1.63$ . From these conditions one can follow different paths by: a) shutting-off the ARIS (upper curve); b) orienting the test cell without ARIS and c) orienting the test cell with ARIS.

The TFD distortions are only partially reduced by the ARIS (in the worst situation, corresponding to both residual-g and g-jitter, the average Nusselt number is 1.8).

Orienting the facility without ARIS, the average Nusselt number is decreased to 1.2. this means that, at least for COF, where the residual-g is sufficiently large, the facility orientation improves the diffusive conditions more than the ARIS. Using both experiment orientation and ARIS, a purely diffusive situation is established and the Nusselt number  $Nu$  becomes almost unitary.

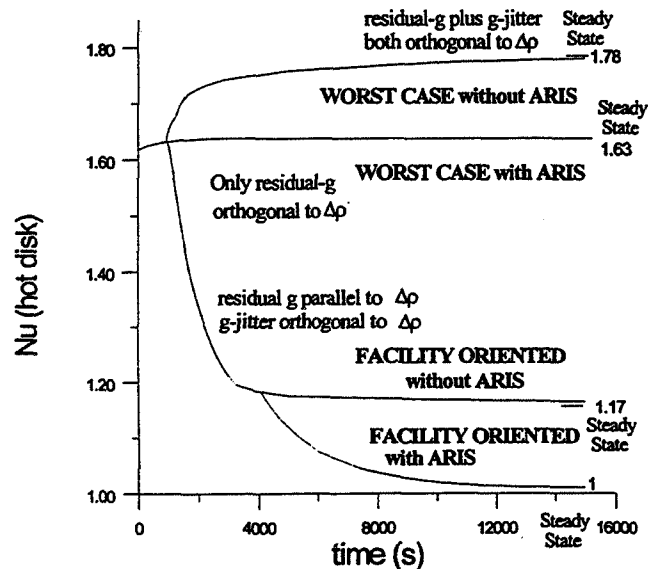


Fig. 22. Summary of the numerical results

All the numerical results presented so far need an experimental check both on ground and on board a microgravity platform. On ground activities are in progress for the measurement of Nusselt numbers in cylindrical enclosures filled with liquid in presence of temperature differences, changing the experiment orientation with respect to the steady and to the periodic acceleration vectors. Objectives of these experiments are: 1) correlation of experimental results with numerical results obtained by three dimensional CFD codes; 2) simulations of flight experiments taking into account the typical microgravity conditions on the ISS; 3) numerical computations for the comparison between effects of ARIS and of the facility orientation.

### Acknowledgments

This work has been supported by the European Space Agency under contract P.O. 171701/96/F/FL.

### REFERENCES

- [1] R. Monti, R. Savino, "Study on g-jitter for the evaluation of tolerability limits". *ESA Final Report N. 22054/94/F/FL* (June 1995)

- [2] R. Monti, R. Savino, "Study on g-jitter for the evaluation of tolerability limits". *ESA Final Report N. 11597/95/F/FL* (December 1997)
- [3] R. Monti, R. Savino, "Influence of g-jitter on fluid physics experimentation on-board the International Space Station". *ESA SP-385*, 215-224 (1996).
- [4] R. Monti, R. Savino, "A new approach to g-level tolerability for Fluid and Material Science experiments". *Acta Astronautica* 37, 313-331 (1994)
- [5] R. Monti, R. Savino, G. Alterio, "Modelling and simulation of g-jitter effects on fluid science experimentation. Impact on the utilization of ISS". Paper IAF-96-J.2.03. In course of publication on *Acta Astronautica*
- [6] R. Savino, R. Monti, "Improving diffusion-controlled microgravity experiments by facility orientation". *In course of publication* (1998)

Paper Number: 24

# **Containerless Processing in Reduced Gravity Using the TEMPUS Facility during MSL-1 and MSL-1R**

---

Dr. Jan R. Rogers, NASA Marshall Space Flight Center, Huntsville, Alabama

# **Containerless Processing in Reduced Gravity Using the TEMPUS Facility During MSL-1 and MSL-1R**

Author:

Jan R. Rogers, NASA Marshall Space Flight Center  
Biophysics and Advanced Materials Branch, Huntsville, AL 35812

## **ABSTRACT**

Containerless processing provides a high purity environment for the study of high-temperature, very reactive materials. It is an important method which provides access to the metastable state of an undercooled melt. In the absence of container walls, the nucleation rate is greatly reduced and undercooling up to  $(T_m - T_n)/T_m \sim 0.2$  can be obtained, where  $T_m$  and  $T_n$  are the melting and nucleation temperatures, respectively. Electromagnetic levitation represents a method particularly well-suited for the study of metallic melts. The TEMPUS (Tiegelfreies ElektroMagnetisches Prozessieren Unter Schwerelosigkeit) facility is a research instrument designed to perform electromagnetic levitation studies in reduced gravity. TEMPUS is a joint undertaking between DARA, the German space agency, and the Microgravity Science and Applications Division of NASA. The George C. Marshall Space Flight Center provides the leadership for scientific and management efforts which support the four US PI teams which performed experiments in the TEMPUS facility.

The facility is sensitive to accelerations in the 1-10 Hz range. This became evident during the MSL-1 mission. Analysis of accelerometer and video data indicated that loss of sample control occurred during crew exercise periods which created disturbances in this frequency range. Prior to the MSL-1R flight the TEMPUS team, the accelerometer support groups and the mission operations team developed a strategy to provide for the operation of the facility without such disturbances. The successful implementation of this plan led to the highly successful operation of this facility during MSL-1R.

## **1. INTRODUCTION**

Containerless processing is one area of interest in materials science.<sup>1,2</sup> Levitation, positioning and processing of materials which are not in direct contact with container surfaces

provides a unique opportunity to study a number of phenomena. In particular, the lack of contact with container walls reduces the possibility for heterogeneous nucleation in studies of the processing of molten materials. The study of the properties and solidification of undercooled materials is facilitated by containerless processing. Electromagnetic levitation represents a method well suited for the study of metallic melts.

Ground-based processing necessitates the use of strong magnetic fields to levitate samples against the force of gravity. Several limitations exist for ground-based electromagnetic levitation:

- high electromagnetic fields deform the shape of a molten sample
- high electromagnetic fields also induce turbulent flow inside the sample
- required fields are so strong that samples must be cooled convectively with high-purity inert gas

In microgravity, the required electromagnetic fields are greatly reduced. This offers the following advantages:

- very little deformation of the sample; spherical shape is maintained
- reduced opportunity for turbulence in the melt
- positioning field generates greatly reduced heating in the sample, and gas cooling is not required--ultra high vacuum processing is possible
- greatly diminished power dissipation as a result of the reduced positioning field permits access to a wide temperature range and facilitates temperature control

Terrestrial levitation experiments are essentially restricted to refractory metals and good conductors. In microgravity, processing and undercooling of metals with low melting points becomes possible. This permits the study of alloys with deep eutectic temperatures and glass forming alloys. The TEMPUS facility is an electromagnetic levitation instrument designed to process samples in the microgravity environment of the Space Shuttle. The equipment was developed by Daimler-Benz Aerospace, with funding from the German space agency (DARA).

Scientific investigations in TEMPUS are categorized using four experiment classes:

Class A: Studies of undercooling phenomena and the kinetics of nucleation

Class B: Measurement of specific heat in liquid metals using an AC calorimetry technique

Class C: Measurement of viscosity and surface tension of undercooled metals

Class D: Measurement of thermal expansion in undercooled materials

Studies of undercooling and solidification are central to materials science. Class A experiments examine the fundamentals of nucleation and include studies of solidification

velocities as a function of undercooling. Class B studies often focus on metallic glass forming materials. Information obtained from the levitation studies seek thermodynamic data which provide insight into the formation of metallic glasses. This is an industrially important new class of materials. Metallic glasses are ductile, isotropic and corrosion resistant. Metallic glasses are used in magnetic storage media films. Applications for metallic glasses have been limited to thermal quench methods which produce thin films and powders. Better insight into the formation of these materials may provide the information needed to better exploit these materials. Class C and D studies provide important thermophysical property data on undercooled materials. Accurate modeling of materials processing requires such data.

## **2. FACILITY DESCRIPTION**

Knauf et al. provide technical data on the capabilities of the TEMPUS facility.<sup>3</sup> Four subsystems housed in a single Space Shuttle rack comprise the facility. The subsystems consist of: the Process control and Data Acquisition Module (PDM), the Experiment Unit (EU), the High Power Supply (HPS), and the Cold plate/ Heat Exchanger (CHEX). A rotating sample exchange mechanism provides access to the different samples within TEMPUS. Samples may be processed under vacuum or selected gas environments.

The levitation and heating coils represent the heart of the facility. The performance of the coil systems determines the ability of an electromagnetic levitator to provide the magnetic fields required to meet the specified scientific objectives. The coils provide the electromagnetic forces to heat, position and manipulate the samples during experiments. The coil system is comprised of two differently shaped coils, one for heating and one for positioning. Pyrometers provide temperature data. A detailed analysis of pyrometry on TEMPUS can be found in Hofmeister.<sup>4</sup>

## **3. REDUCED GRAVITY PERFORMANCE**

The first mission for TEMPUS occurred in July 1994 as part of the Second International Microgravity Laboratory (IML-2) Payload on the National Aeronautics and Space Administration's (NASA's) Space Shuttle. Four NASA sponsored and four DARA sponsored investigation teams had 22 samples of different compositions. During the initial processing studies it became evident that the samples were often unstable. Several samples were lost during processing. These problems were due to inhomogeneities in the magnetic field. The TEMPUS investigation team developed procedures to process samples and collect some data

despite the problems with the magnetic fields. Egry et al. REFERENCE provide a summary of the findings from IML-2.<sup>5</sup> Achievements on IML-2 include: 48 hours of levitation time, melting and heating Zr to 2000 C, measurement of the specific heat of NiNb and ZrNi in the slightly undercooled state, solidification of NiNb into a possible metastable state and surface tension measurements of liquid Au, AuCu and ZrNi.

Additionally, because of magnetic field inhomogeneities during IML-2, stable positioning required the application of much higher magnetic fields than called for in the nominal experiment protocols. Flows induced by the high magnetic fields precluded the quiescent conditions required by many of the scientific investigations. The design and evaluation of a new coil system represented a major undertaking in the modification of TEMPUS facility for future Space Shuttle missions. Design efforts included theoretical/modeling studies as well as field mapping and torque measurements on candidate coil systems.

Because TEMPUS is unable to levitate samples against 1-g acceleration, ground-based performance testing is not possible. Therefore, performance tests were undertaken in reduced gravity on NASA's KC-135 aircraft. This KC-135 aircraft is a research platform for reduced gravity experimentation and astronaut training. When flown in a special parabolic trajectory, the plane provides approximately 20 seconds of reduced gravity.<sup>6</sup> Under good conditions, the plane can provide acceleration levels of approximately 0.01g. Under turbulent flying conditions the acceleration environment in the reduced gravity portion of the parabola can vary greatly in both magnitude (up to 0.1g) and direction (up vs. down). This aircraft presented a challenging test environment for the TEMPUS coil systems, designed to operate in the microgravity environment of the Space Shuttle.

The engineering development model of TEMPUS system with selected candidate coil systems was loaded in the KC-135 aircraft for testing. Testing included procedures to examine the positioning stability of a variety of solid and molten samples. A preliminary campaign in June 1995 indicated that the newly designed coil systems showed superior performance than the coil system used on IML-2. A second campaign, in January 1996 demonstrated that the coil system designated E2A3 could stably position molten samples against disturbances on the order of 100 milli-g. The coil was able to melt and position a number of materials, including Zr, CoPd, Ni and AuCu.<sup>7</sup>

This coil system was used in the TEMPUS facility during the Microgravity Science Laboratory (MSL-1 and MSL-1R) Spacelab missions. MSL-1 launched on April 4, 1997 and landed on April 8, 1997. The mission which had been planned for 16 days was cut short due to fuel cell problems. However, the TEMPUS facility was able to perform a limited number of

experiments. Prior to the mission it had been recognized that the TEMPUS facility was sensitive to accelerations in the 1-10 Hz range. Crew exercise on the bicycle ergometer produces such disturbances. It had been anticipated that the vibration isolation of the bicycle ergometer in the mid-deck would provide sufficient damping to permit experiment operations during exercise periods. However, during MSL-1 the loss of control of several molten samples occurred during crew exercise periods. Video of sample processing during these periods shows oscillations in the position of the sample which occur with increasing amplitude. In some cases the molten sample was no longer contained by the positioning field, and struck the sample containment fixtures. This resulted in the loss of some samples and significant loss of data return. Additionally, the coils of the facility could be destroyed by contact with a molten sample. Analysis of the accelerometer data from PIMS (Principal Investigator Services), QSAM (Quasi-Steady Acceleration Measurement) and MMA (Microgravity Measurement Assembly) and TEMPUS video confirmed that in many instances, loss of sample control occurred when the 1-10Hz accelerations were present.

After NASA decided to reflly the MSL-1 payload in July 1997 (as MSL-1R), the TEMPUS team sought an improved operations strategy. Sample processing during crew exercise was deemed unacceptable due to the risk of sample loss and facility damage. Mission management had already prepared the timeline which indicated when the different facilities could operate and when exercise would occur. Power and other resource constraints made simultaneous operation of all experiment facilities impossible. Crew exercise periods are essential to astronaut health and performance. Pre-mission scheduling of TEMPUS operations during periods without crew exercise was not possible. However, because many of the TEMPUS experiments had some runs of relatively short duration (minutes to hours), the investigation teams could schedule pauses in their experiment operations during crew exercise. The crew had been alerted to the concerns of the TEMPUS facility and would call the ground operations team to indicate when they would be exercising. Accelerometer teams from PIMS and MMA monitored their real-time acceleration data and alerted the TEMPUS operations team of any accelerations in the 1-10Hz range. Mission management often permitted experiment teams extension of their allotted processing time, to compensate for the pauses during exercise.

The acceleration environment also has an impact on the temperature measurements obtained during the experiments. G-jitter can induce motions of the spherical samples which alter the intensity of signal at the detector of the pyrometer. This can produce errors in temperatures calculated from pyrometer data. The TEMPUS facility was permitted to run some brief experiments at the end of the minimum duration flight. Because of the fuel cell problems,

facilities had been turned off in order to conserve power and prepare for landing. During these final runs, all other facilities in the Spacelab had been deactivated and the environment was free from the accelerations caused by the equipment and operations associated with other experiments. This provided the facility was some very quiescent processing time. Egry has performed preliminary analysis of thermophysical properties as functions of temperature using data obtained during these runs. Comparison with data obtained during normal mission operations and has indicated that the data from the quiescent operations provide much smoother curves; much less scatter is observed from the temperature data.<sup>8</sup>

It is important to note that the microgravity environment dictates the strength of the field required to position samples during experiments. In order to maximize the benefits of microgravity processing in the facility, it is important to use the minimum necessary positioning field. Accurate knowledge of the microgravity environment is required to appropriately define this parameter. Strong transient accelerations or impulses can exceed the force of the positioner field and may also lead to loss of sample control. Also, during MSL-1 some sample containment fixtures were equipped with reflectors which had been included to facilitate thermal expansion measurements. During the minimum duration flight it became evident that these reflector perturbed the magnetic field during sample processing. The reflectors were eliminated for MSL-1R.

#### **4. SUMMARY OF RESULTS**

TEMPUS flew on MSL-1 and MSL-1R in 1997. The payload supported 10 principal investigators, listed in Tables 1 and 2.

| Principal Investigator   | Institution                        | Experiment Title  |
|--|------------------------------------|---|
| Dr. Bayuzick   | Vanderbilt Univ.                   | Effects on Nucleation by Containerless Processing in Low Earth Orbit  |
| Dr. Flemings   | MIT                                | Alloy Undercooling Experiments  |
| Dr. Johnson  | California Institute of Technology | AC Calorimetry and Thermophysical Properties of Bulk Glass Forming Metallic Liquids--A Flight Experiment Employing the TEMPUS hardware                  |
| Dr. Szekely(deceased)<br>Drs. Flemings/Trapaga<br>(continuation PI team) | MIT                                | Measurement of the Viscosity and Surface Tension of the Undercooled Melts Under Microgravity Conditions and Supporting Magnetohydrodynamic Calculations |

Table 1. NASA sponsored research teams

| Principal Investigator | Institution   | Experiment Title   |
|------------------------|---|--|
| Dr. Egry               | DLR, Institute for Space Simulation                               | Thermophysical Properties of Undercooled Metallic Melts  |
| Dr. Fecht              | TU Berlin, Institute for Metal Research                           | Thermophysical Properties of Advanced Materials in the Undercooled State                                   |
| Dr. Frohberg           | TU Berlin, Institute of Metallic Materials and General Metallurgy | Measurement of the Surface Tension of Liquid and Undercooled Metallic Alloys by Oscillating Drop Technique |
| Dr. Herlach            | DLR, Institute for Space Research                                 | Comparative Dendrite Velocity Measurement on Pure Ni and a Dilute Ni-C alloy                               |
| Dr. Herlach            | DLR, Institute for Space Research                                 | Undercooled Melts of Alloys with Polytetrahedral Short-Range Order   |
| Dr. Samwer             | University of Augsburg, Institute for Physics                     | Thermal Expansion of Glass Forming Metallic Alloys in the Undercooled State                                |

Table 2. DARA sponsored research teams.

TEMPUS operated throughout the MSL-1R mission, with almost 200 hours of containerless processing. Experiments from 6 German and 4 US PI teams were performed successfully, providing the teams with wealth of data in an up-to-now inaccessible for this kind of research.

For the first time it was possible to conduct a systematic study on the thermophysical properties and solidification behavior of undercooled liquid metals and alloys. Most of the experiments exceeded the expectations of the investigator teams, and some were spectacular. Among the highlights, the following deserve special mention:

- First measurements of specific heat and thermal expansion of glass-forming metallic alloys. These measurements have never been done before and are not possible on Earth.
- More than 120 melting cycles on Zirconium with a maximum temperature of approximately 2000°C and consistently an undercooling of 340°C. This is the highest temperature and possibly the largest absolute undercooling ever achieved in space.
- First measurements of viscosity of PdSi alloys and a relative undercooling of 26%. Viscosity measurements on undercooled liquid metals and alloys are not possible on Earth, and such a high relative undercooling has never been reported before on this sample.
- Systematic study of commercially important FeNiCr- steels of different compositions in the entire undercooled regime from 20 - 300 K including both, spontaneous and triggered nucleation.
- Greater than 330 K undercooling of a CoPd alloy thus potentially creating a liquid magnet.

## 5. ACKNOWLEDGEMENTS

Research with the TEMPUS facility is supported by DARA and NASA.. Daimler-Benz Aerospace is the primary hardware developer. The German Aerospace Research Establishment (DLR-MUSC) provides user support services.

## 6. REFERENCES

1. R.J. Bayuzick, W.H. Hofmeister and M.B. Robinson, "Applications of Containerless Processing in the Study of Metals and Alloys," *Proceedings of the AIAA/IKI Microgravity*

- Symposium, Moscow, USSR, May 13-17, 1991*, H.C. Gatos and L.L. Regel, eds., AIAA, Washington, D.C., 1991.
2. R.J. Naumann and D.D. Elleman, "Containerless Processing Technology," *Materials Sciences in Space*, B. Feuerbacher, H. Hamacher and R.J. Naumann, eds., 294-314, Springer-Verlag, Berlin, 1986.
  3. R. Knauf, J. Piller, A. Seidel, M. Stauber, U. Zell and W. Dreier, *6th International Symposium on Experimental Methods for Microgravity Materials Science*, R. Schiffman ed., 43-51, The TMS Society, Warrendale, 1994.
  4. W. Hofmeister and R.J. Bayuzick, "Optical Pyrometry on TEMPUS: A Critical Assessment of Non-contact Temperature Measurement in Low Earth Orbit," *Space Processing of Materials-SPIE Proceedings Vol. 8513*, SPIE, 1994 (submitted).
  5. I. Egry et al., "Containerless Processing in Space," *Materials and Fluids Under Low Gravity*, L. Ratke, H. Walter and B. Feuerbacher, eds., Springer-Verlag, Berlin, 1996.
  6. G.A. Smith and G.L. Workman, "KC-135 Acceleration Levels during Low- and High-Gravity Trajectories," *Materials Science on Parabolic Aircraft*, P.A. Curreri, ed., NASA Technical Memorandum 4456, 1993.
  7. J. Piller et al., "KC-135 Experiment Data Package," *January 1996 TEMPUS Working Group Proceedings*, Daimler Benz, Friedrichshafen, Germany, 1996.
  8. I. Egry unpublished data.

# Planning Experiments for a Microgravity Environment

---

Melissa J. B. Rogers, National Center for Microgravity Research of Fluids and Combustion, Cleveland, Ohio

# **Planning Experiments for a Microgravity Environment**

Author:

Melissa J. B. Rogers

Microgravity Environment Scientist  
National Center for Microgravity Research on Fluids and Combustion  
21000 Brookpark Rd. MS 110-3  
Cleveland, OH 44135

## **ABSTRACT**

Prior to performing science experiments in a microgravity environment, scientists must understand and appreciate a variety of issues related to that environment. The microgravity conditions required for optimum performance of the experiment will help define an appropriate carrier: drop facility, sounding rocket, free-flyer, or manned orbiting spacecraft. Within a given carrier, such as the International Space Station, experiment sensitivity to vibrations and quasi-steady accelerations should also influence the location and orientation of the experiment apparatus; the flight attitude of the carrier (if selectable); and the scheduling of experiment operations in conjunction with other activities. If acceptable microgravity conditions are not expected from available carriers or experiment scheduling cannot avoid disruptive activities, then a vibration isolation system should be considered. In order to best interpret the experimental results, appropriate accelerometer data must be collected contemporaneously with the experimental data. All of this requires a good understanding of experiment sensitivity to the microgravity environment.

## **BACKGROUND**

Presentations made earlier in this meeting discussed the microgravity environment of the Space Shuttle Orbiters, the Mir space station, Terrier-Black Brant sounding rockets, and the FOTON free-flyer. One session was devoted to predictions of the microgravity environment that will be provided on the International Space Station. Several speakers provided overviews of the sensitivity of broad categories of experiments to variations in the microgravity environment and some specific examples of experiments that were affected by vibrations in flight were given. This paper takes these various topics and combines them to discuss the implications they have to investigators planning to run experiments in a microgravity environment.

Many types of scientific experiments may benefit by being conducted in a microgravity environment. There are many variables that should be considered by the experimenter before the

experiment operations are started. These include the environment provided by different microgravity carriers; the experiment location and orientation within the carrier; the carrier attitude while falling, flying, or orbiting; the accessibility of accelerometer data measuring the environment; and the impact of other operations which might occur during the experiment runs. These various topics are discussed in the remaining sections of this paper.

## MICROGRAVITY CARRIERS

There are several carriers commonly used by researchers for microgravity experiments. If we consider a microgravity environment, in general, to be an environment in which the effects of gravity are reduced compared to what we experience on Earth, then the different carriers provide a range of microgravity environments. Pertinent attributes of common microgravity carriers are listed in Table 1. Selecting a carrier with an appropriate microgravity environment is a good early step in the planning of an experiment.

**Table 1.** Typical microgravity environments on selected carriers.

| Carrier                                    | Duration of Microgravity               | Acceleration Levels                      | Notes   |
|--|--|--|---|
| Drop Facilities                            | <10 sec.                               | $10^{-3}$ g                              | longest available time at Japanese tower  |
| NASA KC-135                                | 15-25 sec.                             | $1.5 \times 10^{-2}$ g                   | approximately 40 parabolas per flight   |
| Sounding Rockets                           | several minutes                        | $10^{-5}$ g                              | based on information from various rocket flights  |
| STS SPACEHAB Module                        | typical flight: 9 days                 | $<5.5 \times 10^{-4}$ g<br>combined axes | 99.73% of data for frequency range 0.01 to 25 Hz; SH-2  |
| STS Spacelab MPESS                         | typical microgravity allotment: 9 days | $<1.4 \times 10^{-3}$ g<br>combined axes | 99.73% of data for frequency range 0.01 to 25 Hz; USMP-2, USMP-3  |
| STS Spacelab Module                        | typical microgravity flight: 15 days   | $<3 \times 10^{-3}$ g<br>combined axes   | 99.73% of data for frequency range 0.01 to 25 Hz; LMS, MSL-1, IML-2   |
| STS Keel Bridge (quasi-steady environment) | typical microgravity flight: 15 days   | $<1 \times 10^{-6}$ g<br>combined axes   | average values for typical microgravity Orbiter attitudes; Spacelab module or MPESS carriers in Payload Bay |

## **EXPERIMENT AND CARRIER CONFIGURATION**

Once an appropriate carrier is selected for an experiment, the sensitivity of the experiment to the microgravity environment may dictate a particular placement of the apparatus within the carrier and the orientation the experiment will have with respect to the motion of the carrier. Experiments sensitive to variations in the quasi-steady environment may benefit from a location close to the vehicle center of gravity. Such experiments may also be oriented such that certain features of the quasi-steady environment are aligned with specific experiment axes. In addition, the flight orientation of the vehicle should also be considered. For some vehicles, such as the NASA Orbiters, vehicle orientation can be tightly controlled while in flight and can also be specified by the experimenter. Unfortunately, other experimenters and payload constraints may require specific attitudes that are in conflict with those required by a particular experiment.

An example of experiment-specific attitude requests is the Geophysical Fluid Flow Cell experiment on the second United States Microgravity Laboratory mission. On this mission (STS-73, November 1996), the Geophysical Fluid Flow Cell experiment required an attitude during operations that allowed the principal axis of the facility (which was co-aligned with the Orbiter Z-axis) to be nearly perpendicular to the orbit plane, while also minimizing disruptions of the microgravity environment.

Experiment location may also be important to experiments sensitive to certain types of vibrations. Many pieces of equipment that control vehicle and experiment operations contain fans, pumps, and other mechanical devices that can excite local structure. An example of this is the water pump that is part of the TEMPUS electromagnetic containerless processing facility used in the Spacelab on the NASA Orbiters. On the second flight of the International Microgravity Laboratory mission (STS-65, May 1994), the water pump operated at a frequency of 80.3 Hz with resulting vibrations transmitted to neighboring racks in the Spacelab module. Modifications to the apparatus for the first Microgravity Science Laboratory mission (STS-83, April 1997 and STS-94, July 1997) lowered the operating frequency to 42-43 Hz. Similar phenomena have been identified across the frequency range from 1 Hz to 100 Hz, for activities and operations as varied as crew exercise, experiment disk drive rotation, vehicle life-support systems, biological sample refrigerator/freezer compressors, and experiment cooling fans. Different accelerations transfer differently across the structure of microgravity carriers and vehicles. Testing of the microgravity environment to identify

the presence of such vibration sources prior to experiment location should be attempted for experiments with known sensitivities to particular vibration frequencies.

## **EXPERIMENT TIMELINING**

An important aspect of the issues introduced in the previous section is that experiment, crew, and vehicle operations are not always continuous in nature. For this reason, careful scheduling of operations may avoid conflicts among requested vehicle attitudes, and may obviate the locating of experiments away from others that may cause disruptive vibrations. Several examples of such scheduling have occurred on NASA Orbiter microgravity missions. During the fourth United States Microgravity Payload mission (STS-87, November 1997), pre-mission discussions among several experiments resulted in an Orbiter attitude plan for the mission. Real-time activities during the mission necessitated the replanning of the attitude schedule several times during the mission. Knowledge of experiment sensitivity, which was slightly modified during the mission based on preliminary results, allowed the experimenters to negotiate new attitudes with more confidence.

On the first flight of the first Microgravity Science Laboratory mission (STS-83, April 1997), TEMPUS experimenters became aware that vibrations caused by crew ergometer exercise were potentially disruptive to their experiments. Careful monitoring of real-time acceleration data and of the mission schedule during the second flight (STS-94, July 1997) allowed them to plan their most sensitive operations around the exercise times. On the second flight of this mission, investigators on the combustion experiment Structure of Flameballs at Low Lewis-numbers realized that the experiment was sensitive to Orbiter thruster firings. After noting the sensitivity, investigators requested that their remaining experiments be conducted with the Orbiter in a free drift mode during which there are no thruster firings.

## **ACCELEROMETER SELECTION**

Investigators with experiments sensitive to any aspect of the microgravity environment should consider requesting that an appropriate accelerometer sensor be located on their experiment apparatus. The sensitivity of the experiment should dictate the appropriate accelerometer. In particular, for vibration sensitivity, the lowpass cutoff frequency of the accelerometer sensor should be above the highest frequency to which the experiment is sensitive. For most space accelerometer systems currently in use, the sampling and filter characteristics are usually determined by the accelerometer team based on the cutoff frequency specified by the experimenter.

Accelerometer sensor location is also an important issue. To most accurately represent the microgravity environment experienced by an experiment, the accelerometer sensor should be as close as possible to the sensitive part of the experiment. The means of mounting the sensor to carrier structure should be similar in nature to the experiment mounting. Transmission of accelerations varies with structure. Sensor axis alignment with experiment axes of interest is also desirable.

## **VIBRATION ISOLATION PLATFORMS**

Once an experiment has been manifested on a particular microgravity carrier, the issues discussed in the previous sections should be considered. If the combined tactics of experiment placement, vehicle flight orientation, and experiment timelining cannot be coordinated in such a way to provide a desirable microgravity environment for the experiment, then vibration isolation platforms should be considered. Several such platforms exist for the NASA Orbiters and Mir Space Station and others are being developed for use on the International Space Station and for other uses. Presentations about some of these isolation platforms were given at the seventeenth Microgravity Measurements Group meeting. These papers should be referred to for more information.

## **SUMMARY**

Prior to performing science experiments in a microgravity environment, scientists must understand and appreciate a variety of issues related to that environment. The microgravity conditions required for optimum performance of the experiment will help define an appropriate carrier. Once an appropriate carrier is selected, experiment sensitivity to vibrations and quasi-steady accelerations should dictate the location and orientation of the experiment apparatus; the flight orientation of the carrier; and the scheduling of experiment operations in conjunction with other activities. If acceptable microgravity conditions are not expected from available carriers or experiment scheduling cannot avoid disruptive activities, then a vibration isolation system should be considered. In order to best interpret the experimental results and aid in assessing needed modifications to experiment operations, appropriate accelerometer data must be collected contemporaneously with the experimental data for real-time or off-line correlation.

## ACKNOWLEDGEMENTS

This paper was developed based on a presentation made at the first Microgravity Environment Interpretation Tutorial sponsored by the NASA Lewis Research Center Acceleration Measurement Program (September 1997). The suggestions proposed herein are based on the experiences of numerous microgravity principal investigators, operations timeline engineers, and acceleration data analysts from The University of Alabama in Huntsville, the now defunct Acceleration Characterization and Analysis Project at the Marshall Space Flight Center, and the Principal Investigator Microgravity Services project at the Lewis Research Center. The author would particularly like to acknowledge conversations over the years with J. Iwan D. Alexander, Charles Baugher, Walt Roark, Bob Galletly, Brian Matisak, Richard DeLombard, Kenneth Hrovat, Milton Moskowitz, and Kevin McPherson.

**Session F**  
**MICROGRAVITY MEASUREMENT OPERATIONS**  
**DURING ISS ERA**

---

Chair: Thomas J. Sutliff, NASA Lewis Research Center, Cleveland, Ohio

Paper Number: 26

# **g-LIMIT: A Vibration Isolation System for the Microgravity Science Glovebox**

---

Dr. Mark S. Whorton, NASA Marshall Space Flight Center, Huntsville, Alabama

# **g-LIMIT: A Vibration Isolation System for the Microgravity Science Glovebox**

Author:

Mark S. Whorton, NASA Marshall Space Flight Center, Huntsville, Alabama

## **Abstract**

For many microgravity science experiments using the Microgravity Science Glovebox (MSG), the ambient acceleration environment will be exceed desirable levels. To provide a more quiescent acceleration environment, a vibration isolation system named g-LIMIT (GLovebox Integrated Microgravity Isolation Technology) is being designed. g-LIMIT is the next generation of technology developed for and demonstrated by STABLE on the USML-2 mission in October 1995. Although g-LIMIT is a sub-rack level isolation system that can be used in a variety of applications, g-LIMIT is uniquely optimized for MSG implementation. Standard MSG structural and umbilical interfaces will be used so that the isolation mount is transparent to the user with no additional accommodation requirements. g-LIMIT consists of three integrated isolator modules, each of which is comprised of a dual axis actuator, two axes of acceleration sensing, two axes of position sensing, control electronics, and data transmission capabilities in a minimum-volume package. In addition, this system provides the unique capability for measuring absolute acceleration of the experiment independent of accelerometers as a by-product of the control system and will have the capability of generating pristine accelerations to enhance experiment operations. g-LIMIT is scheduled for flight during the UF-2 mission and will be available to glovebox investigators immediately after characterization testing.

## **Introduction**

As a research facility, the Space Station Microgravity Science Glovebox will be used for numerous investigations such as protein crystal growth, combustion, and fluid mechanics experiments which require a quiescent acceleration environment. Many of these experiments are especially sensitive to accelerations in the frequency range below 1 Hz which cannot be passively attenuated. Numerous disturbance sources such as crew activity, fans, pumps, and

motors will introduce accelerations significantly larger than acceptable, requiring active vibration isolation to attenuate these disturbances.

The basic objective of a vibration isolation system is to attenuate the accelerations transmitted to an experiment from umbilicals, crew motion, and payload-generated sources. The required attenuation can be derived from the anticipated disturbance environment and required acceleration levels. To provide the desired environment requires that the isolation system pass through the quasi-steady accelerations while providing attenuation above 0.01 Hz. At frequencies above 10 Hz, the required attenuation level is -60 dB, or 3 orders of magnitude of attenuation.

Due to the need to provide data, power, vacuum, and fluid resources to the payload, the isolated experiment is physically connected to the base (MSG) by an umbilical which tends to be too stiff to provide sufficient passive attenuation. From a structural dynamics perspective, the attenuation requirement may be interpreted as requiring a soft spring connection between the base and the isolated experiment. The isolation system must also reject forces transmitted directly to the experiment (such as pumps, fans, motors associated with the experiment to be isolated). To accomplish this effective softening of the umbilicals while rejecting direct disturbances requires an active isolation system. By sensing relative position the isolated experiment can follow the very low frequency motion of the base while attenuating the base motion above 0.01 Hz. High bandwidth acceleration feedback increases the effective mass of the payload thereby attenuating the direct disturbance response. Demonstration of this level of performance cannot be accomplished on the ground due to gravitational coupling, but requires testing in a microgravity environment. Long periods of experimentation are necessary to characterize the low-frequency behavior, which is the critical frequency range for vibration isolation.

Although the space station program has baselined the Active Rack Isolation System (ARIS) for isolation at the rack level, ARIS is not well-suited for MSG and is not designed to attenuate forces directly applied to a rack, as will be the case with MSG. The Suppression of Transient Accelerations by Levitation Evaluation (STABLE) and the Microgravity Isolation Mount (MIM) are sub-rack level isolation systems, but neither is optimized for the glovebox (in fact, MIM requires too much volume for practical glovebox use). Although no current isolation system is well-suited for use in the glovebox, the g-LIMIT system will be uniquely designed to accommodate glovebox investigations. The MSG vibration isolation uniquely fills a niche in the MSG and significantly enhances the capabilities of the MSG for performing microgravity science.

## Design Concept

In order to provide an isolated environment to an experiment, an isolation system must sense and cancel the inertial accelerations applied to the experiment. With g-LIMIT, this is accomplished by six independent control actuation channels that provide six independent forces to a platform upon which the experiment resides. g-LIMIT consists of three integrated isolator modules each of which is comprised of a dual axis actuator, two axes of acceleration sensing, two axes of position sensing, control electronics, and data transmission capabilities. The two axes of control in each module are uncoupled by using co-located acceleration and position feedback to each axis of control actuation. A high-frequency control loop is implemented to cancel the inertial accelerations and a low frequency position loop is used to center the platform in the sway space and cause the experiment to follow the quasi-steady motion of the vehicle. The capability for centralized control laws will be implemented as well. During flight investigation, various control designs will be tested including classical, robust, and adaptive control theory. A novel feature of g-LIMIT is the patent-pending implicit position sensing technology which uses a drive coil to induce a signal on the actuation coil to sense motion much like a standard encoder. A dynamics characterization payload will be implemented to characterize the direct disturbance rejection and robustness capabilities of the various control designs. The g-LIMIT system is shown below in Figure 1.

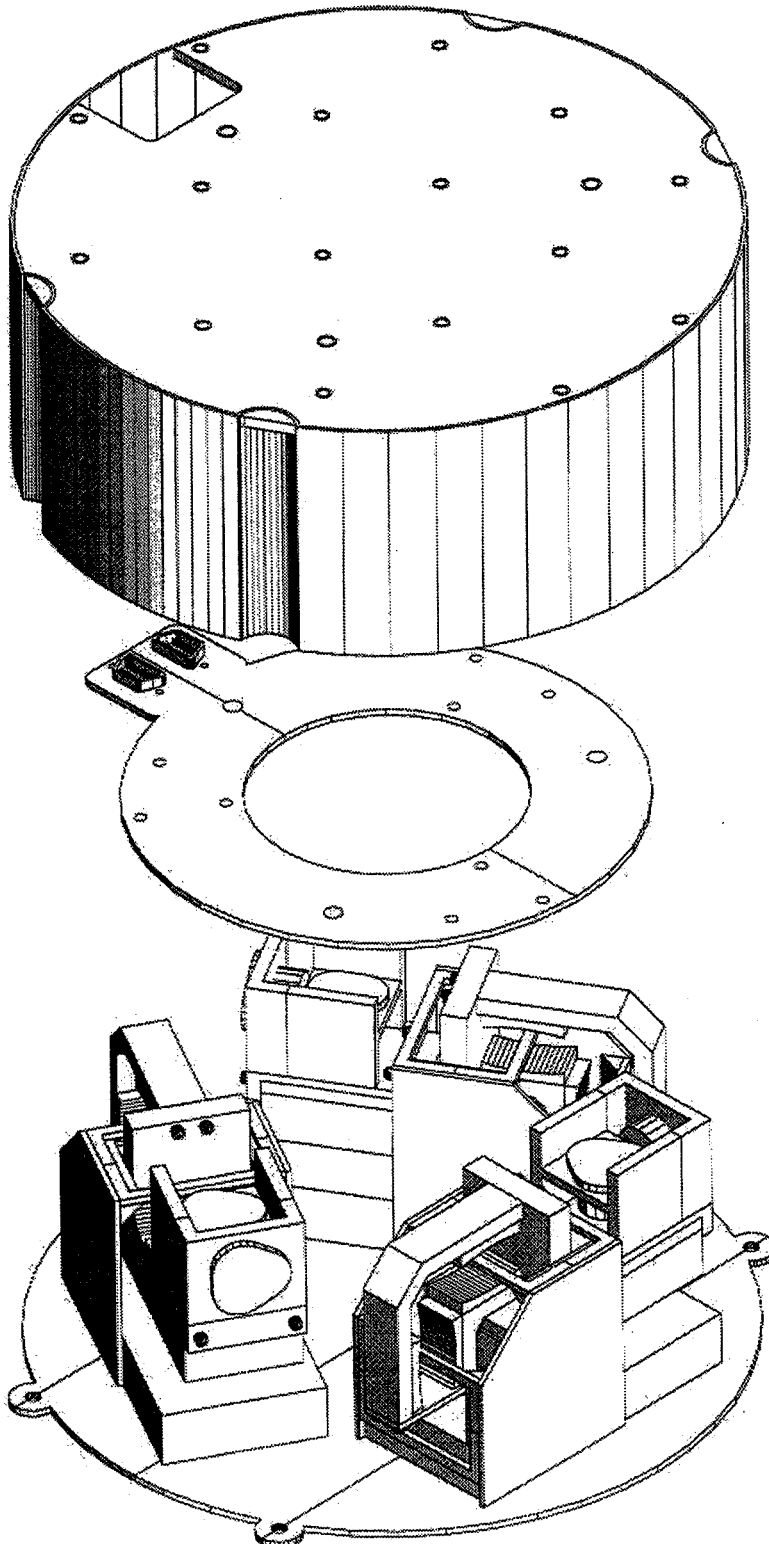
A key aspect of the g-LIMIT design is modularity. Incorporation of two axes of actuation, sensing (position and acceleration), and electronics into an integrated unit (the "Isolator Module", or IM) results in a general-purpose system design. The IM forms the basis of g-LIMIT and also provides the capability for an off-the-shelf kit for other isolation applications such as lockers, drawers, and other small volumes. Use of a co-located control law results in configuration independent software and negligible interfaces. Vibration isolation of larger masses is easily accomplished with g-LIMIT (or the IM kits) as well.

By designing for modularity and optimizing for MSG application, g-LIMIT makes efficient use of the volume inside MSG. To minimize power requirements, a three-axis translation stage will be used to displace the umbilicals such that the null point coincides with the center of the sway space. This will remove the DC component of the force applied by the actuators and hence considerably reduce power consumption. The Umbilical Bias Stage also reduces the peak power requirements of the IM so that the actuator size is minimized.

The g-LIMIT system will not only provide a quiescent environment for MSG investigations, but it will also have the capability to generate pristine accelerations as desired by

certain classes of experiments such as protein crystal growth. In this mode, a user-prescribed acceleration environment (time response or frequency spectrum) will be applied to the experiment while providing isolation from the ambient MSG acceleration environment. An additional capability will be the accelerometer-independent measurement of quasi-steady accelerations as a by-product of the isolation control system.

In order to make the isolation system transparent to the user with respect to interfaces, the structural, electrical, and data interfaces to g-LIMIT will be identical to the MSG. The glovebox provides a standard set of resources including power, data, video, heat dissipation, nitrogen, and vacuum. g-LIMIT will provide the experiments mounted to its isolated platform a subset of the glovebox standard resources consisting of power (+/-12V, +28V, +5V), 8-bits digital input & output, 8 channels analog input, RS422, and video. When operational, g-LIMIT needs approximately 60W peak and about 25W power nominally. This power will be derived from either the 28V or the 120V glovebox power supply, with the remaining power available to the experiment. Also, the internal glovebox MIL1553 connection will be available to the experiment as a shared resource with the g-LIMIT system.



S24-29

Paper Number: 27

## Acceleration Measurements in JEM

---

Toshitami Ikeda, National Space Development Agency of Japan(NASDA), Ibaraki, Japan

Keiji Murakami, National Space Development Agency of Japan(NASDA), Ibaraki, Japan

## **Acceleration Measurements in JEM**

Authors:

Toshitami Ikeda and Keiji Murakami  
NASDA Space Experiment Department, Sengen 2-1-1  
Tsukuba-city, Ibaraki, 305-8505, Japan

### **ABSTRACT**

National Space Development Agency of Japan (NASDA) started the study of microgravity acceleration measurement systems in Japanese Experiment Module (JEM) from summer in 1996. And now the specification determination study is being carried out by some hardware developers. It will be finished by the end of March 1998.

First of all, the development status of Japanese payloads are briefly presented. Second, the development schedule and status of acceleration measurement system in JEM are described. Next, we show the plans for acceleration measurements in Pressurized Module (PM) and on Exposed Facility (EF). Finally, we present a topic about international collaborations on acceleration measurement in JEM-PM.

### **Development Status of Japanese Payloads**

NASDA is now developing 9 equipment for JEM-PM and 4 equipment for JEM-EF. We plan to install 5 International Standard Payload Racks (ISPRs) in JEM-PM.

- (1) ISPR#1: Gradient Heating Furnace (GHF)
- (2) ISPR#2: Cell Biology Experiment Facility (CBEF)  
Clean Bench (CB)
- (3) ISPR#3: Advanced Furnace for Microgravity Experiment with X-ray Radiography (AFEX)
- (4) ISPR#4: Fluid Physics Experiment Facility (FPEF)  
Solution/Protein Crystal Growth Facility (SPCF)  
Image Processing Unit (IPU)
- (5) Others: Electrostatic Levitation Furnace (ELF)  
Isothermal Furnace (ITF)

We plan to launch 3 ISPRs (#1, #2 and #4) on flight 1J/A in May 2001. The Proto-Flight Models of GHF, CBEF and CB are now being manufactured. Equipment loaded into the ISPR#4 are now Engineering Model (EM) manufacturing phases.

On the other hand, statuses of EF payloads are now phase B design.

- (1) Space Environment Data Acquisition Equipment (SEDA)
- (2) Monitor of All-Sky X-ray Image (MAXI)
- (3) Laser Communication Demonstration Experiment (LCDE)
- (4) Superconducting Sub-Millimeter Wave Limb Emission Sounder (SMILES)

### **Development Schedule and Status of Acceleration Measurement System**

NASDA started the concept study of acceleration measurement system in JEM-PM from summer in 1996. The specification determination study is now being carried out by some hardware developers. It will be finished by the end of March in 1998. We will start to measure microgravity accelerations after flight UF-3.

### **Acceleration Measurement in JEM-PM**

There are some preconditions of specification determination study.

- (a) Acceleration should be measured for the five equipment (GHF, CBEF, AFEX, FPEF and SPCF) and it is desirable that measurement points are near the experiment samples.
- (b) Acceleration should be measured simultaneously at more than 3 points (x 3) any time.
- (c) Acceleration data should be transferred to the ground in 24 hours (TBD) since they are measured.
- (d) Downlink data should include time tag.
- (e) It is desirable that the system operates automatically and needs no logistics.
- (f) It is desirable that the life time of the system is more than 3 years.
- (g) It is desirable that the system can be replaced on orbit.
- (h) It is possible that the system uses the Payload Lap Top computer (PLT) as a downlink controller.
- (i) Existing technology would be employed for development so that the development cost can be kept as low as possible. Under this condition, the highest performance should be required.

We are now just under consideration. Therefore, typical configurations of acceleration measurement system which was studied so far will be described next.

- (1) There are two types of system configuration. One is independent type -each set of

### *Acceleration Measurements in JEM*

sensors (3 axes) and amplifier has own controller. And the other is concentration type -some sets of sensors (3 axes) and amplifier are connected to one controller.

- (2) Ethernet lines are used for data downlink.
- (3) Measurement range is from 0.01 Hz to several hundred Hz.

### **Acceleration Measurement in JEM-EF**

NASDA has an acceleration measurement system also on JEM-EF. Space Environment Data Acquisition Equipment (SEDA) which can measure accelerations of JEM-EF is being developed and will be launched on flight 2 J/A in February 2002.

### **International Collaboration**

There are many ways of international collaboration. For example, we can provide on-orbit places and Japanese Communication line. Then we operate it from Japan. And measurement data are owned jointly.

Anyway, international collaborations are always welcome to us.

Paper Number: 28

## **Status of ESA Taskforce on Microgravity Levels on the International Space Station**

---

Dr. Paul Clancy, ESA/ESTEC, Noordwijk, The Netherlands

## **Status of ESA Taskforce on Microgravity Levels On the International Space Station**

Author:

Paul Clancy, ESA/ESTEC, Noordwijk, The Netherlands

### **Columbus Orbital Facility**

The Columbus Orbital Facility COF is the European contribution to the pressurized volume on the International Space Station.

The COF is a cylindrical module with an overall length of 6.7 metres and a diameter of 4,5 metres. The module will be permanently attached to the International Space Station, from which it will receive power and other resources. An environmental control and life-support system in the COF provides a so-called 'Shirt-sleeve Earth-like atmospheric environment' for the crew.

The ceiling and the side walls of the module accommodate payload and storage racks. There are ten locations for payload racks, five of which are permanently allocated to ESA. The floor is used for the accommodation of subsystems and, in addition, contains one storage rack. Further subsystem equipment is located in the end cones.

According to current plans, the COF will be launched to the Station in November 2002 by the Space Shuttle, together with the fully integrated initial European scientific payload. After arrival at the Station, the COF will be attached to Node 2 of the Station.

To utilise the accommodation resources available to ESA in the COF the following facilities are under development by ESA:

- The Biolab, to be launched in the COF
- The Fluid Science Laboratory (FSL), to be launched in the COF
- The European Physiology Modules (EPMs), to be launched in the COF
- The Material Science Laboratory (MSL), which will be composed of two facilities, one to be accommodated in the US Laboratory and one in the COF.

Due to the type of science to be performed the Fluid Science Lab (FSL) and the Material Science Laboratory (MSL) are likely to be sensitive to the microgravity environment. As a result of the decision by NASA to develop an active Rack Isolation System (ARIS) to counter the predicted poor microgravity levels ESA instituted a Task Force in 1997 to advise the agency on what approach ESA should take vis a vis FSL and MSL in the COF. The Task Force consisted of leading microgravity scientists in Europe, microgravity experiments modelling experts and expert agency staff. The group made a number of recommendations as follows.

## **Recommendations dealing with the Microgravity Platform Environment**

- The Agency is encouraged to develop, possibly in coordination with NASA, a scheme for carrying out accurate acceleration measurements in the low frequency domain below 0.1 Hz.
- The Agency is recommended to pursue the course of permanent microgravity measurement within the COF. This measurement course has to be supplemented by mathematical tools for data analysis and for extrapolating acceleration data from the points of measurement to the experiment locations of interest.
- The Agency should undertake a full operational assessment of crew activities and operations to assess impacts of these non-instrument disturbances .
- A comprehensive study/evaluation of the present design concept of the ESA facilities Biolab, European Physiology Modules (EPM) and Modular Cultivation System (MCS) be carried out to identify sources of disturbances in these facilities and which act as threat to adjacent facilities. Technical means to passively isolate and dampen these disturbances at source should be identified and implemented. They should also be located as far as possible from the sensitive facilities listed above.

## **Recommendations dealing with G-Jitters Sensitivity Studies**

- The Agency should consider an experiment programme using fluid cell, tracer particles and temperature measurements to validate the results of the numerical modeling.
- The Agency is recommended to promote a coordination between different groups devoted to acceleration measurements, experimental results and development of numerical models to correlate g-jitter measurement with g-jitter effects.

## **Recommendations dealing with countermeasures to mitigate g-jitter effects**

- A comprehensive study/evaluation of present design concepts of the ESA facilities Fluid Science Lab (FSL), Materials Science Lab (MSL) and Protein Crystallisation Diagnostics Facility (PCDF) should be carried out to identify sources of disturbances in these facilities acting as threat to the proper functioning of the facilities themselves. Technical means to passively isolate and dampen these disturbances at source should be identified.
- The Agency is recommended to systematically investigate the question of the optimum orientation of facilities or test cells with respect to the residual g and g-jitter with a view to minimizing their effects.
- The Agency is recommended to plan the location of the most sensitive facilities i.e. FSL, MSL and the EDR (when carrying protein crystal growth or other sensitive experiments) at

locations within the COF with minimized residual g and at maximum distance from other COF experimental facilities or system racks which induce significant disturbances.

- The Agency is strongly recommended to pursue the development of the passive isolation methods already started in the TRP activities and to investigate how these can be used to isolate sources of disturbances in COF facilities and system racks.
- The Agency is recommended to actively investigate use of active isolation systems capable of offering protection at the experiment cell level, such as the Canadian MIM to be incorporable in the European Drawer Rack and possibly the Fluid Science Lab. The Agency is not recommended to pursue the development of a rack level system such as ARIS.

### **Recommendations dealing with ISS partners coordination**

- Strong coordination with NASA is recommended in regard to what facilities NASA intends to locate in its 49% location allocation in the COF. (If possible a coordination with NASA is recommended for an overall "Functional Allocation" approach for ISS in general where all sensitive facilities are located at the optimum g-level locations far from disturbing facilities.)

The Agency is recommended to pursue a strong policy of coordination with the other partners in particular NASA, NASDA and CSA for a programme of sensitivity prediction, acceleration measurements and mitigation procedures. (Particular emphasis was placed on the advantages of optimised orientation of the facilities or test cells with respect to the residual g vector (s).)

### **Microgravity measurement strategies**

Concerning measurement strategies ESA plans an approach as shown in the following points.

- Fluid Science Lab (FSL) and Materials Science Lab (MSL) will incorporate their own microaccelerometer packages.
- The low frequency (down to  $10^{-8}$  g) Onera system could be adapted to a drawer of the European Drawer Rack (EDR).

In summary and conclusion therefore the ESA approach to the microgravity environment in the COF consists of a multi-faceted approach of isolation at the source, use of passive damping, use of active damping at the experiment level and the use of optimised orientation and location of the sensitive facilities.

# **Procedures and Microgravity Measurements for Commercial Materials Development in Space**

---

Jan A. Bijvoet, CMDS, University of Alabama in Huntsville, Huntsville, Alabama

Philip D. Nerren, CMDS, University of Alabama in Huntsville, Huntsville, Alabama

# **Procedures and Microgravity Measurements for Commercial Materials Development in Space**

Authors:

Jan A. Bijvoet and Philip D. Nerren,  
Consortium for Materials Development in Space,  
The University of Alabama in Huntsville.

## **ABSTRACT**

In this communication we share our thoughts on commercial materials development in space needing repeatable microgravity conditions and desiring reproducible products.

We (re)emphasize the need for initial materials processing with supporting microgravity measurements at a "Reference", very low-g condition, followed by processing under conditions with controlled (set) disturbances and completion under strict and effective Microgravity Management Procedures.

We list some technical measures to reduce the cost of measuring the microgravity environment.

## **BACKGROUND**

The Consortium for Materials Development in Space (CMDS) is one of the NASA / Industry sponsored Commercial Space Centers (CSC) and is administered by the University of Alabama in Huntsville (UAH).

The CMDS pursues a low cost approach on Process Development and System Operations being essential for successful Space Commercialization.

In addition to the development and operation of several Materials Processing Facilities on several Space Shuttle missions and on several Sounding Rocket flights, the CMDS developed and flew the 3- Dimensional Microgravity Accelerometer (3-DMA), a high performance, low cost instrument, and an "Invertable Accelerometer" for adequate measurement of quasi-stationary accelerations at low cost.

Recently we reviewed the effectiveness of the overall process for commercial materials development in space and the success of the use of the measured microgravity environment.

## **DISCUSSION**

No commercially viable products should be expected if we do not have low development costs and low operations costs.

These costs are high because experiments or processes have to be repeated over and over again because of inconclusive results and if we do not achieve a reproducible product and do not insure repeatable microgravity conditions.

A good many of the experiments done so far in space have to be redone for the following reasons:

- Very few successful correlations between materials processing results and "THE" microgravity environment have been achieved;
- Several mechanisms and effects are unexplained as reported by several experimenters;
- Varying results were obtained in seemingly "similar" microgravity conditions;
- Repeatability of results has been limited.

The reason for this poor state of affairs seems to lay for a large part in:

- The lack of experimenting in different (very low-g and controlled), microgravity environments,
- The resulting lack of knowledge of the thresholds for the several microgravity environment components below which a desired effect occurs and
- The resulting reduced understanding of cause and effect.

Little understanding was found of the variety of microgravity components such as the quasi-stationary condition, the vector direction, microvibration frequencies and amplitudes, and transient amplitudes and duration.

Several papers only refer to the microgravity environment as being "in space", or "in microgravity" or even as "different than on the ground".

There are a few glaring exceptions to this such as the MEPHISTO experiment. The good correlations were however with high disturbances in the milli-g range, well standing out

above other disturbances.

What needs to be promoted?

The microgravity measurement activities are not to be blamed: Terabytes of adequate data are generated on the microgravity environment by several organizations and made available to PIs.

For successful commercial development of materials sensitive in say the 0.1 to 100 micro-g range; for reducing the number of futile experiment runs, for achieving conclusive experiments and for obtaining reproducible products we need the following three steps:

STEP 1) Processing in a near zero-g, "Reference" G- Situation (Prof.Monti); for instance on a Sounding Rocket (extremely low-g), SPARTAN, SPAS, EURECA, WSF, etc.

STEP 2) On the platforms of STEP 1, introduction of controlled (set) disturbances, using for instance MIM, platform rotation, etc.

STEP 3) Application of strict and effective Microgravity Management Procedures on STS and ISS.

In all phases knowledge of the microgravity environment by measurement and / or calculation is essential.

Secondary technical measures for cost saving as related to microgravity measurements are:

- No recording on board ISS, but transmission to the ground
- Direct transmission to the ground of the measured environment and via internet to the PI's laboratory for processing,
- Automatic recording using Hard Disk Drives on STS, etc., missions.
- Multiple simultaneous bandwidths for each accelerometer in each remote head.
- Calculation on the ground of the quasi-stationary components from orbital data instead of on board measurement.

## **CONCLUSION**

A three step approach should be followed for successful commercial development in space of materials sensitive in the say 0.1 to 100 micro-g range so as to eliminate inconclusive

*Microgravity Measurements Group Meeting #17*

experiment runs and to achieve reproducible products.

Needed is first processing and microgravity measurement at near-zero-g conditions, followed by processing under set disturbances and finally processing at the ISS with strict Microgravity Management Procedures in effect.

527-14

Paper Number: 30

## **KSC ISS Payload Processing and Facilities**

---

Kevin Zari, NASA Kennedy Space Center, Florida

# **KSC ISS Payload Processing and Facilities**

Author:

Kevin Zari, Payload Engineering Division, NASA, Kennedy Space Center, Florida

## **ABSTRACT**

KSC International Space Station (ISS) payload processing and facilities have changed significantly from what was utilized for many years to prepare Spacelab experiment payloads for the Shuttle.

Presented will be an overview of the processes and facilities to be used for preparing payloads to be launched on the Shuttle to the ISS.

## **INTRODUCTION**

Kennedy Space Center is a launch site for ISS Payloads. As the Spacelab program comes to an end, there have been some changes to KSC payload processing and facilities.

## **TYPES OF UTILIZATION PAYLOADS**

### **ISS Racks**

Rack-mounted payloads are transported to the ISS in the pressurized Multi-Purpose Logistics Module (MPLM). There are five types of racks that are currently planned to fly on ISS. These are facility class payload, EXPRESS flight, EXPRESS transportation, refrigerator/freezer, and resupply stowage racks.

One or more racks comprise a facility class payload. These racks come integrated to KSC. The payload interfaces are tested at KSC before the rack is installed in the MPLM. A facility class payload rack can stay on orbit between missions.

## *KSC ISS Payload Processing and Facilities*

EXPRESS flight racks are composed of 8 single Middeck Locker Equivalents (MLE) and 2 Standard Interface Rack (SIR) drawer equivalents. These racks are integrated and tested at KSC. EXPRESS flight racks can stay on orbit between missions.

EXPRESS transportation racks are composed of 4 MLEs and 10 SIR drawer equivalents. Payloads to fly on this type of rack are tested in the Functional Checkout Unit (FCU) and then installed and integrated into the rack. These racks are used to transport payloads to the EXPRESS racks already on orbit.

Refrigerator/Freezer (R/F) racks are the only type of ISS rack with active interfaces to the MPLM. Two types of R/F racks are the Minus Eighty Degree Laboratory Freezer for ISS (MELFI), and the LSE Transportation Preservation Assembly rack (Cryo Freezer –180 Degree Celsius).

Resupply stowage racks are used to transport stowage trays. These racks are processed by the KSC Resupply and Return Integrated Product Team (IPT).

### **Other Types of Utilization Payloads**

In addition to the rack-based payloads, there are other types of Utilization payloads.

Attached Payloads (truss-attached or EXPRESS pallet) are transported to ISS on an unpressurized structure and remain in an unpressurized environment once on orbit.

Middeck Experiments are transported to ISS in the Orbiter Middeck and receive continuous power within specification.

## **SPACE STATION PROCESSING FACILITY (SSPF)**

The SSPF was built specifically for the processing of ISS components and payloads. This 475,000 square foot building houses a high bay, intermediate bay, air locks, off-line labs, and operations support and control areas.

### **Off-line Labs**

The SSPF houses 19 off-line labs, where payload customers have access to various services. Some of these services include vacuum systems, GN2 and GHe, administrative and

data communication, and various power systems.

### **Experiment Rack Checkout at the SSPF**

Experiment rack checkout includes verification of power, command and data, high-rate telemetry, and fluids and gasses interfaces. These interfaces are tested by the Payload Test and Checkout System (PTCS). One system of PTCS is the United States International standard payload rack Checkout Unit (USICU), which is located in the Intermediate Bay of the SSPF. USICU is used to checkout the electrical and fluid connections of ISS racks and simulates the US Lab payload interface.

## **UTILIZATION KSC PROCESSING TEMPLATES**

For each type of ISS payload, there exists a template to show the flow of payload processing activities. The template for an ISS payloads generic rack shows customer-performed off-line lab processing, turnover of the payload to KSC for rack integration, rack test and checkout, and integration into the carrier.

## **CONTACT INFORMATION AT KSC**

### **Test and Checkout of Payloads:**

John Battcher – (407) 867-2142 email: John.Battcher-1@ksc.nasa.gov

### **ISS Payload Integration:**

Mark Matis – (407) 867-3204 email: Mark.Matis-1@ksc.nasa.gov

### **Schedule/Processing Templates:**

Joann Leotta – (407) 867-9067 email: Joann.Leotta-1@ksc.nasa.gov

### **Utilization IPT website:**

<http://www-ss.ksc.nasa.gov/utilization/>

S28-29

Paper Number: 31

# **The International Space Station Microgravity Acceleration Measurement System**

---

James C. Fox, Canopus Systems Inc., Ann Arbor, Michigan

# **The International Space Station Microgravity Acceleration Measurement System**

Author:

James C. Fox, Canopus Systems Inc., Ann Arbor, Michigan

## **ABSTRACT**

The Microgravity Acceleration Measurement System (MAMS) is a high resolution and wide dynamic range dual sensor-based accelerometry instrumentation system which is under development for an early Utilization Flight installation within the International Space Station's (ISS) U.S. Laboratory Module. The MAMS instrument will provide highly accurate acceleration measurement data over the nano-g to milli-g amplitude range characterizing the U.S. Lab Module environment in the frequency spectrum from 10<sup>-4</sup> Hz to 300 Hz. The data will be transmitted to ground users such as microgravity science investigators and the Microgravity Analysis and Integration Team members.

The MAMS quasi-steady acceleration measurement instrument, the Orbital Acceleration Measurement Experiment (OARE), and a vibratory microgravity disturbance measurement instrument, the High Resolution Accelerometer Package (HIRAP) were previously flown on the Space Shuttle and will be installed with additional interface and control units into a MAMS enclosure. The MAMS will interface to an EXPRESS Rack and provide acceleration measurement data via an Ethernet link to the Rack Interface Controller for subsequent downlink transmission

This paper addresses the MAMS performance specifications imposed and the new design solutions developed to meet the required performance. A description of the MAMS operational modes, calibration techniques and data/command interface is also included..

# THE MICROGRAVITY ACCELERATION MEASUREMENT SYSTEM

---

## SUMMARY

The Microgravity Acceleration Measurement System (MAMS) is a high resolution and wide dynamic range dual sensor-based accelerometry instrumentation system which is under development for an early Utilization Flight installation within the International Space Station's (ISS) U.S. Laboratory Module. The MAMS instrument will provide highly accurate acceleration measurement data over the nano-g to milli-g amplitude range characterizing the U.S. Lab Module environment in the frequency spectrum from  $10^{-4}$  Hz to 300 Hz. The data will be transmitted to ground users such as microgravity science investigators and the Microgravity Analysis and Integration Team members.

The MAMS quasi-steady acceleration measurement instrument, the Orbital Acceleration Measurement Experiment (OARE), and a vibratory microgravity disturbance measurement instrument, the High Resolution Accelerometer Package (HIRAP) were previously flown on the Space Shuttle and will be installed with additional interface and control units into a MAMS enclosure. The MAMS will interface to an EXPRESS Rack and provide acceleration measurement data via an Ethernet link to the Rack Interface Controller for subsequent downlink transmission

## REQUIREMENTS

The requirement for the ISS Vehicle to provide the microgravity environment (acceleration) measurement data to payload experimenters is documented in the ISSA System Specification<sup>1</sup> where it is specified that the Government Furnished Equipment (GFE) Orbital Acceleration Research Experiment (OARE)<sup>2</sup> and the GFE High Resolution Accelerometer Package (HIRAP)<sup>3</sup> are to be incorporated into one MAMS package for attachment to the exterior of a payload rack in the U.S. Lab Module. The

acceleration measurement data is required so that ISS Payloads will be able to correlate microgravity disturbances to experiment anomalies and to understand the unisolated environment in which some experiments will be operating. The MAMS data can also be used to identify unexpected disturbance sources and measure the results of corrective vehicle actions. Further, the measured acceleration data time series can also be utilized to characterize the vehicle structural dynamics response to forcing functions and thus provide an evaluation and verification of vehicle structural models and simulation codes.

The specific type of MAMS measurements required are documented in the USOS Specification<sup>4</sup> as consisting of both unisolated vibratory (high frequency) and quasi-steady (low frequency) accelerations at selected locations within the ISS pressurized modules. The data derived from MAMS can then be utilized to determine if the microgravity acceleration levels specified for the U.S. Lab Module as shown in Figure 1 are within the limits or if exceedances have occurred which may require corrective actions. In order to provide sufficient MAMS data amplitude and frequency resolution to correlate with the Figure 1 limits, the USOS Specification incorporates further detailed requirements on the MAMS instrument which are described in the MAMS specification<sup>5</sup> as follows:

1. The MAMS shall measure quasi-steady accelerations in three orthogonal OARE sensor input axes, and shall have an accuracy and resolution of 100 nano-g or better from  $10^{-4}$  Hz to 1.0 Hz.

and

2. The MAMS shall measure vibratory accelerations in three orthogonal HIRAP sensing input axes, and shall have an accuracy and resolution of 1/10th of the magnitude or one microgravity, whichever is greater, of Space Station system acceleration limits from 0.01 Hz to 300 Hz.

# THE MICROGRAVITY ACCELERATION MEASUREMENT SYSTEM

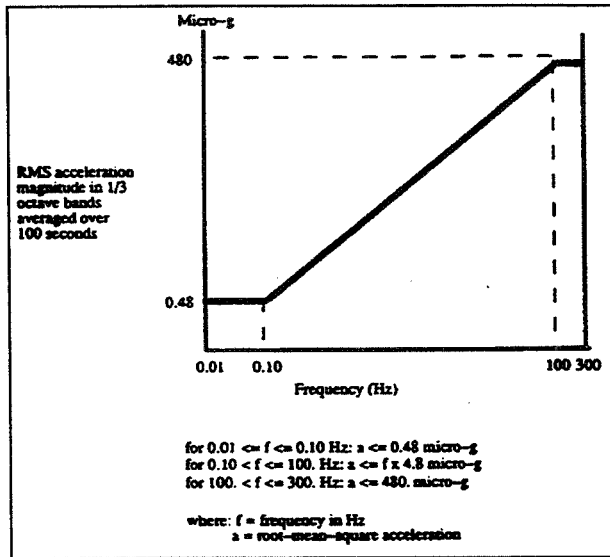


Figure 1. US Lab and US Hab vibro-acoustic microgravity acceleration limits

The balance of this paper is devoted to a system description and hardware/software implementation providing an on-orbit MAMS performance satisfying the difficult acceleration measurement ranges, resolution and accuracy specified above.

## PERFORMANCE OBJECTIVES

The quasi-steady acceleration measurement performance objective will be satisfied by utilizing a repackaged OARE Sensor Subsystem (OSS) containing a triaxial Miniature Electro-Static Accelerometer (MESA) which has performed successfully on eleven Space Shuttle missions through 1997. The OARE MESA has three sensor ranges (A, B, C) for each signal input axis which are controlled by auto-ranging software. The full scale range and sensor resolution for each input axis is shown in Table 1 as follows.

Table 1. OARE Sensor Ranges and Resolutions

| Range | Full Scale Range in Micro-g's |            |
|-------|-------------------------------|------------|
|       | X-Axis                        | Y & Z Axes |
| A     | 10,000                        | 25,000     |
| B     | 1,000                         | 1,970      |
| C     | 100                           | 150        |

| Range | Resolution in Nano-g's |            |
|-------|------------------------|------------|
|       | X-Axis                 | Y & Z Axes |
| A     | 305                    | 763        |
| B     | 30.5                   | 60         |
| C     | 3.05                   | 4.6        |

The MAMS vibratory acceleration measurement performance objective will be met by utilizing a repackaged HIRAP triaxial wideband accelerometer<sup>3, 7</sup> which has flown on numerous Shuttle missions as reported in the References. The triaxial, pendulous suspension, force feedback servo-controlled, gas damped sensors are the highly accurate Bell Aerospace Model XI type with a proven successful flight heritage. Each triaxial sensor has an achievable resolution of 1.0 micro-g and a laboratory test demonstrated bandwidth in excess of 300 Hz.

Based upon the performance objectives and sensor capabilities described above, the overall MAMS Data Performance Specification to be verified in system test and calibration operations is shown in Table 2 below.

Table 2. MAMS Calibrated Data Performance Parameters

| Quasi-Steady Data (OSS MESA)       | Parameters                                 |                                    |
|------------------------------------|--|------------------------------------|
| C Range Resolution                 | 3.05 nano-g X-axis, 4.6 nano-g Radial Axes |                                    |
| C Range Accuracy                   | $\pm 50 \text{ nano-g}$                    | $(\pm 5 \times 10^{-8} \text{ g})$ |
| C Range Full Scale                 | $\pm 100 \text{ micro-g}$                  | $(\pm 10^{-4} \text{ g})$          |
| B Range Full Scale                 | $\pm 1.0 \text{ milli-g}$                  | $(\pm 10^{-3} \text{ g})$          |
| A Range Full Scale                 | $\pm 10 \text{ milli-g}$                   | $(\pm 10^{-2} \text{ g})$          |
| Pre-Sample Filter Bandwidth        | $10^{-5}$ to 1.0 Hz                        |                                    |
| Maximum Data Rate                  | 1.0 Kbps                                   |                                    |
| Input Axis Alignment to Reference  | 20 arc minutes                             |                                    |
| IA Positioning Accuracy            | 5 arc minutes                              |                                    |
| Bias Temperature Coefficient       | 0.05 $\mu\text{g}/^\circ\text{C}$          |                                    |
| <b>Vibratory Data (HIRAP)</b>      |  |                                    |
| Resolution and Accuracy            | $\pm 1.0 \text{ micro-g}$                  | $(\pm 10^{-6} \text{ g})$          |
| Full Scale Dynamic Range           | $\pm 8 \text{ milli-g}$                    | $(\pm 8 \times 10^{-3} \text{ g})$ |
| Pre-Sample Filter Bandwidth        | $10^{-4}$ to 300 Hz                        |                                    |
| Maximum Data Rate                  | 104 Kbps                                   |                                    |
| Input Axis Alignment to Reference  | 10 arc minutes                             |                                    |
| Bias Temperature Coefficient (Max) | 10 $\mu\text{g}/^\circ\text{C}$            |                                    |

# THE MICROGRAVITY ACCELERATION MEASUREMENT SYSTEM

## SYSTEM DIAGRAM

A MAMS functional block diagram depicting the signal and command flow relationship between the six Line Replaceable Units (LRU's) is shown in Figure 2. Four of the LRU's are GFE and two LRU's are new development items, i.e. the Bias Calibration Table Assembly (BCTA) and MAMS Process Control Subsystem (MPCS) units were custom designed for the MAMS program to interface with and control the GFE LRU's.

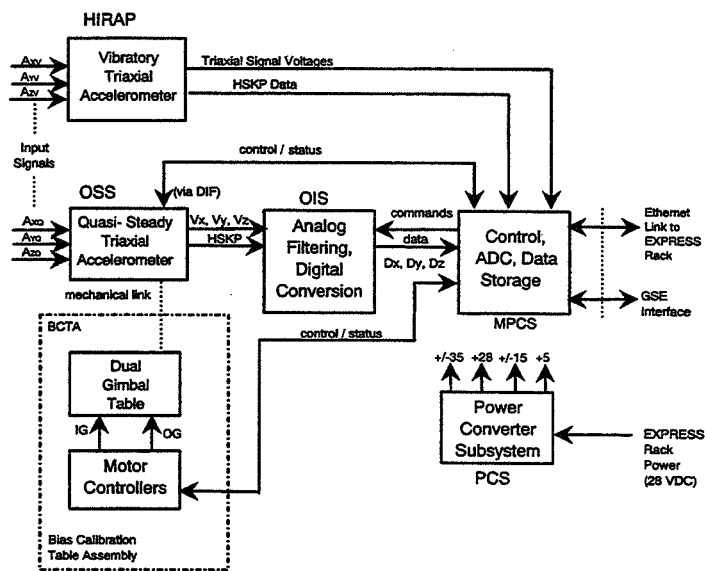


Figure 2. MAMS Functional Block Diagram

## FLIGHT SOFTWARE/OPERATIONS

The MAMS flight software controls the instrument and collects and transmits data (autonomous operation) to the EXPRESS Rack Interface Controller (RIC) which then relays the data to the ground. In

normal operation when MAMS power is turned on, the MAMS instrument will "boot-up" and establish communications with the RIC. Thereafter, MAMS will operate independently of ground

control by collecting and transmitting acceleration data from both the HiRAP and the OARE Sensor Subsystem (OSS) accelerometers. Ground controllers can modify the operation of MAMS in three ways: 1) through a limited number of commands issued from the ground, 2) through the uploading of adaptation parameters which further define the normal mode of operation, and 3) through the uploading of new operational software.

In MAMS Data Collection Mode, after it has "booted-up", performed internal checks of the MAMS memory, interfaces, the BCTA, and established communication with the RIC, MAMS flight software begins collecting the vibratory acceleration data from HiRAP accelerometer at a rate of 2048 samples per second for each axis and the quasi-steady acceleration data from the OSS accelerometer at a rate of 10 samples per second for each axis. In addition, ISS time, housekeeping time, temperatures and voltages are measured for each MAMS instrument and state indicators of sensor range, gimbal status, and OSS sub-mode are collected. Approximate data rates for these data types are shown in Table 3.

In order to provide the specified acceleration measurement accuracy during the MAMS mission, provision has been made to periodically perform a bias calibration of the OSS MESA sensor. In the Bias Calibration submode, the MAMS software controls a bias calibration sequence where each of the OSS input axes are rotated 180° using the Bias Calibration Table Assembly (BCTA). The acceleration signal output is measured at each of

Table 3. MAMS Data Generation Rates

| MAMS Data Types                            | Approximate Average Generation Rate (bits per second) |
|--|---|
| Status and Error Messages                  | 0.1 bps   |
| OSS Raw Acceleration Measurements          | 640 bps   |
| OSS Raw Bias Measurements                  | 13.3 bps  |
| OSS TM* Filtered Acceleration Measurements | 17 bps  |
| OSS TM Filtered Bias Measurements          | 0.4 bps   |
| MAMS Housekeeping/Health Data              | 0.4 bps   |
| HIRAP Raw Acceleration Measurements        | 104 kbps  |

\* Trim-Mean Average

# THE MICROGRAVITY ACCELERATION MEASUREMENT SYSTEM

---

these two orientations for each axis for a period of at least 50 seconds. The sum of these two output acceleration measurements is then a measure of the acceleration bias of that OSS axis at the range being calibrated. The accuracy of this bias measurement will be largely determined by the level of "noise" generated by other activity on the ISS during the time period of the bias calibration. However, with each additional measurement the error on the bias estimation is reduced by a statistical averaging process.

## MAMS GROUND OPERATIONS AND UTILIZATION

The Microgravity Acceleration Measurement System will operate on-board the International Space Station for ten years, providing quasi-steady and vibratory acceleration data to Space Station microgravity scientists, vehicle engineers, structural dynamicists, and other users for the purposes of understanding the microgravity environment and vehicle dynamics of the ISS. The MAMS will also provide atmospheric drag acceleration data to vehicle engineers to help determine ISS reboost activities.

The MAMS will be controlled from the Telescience Support Center (TSC) at the NASA Lewis Research Center (LeRC). Commands to MAMS, and acceleration and engineering data from the instrument, will be routed between the LeRC TSC and the ISS via the ISS ground network. Because of the long-term nature of MAMS operations, the current plan is for MAMS to operate autonomously, without the need for constant ground personnel interaction. However, specific, high-activity commanding and data acquisition periods will require ground personnel and support equipment.

The MAMS project office will be responsible for coordinating the planning of MAMS operations and requesting ISS, crew and ground resource allocations. On-board power, uplink and downlink bandwidth, and crew time will need to be scheduled to support MAMS data acquisition periods. Requests for MAMS data will be coordinated with the MAMS project office at NASA LeRC. It is anticipated that MAMS data

requests and distribution will be provided by an Internet-based service, much like the manner in which SAMS and OARE data from the Space Shuttle is currently provided by NASA LeRC. No unique software, other than a Web browser, will be required to request and receive MAMS acceleration data.

## REFERENCES

1. "System Specification for the ISSA", SSP 41000C, NASA Johnson Space Center
2. R. C. Blanchard, J. C. Fox et al, "The Orbital Acceleration Research Experiment", AIAA Paper 86-1195, AIAA 3rd Space System Technical Conference, San Diego, CA, June, 1986
3. R. C. Blanchard and J. F. Rutherford, "The Shuttle Orbiter HIRAP Experiment", AIAA Paper 84-0490, AIAA 22nd Aerospace Science Meeting, Reno, NV, January, 1984
4. "Segment Specification for the US On-Orbit Segment", SSP41162C, NASA Johnson Space Center
5. "Prime Item Development Specification for the Microgravity Acceleration Measurement System", SP401001, Canopus Systems, Inc, Ann Arbor, MI
6. J. E. Rice, "OARE STS-94 (MSL-1R) Final Report", CSI-9704, Canopus Systems, Inc., Ann Arbor, MI, August, 1997
7. Bonnie Dunbar, R. L. Giesecke et al, "The Microgravity Environment of the Space Shuttle Columbia Payload Bay During STS-32", NASA Technical Paper 3141, NASA Johnson Space Center, November, 1991
8. T. J. Sutliff, "An Acceleration Measurement Capability on ISS Supporting Microgravity Science Payloads", AIAA Paper No. 97-0349, AIAA 35th Aerospace Sciences Meeting, Reno, NV, January, 1997

JCF98027

529-66

Paper Number: 32

## **SAMS-II Requirements & Operations**

---

Lawrence W. Wald, NASA Lewis Research Center, Cleveland, Ohio

## **SAMS-II Requirements & Operations**

Author:

Lawrence W. Wald, NASA Lewis Research Center, Cleveland, Ohio

### **ABSTRACT**

The Space Acceleration Measurements System (SAMS) II is the primary instrument for the measurement, storage, and communication of the microgravity environment aboard the International Space Station (ISS). SAMS-II is being developed by the NASA Lewis Research Center Microgravity Science Division to primarily support the Office of Life and Microgravity Science and Applications (OLMSA) Microgravity Science and Applications Division (MSAD) payloads aboard the ISS.

The SAMS-II is currently in the test and verification phase at NASA LeRC, prior to its first hardware delivery scheduled for July 1998. This talk will provide an overview of the SAMS-II instrument, including the system requirements and topology, physical and electrical characteristics, and the Concept of Operations for SAMS-II aboard the ISS.

### **BACKGROUND**

Acceleration measurement of the microgravity environment has been a feature on Space Shuttle flights since the first flight of the SAMS on STS-40 in June 1991. The SAMS units have been on a total of 20 STS missions, with between 45 to 50 Gbytes of acceleration data collected. In addition to the STS missions SAMS was deployed to the MIR station where it is the longest running US payload on the MIR.

The success of the SAMS instruments led to the go ahead to develop a similar device for the International Space Station (ISS) to support the Office of Life and Microgravity Science and Applications (OLMSA) Microgravity Science and Applications Division (MSAD) payloads. The instrument developed for the ISS, dubbed SAMS-II, was to be significantly different than its predecessors for various reasons. For one, Payloads deployed to the ISS environment would operate in more of a laboratory environment, and over longer durations, compared to ISS science payloads. Another difference was in the operational role of the payload Principal investigator (PI). In the ISS era the PI will have more of a hands-on function with the daily operation and control of their microgravity measurement capabilities. Finally, the development of the SAMS-II for the ISS would utilize technical and operational lessons learned from the

SAMS experience on STS and MIR to attempt to reduce the development time and cost for SAMS-II.

## **REQUIREMENTS**

The Space Acceleration Measurement System-II (SAMS-II) will reside in the United States Laboratory Module (US Lab) of the International Space Station (ISS). The SAMS-II objectives are to provide acceleration measurement capabilities in support of microgravity science payloads in the areas of biotechnology, combustion, fluid physics, and materials science. SAMS-II will acquire acceleration data with a measurement capability better than the acceleration envelope of the ISS program. The acceleration data will be correlated with the on-orbit station time and both provided to the end user. The PI will have control over certain parameters such as gain, acceleration measurement frequency range, and acceleration sampling rate. The acceleration data provided to the end user (PI, facility, etc.) will be in a selectable format and provided in a timely manner.

The SAMS-II is an in-house development effort by the LeRC Microgravity Science Division (MSD). As originally envisioned the SAMS-II instrument is composed of two systems: the Control Unit (CU) and the Remote Triaxial Sensor (RTS). The CU accepts uplink commands, stores and processes acceleration data received from the RTS, and downlinks the processed data. The RTS in turn is composed of two subelements, the RTS Electronics Enclosure (RTS-EE) and the RTS Sensor Enclosure (RTS-SE). The RTS-EE communicates to the CU through the ISS payload ethernet network, accepting commands from the CU and sending data back to the CU. The RTS-SE is connected via cable to the RTS-EE and houses the three accelerometers, which are arranged in an orthogonal, triaxial arrangement. The RTS-SE is placed in close proximity to the on-orbit PI hardware to provide acceleration measurement capability. The acceleration data collected by the RTS-SE during the operations of microgravity science payload is sent to the ground through the RTS-EE, the CU, the ISS, and eventually provided to the payload PI.

## **STATUS**

SAMS-II held its Preliminary Design Review (PDR) in December 1995. Since that time the SAMS-II configuration has undergone several changes. The CU effort was halted due to a reduction in funding, with a planned re-start for FY99. RTS development continued; the engineering unit was built and tested and a successful RTS CDR completed.

In early CY97 the idea for an Interim Control Unit (ICU) was conceived to provide limited

support for science payloads from UF-1 to UF-5. The ICU would allow for some command and control of the RTS systems on the ISS from the ground. The planned ICU would be an ISS Personal Computer System (PCS) loaded with SAMS-II software to provide uplink, downlink, and commanding from the ground to the RTS system. The ICU would be operational from UF-1 to UF-5. In May 1997 the ICU was approved by MSAD management.

In FY98 the SAMS-II project will complete the fabrication and testing of the RTS-EE Qualification Unit. Successful qualification test results will allow the fabrication, testing and delivery of the first RTS-EE, scheduled for delivery to the EXPRESS Rack Project in July 1998, for deployment at UF-1. Additional flight EEs and the RTS-SE Qualification Unit will be built during the remainder of FY98.

The ICU effort has started and will hold a PDR in July 1998. The ICU will be delivered in July 1999 for a UF-1 launch. The Control Unit development will re-start at the beginning of FY99. The CU will be deployed at UF-5, taking the place of the ICU.

## **CONCLUSIONS**

The SAMS-II system will fulfill the requirements for microgravity measurement aboard the ISS. The primary customer for SAMS-II is the Microgravity Research Program, with their associated disciplines and PIs. SAMS-II has used lessons learned from the SAMS experience on the STS and the MIR to provide a significant enhancement in performance and capability for our ISS customers. The first planned delivery of flight hardware is an RTS-EE, in July 1998, to the EXPRESS Rack program for a UF-1 launch. Additional EEs, SEs, and the ICU are being built for future delivery to the EXPRESS program and other users.

Paper Number: 33

# **PI Microgravity Services Role for International Space Station Operations**

---

Richard DeLombard, NASA Lewis Research Center, Cleveland, Ohio

# **PI Microgravity Services Role for International Space Station Operations**

Author:

Richard DeLombard, NASA Lewis Research Center, Cleveland, Ohio

## **ABSTRACT**

During the ISS era, the NASA Lewis Research Center's Principal Investigator Microgravity Services (PIMS) project will provide to principal investigators (PIs) microgravity environment information and characterization of the accelerations to which their experiments were exposed during on orbit operations.

PIMS supports PIs by providing them with microgravity environment information for experiment vehicles, carriers, and locations within the vehicle. This is done to assist the PI with their effort to evaluate the effect of acceleration on their experiments.

Furthermore, PIMS responsibilities are to support the investigators in the area of acceleration data analysis and interpretation, and provide the microgravity science community with a microgravity environment characterization of selected experiment carriers and vehicles.

Also, PIMS provides expertise in the areas of microgravity experiment requirements, vibration isolation, and the implementation of requirements for different spacecraft to the microgravity community and other NASA programs.

## **INTRODUCTION**

The Microgravity Measurement & Analysis Project (MMAP) at the NASA Lewis Research Center supports the Microgravity Research Program and implements the work of the Acceleration Measurement Discipline. The primary support given by MMAP is to advise Principal Investigators (PIs) about the microgravity environment, provide acceleration measurement systems, conduct data analysis, characterize the microgravity environment, and provide PI support before, during, and after experiment operations. The MMAP is composed of five accelerometer

system projects and a PI services project (PI Microgravity Services). The accelerometer system projects are:

- a) Space Acceleration Measurement System (SAMS)
- b) Orbital Acceleration Research Experiment (OARE)
- c) SAMS for ISS (SAMS-II)
- d) SAMS for Free Flyers (SAMS-FF)
- e) Microgravity Acceleration Measurement System (MAMS)

The MMAP has also been delegated the task to maintain an overview of the predicted ISS microgravity environment from the science users' perspective and to maintain an overview of vibration isolation technology.

The PIMS project is responsible for providing the interface between the accelerometer system projects and the PIs in the Microgravity Research Program. This responsibility entails working with the experiment science team (including the PI(s) and project scientist) to establish requirements for acceleration measurement and for the subsequent data dissemination. This generates many areas of work for the PIMS project including a data and information repository, informing PIs and their teams about the microgravity environment, characterizing the microgravity acceleration environment, providing real-time analyses during some experiment operations, and providing post-mission services for data analyses.

## **PIMS SERVICES**

### **Acceleration knowledge base**

The SAMS instruments have flown on twenty Shuttle missions since 1991 and one SAMS instrument has been installed on Mir since September 1994. In addition, the OARE instrument has flown on ten Shuttle missions since 1991. A large base of data has been accumulated from these and other accelerometers in support of microgravity science experiments. For each Shuttle mission with a SAMS instrument, a report has been prepared to summarize the microgravity environment and to highlight features of this environment. For each increment of the Shuttle-Mir and NASA-Mir programs, a summary report was prepared to summarize the Mir microgravity environment.

PIMS utilizes this data base to prepare post-mission analyses in response to PI requests and to prepare overall characteristics of the vehicles' environment. These characteristics are reported

in conference papers, journal articles and reference publications by PIMS. Several such reference publications are:

- a) Compendium of Information for Interpreting the Microgravity Environment of the Orbiter Spacecraft,
- b) Comparison Tools for Assessing the Microgravity Environment of Missions, Carriers and Conditions,
- c) Microgravity Environment Description Handbook, and
- d) Accelerometer Data Analysis and Presentation Techniques.

The archives of acceleration data are also made available to users by means of internet file servers and CD-ROM disk sets. Access to the acceleration data allows a PI to better correlate effects on the science experiment with the acceleration environment.

## **CHARACTERIZATION OF ENVIRONMENT**

The understanding of the microgravity environment has developed over the years so that the many of the measured disturbances in the frequency range below about 200 Hz have been identified and characterized. The level of detail has improved by the critical examination of disturbances on each new set of acceleration data available for analysis. The display techniques have improved with refinement of old standard processes (e.g. power spectral density calculations) and with the development of new processes (e.g. principal component spectral analysis).

The speed of analysis has improved to shorten the response time to requests for information as well as to provide more real-time information along with the data displays. Faster and more powerful computers have helped in this area, but primarily, this has been due to the experience gained by the data analysts over time. The dissemination of data and information has improved with the utilization of the internet, CD-ROM disks, and electronic mail.

All of these efforts to characterize the environment are a major step to begin the characterization of the ISS microgravity environment. The learning curve for understanding the Shuttle microgravity environment is nearly over as demonstrated by the extensive analyses performed for well-informed PIs during the STS-87 mission with the USMP-4 payload. The learning curve to develop an understanding of the ISS microgravity environment should be considerably less than that experienced for the Shuttle. The tools for analyzing acceleration data

and for storing, handling and disseminating large amounts of data and are being adapted for ISS-era operations.

Another feature that will ease some of the analysis burden for the ISS microgravity environment is that the ISS will be assembled in stages. There will be time for the acceleration data for one stage to be analyzed and the environment characterized before the next stage of assembly begins. This will allow the characteristics of the equipment in each phase of assembly to be identified. This step by step analysis of the ISS environment should ease the burden of characterizing the environment.

A neural network and expert system are under development by PIMS to assist in the real-time analysis and classification of the acceleration data. The PIMS staff will be on console for ISS operations for a single shift under normal circumstances. A neural network and expert system will provide much of the analysis during PIMS off-shift hours.

The data processing for ISS operations may also be distributed to the PI operations centers for more PI control of the data displays.

## **PIMS OUTREACH IN ISS ERA**

### **Microgravity Environment Interpretation Tutorial**

PIMS will continue to provide an annual Microgravity Environment Interpretation Tutorial geared toward science teams to educate them on the microgravity environment. These tutorials will explain the components of the microgravity environment as well as the parameters involved in the measurement, display and interpretation of the microgravity environment. These tutorials will also begin to illustrate to PI teams the effects of the microgravity environment on science experiments.

### **Microgravity Measurement Group**

PIMS will continue to sponsor the Microgravity Measurement Group meetings on an annual or semi-annual basis. This series of meetings provides a forum for exchange of information about accelerometer systems, environment analysis results, and effects on science experiments. It also provides a forum for international coordination of environment characterization.

## DISSEMINATION OF DATA

### **Real-time data**

PIMS will continue to use expeditious means to disseminate the data to users. Real-time data products will continue to be delivered via the World Wide Web and internet file transfers. The various data products (e.g., data plots) will be tailored to the requirements of the PIs who have active experiments at the time. Standard displays will also be generated for the microgravity community and others who need a general look at the environment.

An expert system is under development for utilization during ISS microgravity operations. Such a system will aid in the categorization of disturbances to the microgravity environment and will provide a first level interpretation of the microgravity environment on a continuous basis.

A software tool will also be made available to PI teams for local processing of acceleration data at the PI teams' operation center. This method will allow PI teams to directly choose the parameters affecting the display of the acceleration data.

PIMS will continue to assess the quality of the acquired acceleration data available for microgravity science support. This will be primarily data available from the SAMS-II and the MAMS.

### **Off-line data**

A major part of PIMS operations in the past has been off-line support for PIs, either in preparation for a mission or in the post-mission analysis of data. Products have included mission summary reports to describe the mission's microgravity environment and the disturbances to the environment. PIMS will prepare similar summary reports for the ISS environment on a regular basis. Other products include short, informal reports addressing specific requests by PIs or PI team members or others in the microgravity community.

For the expected level of PI requests during ISS operations, an automated system for standard data calculations and displays will be implemented. This system will accept either an e-mail request or a WWW form and produce a product (e.g., a data plot) which would be delivered by e-mail or on the WWW.

## **SUMMARY**

The PIMS project will continue to perform a microgravity environment project scientist role for the PIs and PI teams during ISS operations. The support given to the PIs and their teams will continue the support established during Shuttle microgravity missions and will extend that support for the long duration of ISS operations. Modern methods will continue to be incorporated as appropriate to improve the products delivered to the microgravity science community.

## **BIBLIOGRAPHY**

- a) Compendium of Information for Interpreting the Microgravity Environment of the Orbiter Spacecraft (NASA TM-107032, 1996)
- b) Comparison Tools for Assessing the Microgravity Environment of Missions, Carriers and Conditions, (NASA TM-107446, 1997)
- c) Microgravity Environment Description Handbook, (NASA TM-107486, 1997)
- d) Accelerometer Data Analysis and Presentation Techniques, (NASA TM-113173, 1997)

# **PIMS Data Storage, Access, and Neural Network Processing**

---

Kevin M. McPherson, NASA Lewis Research Center, Cleveland, Ohio

Milton E. Moskowitz, Tal-Cut Company, North Olmsted, Ohio

# **PIMS Data Storage, Access, and Neural Network Processing**

Authors:

Kevin M. McPherson

NASA Lewis Research Center, Cleveland, OH 44135

Milton E. Moskowitz

Tal-Cut Company, North Olmsted, OH 44070

## **ABSTRACT**

The Principal Investigator Microgravity Services (PIMS) project at NASA's Lewis Research Center has supported microgravity science Principal Investigator's (PIs) by processing, analyzing, and storing the acceleration environment data recorded on the NASA Space Shuttles and the Russian Mir space station. The acceleration data recorded in support of the microgravity science investigated on these platforms has been generated in discrete blocks totaling approximately 48 gigabytes for the Orbiter missions and 50 gigabytes for the Mir increments. Based on the anticipated volume of acceleration data resulting from continuous or nearly continuous operations, the International Space Station (ISS) presents a unique set of challenges regarding the storage of and access to microgravity acceleration environment data. This paper presents potential microgravity environment data storage, access, and analysis concepts for the ISS era.

## **INTRODUCTION**

In order to support microgravity science Principal Investigators (PIs), the Principal Investigator Microgravity Services (PIMS) group was formed at the NASA Lewis Research Center in Cleveland, Ohio. PIMS primary function is PI support, achieved by the processing, analysis, storage, and distribution of acceleration data which has been recorded aboard the U.S. Space Shuttles, and the Russian Mir Space Station. PIMS' acceleration data analysis efforts are two-fold: general characterization of the microgravity environment, and the processing of data requests in direct support of microgravity science PIs. Both of these efforts generate unique requirements for data storage, access, and analysis.

The general characterization of the microgravity environment consists of identifying the sources and characteristics of disturbances on a given platform in an effort to maintain a

database of the acceleration environment and its observed characteristics. Toward that end, PIMS has developed a microgravity handbook [1] that presents an overview of known microgravity environment disturbances. Disturbances in the handbook are cross-referenced by carrier, source, acceleration magnitude and frequency. Mission summary reports are generated following each microgravity mission and contain an analysis of the recorded acceleration data. Any unique aspects of the analyzed data are subsequently added to the microgravity handbook in an effort to continually update the knowledge database. These cause and effect relations have been utilized for experiment planning, and may be used for experiment hardware design.

Microgravity PI support is accomplished by the processing, analysis, and correlation of acceleration data as both real-time and post-mission support. Whether real-time or post-mission, analysis of this type assists PIs in understanding the effects of the acceleration environment on their experiment. In addition to this analysis task, PIMS makes the acceleration data readily available to PIs who wish to have access.

The two-fold PIMS data analysis effort divides access to the acceleration data into two major categories: real-time and off-line. The real-time and off-line data processing approaches each generate unique requirements relative to providing PIs access to the analysis results. The current real-time implementation utilizes the World Wide Web (WWW) to allow experiment investigators easy access to a set of plots of the acceleration environment in near-real-time. The requirements for the plots are defined by PI inputs pre-mission. These plots are usually customized to meet the PIs requirements. Limits to the number of plots and the complexity of the plots are imposed, based upon the available computer processing power. Off-line data processing requests are handled individually. Since this type of processing need not be done in real-time, less restrictions are imposed, as computing power is less of an issue. PIMS has created a standard set of processing techniques and algorithms, but specialized requests are often performed. Distribution of these results are handled either electronically (i.e. via the WWW, an ftp server, etc.), or in hard-copy form (i.e. mail, FAX, etc.). Off-line data processing requests performed during a mission are handled by a modified off-line processing system. Post-mission, off-line access to engineering unit data is accomplished using an internet file server. No capability currently exists for providing access to real-time engineering unit data from Orbiter missions.

---

[1] DeLombard, Richard, Kevin McPherson, Kenneth Hrovat, Milton Moskowitz, Melissa J. B. Rogers, and Timothy Reckart. Microgravity Environment Description Handbook. Cleveland: NASA LeRC, July 1997. NASA TM 107486.

## DATA ACCESS

The real-time and off-line differences are also apparent with respect to the data storage format. The PIMS real-time systems strip the data from the telemetry stream, and save the data in a file format required by the real-time processing systems. The primary off-line data source has been processed by the Space Acceleration Measurement System (SAMS) group, and is saved into a different file format. Off-line data processed during a mission needs to be converted from the real-time format to a modified off-line format, via a conversion tool produced by PIMS. Clearly, the primary functions served by these divergent systems need to be merged into a single, more cohesive system for the ISS era.

PIMS will use a standardized data format for storage and archival of acceleration data. If adopted by other accelerometer systems, this format would allow any acceleration data to be used by any processing program (real-time and off-line), without the need for data converters. Ideas regarding this format include a universal file format, and a well-defined directory and file hierarchy. As an example, the current SAMS data reduction for Mir data separates the data based upon year and day, and has time-descriptive file names. The file format should be in the simplest form possible (i.e. without telemetry headers, or the need to process digital counts into engineering units). The two simplest file formats would be binary and ASCII, with binary being the clear choice due to its storage efficiency. A well-defined database of sensor head location and orientation (i.e. configuration management) should be developed for ISS data.

Data access tools should be provided to the microgravity community. These tools would include cross-platform programs to perform binary-to-ASCII conversions, and for data access, retrieval and display. A standard data format becomes most useful with such programs because these data access tools would be available for acceleration data from any accelerometer system.

By providing access to these tools, a PI would be able to request access to the real-time acceleration data, and use the PIMS-provided software to produce real-time (or near-real-time) plots of the data. This also gives each PI ultimate control over their own displays, as opposed to having to share the available PIMS computer resources with other PIs. By providing a modular program design, an analysis "toolbox" could be created, with the tools offering various analyses and display formats. PI requests for a specialized analysis would be accomplished by the creation of a new plug-in tool to be used with both the real-time and off-line systems. The standard data format and modular program design would allow the PI to analyze past data with this new data processing tool.

PIMS is also considering the development of a web-based data analysis package. Here, the PI would fill-out an analysis request form on a web page, a PIMS computer would

automatically process the data, and the results would be placed on a file server for the PI to access within a given period of time (i.e. for 10 days). The imposition of the time limit would be required in order to deal with data storage and archival issues.

## **DATA STORAGE**

The quantity of acceleration data that will be generated during ISS operations requires an overall storage scheme that affords both long term and short term data storage solutions. Short term storage refers to the time the acceleration data is available on the internet file server for ready access by a PI or a PIMS data analyst. Anticipated to be on the order of three months, the short term storage duration could be adjusted operationally based upon available storage space, and the number of active accelerometers and their respective sampling rates. Regardless of the actual number, the duration will be such that long term storage of data will need to be achieved via a different medium.

Issues of data compression are inherent in generic discussions of long term storage. Any compression algorithm employed relative to the recorded acceleration data must be a capable of retaining every aspect of the original recorded data (lossless compression). Table 1 lists some storage media options with their respective amounts of available data storage. Whether compression is utilized or not, in terms of storage capacity, Digital Video Disk (DVD) technology clearly presents the most efficient option for long term storage of data. Anticipated advances in technology will present the capability to store greater volumes of data on a single disk.

Table 1: Storage Media Options

| <b>Storage Media</b>    | <b>Type</b> | <b>Access</b> | <b>Capacity</b> |
|-------------------------|-------------|---------------|-----------------|
| 8-mm Cartridge          | Magnetic    | Sequential    | 5 gigabytes     |
| CD-ROM                  | Optical     | Random        | 650 megabytes   |
| Single Sided DVD-120 mm | Optical     | Random        | 4.7 gigabytes   |
| Dual Layer DVD-120 mm   | Optical     | Random        | 8.5 gigabytes   |

Regardless of the media selected, a PI requiring access to acceleration data that has been moved to long term storage must request the data be returned to the internet file server for ready access or must request the data on an alternate media such as a CD-ROM or DVD.

## ANALYSIS CONCEPTS

During Orbiter microgravity missions, PIMS staff monitored acceleration data, experiment timelines, and voice loop activity continually throughout a given mission. Detailed logbooks were maintained to assist in establishing the relationship between experiment, crew, and vehicle activity and signatures observed in the acceleration data. During post-mission analysis of the acceleration data, PIMS data analysts review the logbook content and experiment timelines when attempting to characterize disturbance signatures. Since the PIMS console will not be staffed continually for ISS operations, the availability of a system that can autonomously detect new events in the microgravity environment would prove invaluable.

Two analysis concepts under consideration by PIMS have application to the real-time and off-line processing of acceleration data. A grant with the Pennsylvania State University (NAS3-1586) investigated the feasibility of utilizing neural networks to classify and cluster events of similar characteristics using Space Acceleration Measurement System (SAMS) data. The resulting work was tested in real-time during the USMP-4 (STS-87) mission. The relatively constant USMP-4 acceleration environment successfully demonstrated the clustering of acceleration data and the successful characterization of similar acceleration events. A neural network would allow the detection of new disturbance sources, prompting an indication to the PIMS data analysts. This indication would precipitate a closer examination of the acceleration data, the experiment timelines, and crew activity around the time the event occurred.

As a by-product of the neural network's support of the USMP-4 mission, an expert system was developed that complemented the real-time PIMS acceleration environment characterization function. The expert system's knowledge base was developed based upon analysis of acceleration data from previous Orbiter missions, and the PIMS microgravity handbook. The cause and effect relationships established prior to the flight of STS-87 allowed descriptive names (such as "crew exercise" and "radiator deployment") to be assigned to clusters detected by the neural network software from a frequency domain analysis of the real-time acceleration data. When detected by the expert system, a simple on/off indication was provided on a computer display. A similar cause and effect knowledge base will be established for ISS operations, allowing a PI to view a simplified display of the microgravity environment instead of trying to interpret a frequency domain representation of the data in real-time.

## CONCLUSIONS

During ISS operations, the real-time and off-line characterization of the microgravity environment in support of microgravity science PIs is the fundamental objective of the PIMS

project at NASA's Lewis Research Center. The volume of acceleration data that will be generated during ISS operations requires significant modification to the access, storage, and analysis techniques used by the PIMS project during Orbiter missions. These modifications will be made in a modular design fashion, such that data access and retrieval will be easier to accomplish, particularly for the experiment PIs. The prototype neural network system (designed by the Pennsylvania State University) will be expanded upon, and used to complement the PIMS monitoring of the acceleration environment in real-time.

| REPORT DOCUMENTATION PAGE   |                             |  | Form Approved<br>OMB No. 0704-0188 |                       |
|---|-----------------------------|--|------------------------------------|-----------------------|
| Public reporting burden for this collection of information is estimated to average 1 hour per response, including the time for reviewing instructions, searching existing data sources, gathering and maintaining the data needed, and completing and reviewing the collection of information. Send comments regarding this burden estimate or any other aspect of this collection of information, including suggestions for reducing this burden, to Washington Headquarters Services, Directorate for Information Operations and Reports, 1215 Jefferson Davis Highway, Suite 1204, Arlington, VA 22202-4302, and to the Office of Management and Budget, Paperwork Reduction Project (0704-0188), Washington, DC 20503.  |                             |  |                                    |                       |
| 1. AGENCY USE ONLY (Leave blank)  | 2. REPORT DATE<br>June 1998 | 3. REPORT TYPE AND DATES COVERED<br>Conference Publication   |                                    |                       |
| 4. TITLE AND SUBTITLE<br><br>17th International Microgravity Measurements Group Meeting   |                             | 5. FUNDING NUMBERS<br><br>WU-974-73-0C-00  |                                    |                       |
| 6. AUTHOR(S)<br><br>Richard DeLombard   |                             | 7. PERFORMING ORGANIZATION NAME(S) AND ADDRESS(ES)<br><br>National Aeronautics and Space Administration<br>Lewis Research Center<br>Cleveland, Ohio 44135-3191 |                                    |                       |
| 8. PERFORMING ORGANIZATION REPORT NUMBER<br><br>E-11229   |                             | 9. SPONSORING/MONITORING AGENCY NAME(S) AND ADDRESS(ES)<br><br>National Aeronautics and Space Administration<br>Washington, DC 20546-0001                      |                                    |                       |
| 10. SPONSORING/MONITORING AGENCY REPORT NUMBER<br><br>NASA CP-1998-208414   |                             | 11. SUPPLEMENTARY NOTES<br><br>Responsible person, Richard DeLombard, organization code 6727, (216) 433-5285.  |                                    |                       |
| 12a. DISTRIBUTION/AVAILABILITY STATEMENT<br><br>Unclassified - Unlimited<br>Subject Categories: 19 and 18<br><br>This publication is available from the NASA Center for AeroSpace Information, (301) 621-0390.  |                             | 12b. DISTRIBUTION CODE<br><br>Distribution: Nonstandard  |                                    |                       |
| 13. ABSTRACT (Maximum 200 words)<br>The Seventeenth International Microgravity Measurements Group (MGMG) meeting was held 24-26 March 1998 at the Ohio Aerospace Institute (OAI) in Brook Park, Ohio. This meeting focused on the transition of microgravity science research from the Shuttle, Mir, and free flyers to the International Space Station. The MGMG series of meetings are conducted by the Principal Investigator Microgravity Services project of the Microgravity Science Division at the NASA Lewis Research Center. The MGMG meetings provide a forum for the exchange of information and ideas about the microgravity environment and microgravity acceleration research in the Microgravity Research Program. The meeting had participation from investigators in all areas of microgravity research. The attendees included representatives from: NASA centers; National Space Development Agency of Japan; European Space Agency; Daimler Benz Aerospace AG; Deutsches Zentrum fuer Luft- und Raumfahrt; Centre National d'Etudes Spatiales; Canadian Space Agency, national research institutions; Universities in U.S., Italy, Germany, and Russia; and commercial companies in the U.S. and Russia. Several agencies presented summaries of the measurement, analysis, and characterization of the microgravity environment of the Shuttle, Mir, and sounding rockets over the past fifteen years. This extensive effort has laid a foundation for pursuing a similar course during future microgravity science experiment operations on the ISS. Future activities of microgravity environment characterization were discussed by several agencies who plan to operate on the ISS. |                             |  |                                    |                       |
| 14. SUBJECT TERMS<br><br>Microgravity environment; Acceleration; Accelerometers; Orbiter; Mir; International Space Station  |                             | 15. NUMBER OF PAGES<br>298   |                                    |                       |
| 17. SECURITY CLASSIFICATION OF REPORT<br>Unclassified   |                             | 18. SECURITY CLASSIFICATION OF THIS PAGE<br>Unclassified   |                                    | 16. PRICE CODE<br>A13 |
| 19. SECURITY CLASSIFICATION OF ABSTRACT<br>Unclassified   |                             | 20. LIMITATION OF ABSTRACT   |                                    |                       |